Quantification and assessment of environmental and health risk in post-combustion carbon capture—An Australian study

Thesis submitted for the degree of Doctor of Philosophy

By

Ye Wu

Department of Environmental Sciences

Faculty of Science and Engineering

Macquarie University

August 2016

MACQUARIE
University
SYDNEY·AUSTRALIA

Table of Contents

Table of Figures

Table of Tables

List of Abbreviations

AAQS	Ambient Air Quality Standards
ALD2	Acetaldehyde
AQMS	Air Quality Monitoring System
CALPUFF	A puff model to process dispersion, chemical transportation and deposition.
Carbon Bond 6	A kinetic mechanism used to model the chemical transformation of gas-phase species
Carbonyls	The group of organic compounds that include the formaldehyde and the ketones
CCS	Carbon Capture and Sequence
CSIRO	Commonwealth Scientific and Industrial Research Organization
CTM	The CTM is a three-dimensional Eulerian chemical transport model with the capability of modelling the emission, transport, chemical transformation, wet and dry deposition of a coupled gas and aerosol phase atmospheric system
DNPH	2,4-Dinitrophenylhydrazine
EC	Elemental carbon
HCHO	Formaldehyde
HPLC	High Performance Liquid Chromatography
KPP	Kinetic PreProcessor Model
MEA	Monoethanolamine
MU	Macquarie University
NPI	National Pollutant Inventory (see http://www.npi.gov.au/)
OC	Organic carbon
OEH	Office of Environment and Heritage, NSW
PCC	Post-combustion Carbon Capture
PTR-TOF-MS	Proton Transfer Reaction Time-of-Flight Mass Spectrometry
TAPM	The Air Pollution Model. A prognostic meteorological and air pollution dispersion model developed by CSIRO Atmospheric Research
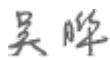
Declaration

I certify that the work in this thesis entitled "Quantification and assessment of environmental and health risk in post-combustion carbon capture—An Australian study" has not previously been submitted for a degree nor has it been submitted as part of requirements for a degree to any other University or institution other than Macquarie University.

I also certify that the thesis is an original piece of research and it has been written by me. Any help and assistance that I have received in my research work and the preparation of the thesis itself have been appropriately acknowledge. In addition, I certify that all information sources and literature used are indicated in the thesis.

I consent to this thesis being made available for photocopying and loan under the appropriate Australian copyright laws.

吴晔

Ye Wu (42622077)

Acknowledgements

Abstract

Post-combustion carbon capture (PCC) technology is an innovation technology to capture carbon dioxide (CO_2) from flue gas through solvents absorption typically using monoethanolamine (MEA). PCC technology is a facility installed after the combustion units. In Australia, most power stations are coal-burning power stations. PCC technology is more likely to be applied on these stations to reduce CO_2 emissions into the atmosphere. However, the technology also emits amine and its degradation products into the atmosphere. Amine can react with OH radicals to form nitrosamine and nitramine under photolysis. A review of literatures in human health impacts reveals that nitrosamine is suspected to be human carcinogenic and aldehydes as the degradation products of amine are known to be toxic. In addition, PCC technology emits ammonia, which is a contributor to fine particle formation.

In order to assess potential environmental and human health impacts from the technology, this study hypothesizes a PCC project in Bayswater Power Station in the Upper Hunter region, NSW, Australia and conducts many tasks including an experimental sampling of aldehydes, KPP modelling simulation for amine's chemical scheme, atmospheric dispersion simulations for amine, nitrosamine, nitramine and other primary air pollutants, and risk assessments of formaldehyde and $PM_{2.5}$.

In the experimental sampling of aldehydes, the study used an active sampling system to conduct air sampling of aldehydes following TO-11A method to determine baseline concentrations of aldehydes on MU campus and in Upper Hunter industrial area. The measured concentration was further used to represent the background value of formaldehyde and acetaldehyde in TAPM-CTM setting. The measured average daily HCHO concentration was 2.2 ppb in late spring, 1.1 ppb in summer, 1.3 ppb in late autumn, and 0.5 ppb in winter on the MU campus. Ambient acetaldehyde concentrations on the MU campus were only available in summer and winter with mean values of 0.6 ppb and 1.2 ppb, respectively. In the Upper Hunter area, the HCHO values were measured in summer and winter. The average concentration of ambient HCHO was 1.0 ppb and 0.9 ppb in summer and in winter, respectively. The acetaldehyde was only detected in summer with mean value of 1.8 ppb in the Upper Hunter area.

Chemical scheme of amine in the atmosphere was simulated in KPP model under two scenarios: chamber scenario and atmosphere scenario. In the chamber scenario, the MEA decreased sharply in the first 3 hours. Nitramines and nitrosamines increased quickly at the beginning of the experiment, then decreased slightly. In the atmospheric scenario, the concentration changes were slower than the chamber experiment. Atmospheric dispersion of amine and its degradation products were simulated in CALPUFF model. The highest concentrations of amines, nitrosamine, and formaldehyde occurred in December which is the hottest months in southern hemisphere. All values of these compounds did not exceed the US EPA's recommended threshold level for health impacts.

TAPM-CTM model was employed to simulate atmospheric dispersion of primary air pollutants in the study area using 2003 NSW emission inventory data under different meteorological conditions. The study assumed a 70% decrease of NO_x emissions and a 95% decrease of SO_2 emission from the Bayswater Power Station. As there is not emission control of NO_x and SO_2 in the power station, the decreased NO_x and SO_2 emission led to a significant decrease on atmospheric NO_x and SO_2 concentrations. Due to the largely decreased NO_x and SO_2 emission, the meteorological conditions is likely to play a less significant impacts on the change of near surface concentrations of NO_x and SO_2. In addition, the increased aldehyde emissions did not significantly change the concentrations of formaldehyde and acetaldehyde.

NH_3 is reported to be favored reacting with nitrate acid to form nitrate aerosol (NIT) in low temperatures (Ansari and Pandis, 1998; Heo et al., 2015; Pinder et al., 2008). Due to increased NH_3 from PCC projects, more nitrate aerosol (NIT) may be formed in low temperature under reactions of NH_3 and nitrate acid. The modelled results showed that the average change of NIT were smaller in winter than other months under largely decreased NO_x emission. The results indicated nitrate aerosol formation is favored in the low temperature environments. In addition, this study's results showed the nitrate aerosol formation does not increase linearly with an increase in NH_3. $PM_{2.5}$ formation also did not show a linear relationship with NIT, NH_4 or ASO_4.

To assess the health impacts exposure to formaldehyde and $PM_{2.5}$, a Monte-Carlo risk model (@RISK) was employed to simulate lifetime exposure to these air pollutants. The cancer risk

due to HCHO exposure decreased slightly after PCC technology installation. The mortality risk due to exposure to PM$_{2.5}$ decreased by 9.3×10^{-6} and 5.7×10^{-6} on mortality from all causes diseases and mortality from lung cancer after installing PCC technology, respectively.

Chapter 1 Introduction

1.1 Global and Australian carbon dioxide emission

As the climate changes, global warming is of greater concern across all sectors of society. Greenhouse gas emissions have been recognized as a main factor to cause the global warming. About two-thirds of annual anthropogenic greenhouse gas emissions originated from the energy sector (IEA, 2015). Global carbon dioxide (CO_2) emissions have increased by more than 50% over the past 25 years (IEA, 2015), and in the last decades of the 20th century, global CO_2 emissions have increased at a rate of 1.2% per year (IEA, 2015). However, the average annual increase of CO_2 emissions between 2000 and 2014 was 2.3%, primarily due to a large increase in CO_2 emissions from power generation in countries outside the Organisation for Economic Cooperation and Development (OECD), such as China and India (IEA, 2015). In 2014, global energy-related CO_2 emissions were estimated to be 32.2 Gt (10^9 tonnes) (IEA, 2015).

The Australian government has committed to reduce emissions by 5-15 % by 2020 compared to year 2000 levels under the United Nations Framework Convention on Climate Change (UNFCCC), and to keep average annual emissions between 2013 and 2020 to 99.5 % of 1990 levels (Climate Change Authority, 2014). The Australian Greenhouse Emissions Information System (AGEIS) has reported (AGEIS, 2013) that Australian CO_2 equivalent emissions in 2013 based on Kyoto accounting was 0.54 Gt (10^9 tonnes). The CO_2 equivalent emissions from the energy sector was 0.4 Gt, which is 74.1% of total national greenhouse gas inventory. Greenhouse gas emissions trap heat radiated from the Earth's surface within the atmosphere (Climate Change Authority, 2014). As more heat is retained, the climate warms. As a result, global average sea levels rose 0.19 meters between 1901 and 2010 (IPCC, 2013). In Australia, record high temperatures have been increasing in frequency since the 1950s (Climate Change Authority, 2014). The coral population in the Great Barrier Reef has decreased half since the 1980s (De'Ath et al., 2012). Control and reduction of CO_2 emissions is a primary way to reduce the effects of global warming.

1.2 Criteria air pollutants in the atmosphere

Air quality is affected by the concentrations of air pollutants in the atmosphere. The main air pollutants are carbon monoxide (CO), ozone (O_3), sulfur dioxide (SO_2), oxides of nitrogen

(NOx), particulate matter (PM) and air toxics. About two-thirds of CO is from anthropogenic sources, and the remainder is primarily from the oxidation of methane (Seinfeld and Pandis, 1998). Particles come from both natural and anthropogenic sources (Seinfeld and Pandis, 1998). The main biogenic sources of particles are "soil and rock debris, volcanic action, sea spray, biomass burning, and reactions between natural gaseous emissions", while anthropogenic sources arise mainly from "fuel combustion, industrial processes, nonindustrial fugitive sources and transportation sources" (Seinfeld and Pandis, 1998). Particles are grouped according to size: particles smaller than 10 μm in diameter (PM_{10}) and those smaller than 2.5 μm ($PM_{2.5}$). $PM_{2.5}$ are related to increased mortality and hospital admissions (Greene and Morris, 2006; Krewski et al., 2009; NSW EPA, 2015; Pope III et al., 2002). The health impact of $PM_{2.5}$ is more pronounced because the smaller particles can be inhaled more deeply into the lungs and are often able to pass into the bloodstream (NSW EPA, 2015). Ozone exists in both stratosphere and troposphere. About 90% of atmospheric ozone is found in the stratosphere (Seinfeld and Pandis, 1998), where it absorbs ultraviolet radiation ranging 290-320nm (UV-B) and thus protects against skin cancer (Seinfeld and Pandis, 1998). Tropospheric ozone concentrations from biogenic sources are normally very low, with background levels in the range of 10-40 ppb in unpolluted regions (Seinfeld and Pandis, 1998). However, tropospheric ozone is harmful to human health and the environment, for example, ozone exposure can decrease the ability of lungs to perform normal functions (WHO, 1998). Ozone can cause agricultural crop yield loss (US EPA, 2016). The majority of tropospheric ozone is formed by precursor compounds, typically NO_x and volatile organic compounds (VOCs), in warm and sunny meteorological conditions (NSW EPA, 2015). SO_2 is significantly from anthropogenic sources, such as industrial activities (NSW EPA, 2015; Seinfeld and Pandis, 1998). Exposure to SO_2 can irritate nose, throat, and cause coughing, shortness of breath, or a tight feeling in the chest (Department of Environment, 2005c). The lifetime of SO_2 is based on reaction with OH radical which is a dominant reaction in gas phase (Seinfeld and Pandis, 1998). NO_x is the combination of NO and NO_2. NO is a product of both natural and anthropogenic emissions. NO_2 is formed by oxidation of NO and is a product of the combustion process along with NO (Seinfeld and Pandis, 1998). NO_2 is a contributor to photochemical smog which impacts human health (Department of Environment, 2005b). Air toxics such as benzene, toluene, xylenes, and formaldehyde, are a range of air pollutants that are present in the atmosphere at low concentrations but are harmful to human health and the environment. These air pollutants can increase the

2

incidence of "cancers, birth defect, genetic damage, central nervous system defects, immunodeficiency, and disorders of the respiratory and nervous systems" (Department of Environment, 2005a).

In New South Wales (NSW), Australia, the NSW Environmental Protection Agency (EPA) has built a statewide network to monitor criteria air pollutants levels and reach ambient air quality standards and goals set under National Environment Protection (Ambient Air Quality) Measure (AAQ NEPM) by the National Environment Protection Council (NEPC) in 1998. The AAQ NEPM emission targets for CO, NO_x, and SO_2 have been met , but O_3 and PM concentrations still exceed targets and remain of concern (NSW EPA, 2015). The air toxics monitoring program, which includes benzene, toluene, xylenes, formaldehyde and benzo(α)pyrene (BaP) shows that concentrations are relatively low (NSW EPA, 2015). In the Upper Hunter industry region, which is, located about 300 km northern of Sydney, PM is one of the most concerning air quality issues. The NSW 2008 Air Emission Inventory Investigation (NSW EPA, 2012b) reported top 10 anthropogenic emissions sources of $PM_{2.5}$ in the non-urban regions of NSW. The detailed proportion of the top anthropogenic emissions is shown in Figure 1-1. Electric power generation is the second largest anthropogenic contribution to $PM_{2.5}$ concentrations outside the Sydney metro area.
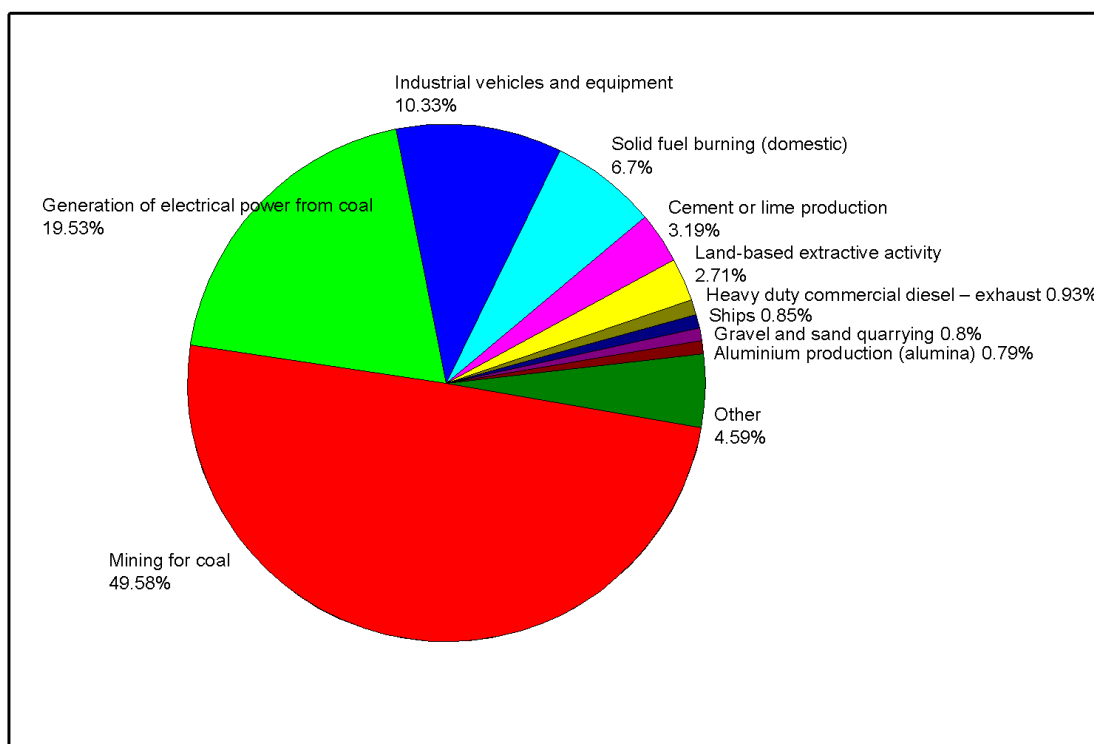
Figure 1-1 The proportion of the top 10 anthropogenic emissions of PM$_{2.5}$ in non-urban region in NSW

1.3 Carbon capture and sequestration

1.3.1 Carbon Capture and Sequestration Technology

Carbon capture and sequestration (CCS) is an innovative technology that seeks to significantly reduce or eliminate carbon dioxide emissions from industrial sources including power stations. The main types of CCS are pre-combustion, post-combustion, and oxy-fuel combustion technologies.

Pre-combustion

Pre-combustion is a process to remove CO_2 from a fuel before it is combusted in a power plant. Pre-combustion technology is normally applied in natural gas processing, natural gas refining, and Integrated Gasification Combined Cycle (IGCC) power plants (Global CCS Institute, 2012). The fuel, such as coal, is oxidized into synthesis gas under high temperature and pressure (Office of Fossil Energy, 2016). The synthesis gas, which is a mixture of hydrogen (H_2), CO, CO_2, and small amounts of other gaseous compounds, can react CO with water to form a H_2 and CO_2 rich gas (Office of Fossil Energy, 2016). The CO_2 can be captured

4

and stored, and the H_2-rich synthesis gas can then be combusted to generate power (Office of Fossil Energy, 2016).

The CO_2 is captured via absorption in a solvent to remove acid gas (e.g., CO_2, H_2S) in one of two ways: chemical or physical (Global CCS Institute, 2012). Chemical absorption uses chemical absorbents to react with the acid gases and to reverse the reactions under heat to release the acid gases (Global CCS Institute, 2012). Physical absorption is a process by which CO_2 gas is dissolved in physical absorbents (e.g., Selexol, Rectisol) under increasing pressure and then released while decreasing the pressure and increasing the temperature (Global CCS Institute, 2012).

Oxy-fuel combustion

Most existing power plants burn coal in air, which produces flue gas containing large amounts of nitrogen (Herzog et al., 2009). Without nitrogen the CO_2 removal can be easier (Herzog et al., 2009). Therefore, oxy-fuel combustion uses high purity oxygen, generated in an air separation plant, instead of ambient air in coal burning process to achieve CO_2 removal (Herzog et al., 2009).

Post-combustion carbon capture

Post-combustion capture (PCC) is a carbon capture technology normally requires retrofitting new technology into existing fossil fuel power plants. The technology captures CO_2 from exhaust gas after fuel combustion. The capture process in PCC employs absorption, adsorption, membrane-based separation, and other approaches to capture CO_2 from flue gas (Herzog et al., 2009). The conventional approach uses amines-based absorption to capture CO_2. In this absorption approach, the flue gas flows along beds of liquid solvents in the scrubber tower where the turbulent flow can boost CO_2 conversion from gas into liquid (Herzog et al., 2009). In the stripper, the captured CO_2 is then desorbed under high temperature to release CO_2 for compression and storage (Herzog et al., 2009). This study focus on this amines-based absorption to assess emission impacts on environment and human health.

1.3.2 Potential air pollutants from the PCC technology

There are a number of species that occur in flue gas, which can be emitted into the atmosphere. Previous studies (de Koeijer et al., 2013; Låg et al., 2009; Morken et al., 2014;

Thong et al., 2012) have reported that gas phase chemical compounds including nitrosamines, formaldehyde, acetaldehyde, ammonia, acetone, and amides (formamide and acetamide) are potentially emitted from post-combustion carbon capture projects. Some of these air pollutants are very toxic, and others, such as formaldehyde, acetaldehyde, and ammonia, can be found in the atmosphere from other sources. Formaldehyde and acetaldehyde in the atmosphere are contributors to the formation of ozone (Luecken et al., 2012). Additionally, formaldehyde is a potential carcinogenic compound that may affect human health. Ammonia is a critical component in the formation of PM (Gong et al., 2013) and has been shown to have eutrophication effects after precipitation (de Koeijer et al., 2013). The more detailed impacts and risks for potential air pollutants from the PCC technology are discussed in Chapter 2.

1.4 Description of the research project

1.4.1 Why is the research project needed?

CCS is a proposed technology to reduce CO_2 emissions from fossil fuel combustion power generation. Post-combustion carbon capture technology is compatible with and can be retrofitted to existing coal combustion power generation plants (Herzog et al., 2009). As large number of power stations employ coal combustion, post-combustion carbon capture is a competitive candidate technology to achieve carbon capture from power stations on a commercial scale.

A potentially significant component of risk associated with post-combustion carbon capture is amines and oxidation products produced in the capture process due to solvent recycling and solvent oxidation reactions. These emission species will determine the application and development of post-combustion technology on the commercial scale. This study combines a field sampling program for existing aldehydes, computer modelling for atmospheric transport, and a Monte-Carlo risk assessment for human health impacts to obtain more information on potential impacts from commercial scale post-combustion carbon capture projects.

It is known that amine-based post-combustion carbon capture projects can emit ammonia, formaldehyde, acetaldehyde, formamide, acetamide, acetone, amines and other degradation products (Morken et al., 2014; Thong et al., 2012).

It is important to understand potential environmental risks before implementing post-combustion carbon capture projects on a commercial scale. Amine degradation in the atmosphere is also of concern as it carries environmental risks and impacts human health. Amines are capable of forming nitrosamines under certain conditions. The nitrosamines are very toxic and are suspected to be a human carcinogen (Låg et al., 2009).

This study simulates potential atmospheric movement and dispersion under different meteorological conditions to determine potential near surface concentrations of targeted air pollutants. Risk probability of selected air pollutants is conducted using the @RISK Monte-Carlo risk model to find out potential risks on human health. In this study, particle pollution is an existing issue in the Upper Hunter study area. This study assesses mortality risk of exposure to $PM_{2.5}$ on long-term exposure.

1.4.2 Project objectives

Upon reviewing the available literature on post-combustion carbon capture technology, its potential emissions and their atmospheric transport and dispersion, a scheme was derived for the fieldwork component of the thesis. A detailed representation of the scheme is presented in the methodology chapter. The field studies were made at an urban location and near a power station in the Upper Hunter Valley in NSW, Australia.

The objectives of the field study were to quantify atmospheric aldehydes values by the collection and analysis of air samples

This information was then used to:
- To develop a simple chemical mechanism including amines reactions to run a transport and dispersion model

- To conduct risk analysis of the risk probability of impacts from the emissions of a post-combustion carbon capture project on health

- To provide suggestions on future policy and regulation development on post-combustion project

1.5 Thesis structure

The study starts with literature review to determine potential emissions from post-combustion carbon capture projects, and potential impacts caused by the emissions. A methodology chapter describing sampling methods for formaldehyde and acetaldehyde follows. After obtaining formaldehyde and acetaldehyde atmospheric concentrations, two

modelling chapters follow to discuss atmospheric dispersion of amines and degradation products, and atmospheric dispersion and movement of critical air pollutants. After considering different meteorological conditions on atmospheric dispersion, a risk assessment is conducted to assess potential human health impacts from atmospheric formaldehyde and $PM_{2.5}$ after installing PCC technology into conventional coal combustion power stations.

Chapter 2 Literature review

This chapter reviews the current state of knowledge regarding atmospheric emissions from post-combustion carbon capture (PCC) projects, atmospheric reactions, and potential environmental and health impacts. In the third and fourth sections of this chapter, the current state of knowledge on the existing atmospheric concentrations of formaldehyde and ammonia which are components of the emission from PCC projects are reviewed. Some of these compounds are suspected to be toxic according to known knowledge. The potential risks and impacts associated with them are reviewed in this chapter. As PCC is an innovative technology, there is no commercial scale operation for large scale coal combustion. There is still uncertainties on emissions, dispersion after atmospheric transport, and the potential impacts on environment and human health. To consider the atmospheric transport and dispersion, and the risk probability of relative emissions, computer modelling is employed to do these tasks. Two atmospheric dispersion models are reviewed in this chapter, and one of Monte-Carlo simulation model employed for the risk probability assessment will also be discussed in the chapter. As PCC is not yet a commercial operation, the regulations and policy regarding PCC operation, design, and emission rules are still under development. Current relevant regulations and policy development in the world, and knowledge gaps are considered in this review.

2.1 Post-combustion emissions

Post-combustion carbon capture technology especially amine scrubbing technology, is a well-developed and innovative technology to capture carbon dioxide (CO_2) from the flue gas of coal-fired power stations. The carbon dioxide capture process involves CO_2 rich flue gas from power stations contacting with aqueous amines such as conventional 30 per cent w/w monoethanolamine (MEA) (Thong et al., 2012) in an absorber tower. The captured CO_2 is then pumped to a stripper tower, where the solution is heated up to release the CO_2 at high temperature. The released CO_2 is stored and compressed for future use or sequestration, and the lean solvent is recycled back to the absorber tower for re-use (Rochelle, 2009). In the capture process, solvent loss needs to be considered (Moser et al., 2011). The loss of solvent occurs by two mechanisms: one is loss by entrainment and solvent vapour pressure, while the second involves consumption by degradation and solvent blocking (Moser et al.,

2011). Due to solvent recycling, PCC technology may release emissions into the atmosphere (Karl et al., 2011). These emissions can be either chemical compounds already existing in CO_2-rich flue gas, or those added during the carbon capture process, including amines and their degradation products (de Koeijer et al., 2013; Karl et al., 2011). Lepaumier and co-workers show that MEA is primarily degraded by oxidation rather than by thermal reactions (Lepaumier et al., 2011). The products from thermal degradation are very stable and in the liquid phase while the oxidation products are volatile (Lepaumier et al., 2011). Similar results were reported by Sexton and Rochelle (Sexton and Rochelle, 2011) which showed that oxidation products can be significant components of the flue gas in the presence of 3-15 per cent oxygen. It is also claimed (Sexton and Rochelle, 2011) that products from oxidative degradation can have impacts on the environment and human health, and contribute to the risk of equipment corrosion.

These oxidative reactions occur mainly in the absorber tower due to the present of oxygen (Gouedard et al., 2012). Two chemical mechanisms have been studied for amine oxidation reactions: electron abstraction and hydrogen abstraction (Gouedard et al., 2012; Sexton and Rochelle, 2011). Electron abstraction includes oxidation reactions of amines by chlorine dioxide and other oxidants (Chi and Rochelle, 2002). The electron abstraction has been verified for tertiary amines only (Gouedard et al., 2012), and been proposed for primary amines (MEA) by several researchers (Chi and Rochelle, 2002; Lepaumier et al., 2011). The mechanism of the electron abstraction by introducing oxygen has been described (Chi and Rochelle, 2002). Figure 2-1 shows the mechanism of electron abstraction from MEA. In this mechanism, the imine radical is oxidised by oxygen to form the peroxide radical, which can further react to form imine and hydrogen peroxide. The imine molecule is not only hydrolysed to form ammonia and hydroxyacetaldehyde, but this can also occur via oxidative fragmentation to form formaldehyde and ammonia. Hydrogen abstraction has been studied by Lepaumier et al. (Lepaumier; et al., 2009). Lepaumier's study shows that hydrogen abstraction occurs at the α-position of nitrogen atom which then reacts to form imine, which is further hydrolysed into ammonia and glycolaldehyde (Lepaumier; et al., 2009). The MEA dealkylation is shown in Figure 2-2.
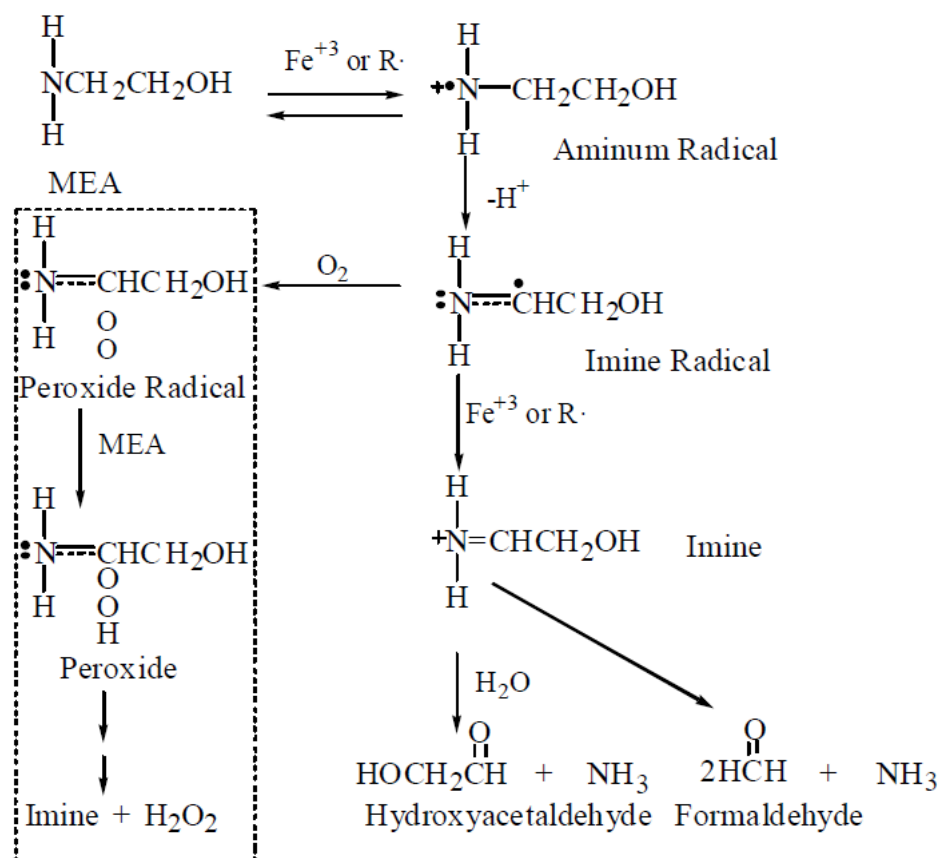
Figure 2-1: Degradation of MEA by electron oxidation, based on Chi & Rochelle study (Chi and Rochelle, 2002)

Previous studies of oxidative degradation products focus on the liquid phase. The main products of oxidative degradation are formic, acetic, glycolic and oxalic acids (Lepaumier et al., 2011). A recent study suggests that it is necessary to consider the environmental impact of these gaseous phase compounds (Zhu et al., 2013). Due to solvent recycling and volatile oxidative products, the flue gas from post-combustion projects can contain amines, ammonia, carboxylic acids, and aldehydes, among others (Gouedard et al., 2012; Lepaumier et al., 2011; Sexton and Rochelle, 2011). The details of these emissions from post-combustion projects are discussed below.
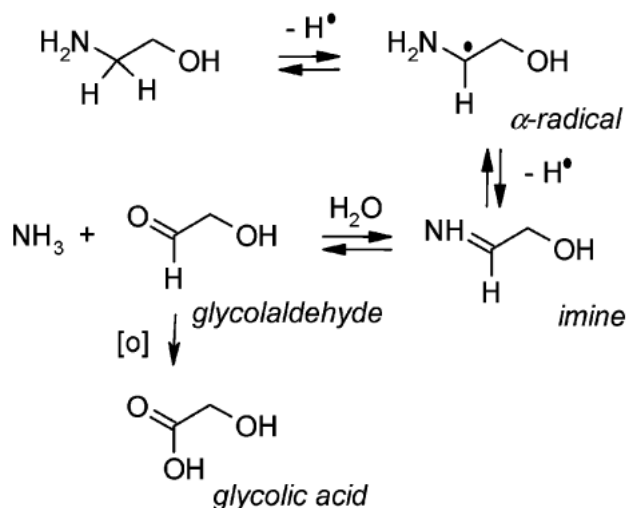
Figure 2-2: MEA Dealkylation, based on (Lepaumier; et al., 2009)

2.1.1 Amine emissions

After releasing CO_2 from the stripper, the lean solvent amines are recycled back to the absorber tower for re-use. Due to solvent recycling, amines can be emitted into the atmosphere. Amines emissions from carbon capture projects depend on the carbon capture processing conditions (Moser et al., 2011). Moser et al., (2011) have undertaken an investigation of trace elements in the inlet and outlet streams from Niederaussem pilot plant in Germany. This pilot plant which is a post-combustion capture facility has the capability to capture up to 7.2 tonne CO_2 per day and a capacity of 1,000 MW_{el} 1 unit (Moser et al., 2011). The measured MEA concentration in CO_2-lean flue gas with values between 0.02 − 0.03 mg/Nm^3 (dry) (Moser et al., 2011). In addition to the measurement of trace elements, the study also discussed the influence of other factors on emission. An additional packed bed at the top of absorber can be used to reduce emission of solvent (Moser et al., 2011). The result of the study (Moser et al., 2011) showed that the MEA concentration values were significantly higher when no make-up water was in the water section or high temperature was operating in the water section.

In an Aspen-Plus process simulation study (Thong et al., 2012), parameters of Australia Tarong coal-fired power plant, which has four 350 MW units with a 30 per cent w/w MEA carbon capture plant, were employed to set up the process simulation. During the capture process, the operational temperature of the absorber tower and the water wash tower conditions were proved to be the factors determining MEA emission and degradation

products (Thong et al., 2012). These results are in good agreement with the Moser et al., study. In the Aspen-Plus simulation study, atmospheric emission of MEA, considering both the vapour and droplet phase, was estimated to be about 0.14 mg/Nm^3 CO$_2$-lean flue gas (Thong et al., 2012). The vapour phase loss of MEA only depended on the vapour pressure of MEA and its solubility in water at a given absorber operating temperature, while entrainment loss of MEA from the wash tower was determined by the chemical composition of the wash water in the wash tower with volume flux of 0.13 m^3 per million m^3 of CO$_2$-lean gas (Thong et al., 2012).

2.1.2 Emission of amines degradation products

As mentioned above, amine degradation processes include thermal degradation and oxidative degradation. Normally, the industrial operating temperature in the reboiler is around 120˚C, as MEA is stable at this temperature (Thong et al., 2012). Thermal degradation occurs mainly at this temperature due to solvent reactions with CO$_2$ to form carbamate (Sexton and Rochelle, 2011; Thong et al., 2012). The main products of thermal degradation have been identified as heat stable salts, oxazolidone-2, 1-(2-hydroxyethyl) imidazolidone-2 (HEIA), N-(2-hydroxyethyl)-ethylenediamine (HEEDA), N-(2-hydroxyethyl)-diethylenetriamine (Trimer), N-92-hydroxyethyl)-triethylenetetraime (Polymer), and cyclic urea of trimer (Thong et al., 2012). These products are unlikely to be emitted into the atmosphere due to their low volatility (Lepaumier et al., 2011; Thong et al., 2012).

The degradation products that can be emitted into the atmosphere are mainly formed by oxidative degradation in the absorber tower (Lepaumier et al., 2011; Moser et al., 2011; Sexton and Rochelle, 2011; Thong et al., 2012). The composition of flue gas from power stations is likely to have an impact on the degradation rate of MEA (Moser et al., 2011). Ammonia (NH$_3$) is one of the primary products of the oxidative degradation of MEA in the presence of oxygen in the liquid solvent (Chi and Rochelle, 2002; Thong et al., 2012). It has been shown (Pedersen et al., 2010) that ammonia formation is also strongly related to the NOx concentration in the flue gas. In addition, NH$_3$ generated during the degradation process can react with MEA to form amides and alkylamines (Goff; and Rochelle, 2004; Sexton and Rochelle, 2011; Thong et al., 2012). Ammonia gas has been detected and measured in many studies. Moser et al., have observed 26.9 to 46.6 mg/Nm^3 NH$_3$ in exhaust gas from absorber tower (Moser et al., 2011). In the Aspen-Plus modelling study, the

simulated NH_3 value was lower than data from CSIRO's own pilot plant as the model did not consider the kinetics of decomposition of MEA (Thong et al., 2012). Considering the emission data from Moser et al., measurement, the atmospheric emission value of NH_3 is between 1 $\mu g/Nm^3$ and 0.12 mg/Nm^3 (Thong et al., 2012). In the presence of SOx, it is known that MEA is likely to be degraded to form organo-sulphates (Thong et al., 2012).

NOx in flue gas has been a significant concern as NOx is likely to react with amines to form nitrosamines and nitramines (Dai and Mitch, 2014; Fostås et al., 2011; Gouedard et al., 2012; Lepaumier; et al., 2009; Moser et al., 2011; Sexton and Rochelle, 2011; Thong et al., 2012). The detailed effect of NOx on nitrosamines and nitramines formation is still not fully understood. There is limited information available from pilot plant operations and industrial projects. However, recent studies (Dai and Mitch, 2014; Thong et al., 2012) have reported emission data from simulation and pilot plant operations. Dai and Mitch's study (Dai and Mitch, 2014) has noted the accumulated nitrosamines (N-nitrosomorpholine) in both the absorber tower and the wash water had a positive linear relationship with NO and NO_2 with concentration values of up to about 20 ppmv, while nitramines (N-nitromorpholine) increased with increasing NO_2 concentrations but not with NO values. As a primary amine, MEA is not expected to form stable nitrosamines (Morken et al., 2014; Thong et al., 2012) but Pedersen et al. (2010) confirmed that nitrosamines are detected at 5 ppm (by weight) in CO_2-lean solvent after 100 hours exposure to 25 -50 ppmv NOx due to solvent impurity or the nitrosation reaction of MEA with NO and HNO_2. Morken et al., and Strazisar studies (Morken et al., 2014; Strazisar et al., 2003) also found that nitrosamine was present in MEA solutions at levels of 797 $\mu mol/L$ and 2.91 $\mu mol/mL$, respectively. However, all nitrosamines and nitramines in the flue gas were below detection limits in one study (Morken et al., 2014). This was thought to be because the nitrosamines from high molecular weight amines have low volatility (Morken et al., 2014). In the Aspen-Plus simulation model study (Thong et al., 2012), the simulation results showed that nitrosamines (Nitrosomorpholine) atmospheric emissions were estimated to be up to 0.003 $\mu g/Nm^3$ CO_2 lean gas.

In addition to NH_3 and potential nitrosamines and nitramines emissions, the post-combustion carbon capture plants also emit formaldehyde, acetaldehyde, and acetone as primary chemical compounds into the atmosphere (Morken et al., 2014; Moser et al., 2011; Thong et al., 2012). Morken et al., measured the isokinetic gaseous emissions of

formaldehyde and acetaldehyde at 3.1-4.4 µg/m^3 and 18.1-31.7 µg/m^3, respectively (Morken et al., 2014). This study also used different measurements to monitor gas emissions from post-combustion carbon capture plant, including Proton Transfer Reaction Time-of-Flight Mass Spectrometry (PTR-TOF-MS) and third party measurement. The emission data are listed in Table 2-1 below. Moser et al., study reported the observed acetaldehyde and acetone in CO_2-lean flue gas with values less than 0.2 mg/Nm^3 and 0.5-1.0 mg/Nm^3, respectively. The Aspen-Plus simulation study estimated the atmospheric emission of formaldehyde, acetaldehyde, and acetone would be 0.26-0.27 mg/Nm^3, 0.3 mg/Nm^3, and up to 0.31-0.33mg/Nm^3, respectively. The detailed summary for atmospheric emissions is shown in Table 2-1.

Table 2-1: Summary of atmospheric emissions of the main chemicals from post-combustion carbon capture

Chemical emissions	Concentration values	Unit	Notes	References
MEA	0.14	mg/Nm^3		(Thong et al., 2012)
	0.02-0.03	mg/Nm^3		(Moser et al., 2011)
	3.5-848	µg/m^3	Isokinetic gas emission measurement	(Morken et al., 2014)
	8.9	ppbv	PTR-TOF-MS measurement	(Morken et al., 2014)
NH$_3$	0.001-0.12	mg/Nm^3		(Thong et al., 2012)
	26.9-46.6	mg/Nm^3		(Moser et al., 2011)
	4907-10031	µg/m^3	Isokinetic gas emission measurement	(Morken et al., 2014)
	18265.7	ppbv	PTR-TOF-MS measurement	(Morken et al., 2014)
Formaldehyde	0.26-0.27	mg/Nm^3		(Thong et al., 2012)
	3.1-4.4	µg/m^3	Isokinetic gas emission measurement	(Morken et al., 2014)
	43.1	ppbv	PTR-TOF-MS measurement	(Morken et al., 2014)
	<70	µg/m^3	Third Party measurement	(Morken et al., 2014)
Acetaldehyde	0.3	mg/Nm^3		(Thong et al., 2012)
	Less than 0.2	mg/Nm^3		(Moser et al., 2011)
	18.1-31.7	µg/m^3	Isokinetic gas emission measurement	(Morken et al., 2014)
	454.9	ppbv	PTR-TOF-MS measurement	(Morken et al., 2014)
	310	µg/m^3	Third Party measurement	(Morken et al., 2014)
Acetone	0.31-0.33	mg/Nm^3		(Thong et al., 2012)
	0.5-1.0	mg/Nm^3		(Moser et al., 2011)
	88.2	ppbv	PTR-TOF-MS measurement	(Morken et al., 2014)
Nitrosamines & Nitramines	Up to 0.003	µg/Nm^3		(Thong et al., 2012)
	<0.2 (total Nitrosamines)	µg/Nm^3	Isokinetic gas emission measurement	(Morken et al., 2014)
	<0.08 (total nitrosamines)	µg/m^3	Third Party measurement	(Morken et al., 2014)

2.2 Amines atmospheric reactions

It is known that amines emitted into the atmosphere can undergo photo-oxidation reactions (Nielsen et al., 2011). The photo-oxidation reactions of amines are primarily the result of reactions with OH radical in daylight (Karl et al., 2012) and are initiated in H-abstraction by the OH radical (Nielsen et al., 2011). The H-abstraction mainly occurs at three groups: the -CH_2OH group, the -CH_2- group, and the NH_2-group (Nielsen et al., 2011). Hydrogen abstraction from the -CH_2OH group results in the production of formamide and 2-oxo-acetamide with NO after reactions initiated by the OH radical while the –CH_2- group hydrogen abstraction produce formamide and formaldehyde (Nielsen et al., 2011). Hydrogen abstraction from the NH_2- group is more concerned as the intermediate product can form nitrosamines with NO, and can form nitramines with NO_2 (Karl et al., 2012; Nielsen et al., 2011). Most nitrosamines exhibit carcinogenicity in laboratory animals and bioassay studies, and nitramines are suspected to be carcinogenic (Låg et al., 2009). A chamber study of atmospheric photo-oxidation of MEA has been undertaken in the European Photochemical Reactor, EUPHORE, in Spain. This study (Nielsen, 2010; Nielsen et al., 2011) reported that the average branching ratios of hydrogen abstraction are 8 per cent from the NH_2- group, 84 per cent from the –CH_2- group, and 8 per cent from the –CH_2OH group (Karl et al., 2012). However, the chamber study did not detect any signal for nitrosamines (Nielsen et al., 2011). It was also reported (Karl et al., 2012) that the nitrosamines from primary amines (e.g. MEA) are not stable due to photolysis of nitrosamines. The mechanism of formation of nitrosamines is still not completely understood.

2.3 Atmospheric aldehydes

Aldehydes that contain carbonyl group play critical and important roles in atmospheric photochemistry and air quality (Andreini et al., 2000; Luecken et al., 2012). The main aldehydes concerned are formaldehyde (HCHO) and acetaldehyde (CH_3CHO), as they can provide new radicals to form ozone (Luecken et al., 2012) and also have potential carcinogenicity to cause health risk (Andreini et al., 2000; Luecken et al., 2012; Tang et al., 2009). Ambient formaldehyde and acetaldehyde concentrations include primary formaldehyde and acetaldehyde from anthropogenic emissions such as exhaust gas from motor vehicles, incomplete combustion of fuels, and biomass burning, and are concentrated

in urban area; and secondary formaldehyde and acetaldehyde that are mainly formed from hydrocarbon oxidation (Lei et al., 2007; Lü et al., 2009; Luecken et al., 2012). As the lifetime of both aldehydes can be of the order of a few hours, both chemicals can be transported distance of several kilometres from the emission source and have photochemical pollution effects over large areas (Jones et al., 2009; Possanzini et al., 2002). Recently, researchers have investigated the atmospheric concentrations of both aldehydes particularly formaldehyde to examine seasonal and temporal variations in concentrations. These studies are detailed in the following sub-sections.

2.3.1 The United States

2.3.1.1 Ambient formaldehyde values in New York City

In New York City, Lin et al., study measured ambient HCHO concentrations in New York in the summer of 2009 at the Queens College site, a residential area with a busy interstate express way 0.6 km further north and a highway within a radius of 5 km (Lin et al., 2012). A quantum cascade laser (QCL) was employed for the measurements, which ran from 15 July to 3 August 2009. The results showed that the HCHO concentration was approximately 0.4 - 7.5ppb, with an average value of 2.2 ± 1.1 ppb (Lin et al., 2012). The daily peak concentration value was reached between 11:00am and noon, while the minimum concentration was observed in the early morning (Lin et al., 2012). The sources of HCHO were reported as both primary and secondary. During the sampling period, primary sources contributed to ambient HCHO predominantly between midnight and 8 am, and were significantly enhanced during peak traffic periods. After 9 am, secondary sources became the major contributor to ambient HCHO concentrations, and reached a maximum value between 12pm and 3pm. Isoprene counted for 44 per cent of the secondary HCHO source, followed by methane (25 per cent), and propene (18 per cent) (Lin et al., 2012). OH radical formation was assessed as well in this study with 67 per cent arising from HONO, 18 per cent from HCHO, and 13 per cent from O_3.

2.3.1.2 Ambient formaldehyde and acetaldehyde in the Houston area

Houston has the top ranking seaport in the United States (Wikipedia, 2013). Several studies have been conducted in the area (Chen et al., 2004; Dasgupta et al., 2005). In Dasgupta et al study, the UCLA multipath DOAS instrument was placed at La Porte Airport, near the ship

channel (Dasgupta et al., 2005). The Houston Regional Monitoring site (HRM-3), which is located downwind from the heavily industrialised area of the Houston ship channel and in the middle of a petrochemical and chemical manufacturing complex, was also considered as part of the Texas Air Quality Study 2000 experiment (Dasgupta et al., 2005). Peak HCHO mixing ratios of more than 47 ppb were observed at both the HRM-3 and La Porte Airport sites, with 3.3 ppb overall average mixing ratio between 12th August and 25th September, 2000. The high concentration in Houston was caused by emissions near the ship channel (Dasgupta et al., 2005). In addition, the investigation in Houston found that high daytime formaldehyde peaks positively correlated with HNO_3 and SO_2 concentrations. In another study (Chen et al., 2004), most of the formaldehyde peak values observed in the summer of 2002 were less than 20 ppbv except on two days. The peak values on these days were approximately 25 ppbv and 30 ppbv, respectively. Chen et al., study (Chen et al., 2004) employed a laser spectrometer based on difference frequency generation (DFG) to perform sampling in Deer Park, Texas. Most data showed that formaldehyde concentrations in the sampling area predominantly arose from photochemical oxidation of volatile organic compounds (VOCs), as formaldehyde values increased when the ozone concentration values were elevated (Chen et al., 2004).

Salas and Singh study (Salas and Singh, 1986) was run in Houston on 18-19 March 1984. Their results showed that the maximum value of formaldehyde was approximately 22.5 ppb, with an average value of 3.8 ± 8.3 ppb. This value was lower than the summer value. During these sampling dates, considerable rain was recorded at the Houston site. The study also recorded the acetaldehyde concentrations. The maximum value of acetaldehyde was 6.7 ppb with average value of 2.2 ± 1.7 ppb. Salas and Singh found that the concentration of formaldehyde was normally higher than that of acetaldehyde, but formaldehyde values showed seasonal variability in that the summer values were higher than the winter values (Salas and Singh, 1986).

2.3.1.3 Other U.S cities

In midtown Atlanta, a maximum formaldehyde concentration of 18 ppb was detected on Jefferson Street near a bus repair depot (Dasgupta et al., 2005). This peak value was reached by 11 am. By association with the HNO_3 peak, HCHO formation was partly caused by atmospheric oxidation reactions (Dasgupta et al., 2005). The maximum value range in rural

Tampa, Philadelphia, and Nashville were observed to be between under 10 ppb and just under 13 ppb (Dasgupta et al., 2005). The study found that local micrometeorology was another factor impacting formaldehyde levels, such as land-sea breezes, which played an important role in generating the lowest formaldehyde level observed in Tampa (Dasgupta et al., 2005).

Acetaldehyde data are relatively sparse, with only a few studies reporting acetaldehyde values. Salas and Singh reported both formaldehyde and acetaldehyde concentration values in five cities (Salas and Singh, 1986). These values are listed in Table 2-2. All the acetaldehyde values tended to be lower than the matching formaldehyde values at the five sampling sites. Biomass burning is an emission source of formaldehyde and acetaldehyde (Lei et al., 2009; Lü et al., 2009; Luecken et al., 2012). A recent study (Na and Cocker, 2008) investigated the effects of wildfire activity on fine organic particles, formaldehyde and acetaldehyde levels. Formaldehyde, acetaldehyde, and elemental carbon values were found to more than double after fire activities. During fire events, the average concentration values of formaldehyde and acetaldehyde were 9.9 and 6.3 ppb, respectively, which are about twice than annual average values (3.1 and 1.2 ppb, respectively) as reported by the California Air Resources Board (Na and Cocker, 2008).

Table 2-2: Ambient formaldehyde and acetaldehyde levels from Salas and Singh observation

Field site	Sampling period	Formaldehyde concentration (ppb)		Acetaldehyde concentration (ppb)	
		Max	Average ± δ	Max	Average ± δ
Pittsburgh, PA	15-16 April, 1981	28.5	18.5 ± 6.7	2.6	1.4 ± 0.8
Chicago, IL	27-28 April, 1981	15.6	11.3 ± 3.8	3.4	2.1 ± 0.9
Downey, CA	28 Feb.-1 Mar., 1984	67.7	15.5 ± 11.9	28.4	8.5 ± 6.3
Houston, TX	18-19 March, 1984	22.5	3.8 ± 8.3	6.7	2.2 ± 1.7
Denver, CO	2-4 April, 1984	5.5	2.3 ± 1.8	2.1	1.0 ± 0.5

2.3.2 Mexico

2.3.2.1 US and Mexico border—Tijuana

The Cal-Mex 2010 air quality study (Zheng et al., 2013) measured formaldehyde concentrations at the US-Mexico border using proton transfer reaction mass spectrometry

(PTR-MS). The sampling site was near the city centre in Tijuana. The HCHO mixing ratio in the sampling period was in the range of 1.0 ppb to 13.7 ppb (Zheng et al., 2013). The daily peak value of 6.3 ± 2.6 ppb was reached at 10 am and the minimum of 2.8 ± 1.3 ppb occurred near midnight. The early HCHO peak is likely to be caused by primary vehicle emission (Zheng et al., 2013). After sunrise, photolysis of HCHO decreased the HCHO value, while maintaining a similar amount of OH production (Zheng et al., 2013). The study results show that secondary organic aerosol (SOA) in this study area is likely to be related to the OH generation from HCHO photolysis (Hodzic and Jimenez, 2011; Zheng et al., 2013). The study in Tijuana (Zheng et al., 2013) also showed that HCHO played a more important role than O_3 in contributing OH radicals, and the diesel vehicles contributed more primary HCHO emissions than gasoline vehicles in this study area.

2.3.2.2 Mexico City

The Mexico City Metropolitan Area (MCMA) is one of the most polluted cities in the world (Molina and Molina, 2002) with more than 3.5 million vehicles (Lei et al., 2007). The city is located "in an elevated basin at an altitude of 2240 m above sea level, surrounded by mountain ridges on the west, south and east, with a broad opening to the north and a narrow gap to the south-southwest" (Lei et al., 2007). A local ambient air monitoring network and the MCMA-2003 campaign measured formaldehyde concentrations in Mexico City, observing a maximum medium daily concentration of around 17 ppb (Molina et al., 2007). As Mexico City is one of the most polluted city in the world, high anthropogenic emission of formaldehyde is a major contributor to the ambient formaldehyde level (Lei et al., 2009). Lei et al., study (Lei et al., 2009) found that up to 50 per cent of the ambient formaldehyde levels on daily basis were from primary formaldehyde which were contributed by anthropogenic activities. Primary formaldehyde was also dominant contributor (up to 80 per cent) to ambient formaldehyde level at night and in the morning (Lei et al., 2009). A local study (Baez et al., 1995) measured both acetaldehyde and formaldehyde concentrations at the University of Mexico campus. This study observed acetaldehyde concentration ranges from 2 to 66.7 ppbv with an average value of 15.9 ppbv, while formaldehyde was recorded at levels ranging from 5.9 to 110 ppbv with an average value of 35.5 ppbv (Baez et al., 1995). Ambient formaldehyde was dominated by primary formaldehyde in Mexico City as the maximum value was recorded during the heavy traffic period of 10:00 am to 12:00 pm (Baez et al., 1995). Meteorological conditions, such as winds

and clouds, atmospheric stability, and smog conditions were the main factors influencing ambient aldehydes levels in the city (Baez et al., 1995).

2.3.3 China

Due to the economic boom in China, energy consumption and the number of vehicles have increased rapidly (He et al., 2001). Recently, many cities of China have suffered severe air pollution. Formaldehyde can be generated from both primary sources, such as emissions from vehicles and secondary sources, such as photochemical oxidation (Duan et al., 2012). In addition, aldehydes play a major role as contributors to urban photochemical smog (Ras et al., 2009), and are carcinogenic (Låg et al., 2009). As a result, HCHO and CH_3CHO are concerned in China due to environmental and human health impacts. Detailed studies from three main cities (Beijing, Shanghai and Guangzhou) are outlined below.

2.3.3.1 Beijing

Beijing, the capital city of China, has a large population and has experienced a dramatic increase in the number of vehicles (Li et al., 2010; Wang et al., 2006). Recently, Beijing has suffered severe air pollution problems and haze days have become more frequent (Duan et al., 2012). Previous studies (Li et al., 2010; Sun et al., 2006) found that volatile organic compounds (VOCs) including carbonyls were frequently present in the ambient air of with higher atmospheric concentration of carbonyls being observed on haze days than on normal days (Lü et al., 2009).

A recent study (Duan et al., 2012) has been conducted during haze days in Beijing. The sampling site was located on the Tsinghua University campus, which is surrounding by several institutes, a residential area, and two roads, and the area has no industrial zones. The samples were collected by DNPH-coated cartridges in August 2006. The meteorological data was measured as mean values of visibility, wind speed, relative humidity, and temperature, at 4.6 km, 2.2 m/s, 83.4%, and 27.3°C, respectively (Duan et al., 2012). The results (Duan et al., 2012) showed that formaldehyde was the most abundant component of all samples, with ratios of 26.3-53.6% of total carbonyls. The ambient formaldehyde ranged from 10.39 to 62.34 ppb (converted to ppb unit), with an average of 28.98±11.98 ppb. The acetaldehyde values ranged from 3.46 to 29.54 ppb (a conversion factor of 1.8), with an average value of 8.69 ± 6.87 ppb. The formaldehyde/acetaldehyde (C_1/C_2) ratio is usually

used as an indicator of biogenic sources of formaldehyde (Feng et al., 2005; Grosjean, 1992). The C_1/C_2 ratio varies from 1 to 2 in urban areas and is approximately 10 in forested areas. The acetaldehyde/propionaldehyde (C_2/C_3) ratio is normally used as indicator of anthropogenic origin for ambient carbonyls as propionaldehyde is believed to correspond to anthropogenic emission (Feng et al., 2005). The ratio is often higher in rural areas and lower in polluted urban environment (Duan et al., 2012; Feng et al., 2005). Duan et al., study showed that the average C_1/C_2 ratio in Beijing was 2.69, while the average C_2/C_3 value was 6.29. These two values indicate that anthropogenic emissions have a significant influence on ambient formaldehyde levels (Duan et al., 2012). Considering the diurnal variations of carbonyls and ozone together, ambient carbonyls during haze days in Beijing are dominantly contributed by photochemical formation (Duan et al., 2012).

A previous study (Pang and Mu, 2006) has reported a seasonal measurements in Beijing from November 2004 to October 2005 comparing pollutant concentrations at different sites and seasons. The sampling sites included an urban site, a botanical park, a commercial site, a transport hub site, and a rural site. The samples were collected by DNPH-coated cartridges at a flow rate of 1 L/min. The urban site environment was similar to the sampling site in Tsinghua University. The results (Pang and Mu, 2006) showed that the average value of formaldehyde and acetaldehyde in the urban site during the June-August 2005 sampling period were 19.5 ± 8.9 $\mu g/m^3$ (equal to 15.85 ± 7.24 ppb) and 7.83 ± 4.11 ppb, respectively. The winter mean values of formaldehyde and acetaldehyde at the same site were observed at 3.41 ± 2.28 ppb and 4.22 ± 2.94ppb, respectively. Interestingly, the acetaldehyde value was higher than the formaldehyde during the winter. Formaldehyde degradation in the atmosphere was likely to be stronger than its formation. Comparing the different sites during the same season (spring), the highest mean values of formaldehyde and acetaldehyde were both detected at the transport hub site, with values of 24.15 ± 7.80 ppb and 11.56 ± 4.72 ppb, which were nearly double those detected at the other urban sites. Vehicle exhaust emissions are likely to be the main sources of these pollutants at the transport hub site. The lowest mean value of formaldehyde and acetaldehyde were both observed at the botanical park site, with values of 3.58 ± 1.14 ppb and 2.28 ± 1.17 ppb, respectively (Pang and Mu, 2006). Natural emissions could be the main source in botanical park as the site is 30km away from Beijing's urban area (Pang and Mu, 2006).

2.3.3.2 Shanghai

Shanghai is the largest industrial city in the Yangtze River Delta and the economic centre of China (Huang et al., 2008). An investigation of ambient carbonyls (Huang et al., 2008) was conducted from 25 to 28 January, and 27 -- 31 March (high air pollution days), and during 10 -- 15 May, 25 -- 30 July, and 10 -- 16 October in 2007. DNPH coated cartridges were employed to collect samples at a flow rate of 1 L/min during the daytime and 0.2-0.3 L/min at night. The results showed that the highest mean values of formaldehyde and acetaldehyde were both found in summer, with levels of 25.91 ± 5.96 ppb and 17.18 ± 10.69 ppb, respectively. The lowest values of formaldehyde and acetaldehyde were observed in autumn, with levels of 5.54 ± 1.46 ppb and 4.58 ± 1.04 ppb, respectively. High mean values of formaldehyde and acetaldehyde (23.96 ± 7.41 ppb and 10.56 ± 3.24 ppb, respectively) were found on the high air pollution days, but these were still lower than the values detected in summer (Huang et al., 2008). The daily peak of formaldehyde occurred in the early morning or early afternoon. This diurnal profile is similar to that observed in other cities (Zheng et al., 2013). Primary sources are an important local source, but secondary sources form a large proportion of these in summer (Huang et al., 2008). The high concentrations on high air pollution days could be caused by long range transport sources (Huang et al., 2008).

2.3.3.3 Guangzhou

Guangzhou study site was in Guangzhou Institute of Geochemistry, Chinese Academy of Sciences with two residential areas and an expressway nearby (Lü et al., 2009). The study collected samples on clear days (17 -- 19 November, 2005) and haze days (30 November -- 2 December, 2005). During the clear days, visibility was 20-23 km, the temperature was between 16.5 and 29.5 ˚C, visibility, temperature, on haze days were 1.5-3 km, 20-31 ˚C, respectively (Lü et al., 2009). The concentration of formaldehyde ranged from 3.75 to 5.99 ppb, with a mean value of 4.89 ppb on the clear days. The value on the haze days was observed in a range of 5.07 to 20.08 ppb with a mean value of 11.87 ppb (Lü et al., 2009). Acetaldehyde was also measured in this study. The concentration range of acetaldehyde on clear days ranged from 2.67 to 5.83 ppb, with a mean value of 4.09 ppb. On haze days, the acetaldehyde values were higher than those on clear days, with a range of 5.14 to 13.1 ppb and a mean value of 9.22 ppb. These results were both lower than those in previous study (Feng et al., 2005) which was measured during June to September 2003. That study (Feng et

al., 2005) measured carbonyls at seven different sites: a bus station, a restaurant area, a small downtown, an industrial area, a botanical garden, a semi-rural site, and a residential area. The results showed that the bus station and restaurant areas had the top two highest concentrations of formaldehyde with 54.45 ± 12.11 ppb and 54.39 ± 16.26 ppb, respectively. Acetaldehyde values were recorded at 12.86 ± 1.88 ppb at the bus station, and 47.32 ± 10.77 ppb in the restaurant areas. The average value of formaldehyde and acetaldehyde in Guangzhou were 11.12 ppb and 4.63 ppb, respectively.

2.3.3.4 Other cities in China

Atmospheric concentrations of carbonyls have been measured in many cities in China. For Example, observations in Xi'an in July-August 2004 showed a level of 8.05 ppb (Wang et al., 2007). Measurement conducted in March--April 2006 in Hangzhou showed a level of 18.05 ppb in public places (Weng et al., 2009), while a recent study in Guiyang (December, 2008--August, 2009) showed a lower value (3.9 ppb) of formaldehyde (Pang and Lee, 2010).

2.3.4 Australia

CSIRO conducted a Clean Air Research Program project in Sydney, the largest city in Australia. This study (Galbally et al., 2008) employed active sampling and PTR-MS instrument for sampling in two suburban Bringelly (a semi-rural area) and Randwick (a residential area). During the sampling periods (18 January to 27 February, 2007 in Bringelly and 28 February to 19 March, 2007 in Randwick), the concentrations of formaldehyde ranged from 0.52 to 4.28 ppb with a mean value of 2.11 ppb in Bringelly and a range of 0.04 to 4.24 ppb with a mean value of 1.22 ppb in Randwick. The acetaldehyde concentration ranged from 0.05 to 0.88 ppb with a mean value of 0.30 ppb were recorded in Bringelly, and a range of 0.04 to 0.27 ppb with a mean value of 0.09 ppb was recorded in Randwick.

2.3.5. Italy

A study (Possanzini et al., 2002) in Rome, the capital of Italy, investigated four years of observational data from 1994 to 1997. The study considered seasonal profiles based on winter and summer samplings, with the samples collected using DNPH cartridges. The results showed hourly concentrations of formaldehyde were in a range of 8 to 28 ppb in summer and 7 to 17 ppb in winter (Possanzini et al., 2002). Acetaldehyde values in summer ranged from 3 to 18 ppb, while these values were 2-7 ppb in winter. There was no obvious

difference between sources from primary emissions or from photochemical formation in winter (Possanzini et al., 2002). This study also showed that secondary sources contribute up to 30 – 35 per cent of formaldehyde and acetaldehyde emission in winter and 80-90 per cent in summer in urban area (Possanzini et al., 2002). In addition, formaldehyde and acetaldehyde are significant sources of free radicals, such as OH radicals (Possanzini et al., 2002). The rate of OH production was calculated as, between one and two orders of magnitude higher than that of ozone and acetaldehyde (Possanzini et al., 2002).

2.3.6. Brazil

2.3.6.1 Rio de Janeiro

The state environmental agency conducted air quality monitoring in downtown Rio de Janeiro the second largest city in Brazil, which has a population of about 11 million and approximately 1.2 million vehicles (Grosjean et al., 2002). The study collected samples from May to November 2000, including the winter season during June to September. The samples were collected over three hours using DNPH cartridges. Average concentrations of 8.78 ± 3.33 ppb were observed for formaldehyde with a peak value of 28.14 ppb reached at 9:55 am to 12: 05 pm interval on 3 May (Grosjean et al., 2002). The average acetaldehyde value was 5.78 ± 2.56 ppb. Extensive use of ethanol fuels in Brazil may increase primary formaldehyde and acetaldehyde. The results also showed that 43 per cent ozone formation was dominated by formaldehyde. In this study, no clear seasonal variation was seen which was likely to be due to the low sampling frequency (Grosjean et al., 2002).

2.3.6.2 Niteroi

The Niteroi sampling site was located in a commercial-residential area near Niteroi City (Ochs et al., 2011). Sampling was conducted from 9th -- 14th January, 2010 using DNPH cartridges at a flow rate of 0.5 L/min flow rate. A mean value of 2.62 ppb and a range of 0.23 to 7.19 ppb were observed for formaldehyde during the study period, while acetaldehyde concentrations ranged from 1.61 to 7.36 ppb, with mean value of 3.63 ppb (Ochs et al., 2011). These values were lower than those observed in the Rio de Janeiro study (Grosjean et al., 2002). School holiday and summer vacations were likely to reduce traffic in the city and

result in the low concentrations (Ochs et al., 2011). The observation that the acetaldehyde value was higher than those of formaldehyde showed that the main emission source was local traffic (Ochs et al., 2011). The high acetaldehyde value was caused by the increased use of ethanol as vehicular fuel (Martins et al., 2008).

The summary is listed in Table 2-3 includes the data from above discussion as well as other data not described in detail.

Table 2-3: Summary of existing atmospheric concentrations of formaldehyde in different cities worldwide

Location (ambient air)	Concentration (ppb)		Comment	References
New York City, USA	0.4-7.5	Range	15 July-3 August,2009	(Lin et al., 2012)
	2.2±1.1	Median	15 July-3 August,2009	(Lin et al., 2012)
Houston, USA	47	Maxima	August-September, 2000	(Dasgupta et al., 2005)
	3.3	Mean	August-September, 2000	(Dasgupta et al., 2005)
	30	Maxima	20 July-25 Sept. 2002	(Chen et al., 2004)
Nashville, USA	1.43-12.67	Range	26 June-07 July, 1999	(Dasgupta et al., 2005)
	4.78	Median	26 June-07 July, 1999	
Atlanta, USA	0.42-18.25	Range	03-31 August, 1999	(Dasgupta et al., 2005)
	7.82	Median	03-31 August, 1999	
Philadelphia, USA	0.33-9.53	Range	27 June-31 July, 2001	(Dasgupta et al., 2005)
	2.89	Median	27 June-31 July, 2001	
Tampa, USA	0.37-9.38	Range	25 April-01 June, 2002	(Dasgupta et al., 2005)
	2.32	Median	25 April-01 June, 2002	
Tijuana, Mexico	1-13.7	Range	15 May-30 June, 2010	(Zheng et al., 2013)
Mexico City, Mexico	3-27	Range	April-May, 2003	(Grutter et al., 2005)
	35	Maxima	2003, Monthly	(Volkamer et al., 2005)
	17	Maxima	Daily, 2003	(Molina et al., 2007)
Beijing, China	10.39-62.34	Range	August, 2006	(Duan et al., 2012)
	28.98±11.98	Average		
	15.85±7.24	Average	Urban Site, Aug.-Oct., 2005	(Pang and Mu, 2006)
	3.41±2.28	Average	Urban site, Nov.04-Jan. 05	
	24.15±7.80	Average	Transport site, Spring 2005	
	3.58±1.14	Average	Botanical park, Spring 2005	
Shanghai, China	9.9-40.4	Range	Mar. 2007, high air pollution	(Huang et al., 2008)
	23.96±7.41	Mean		
	25.91±5.93	Mean	Summer, 2007	
Guangzhou, China	3.75-5.99	Range	17-19 Nov. 2005, Clear days	(Lü et al., 2010)

	4.89	Mean		
	2.07-20.08	Range	30 Nov-2 Dec.2005, haze days	(Lü et al., 2010)
	11.87	Mean		
	54.45±12.11	Maxima	July-September, 2003	(Feng et al., 2005)
	11.22	Average		
Xi'an, China	8.05	Average	July-August, 2004	(Wang et al., 2007)
Hangzhou, China	18.05	Average	March-April, 2006	(Weng et al., 2009)
Guiyang, China	3.9	Average	Dec. 2008-Aug. 2009	(Pang and Lee, 2010)
Sydney, Australia	0.52-4.28	Range	18 Jan.-27 Feb.2007, Bringelly	(Galbally et al., 2008)
	0.04-4.24	Range	28 Feb-19 Mar2007,Randwick	

Table 2-4: Summary of existing atmospheric concentration value of acetaldehyde in cities worldwide

Location (ambient air)	Concentration (ppb)		Comment	References
Houston, USA	6.7	Maxima	18-19th March, 1984	(Salas and Singh, 1986)
	2.2 ± 1.7	Mean	18-19th March, 1984	
Pittsburgh, PA	2.6	Maxima	15-16th April, 1981	(Salas and Singh, 1986)
	1.4 ± 0.8	Mean	15-16th April, 1981	
Chicago, IL	3.5	Maxima	27-28th April, 1981	(Salas and Singh, 1986)
	2.1 ± 0.9	Mean	27-28th April, 1981	
Downey, CA	28.4	Maxima	28 Feb-1 Mar, 1984	(Salas and Singh, 1986)
	8.5 ± 6.3	Mean	28 Feb-1 Mar, 1984	
Denver, CO	2.1	Maxima	2nd - 4th April, 1984	(Salas and Singh, 1986)
	1.0 ± 0.5	Mean	2nd - 4th April, 1984	
Mexico City	2 - 66.7	Range	March – May, 1993	(Baez et al., 1995)
	15.9	Mean	March – May, 1993	
Beijing	3.46 – 29.54	Range	August, 2006	(Duan et al., 2012)
	8.69 ± 6.87	Mean	August, 2006	
	7.83 ± 4.11	Mean	June-August, 2005	(Pang and Mu, 2006)
	4.22 ± 2.94	Mean	Nov. 2004– Jan, 2005	
Shanghai	17.18 ± 10.69	Mean	Summer, 2007	(Huang et al., 2008)
Guangzhou	2.67 – 5.83	Range	Clear days, 17-19th Nov, 2005	(Lü et al., 2009)
	4.09	Mean	Clear days, 17-19th Nov, 2005	
	5.14 – 13.1	Range	Haze days, 30 Nov-2 Dec, 2005	
	9.22	Mean	Haze days, 30 Nov-2 Dec, 2005	
Sydney, Australia	0.05 – 0.88	Range	18th Jan to 27th Feb, 2007	(Galbally et al., 2008)
	0.30	Mean	18th Jan to 27th Feb, 2007	
	0.04 – 0.27	Range	28th Feb to 19th March, 2007	
	0.09	Mean	28th Feb to 19th March, 2007	
Rome, Italy	3 - 18	Range	Summer season, 1994-1997	(Possanzini et al., 2002)
	2 - 7	Range	Winter season, 1994-1997	

Rio de Janeiro, Brazil	5.78 ± 2.56	Mean	May to November, 2000	(Grosjean et al., 2002)
Niteroi, Brazil	1.61 – 7.36	Range	9th to 14th January, 2010	(Ochs et al., 2011)
	3.63	Mean	9th to 14th January, 2010	

2.4 Atmospheric ammonia

As the most abundant alkaline compound in the atmosphere, ammonia (NH_3) plays an important role in atmospheric chemical process (Pinder et al., 2011; Seinfeld and Pandis, 1998). Atmospheric ammonia arises from natural and anthropogenic sources. Anthropogenic emission contributes a significant fraction to atmospheric ammonia levels (Gong et al., 2013). The US EPA has performed source category analysis for US states. The data for Harris County, Texas are shown in Figure 2-3. The main emission sources were from vehicles, industrial operations, and livestock. In Texas, the annual emission of ammonia was about 10.2 million pounds (about 4.63 million kilograms) in 2008 (Gong et al., 2013). In the UK, the annual emission of NH_3 was estimated at 366Gg per year (Blackall et al., 2008). The emitted gas phase NH_3 in the atmosphere contributes to formation of particulate matter (PM) and mass concentration by forming ammonium salts (Gong et al., 2013). Recent studies (Qiu et al., 2011; Zheng et al., 2015) have found that amines that have a stronger nucleation ability than ammonia can react with particulate ammonium salts to form stable aminium salts, which can increase aerosol particles under certain humidity conditions. Meanwhile, the reaction can also release ammonia (Zheng et al., 2015). Atmospheric NH_3 is not only an important component of the nitrogen cycle to cause potential eutrophication and acidification (Blackall et al., 2008; Ferm and Hellsten, 2012), but NH_3 also has potential health impacts as it is corrosive to the skin, eyes, and lungs (Wilson and Serre, 2007b; Yamada et al., 2012). However, NH_3 currently is not under the regulation of the National Ambient Air Quality Standards of the U.S.EPA (Gong et al., 2013), and the spatial and temporal variations in NH_3 still remain unclear due to scarcity of observations of this emission component (Gong et al., 2013).

Past studies (Blackall et al., 2008; Gong et al., 2013; Puchalski et al., 2011; Wilson and Serre, 2007a, b; Yamada et al., 2012; Zbieranowski and Aherne, 2012) mainly used diffusive sampling systems to measure atmospheric ammonia in agriculture areas. The results are shown in Table 2-5. These studies have found that source terms (such as distance to emission source) (Wilson and Serre, 2007a) and weather conditions (such as temperature, wind speed and direction) are the main factors influencing atmospheric ammonia levels (Ferm and Hellsten, 2012; Wilson and Serre, 2007a). Other studies (Hellsten et al., 2007; Yamamoto et al., 1995) have also reported that the atmospheric ammonia level is influenced by temperature and seasonal variations in farming practice. Ferm and Hellsten study found that NH_3 concentration changes as similar as the temperature changes (Ferm and Hellsten, 2012). Zbieranowski & Aherne study (Zbieranowski and Aherne, 2012) have reported that the lowest concentration of ammonia was recorded in winter and the highest value occurred during spring associated with seasonal farming activity.

In New South Wales (NSW) Australia, Manins et al. (1996) have reported ammonia observations in the Upper Hunter Valley using a passive sampling device. The peak concentrations in a range of 8-15 ppb were reported for the observation period from February 1995 to July 1995, while the peak concentrations of 2-4 ppb were observed during the period from August 1996 to February 1996. The annual mean NH_3 concentration was 4.62 ppb. In 2008, the NSW EPA investigated air emission inventory in the Greater Sydney region. The updated inventory provides the latest emission sources for air pollutants. The main ammonia emission source categories are shown in Figure 2-4 based on the 2008 NSW air inventory investigation (NSW EPA, 2012a).

Table 2-5: Ambient ammonia concentration values from existing observations

Location (ambient air)	Concentration (ppb)	Comment	References
Eastern Oklahoma, USA	Mean: 1.8	December 2006 — December 2007	(Sather et al., 2008)
Four Corners Area, USA	Range of Mean values: 0.2-1.5	December 2006— January 2008	(Sather et al., 2008)
Houston, TX, USA	Average: 3.0 ± 2.5	05-09th August, 2008	(Gong et al., 2013)

Location	Value	Period	Reference
North Carolina, USA (High-density industrial hog farm area)	Mean seasonal values: Spring: 10.9 Summer: 16.7 Fall: 10 Winter: 8.1	October 2003 –May 2004 July 2004 – October 2004	(Wilson and Serre, 2007b)
Beijing, China	Mean values: Urban: 18.5 ± 13.8 23.5 ± 18.0 26.9 ± 15.7 Rural: 4.5 ± 4.6 6.6 ± 7.0 7.1 ± 3.5 14.2 ± 10.8	Feb. 2008 – Dec. 2008 Jan. 2009 – Dec. 2009 Jan. 2010 -- Jul. 2010 Jan. 2007 – Dec. 2007 Jan. 2008 – Dec. 2008 Jan. 2009 – Dec. 2009 Jan. 2010 – Dec. 2010	(Meng et al., 2011)
Beijing, China	Range from 10.94 to 54.82 Mean: 26.19 (converted to ppb)	25 November –24 December 2013	(Zhao et al., 2016)
Nanjing, China	Average: 1.7 ± 2.3	Summer 2012	(Zheng et al., 2015)
Ontario, Canada	Annual average: 2.47 (conversion factor of 1.44) Spring: 3.89 Summer: 2.81 Fall: 2.56 Winter: 1.10	April 2010 – March 2011	(Zbieranowski and Aherne, 2013)
Ontario, Canada	Annual average: 0.21 at low agricultural intensity 1.94 at intensive agricultural	August 2007 – December 2010	(Zbieranowski and Aherne, 2012)
Isle of May, Scottish seabird colony, Scotland	Guillemot cliffs: 0.76 to 32.99 with mean of 11.18 Puffin colony: 0.56 to 19.31 with mean of 6.04	April 2000 –November 2001	(Blackall et al., 2008)
Upper Hunter Valley,	8-15 ppb during February	February 1995 –	(Manins et al., 1996)

Australia   1995 to July 1995, and 2-   February 1996

                             4 ppb during August 1995

                             to February 1996

                             Annual average: 4.62 ppb
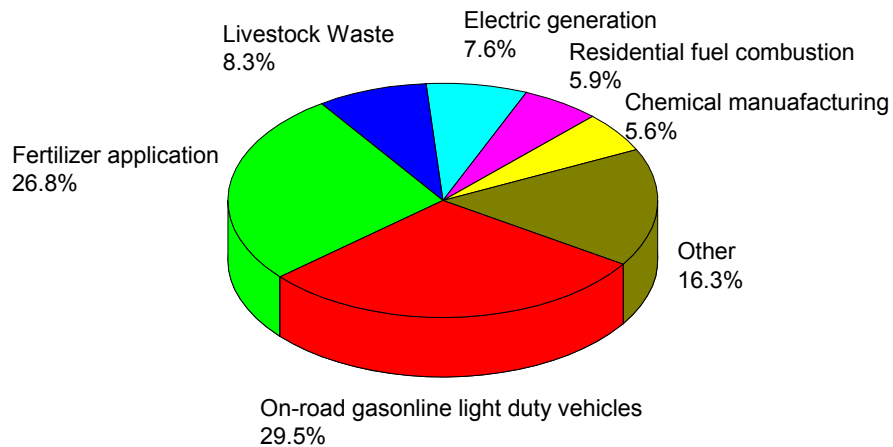
Figure 2-3: Annual NH₃ emissions by source category in Harris County Texas (Gong et al., 2013; U.S.EPA, 2008)
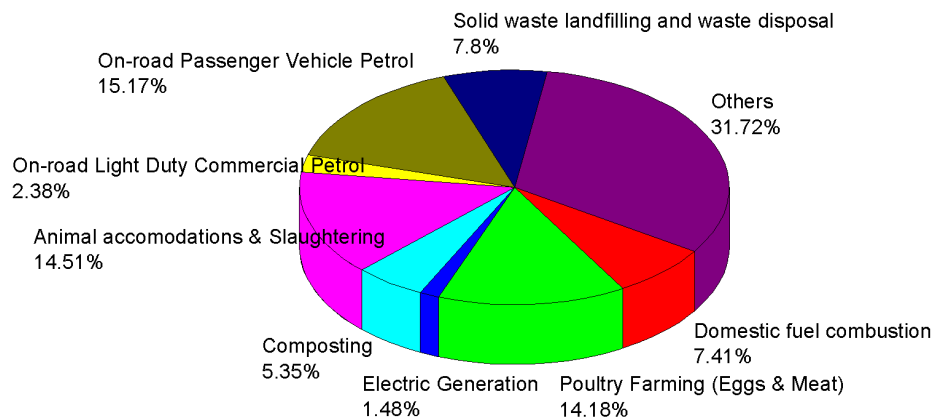
Figure 2-4: annual ammonia emission by source category in the 2008 NSW Greater Metropolitan Region inventory (NSW EPA, 2012b)

2.5 Potential risks

During the capture process, PCC can release chemicals into the environment through lean flue gas, and waste. As stated in previous sections, post-combustion carbon capture technology can emit amines and degradation products into the atmosphere via CO_2 lean flue gas. The emitted chemicals undergo reactions in the atmosphere to form other compounds. These amines and other degradation products can have potential impacts on the environment, and also on human health.

2.5.1 Potential environmental impacts

The main emissions that have been detected from pilot scale post-combustion capture plants are amines, ammonia, formaldehyde, acetaldehyde, acetone, and amides (formamide and acetamide) (Morken et al., 2014; Thong et al., 2012). Trace amounts of certain compounds can also be emitted from the post-combustion capture plants, such as nitrosamines and nitramines. However, these two compounds are most likely below the detection limits of current studies (Morken et al., 2014; Moser et al., 2011). The amines can react with other compounds such as OH radicals, NO_x, and SO_2 to form other degradation products. These chemical compounds can affect the ecosystem after atmospheric transport, deposition and precipitation (Shao and Stangeland, 2009). As there is little available knowledge on the impacts of amines and related products from atmospheric sources, the main toxicity data are from laboratory experiments (Aarrestad and Gjershaug, 2009).

High concentrations of amines have been reported to cause irritation of the skin, eyes, and respiratory tract in animals (Aarrestad and Gjershaug, 2009; Gillner and Loeper, 1993; Shao and Stangeland, 2009). No information is available on the toxicity of amines on terrestrial plants in the literature (Aarrestad and Gjershaug, 2009), but amines as nitrogen-rich compounds may cause eutrophication (Shao and Stangeland, 2009). Eutrophication can increase biomass production and decrease plant biodiversity especially for plant growth in oligotrophic ecosystems (Shao and Stangeland, 2009). In water systems, a previous study (Bieniarz et al., 1996) found that methyldiethanolamine (MDEA) at concentrations above 0.5 mg/L is chronically toxic to fish. MEA is reported to be acutely toxic to fish at concentrations above 60.3 mg/L (Brooks, 2008). Previous studies have found that MEA causes chronic and

acute toxicity in algae at concentration above 0.75 mg/L (Bringmann and Kuhn, 1980) and 6 mg/L (Brooks, 2008), respectively. Based on Norway's PCC plant, an assumed rainfall of 2000 mm, and the lowest MEA impact concentration on algae (0.75 mg/L), the maximum allowable annual amines emission was calculated to be no more than 1,579 tonnes to avoid chronic effects (Karl et al., 2008). This level of emission is unlikely to occur during normal operation of a PCC plant, as the annual emission of amines is estimated to be around 40-160 tonnes (Shao and Stangeland, 2009).

The maximum allowance of amides for chronic toxicity on invertebrates is 1.2 mg/L (Brooks, 2008). The toxicity effect on fish and algae is lower than the effect on invertebrates (Brooks, 2008).

After precipitation into the soil and water systems, ammonia is likely to cause eutrophication effects in the environment (de Koeijer et al., 2013; Shao and Stangeland, 2009). In addition, atmospheric ammonia is known to contribute to the formation of particulate matter, which can cause haze and change visibility (Gong et al., 2013). However, a recent study (Zheng et al., 2015) has reported that amines have a stronger nucleation ability than ammonia and react with particulate ammonium salts to form stable aminium salts, which can increase aerosol particles.

2.5.2 Potential health impacts

As chemical compounds can be emitted into the atmosphere, it is necessary to understand and evaluate the potential health impacts of amine related compounds from post-combustion capture plants.

2.5.2.1 Monoethanolamine (MEA)

The major sites for the metabolism of MEA are the liver, heart and brain (Låg et al., 2009). A previous study (Knaak et al., 1997) reported that the LD_{50} (after which 50% of the tested animals died) in rats was an oral dose vale of 1.1-2.7 g/kg body weight. MEA shows relatively low acute oral toxicity. Weeks et al., study indicated that chronic toxicity of MEA could cause behavioural effects and degenerative changes in different organs, particularly in the liver and kidneys at doses below 1.2 mg/m^3 of MEA after 2--3 weeks exposure (Weeks et al., 1960). Låg et al., study (Låg et al., 2009) reported that MEA and piperazine (PIPA) have

reproductive and developmental toxicity, but none of the amines have been reported to be carcinogenic. It has been suggested that exposure to ambient MEA should not exceed 10 µg/m^3 (Låg et al., 2009).

2.5.2.2 Aldehydes

Aldehydes are known to be genotoxic (Låg et al., 2009) and human carcinogens (Tang et al., 2009; USEPA, 2013). The main aldehydes emitted from post-combustion capture projects are formaldehyde and acetaldehyde. Acetaldehyde has a similar mechanism of carcinogenicity to that of formaldehyde (Låg et al., 2009). The US EPA has conducted an investigation into the carcinogenicity of formaldehyde, and found that the available data is still limited (USEPA, 2015b). Based on the available studies, the US EPA has undertaken quantitative estimation of the carcinogenic risk of inhalation exposure to formaldehyde, and estimated values of 0.08 µg/m^3 and 8 µg/m^3, respectively, corresponding to a 1 in 1,000,000 and 1 in 10,000 risk level (USEPA, 2015b). The inhalation unit risk is estimated to be 1.3×10^{-5} (µg/m^3)$^{-1}$ (USEPA, 2015b). The acetaldehyde cancer risk value is estimated to be 0.5 µg/m^3 at 1 in 1,000,000 (USEPA, 2015a)

2.5.2.3 Nitrosamines

Nitrosamine is the most concerning amine degradation product due to its extremely potent carcinogenicity, based on experimental data (Låg et al., 2009). Most nitrosamines are suspected to be carcinogenic in humans (Karl et al., 2011). Many studies have reported tumours of the nasal cavity and other neoplasms in experimental animals (Låg et al., 2009). The carcinogenicity in humans has also been studied, and previous reports have shown that there is circumstantial evidence that nitrosamines could cause cancer (Olajos and Coulston, 1978; Verna et al., 1996). The Norwegian Institute of Public Health (NIPH) guidelines indicate that a lifetime exposure to nitrosamine corresponding to a 1 in 1,000,000 cancer risk is a concentration of 0.3 ng/m^3 in air and 4 ng/L in water (de Koeijer et al., 2013). The integrated Risk Information System of the US EPA states that concentration values of inhalation exposure to nitrosamines (N-Nitrosodimethylamine) corresponding to 1 in 1,000,000 and 1 in 10,000 risk values are 0.07 ng/m^3 and 7 ng/m^3, respectively (USEPA, 2015c). The inhalation unit risk is 1.4×10^{-2} (µg/m^3)$^{-1}$ (USEPA, 2015c).

2.5.2.4 Nitramines

Nitramines have a longer lifetime in the environment than nitrosamines (de Koeijer et al., 2013). The nitramines biodegrade by 33 % reduction in 28 days compared to a half-life of 15 days for nitrosamines degradation (de Koeijer et al., 2013). This longer lifetime means that nitramines could have a more significant impact than nitrosamines. However, only a few studies are available on the health impacts of nitramines (NIPH, 2015 Access). A previous study (Goodall and Kennedy, 1976) found that tumours were caused predominantly in the liver and kidney of mice and rats after oral exposure through their drinking water. The available studies indicate that compared to the nitrosamines, the nitramines are less potent carcinogens (NIPH, 2015 Access).

Table 2-6: Summary of the concentration values of the main chemicals concerned with inhalation exposure risk at a 1 in 1,000,000 value

Chemicals	Threshold Concentration	US EPA in 10^{-6} risk	NIPH in 10^{-6} risk
MEA	10 µg/m3		
Nitrosamines (NDMA)		0.07 ng/m^3	0.3 ng/m^3
Formaldehyde		0.08 µg/m^3	
Acetaldehyde		0.5 µg/m^3	

2.6 Computer modelling

Air pollution and dispersion model is a useful tool to predict air pollutant concentrations after atmospheric transport and dispersion from emission sources. These models are very important to assist environmental impact assessments for existing industrial updates and new plant development. Various computer models are available to conduct this task, such as The Air Pollution Model (TAPM), and the CALPUFF model. The TAPM model which was developed by Australia CSIRO was selected as an approved method for air pollutant assessment in New South Wales (NSW), Australia (NSWEPA, 2005). The CALPUFF model is a non-steady-state Gaussian puff dispersion model to simulate the effects of meteorological and terrain conditions on air pollutant transport (Scire et al., 2011). The CALPUFF model has been accepted by the US EPA as a guideline model for regulatory application (NSWEPA, 2005). The CALPUFF model was also selected as an approved model for air pollution assessment by the NSW EPA (NSWEPA, 2005). The fundamental concepts for simulating concentration values on a spatial and temporal basis are described below.

@RISK uses Monte-Carlo simulation to calculate risk values several thousand times to obtain risk probabilities. This model is the most widely used tool for risk analysis. @RISK has been

successfully employed in many areas such as finance, insurance, and the environment (Palisade, 2015). The fundamental concepts related to this model are also described below.

2.6.1 TAPM model

The TAPM model includes two main components: a coupled prognostic meteorological component and an air pollution concentration component (Hurley, 2008b). The model can minimise the need for meteorological observations, and provide flows to local-scale air pollution (Hurley, 2008a). The meteorological component uses momentum equations, the incompressible continuity equation, scalar equations, and turbulence kinetic equation to simulate 3-D meteorological conditions. The air pollution component can use the predicted meteorology to accurately model industrial emissions at fine resolution under the Eulerian grid module, the Lagrangian particle module, the plume rise module, and the building wake module (Hurley, 2006, 2008a). The Eulerian Grid Module calculates prognostic equations for the mean and variance of emission concentrations. Near-source dispersion is calculated more accurately by the Lagrangian Particle Module. The plume rise module calculates plume momentum and buoyancy effects for point sources. The Building Wake Module can be used to consider wake effects on meteorology and turbulence (Hurley, 2008a). The only user-supplied data required is emission information (Hurley, 2006). The TAPM model also includes photochemistry reactions based on a generic reaction set, a dust model for particles, and wet and dry deposition effects (Hurley, 2008a).

2.6.2 CALPUFF model

CALPUFF is a non-steady-state Gaussian puff dispersion model (Scire et al., 2011) recommended by the US EPA to simulate 3-D meteorological conditions and air pollutant transport in complex terrain and wind conditions (MacIntosh et al., 2010). There are three main components in the CALPUFF model: CALMET, CALPUFF, and CALPOST. CALMET is the meteorological component to simulate 3-D wind and temperature data for CALPUFF (Scire et al., 2011). The output files from CALMET also include the 2-D mixing height, surface characteristics, and dispersion properties to be used in CALPUFF (Scire et al., 2011). CALPUFF is an atmospheric time-varying source-to-receptor model to advect puffs of air pollutants from sources to the surface (MacIntosh et al., 2010). CALPUFF uses 3-D local meteorological data from CALMET to maximise accurate simulation for pollutant transport (Fowler and Vernon, 2012a). CALPOST is a component to post-process output from CALPUFF. The most

important characteristic is that CALPUFF is an open-source code model, which means that users can easy modify the code to suit their particular needs, such as those for the chemical mechanisms.

2.6.3 The @RISK model

The @RISK model usually works with EXCEL to calculate risk analysis. The calculation process is a method to generate the distribution of possible outcomes by recalculating the worksheet multiple times by randomly selecting different value sets each time (Palisade, 2013). The method involves the computer testing all valid combinations of input variables to generate all possible outcomes (Palisade, 2013). To develop a @RISK model, variables including certain/uncertain or independent/dependent variables must be set up.

2.7 Worldwide regulation and knowledge gaps

2.7.1 Worldwide regulations

Standards and regulations for industrial emissions in the air can be grouped into three categories: emission standards, ambient air quality standards, and occupational exposure limits.

Emission standards are set to regulate the amount of a pollutant that can be emitted from an industrial facility. In the US, the New Source Performance Standard regulates the emission amounts of a range of pollutants such as SO_2, NOx, particulate matter, and various others (IEAGHG, 2012). The National Emission Standards for Hazardous Air Pollutants Compliance Monitoring (NESHAP) sets emission standards for hazardous air pollutants from stationary sources. In the EU, Directive 2001/81/EC is a regulation to address the emission amounts of pollutants that can be emitted in individual countries (IEAGHG, 2012). From the limited existing studies, post-combustion can emit compounds that have been regulated in most countries, but can also emit some new chemicals that are not specifically considered in existing emission standards. The IEAGHG report (IEAGHG, 2012) has stated that general emission level for new chemicals from post-combustion projects "have yet to be established".

Ambient air quality standards are related to the concentration values of a given air pollutant in the ambient air environment. Many countries set air quality standards based on the World Health Organisation's Air Quality Guidelines, which recommend maximum exposure limits for a range of compounds (IEAGHG, 2012). In the EU, Directive 2004/107/EC and Directive 2008/50/EC are the air quality standards for the main air pollutants (IEAGHG, 2012). The US air quality standards are similar to the European limits, but some states have stricter requirements. For example, California has the most rigorous air quality standards in the world (IEAGHG, 2012). Although there are no specific ambient air quality standards related to potential emissions from post-combustion capture projects, some studies have conducted investigations of the toxicity of amines and related products. The US EPA integrated risk information system has set up exposure limit for nitrosamines, and aldehydes on a 1 in 1,000,000 cancer risk basis. In Norway, the NIPH has also examined the toxicity of these products, and has regulated a guideline for lifetime exposure limit of nitrosamines and nitramines corresponding to a 1 in 1,000,000 cancer risk. These values are summarised in Table 2-6.

Occupational exposure limit is workplace standard to manage exposure of workers. Normally, chemical compounds that could cause cancer in human are considered to determine exposure limit (IEAGHG, 2012). In US, The National Institute for Occupational Safety and Health (NIOSH) is the government agent to develop occupational exposure standard.

2.7.2 Knowledge gaps

Amine-based post-combustion carbon capture projects are the most mature technology available to capture carbon dioxide. Studies conducted worldwide have found this technology can emit solvents and degradation products into the atmosphere. The main chemical compounds of these emissions are amines, aldehydes, ammonia, and acetone. The fate of amines and their degradation products in the atmosphere is still under investigation. The possible impacts on the environment and health are not yet fully understood. A survey of the literature on atmospheric emission from post-combustion projects reveals that:

- Few field based studies have been carried out to measure atmospheric aldehydes concentrations in Australia

- Few field based atmospheric dispersion simulations of amines, ammonia, and aldehydes have been performed in Australia

- No analysis of cancer risk probabilities has been carried out to consider emission impacts based on Australian meteorology and terrain conditions

- No detailed regulations specify the allowable emissions from post-combustion carbon capture projects

The project therefore aims to determine atmospheric aldehyde concentration in Australia, and assess the potential cancer risks of the possible emissions from the post-combustion carbon capture project.

Chapter 3 Experimental sampling methodology for aldehydes

Based on the knowledge gaps identified in Chapter 2, this chapter focuses on the measurement of atmospheric aldehydes as risk assessment considerations for the installment of post-combustion carbon capture technology. The chapter begins with a description of the study region where the samplings were performed.
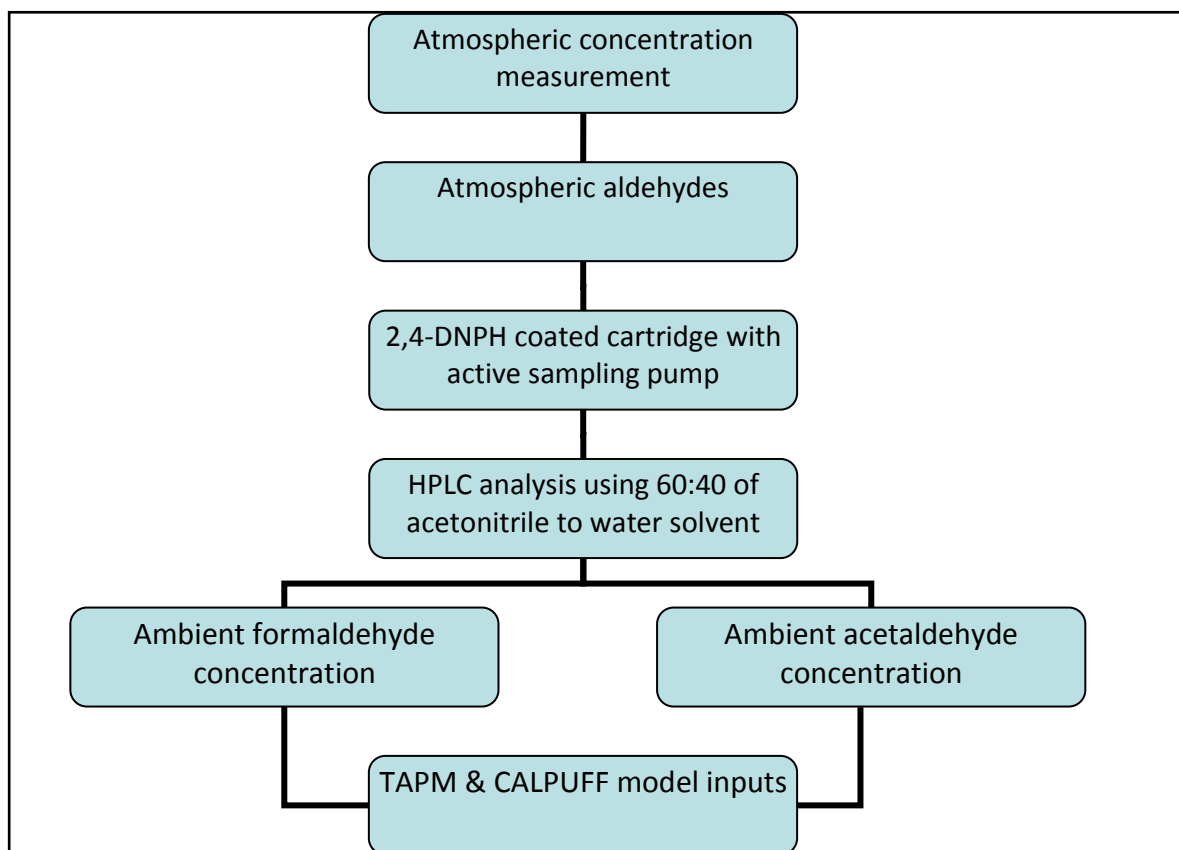
Figure 3-1: Overall experimental framework for ambient aldehydes measurement

Atmospheric formaldehyde and acetaldehyde measurements were performed to quantify the existing gas phase concentration values of these compounds before introducing post-combustion technology. The aldehydes were measured by High Performance Liquid Chromatography (HPLC) system. The results from these measurements were later treated as inputs for modelling simulation. The overall measurement framework is shown in Figure 3-1.

3.1 Study region

New South Wales (NSW) is located on the Eastern coast of Australia. The state is geographically divided into four sections: a narrow coastal strip, the mountainous area of the Great Dividing Range, the agricultural plains, and the western plains (Wikipedia, 2012).

The three main cities of NSW located in the narrow coastal strip including Sydney, Newcastle, Wollongong, Central Coast, and the Hunter region. The state has a climate varying from cool oceanic in the south to humid subtropical in the north (Borweina et al., 2014). With international and domestic migrations, the population in New South Wales has grown fast. In 2011, it reached 7.21 million (NSWEPA, 2012). Two-thirds of the state's population live in the Greater Sydney region (Australian Bureau of Statistics, 2012). Along with this population growth, as well as economic and urban development, air quality has become more of a concern. In general, NSW air quality meets Ambient Air Quality National Environmental Protection Measure (AAQ NEPM) goals for carbon monoxide, nitrogen dioxide, sulfur dioxide and lead, but Ozone and particles levels still exceed the goal (NSWEPA, 2012).

Volatile organic compounds (VOCs) are one of the precursors for ozone formation especially in warm sunny conditions (Luecken et al., 2012; NSWEPA, 2012). Aldehydes, the main emission from post-combustion carbon capture projects are one of the VOCs providing a positive contribution to ozone formation. Ammonia as the most abundant emission from post-combustion projects is a contributor to particle formation. Aldehydes and ammonia are therefore selected as the main compounds for the sampling and measurements in this study. The sampling sites selected for the study are located in a Sydney urban site (Macquarie University Campus) and an Upper Hunter industrial area, which are both within the same narrow coastal strip climate zone. Figure 3-2 shows that the historical observation meteorological data over two decades in the two study areas. The Macquarie Park (Willandra Village) station data which was selected to represent the meteorological data for the Macquarie University campus, only covers data from 1971 to 1995. Singleton Army station was selected to represent the Upper Hunter industrial area data from 1969 to 1990, while Singleton STP station data was selected for data from 2002 to 2015 after Singleton Army station closed.

3.1.1 Sydney Metropolitan

Sydney, the capital city of New South Wales, is a coastal basin surrounded by Tasman Sea in the east, the Blue Mountain in the west, the Hawkesbury River in the north, and the Woronora Plateau in the south (Wikipedia, 2014). The population of Sydney is about 4.39 million, based on the 2011 census (Wikipedia, 2015b). Sydney has temperate climate, with rainfall spreading throughout the year, but slightly higher rainfall in the first half of the year

due to the domination eastern wind (Wikipedia, 2014). Figure 3-2 illustrates the monthly average temperatures and rainfall and shows the higher rainfall in the first six months of the year at the Macquarie Park monitoring station.

The NSW Environment Protection Authority (EPA) has reported that ozone level excesses are more frequent in summer than in winter, based on data from 1994 to 2011 (NSWEPA, 2012). These records showed that the ozone level was higher than the 1-hour and 4-hour standards on up to 19 days per year and 21 days per year, respectively (NSWEPA, 2012). A previous study (Galbally et al., 2008) by the Commonwealth Scientific and Industrial Research Organization (CSIRO) has investigation the sources of ozone precursors in Sydney. The study involved measurement and modelling of ozone levels and their precursors in the Sydney urban area. Using advanced monitoring technology including PTR-MS, the study conducted measurements in the summer of 2007 in two Sydney suburbs: Randwick (inner urban) and Bringelly (outer urban). The results have shown that the maximum ozone concentration in Randwick and Bringelly are 51.1 ppb and 78.9 ppb, respectively. Aldehydes as precursors were also measured, and the mean values for formaldehyde were 1.22 ppb in Randwick and 2.11 ppb in Bringelly, while the mean values for acetaldehydes were recorded as 0.09 ppb in Randwick and 0.30 ppb in Bringelly.

3.1.2 Upper Hunter Valley Region

The Upper Hunter Valley region is located approximately 200 km north of Sydney. The main industries in this region are coal mining, electricity generation, viticulture, and horse breeding (Wikipedia, 2015a). This study focuses on two population centres in the Upper Hunter Valley region, Singleton and Muswellbrook. The area is adjacent to the New England Highway, coal mining sites, and the Bayswater power station. The climate of the Upper Hunter Valley is characterised by hot summer days and dry winters. The rainfall is predominantly in summer, but heavy isolated rains have been recorded in winter (Muswellbrook Shire Council, 2015). Air quality issues in the area are a concern for the local community, especially particulate emissions from coal mining and other air pollutants from the power station.

CSIRO has conducted a particle study (Hibberd et al., 2013) in the area, and has reported that the 15-day running average $PM_{2.5}$ values showed a seasonal trend of higher

concentrations in the cooler months of May to October, with a maximum of around 17.5 µg/m³ in Muswellbrook and 12.5 µg/m³ in Singleton. Ambient ammonia concentrations have rarely been studied in NSW, although a few studies have investigated the Hunter region. One previous study (Todoroski and Kjellberg, 2013) measured ambient ammonia levels in the Lower Hunter at Fullerton Street in Stockton, NSW in May, 2013. This study reported that the ambient ammonia level was far below the air quality impact criteria level of 0.46 ppm, and showed that ammonia values above 0.1 ppm were associated with winds from west and west-northwest (Todoroski and Kjellberg, 2013). Manins et al. (1996) have reported ammonia observations in the Upper Hunter Valley using a passive sampling device. The annual mean NH3 concentration was 4.62 ppb.
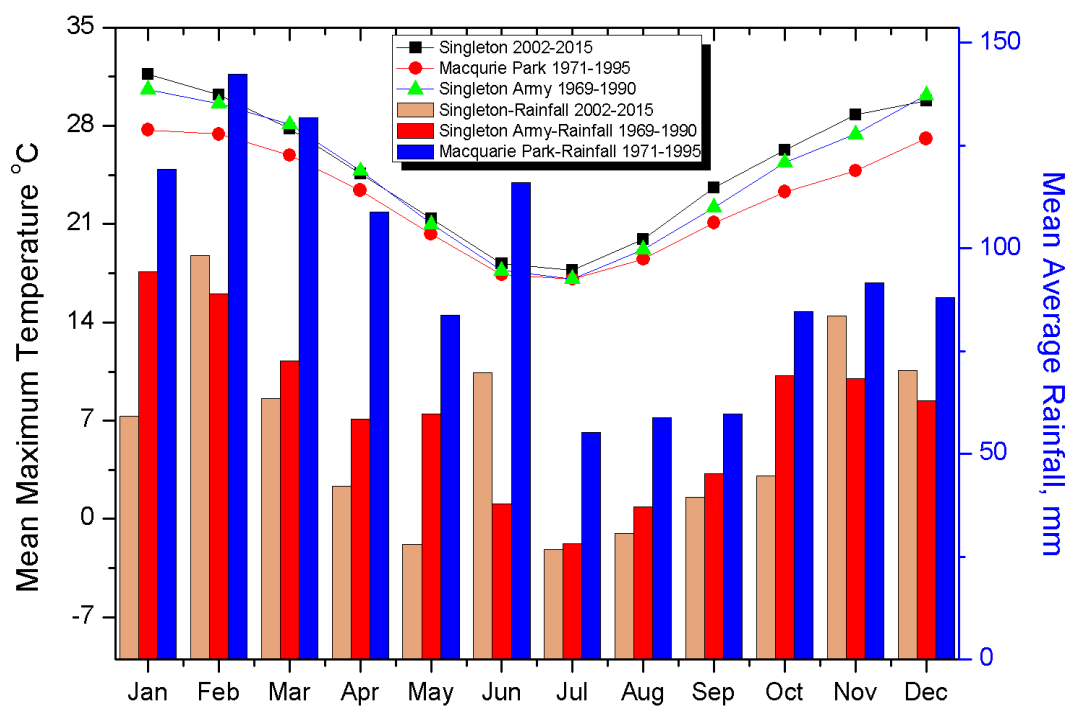
Figure 3-2 Monthly average rainfall and maximum temperatures in the two regions of NSW based on observation data from the Bureau of Meteorology (BoM)
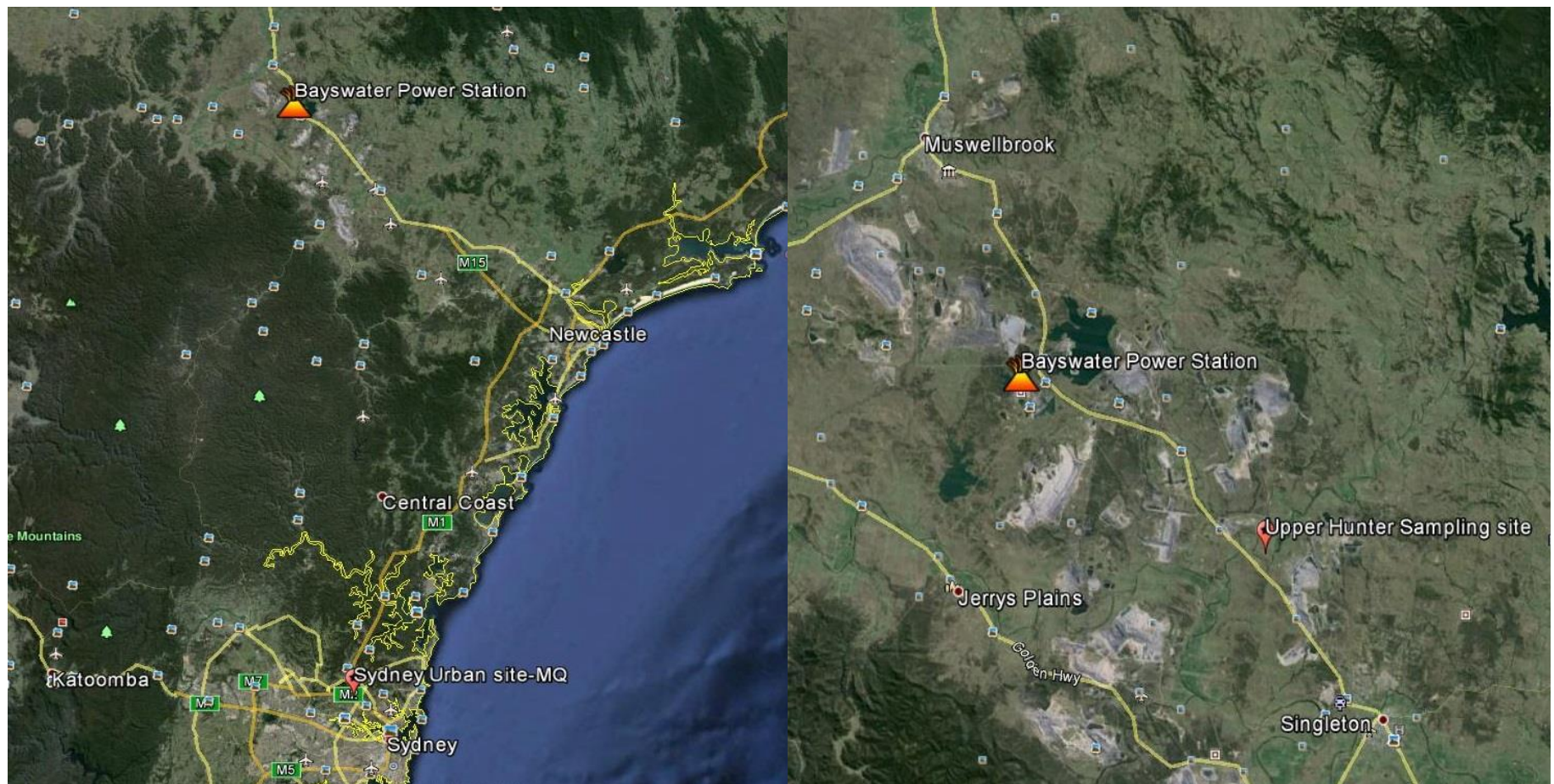
Figure 3-3: Left: Two sampling sites in the NSW region. Right: Near-field study site with an Upper Hunter sampling site

3.2 Sampling sites

3.2.1 The urban site—Macquarie University

The urban site was selected in Macquarie University North Ryde campus which is adjacent to one of major hi-tech business parks. Many international hi-tech corporations have established regional headquarters in the area. The campus is located at a 150 km straight-line distance south-east of the Bayswater Power Station (see Figure 3-3 Left), and is surrounded by a motorway on north-east side of the campus and a 4-lane major road on the south-west side. A national park is near the campus.

The air sampling was carried out in the south-east section of the campus on the roof of a four-floor building. The urban site sampling was conducted in both winter and summer. A few short-time samplings were performed in late autumn and late spring.

3.2.2 The Hunter Valley site

A private property near Glennies Creek in Singleton was selected as the Upper Hunter Valley sampling site. The site is surrounded by several open-cut mining sites and is about 17 km straight-line distance away from the Bayswater power station (see Figure 3-3 right panel). The area is sparsely populated. A five-day summer season sampling was conducted on 17-22 January, 2015. The weather on the sampling days was showery and windy.

3.3 Field sampling

3.3.1 Sampling schedule

Fieldwork components preparation was initially undertaken at the Macquarie University campus site, which helped to develop the experience to an enable efficient sampling process at the Upper Hunter Valley site. The scheduled field activities were mainly undertaken over a short period in 2013, during the winter and summer of 2014 and the summer season of 2015. The detailed sampling activities are listed in Table 3-1 below.

Table 3-1 The schedule of field sampling undertaken during the study

Sampling Activities	Urban Site—Macquarie University North Ryde campus	Upper Hunter Site— Glennies Creek
24-hour sampling, summer	6 January - 5 February, 2015	17-22 February, 2015
24-hour sampling, late autumn	29-31 May, 2013	N/A
24-hour sampling, late spring	7-14 November, 2013	N/A
24-hour sampling, winter	8 August - 8 September, 2014	13-14 August, 2013

3.3.2 Sampling protocols

3.3.2.1 Aldehydes sampling (TO-11A)

Numerous methods have been developed for the sampling and analysis of aldehydes. Passive sampling devices have been designed to assess inhalation exposure to formaldehyde in industrial workers. These devices have a limited flow rate, resulting in a requirement for long exposures times. As aldehydes concentrations remain at low levels in the atmosphere, these passive devices have limitations on ambient aldehydes sampling. The US EPA has developed an active sampling methodology for the determination of formaldehyde in the ambient environment, namely the TO-11A method. This method employs wet chemistry and a solid adsorbent with a chemical (2,4-Dinitrophenylhydrazine; DNPH) that reacts with carbonyl compounds in order to sample a greater amount air for better sensitivity (William et al., 1999).   The chemical reaction shown in Equation (3.1) which shows that aldehydes reacts with DNPH to form a stable colour hydrazine derivative, is the basic principle for this method.

$$R-\overset{\overset{\displaystyle O}{\|}}{C}-H+H_2N-NH-\overset{\overset{\displaystyle NO_2}{|}}{CH_3}-NO_2 \xrightarrow{H+} \overset{\overset{\displaystyle R^1}{|}}{C}=N-NH-CH_3-NO_2+H_2O \quad (3.1)$$

$$Aldehydes \qquad (DNPH) \qquad \qquad \overset{|}{R}$$
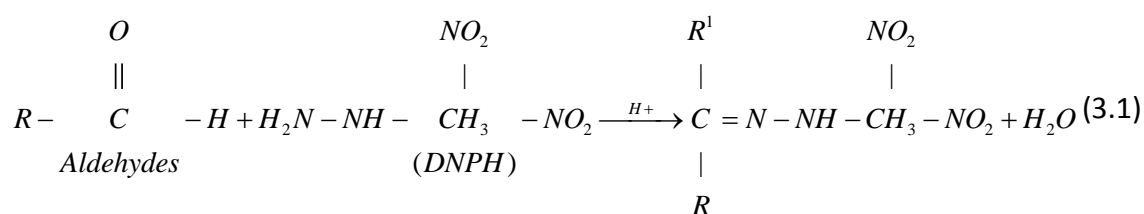
3.3.2.1.1 Sampling requirements

As formaldehyde can be emitted from materials like rubber at high temperatures, the sampling system uses Teflon or silica materials as tubing, caps, and connectors to avoid potential contamination. The sample cartridges must be stored in a refrigerator or freezer (below 4°C) during storage and transportation to remain stable. During the sampling process, the cartridges must be covered with aluminum paper to prevent sunlight induced

artifacts. In the sampling system, an ozone scrubber must be placed in the front of the DNPH-coated sampling cartridge to avoid ozone interference. Normally, the ozone scrubber has an effective capacity of up to 80 hours without breakthrough at ozone levels of about 700ppb (William et al., 1999).

3.3.2.1.2 Sampling calibration

The sampling system, and particularly the flow rate of the sampling pump must be calibrated before and after sampling. Normally, a flow rate of 1-2 L/min is employed to allow enough air through the DNPH-coated cartridge to form stable hydrazine derivatives for further analysis. A soap bubble flow meter was employed to calibrate the flow rate and ensure it was within the required range. Given that the flow rate may change during the sampling procedure, a calibrated dry gas meter was placed between the sampling cartridge and the sampling pump to record the total volume of air taken into the sampling cartridge.

3.4 Measurement of aldehydes

As discussed briefly above, the sampling and analysis of formaldehyde was conducted by standardized sampling and analytic procedures based on the US EPA TO-11A method. The air samples were analysed using an HPLC system. The detailed sampling and analytical procedures are described below.

3.4.1 Sampling device and system

Air sampling was conducted using a sampling train consisting of an active sampling device from SKC Universal Sample Pump (Model 224-PCXR7), a flow controller and a dry gas meter (Shinagawa DC-1 model). This configuration allowed for the accurate determination of the total volume sampled. The entire gas flow lines were constructed of Teflon PTFE tubing (1/8 in I.D.) and silica tubing (6mm I.D). An ozone scrubber was placed before the sampling cartridge to reduce ozone interference. Both the ozone scrubber and 2, 4-dinitrophenylhydrazine (2, 4-DNPH) coated LpDNPH cartridges were purchased from Sigma-Aldrich Australia. Air samplings were made over 24 hours and for continuous periods. These sampling activities were conducted to determine existing ambient aldehydes before installing a post-combustion carbon capture facility to the current coal-fired power station. As seasonal differences in ambient aldehydes concentrations are known, two one-month air sampling campaigns were conducted in winter season of year 2014, and summer season of

year 2015 at the Macquarie University campus site. A five-day summer sampling campaign was undertaken at the Upper Hunter site.
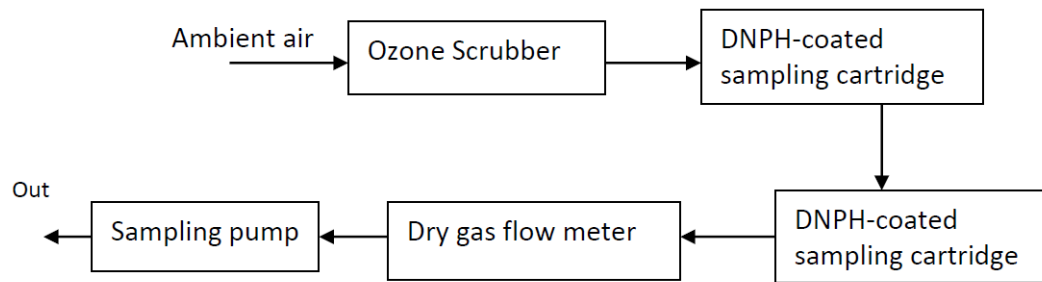
Figure 3-4 Sampling system flow chart

Figure 3-5 Air Sampler at Sydney urban site (MQ)

Figure 3-5 were operated at the Macquarie University site (MQ) and the Upper Hunter site to prevent system failure. A second cartridge was placed after the sampling cartridge in case of breakthroughs in the first cartridge. All cartridges were sealed in individual aluminum zipper bags before and after sampling, and these were stored in refrigeration prior to further analysis.

3.4.2 Description of HPLC system

A Shimadzu HPLC system was employed to analyse the air samples. The HPLC system comprised several components, including a system controller (SCL-10A), an auto injector (SIL-10AD), a liquid chromatograph (LC-10AD), an auto degasser (DGU-12A), and a diode array detector (SPD-M10A). The HPLC column was a 4.6 mm internal diameter x 25cm Supelcosil™ LC-18 5μm column purchased from Sigma-Aldrich. To protect the column, a Supelguard™ guard column was placed in front of the HPLC column, see Figure 3-6.
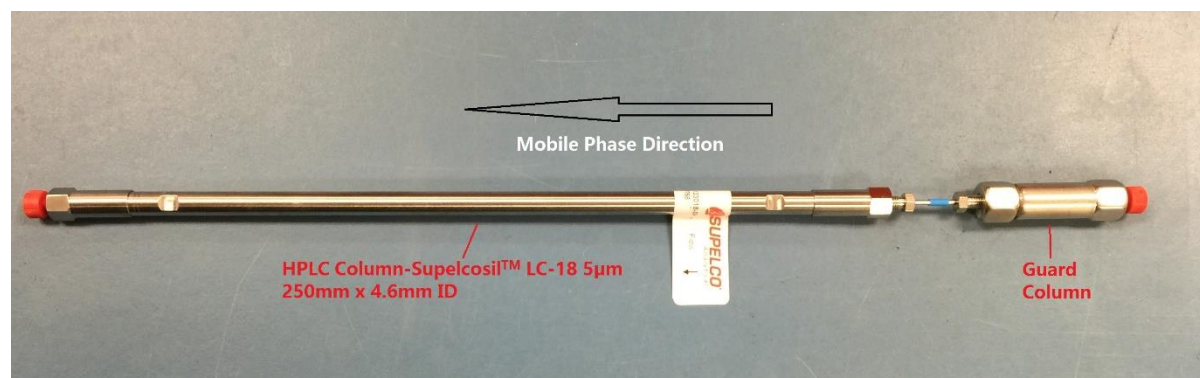
Figure 3-6: HPLC column & Guard column

3.4.3 Analysis process

Before the HPLC analysis, the samples were eluted from DNPH-coated sampling cartridges with 10ml acetonitrile. Diluted samples were pipetted into HPLC vials with TFE-fluorocarbon-lined septa. In HPLC analysis, baseline checks were conducted before injection of the sample. During sample analysis process, a 25 μL sample was injected into the system using an auto sampler. The injected samples were separated and detected at a UV wavelength of 360 nm. The pump flow rate was set at 1.0 mL/min and the analysis cycle was 25 minutes for each sample. Each sample was analysed three times to obtain an average HPLC peak area.

3.4.4 Calibration standard preparation of aldehydes-DNPH mix

Calibration standards were prepared in acetonitrile from a commercial DNPH-aldehydes liquid standard purchased from Sigma-Aldrich. The liquid standard is TO11/IP-6A Aldehyde/Ketone-DNPH mix (Catalog No. 47285-U) containing 15 components including formaldehyde, acetaldehyde, acrolein, acetone, propionaldehyde, and others with each component at a concentration value of 15 μg/mL. Each ampule of the standard contains 1mL of the mixed standard. In the calibration standard preparation, two ampules of the liquid

standard were diluted with acetonitrile to 10mL in a volumetric flask to obtain a concentration of 3,000 ng/mL. The diluted standard was further diluted into different concentrations for the HPLC analysis. In the working standard, there were 6 levels concentration values: 3000, 1500, 1200, 750, 300, and 150 ng/mL. Each standard was analysed three times to obtain an average HPLC peak area for HPLC calibration. The detection limit of formaldehyde in acetonitrile solvent was 60.7 ng/mL. The concentrations of all working standards and samples were far higher than the detection limit.

Chapter 4 Existing atmospheric aldehyde concentration values in the greater Sydney urban area

In order to assess the impact of PCC emission of aldehydes on human health risk, it is necessary to determine background aldehyde concentrations in the absence of PCC. This chapter presents the results of measurement of atmospheric concentration of aldehydes at both the Macquarie University site and the Upper Hunter site. As aldehydes in the atmosphere are impacted by many factors, the chapter also provides data on the daily variations of aldehyde concentrations and considers the relationship between aldehyde levels and the photochemical oxidation of hydrocarbons and meteorological conditions. At the end of this chapter, the ratio of formaldehyde and acetaldehyde is discussed to evaluate the sources of atmospheric carbonyls.

4.1 Aldehyde concentrations at an urban site—the Macquarie University campus

In this study, the main aldehydes, formaldehyde and acetaldehyde were measured in both summer and winter seasons. 24-hour measurements of aldehyde concentrations conducted between August 2014 and February 2015 are summarised in Table 4-1 and Table 4-2. The concentration of formaldehyde ranged from 0.45 to 3.19 ppb and 0.12 to 1.35 ppb in summer and in winter, respectively. The average formaldehyde value was 1.07 ppb with a standard deviation of 0.69 ppb in summer, and 0.48 ± 0.35 ppb in winter. Over four seasons of formaldehyde measurement, the winter season values showed a higher coefficient of variation compared to those of the other seasons, while the highest average formaldehyde value was observed in late spring. The minimum and maximum concentrations of acetaldehyde were 0.23 and 2.17 ppb in summer, respectively, while the average summer time value of acetaldehyde was 0.85 ± 0.47 ppb. The concentration of acetaldehyde in winter was slightly higher than that in summer. The values ranged from 0.27 ppb to 3.75 ppb with an average value of 1.16 ± 0.93 ppb. Late spring and late autumn samplings were also taken on the Macquarie University campus. The average concentrations of formaldehydes were 2.18 ± 0.84 ppb and 1.33 ± 0.16 ppb in late spring and late autumn, respectively. No acetaldehyde value is available for these two seasons. Propionaldehyde was below the limits of detection in this study. A large peak was detected in both summer and winter season samples during the study. The retention time of the peak was similar to retention time of

crotonaldehyde. The values in the measurement are higher than both formaldehyde and acetaldehyde values. As formaldehyde and acetaldehyde are normally the two dominant compounds in ambient aldehydes, the peak is unlikely to be crotonaldehyde. The possibility of the peak is needed to be investigated further. The unknown peak may be formed by reaction of NO_2 with DNPH or by reactions of unsaturated carbonyls with DNPH. A previous study (Ho et al., 2013) reported that NO_2 can react with DNPH to form 2,4-dinitrophenylazide (DNPA). The DNPA has similar chromatography property to formaldehyde-DNP-hydrazone. However, the unknown peak was closer to the retention tine of crotonaldehyde. It is not likely to be DNPA. In addition, Ho et al. (2011) also reported that unsaturated carbonyls such as acrolein and crotonaldehyde can react with DNPH to form dimers or trimers. In the study, acrolein reacted with DNPH to form acrolein-DNP-hydrazone-DNPH, one of which has significant quantity and its retention time closes to retention time of crotonaldehyde (Ho et al., 2011). Therefore, the unknown peak may be more likely due to the reactions of unsaturated carbonyls with DNPH.

These results show lower values of aldehydes in ambient air in NSW, Australia compared to those reported in other worldwide studies of carbonyl compounds. However, most of these studies were conducted in highly polluted areas. To evaluate the levels of carbonyl compounds in NSW, a comparison has been made with a previous study where these compounds were measured in other suburbs of the Sydney region in 2007, shown in Table 4-3. The previous study (Galbally et al., 2008) measured ozone precursors, including formaldehyde and acetaldehyde concentrations, in two suburbs: Bringelly and Randwick. The carbonyl measurements were conducted in the summer of 2007 from 12:00 to 19:00 each day for a 7-hour average value per day (Galbally et al., 2008). The results shown in Table 4-3 demonstrate a slightly lower average and maximum concentrations of formaldehyde at Macquarie University (MU) campus compared to the other two suburbs. In contrast, the acetaldehyde concentration at the MU site is slightly higher than the values measured in Bringelly and Randwick. The differences between the two studies may be the result of differences in the sampling duration. In this study, sampling was conducted on a 24-hour basis, while Galbally's study took samples for only 7 hours each day for carbonyl measurements. Previous studies (Duan et al., 2012; Lü et al., 2009) have found that the concentrations of formaldehyde and acetaldehyde show diurnal variations between morning and afternoon or daytime and evening. Based on these previous studies, the formaldehyde

value is more likely to show a peak in the afternoon. These diurnal variations may explain the results measured in this study. The longer sampling period could result in an average concentration of formaldehyde that is lower than that seen with a shorter sampling period. However, the concentration levels of the carbonyls are impacted by many conditions, and a more detailed analysis will be presented in the following sections.

Table 4-1 Summary of 24-hour measurement of Formaldehyde at the Macquarie University Site Sydney, Australia between 29 May 2013 and 5 February 2015. Concentrations are in ppb.

Sampling Period	Summer Sampling Jan. & Feb. 2015	Winter Sampling Aug. & Sep. 2014	Late Spring 7-14 Nov. 2013	Late Autumn 29 May-1 Jun 2013
Median	0.84	0.42	2.45	1.39
Coefficient of variation	64.99%	72.38%	38.39%	11.72%
Count	26	19	6	3
Mean ± std. dev.	1.07 ± 0.69	0.48 ± 0.35	2.18 ± 0.84	1.33 ± 0.16
Minimum concentration	0.45	0.12	1.10	1.15
Maximum concentration	3.19	1.35	3.11	1.44

Table 4-2 Summary of 24-hour measurement of acetaldehyde at the Macquarie University Site Sydney, Australia between 8 August 2014 and 5 February 2015. Concentrations are in ppb.

Sampling Period	Summer sampling Jan. & Feb. 2015	Winter Sampling Aug. & Sep. 2014
Median	0.48	0.72
Coefficient of variation (%)	49.07%	80.27%
Count	26	19
Mean ± std. dev.	0.55 ± 0.27	1.16 ± 0.93
Minimum concentration	0.15	0.27
Maximum concentration	1.31	3.75

Table 4-3 Comparison of Formaldehyde & Acetaldehyde value in three suburbs of Sydney region (Unit:ppb)

	Bringelly*				Randwick*				MU Site, Summer			
	Mean	St.dev	Min	Max	Mean	St.dev	Min	Max	Mean	St.dev	Min	Max
Formaldehyde	2.11	1.00	0.52	4.28	1.22	1.32	0.04	4.24	1.07	0.69	0.45	3.19
Acetaldehyde	0.30	0.26	0.05	0.88	0.09	0.07	0.04	0.27	0.55	0.27	0.15	1.31

*Data from Galbally et al. (2008)

4.2 Aldehyde concentrations in the Hunter Valley

The 24-hour aldehyde sampling in the Hunter Valley region was only taken in a 5-day period in summer 2015 and a one-day sample was taken in winter 2013. The results are shown in Table 4-4 and Table 4-5. There was no significant difference between summer and winter in terms of changes in formaldehyde concentration. The averaged formaldehyde concentration in summer was slightly higher than that in winter in the Upper Hunter Valley. However, the winter 24 hour sampling was conducted on 13-14 August 2013 and a 24-hour concentration

cannot fully represent the average concentration level. Acetaldehyde values were only analysed in the summer samples. The concentrations of acetaldehyde in summer ranged from 0.49 to 4.47 ppb, with an average of 1.75 ± 1.65 ppb. The variation in acetaldehyde concentration is large compared to the summer formaldehyde levels. The unknown peak was also detected in the Upper Hunter samples, and the values in the Upper Hunter (Singleton) were higher than that value measured at the Macquarie University site. Again, propionaldehyde was not detectable in the samples.

Table 4-4 Summary of 24-hour measurement of formaldehyde at the Upper Hunter site, NSW, Australia 17-22 February 2015 and 13-14 August 2013. Concentrations are in ppb.

Sampling Period	Summer sampling 17-22 Feb. 2015	Winter Sampling 13-14 Aug. 2014
Median	0.67	Two 24-hrs samples
Coefficient of Variation (%)	54.87%	
Count	5	
Mean ± Std. Dev.	0.95 ± 0.59	Average: 0.85
Minimum Concentration	0.65	
Maximum Concentration	2.01	

Table 4-5 Summary of 24-hour measurement of acetaldehyde at the Upper Hunter site, NSW, Australia, 17-22 February 2015. Concentrations are in ppb.

Sampling Period	Acetaldehyde
Median	1.16
Coefficient of Variation (%)	94.17%
Count	5
Mean ± Std. Dev.	1.75 ± 1.66
Minimum Concentration	0.49
Maximum Concentration	4.47

Compared to the results from the MU site samples in summer time 2015, formaldehyde showed a similar concentration range at the Upper Hunter site with slightly lower average concentrations. However, the acetaldehyde concentration in Singleton was double than that at the MU site. In comparison with a previous Sydney urban study (Galbally et al., 2008), the summer acetaldehyde values in Singleton are significantly higher than those from both Bringelly (outer urban, a council reserve) and Randwick (inner urban, a residential area), as summarised in Table 4-6. Based on 2008 Air Emission Inventory dataset (NSW EPA, 2012a), yearly acetaldehyde emission in Singleton and Muswellbrook was 238,511 kg and 122,741kg respectively; the emission was only 9,162 kg in Randwick. The acetaldehyde emission at the Upper Hunter sampling site was orders of magnitude larger than that in Randwick. The 2008 Air Emission Inventory dataset also provided detailed emission sources for each criteria pollutant. Acetaldehyde in Singleton was emitted mainly from natural source and off-road

mobile (e.g. dump trucks, bulldozers and marine vessels) (NSW EPA, 2012a), particularly industrial vehicles and equipment. In Randwick, the main acetaldehyde emission sources were domestic-commercial and natural sources (NSW EPA, 2012a). As mentioned in Chapter 3, the sampling site in the Upper Hunter region is surrounded by open-cut mining sites and farms. The measured results are in good agreement with the emission sources investigation in the 2008 Air Emission Inventory.

In addition, acetaldehyde is a significant emission from biodiesel blended with ethanol (Peng et al., 2008). Acetaldehyde emitted from diesel vehicles is also significantly higher than in the emission from petrol vehicles (Coffey, 2000; Schauer, 1999). The 2008 Air Emission Inventory also reported that vehicles using E10 petrol emit higher acetaldehyde than vehicles using petrol without ethanol (NSW EPA, 2012a). Considering the Upper Hunter sampling site is surrounded by mining sites, these factors are reasonable to explain higher acetaldehyde concentration recorded in the Upper Hunter than the results from Randwick.

Table 4-6 Comparison of measurement of summer time acetaldehyde concentrations in studies in the Greater Sydney Region, NSW. Concentrations are in ppb.

Sampling Period	Upper Hunter	MU	Bringelly	Randwick
Median	1.16	0.69	N/A	N/A
Coefficient of Variation (%)	94.17%	54.87%	86.67%	77.78%
Count	5	26	15	13
Mean ± Std. Dev.	1.75 ± 1.65	0.85 ± 0.47	0.30 ± 0.26	0.09 ± 0.07
Minimum Concentration	0.49	0.23	0.05	0.04
Maximum Concentration	4.47	2.17	0.88	0.27

4.3 Ozone concentration changes and daily variations of aldehydes during the sampling period

As ozone is usually a product from photo-oxidation of active hydrocarbons, the ozone level can be an indicator to evaluate the impact of photochemical reactions of hydrocarbons (Duan et al., 2012). The ozone levels for the sampling periods were obtained from the NSW EPA air quality monitoring network (Rozelle site,NSW) database based on sampling duration, and are presented in Figure 4-1 and Figure 4-2. From the relationship between ozone levels and aldehyde concentrations in summer, it was evident that higher formaldehyde than acetaldehyde values were more likely to occur when the ozone level was increased (see Figure 4-1). Moreover, formaldehyde and acetaldehyde values reached relative peaks as

ozone levels peaked. This phenomenon is evidence that aldehyde levels are affected by ambient photochemical oxidation of hydrocarbons.
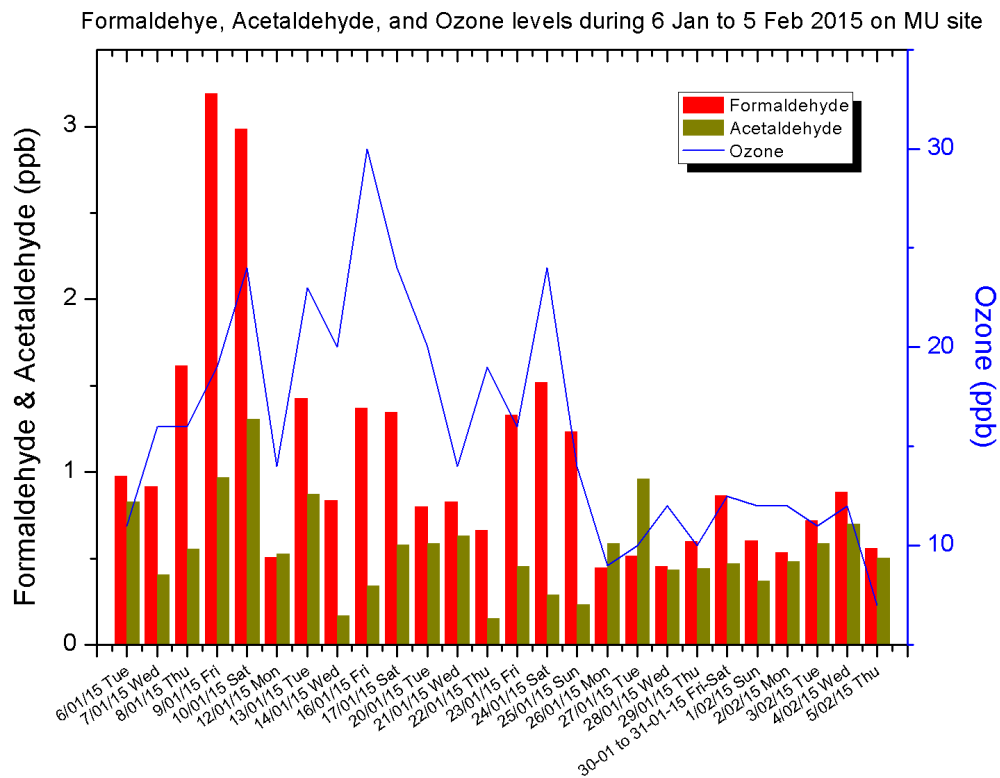
Figure 4-1 Daily variations of aldehydes and ozone levels in summer season at an urban Sydney site
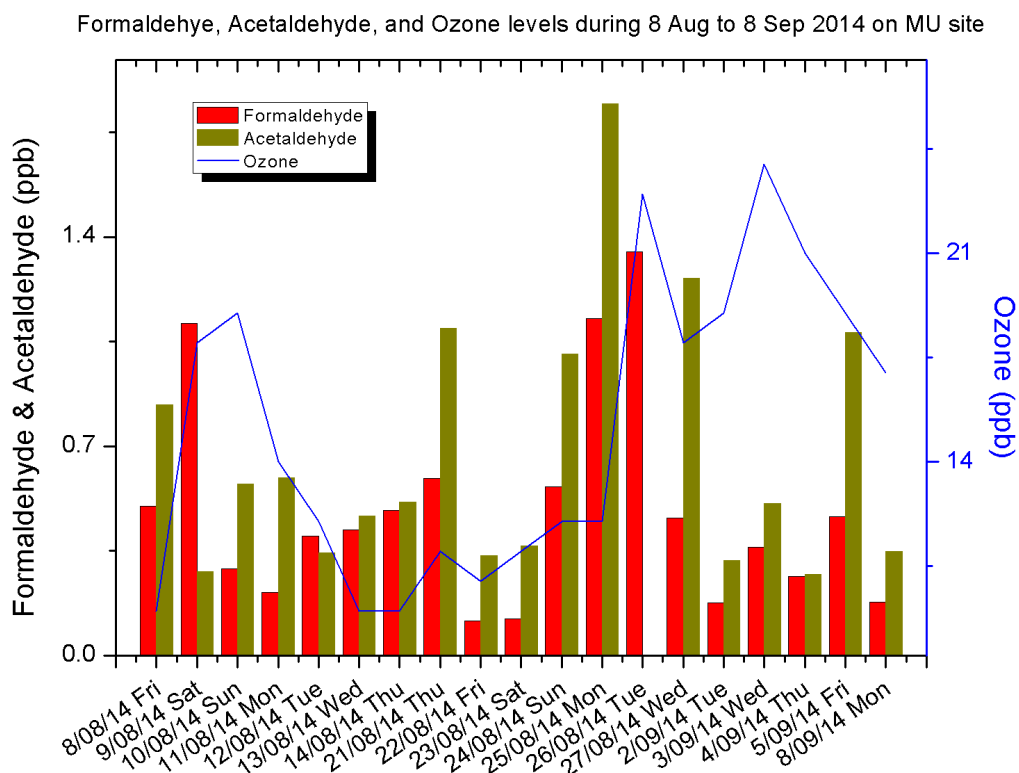
Figure 4-2 Daily variations of aldehydes and ozone levels in winter season at an urban Sydney site

As discussed in Chapter 2, ambient carbonyls can be formed from secondary formation of volatile organic compounds (VOCs), and can be emitted from primary sources, including anthropogenic emission and biogenic emission (Luecken et al., 2012). Human activities such as vehicle exhaust, biomass combustion are major contributions to ambient carbonyls level. The Upper Hunter sampling results can be explained by the influence of human activities ion atmospheric carbonyls values. According to the 2008 Air Emission Inventory investigation (NSW EPA, 2012a), formaldehyde and acetaldehyde emissions were 219,538 kg and 238,511 kg in Singleton, and 70,831kg and 122,741 kg in Muswellbrook, respectively. The average values of formaldehyde and acetaldehyde measured in summer time in this study were 0.95 ppb and 1.75 ppb, respectively (shown in Table 4-4 and Table 4-5). The average acetaldehyde value was higher than that of formaldehyde. This is a good agreement with the Air Emission Inventory investigation.

In addition to the photochemical oxidation of hydrocarbons and primary emission as influence factors, ambient aldehyde levels are influenced by other factors, including meteorological conditions, and atmospheric stability among others. Concentrations of the aldehydes show a temporal variation. This study measured the 24-hour daily concentration,

and so only daily variations are presented in this study. The daily variations of formaldehyde and acetaldehyde were measured at the Macquarie University site, and are also present in Figure 4-1 and Figure 4-2. In this study, the Formaldehyde values were higher than acetaldehyde concentrations on 22 out of 26 days in summer time and three out of 19 days in winter. As formaldehyde is normally the dominant oxidation product from photochemical reactions of hydrocarbons, the relationship between the concentrations of formaldehyde and acetaldehyde in this study demonstrates that photochemical oxidation of hydrocarbons is an important factor in summer and is also not the only factor to influence the carbonyls level. Previous studies (Pang and Mu, 2006; Pang and Lee, 2010) also pointed out that meteorological conditions influences ambient carbonyls concentrations. This factor will be discussed in the next section.

4.4 Meteorological effects on ambient aldehydes concentrations

As meteorological conditions can have impacts on ambient aldehyde concentrations, this study considers the relationship of formaldehyde and acetaldehyde concentrations with different meteorological factors: maximum temperature, wind speed, and daily rainfall. The meteorological data were obtained from observation records from Bureau of Meteorology (BOM). 3pm temperature which is dry-bulb air temperature measured at local time, averaged over the period of recording (BOM, 2015a) was used to represent daily temperature. The mean 3pm temperatures ranged from 19.2 to 35.6 ˚C during the sampling period of January and February 2015, and were 12.8 to 22.6 ˚C during sampling period of August and September 2014. Figure 4-3 and Figure 4-4 present formaldehyde and acetaldehyde concentrations relative to daily temperature changes. The formaldehyde concentration demonstrated similar movement trends as the temperature variations in summer. However, there was no apparent relationship between the formaldehyde concentration variations and temperature in winter (Figure 4-4). In contrast to the variations in formaldehyde levels, there were no clear variations in acetaldehyde levels related to temperature in either summer or winter.

Atmospheric stability is likely to cause concentration changes. Wind speed is an important meteorological condition that impacts on atmospheric stability. In the sampling period between January and February 2015, the 3pm wind speed ranged from 9 to 24 km/h with an average of 17.58 km/h, while between August to September 2014, it ranged from 6 to 20

km/h with an average of 15.84 km/h. From the measured aldehyde concentrations and observed wind speed data presented in Figure 4-5 and Figure 4-6, the aldehyde levels did not demonstrate a close relationship with wind speed. In summer, formaldehyde did not record a relative high concentration value at the lowest wind speed. However, several relative high concentrations of formaldehyde were recorded on high wind speed days. In winter, formaldehyde levels tended to have a negative relationship with wind speed on most days. Radiation is also one of the important meteorological factors that impacts on atmospheric stability. Solar radiation can heat up the air to cause atmospheric instability during the day (Seinfeld and Pandis, 1998). Radiation inversion that radiative cooling of the ground surface during the night cools the air can trap pollutants emitted during the night (Seinfeld and Pandis, 1998). Figure 4-7 and Figure 4-8 present relationship between radiation and aldehydes concentrations. Due to equipment failure at the MQ weather station during the summer sampling season, only winter observation data of radiation were available to analyse correlation with observed aldehydes concentrations in the same period. The results in Figure 4-7 demonstrated that formaldehyde concentrations decreased while the radiation increased in most of days. The results in Figure 4-8 showed a similar trend with formaldehyde. Acetaldehyde levels trended to have negative relationship with radiation on most of days, however, the highest concentration of acetaldehyde did not occur on the lowest radiation level. These results show that formaldehyde and acetaldehyde levels can be impacted by a combination of meteorological conditions. Photochemical oxidation of hydrocarbon could be an important factor that determines the concentration of aldehyde in summer season, but maybe lesser impacts in winter.

As formaldehyde is highly soluble in water, this study also considers the impact of rainfall on aldehyde concentrations, as shown in Figure 4-9 and Figure 4-10. During the summer sampling period, the average rainfall was 5.62mm with a maximum of 71.4mm. The mean rainfall in winter sampling days was 3.02mm with a maximum of 22.2mm. On high rainfall days, formaldehyde levels did not reach relative peaks, but peak acetaldehyde levels were detected on a few days. While it is possible that rainfall could reduce aldehydes concentrations, it did not show any apparent effect on aldehydes levels in this study. These results provide evidence that ambient aldehyde concentration values are determined by many factors, including primary emission, photochemical oxidation reactions of hydrocarbons, and meteorological conditions.

Figure 4-3 Formaldehyde, acetaldehyde, and temperature levels during January and February 2015 at Macquarie University Site

Figure 4-4 Formaldehyde, acetaldehyde, and temperature levels during August and September 2014 at Macquarie University Site

Figure 4-5 Formaldehyde, acetaldehyde, and wind speed during January and February 2015 at Macquarie University Site

Figure 4-6 Formaldehyde, acetaldehyde, and wind speed during August and September 2014 at Macquarie University Site
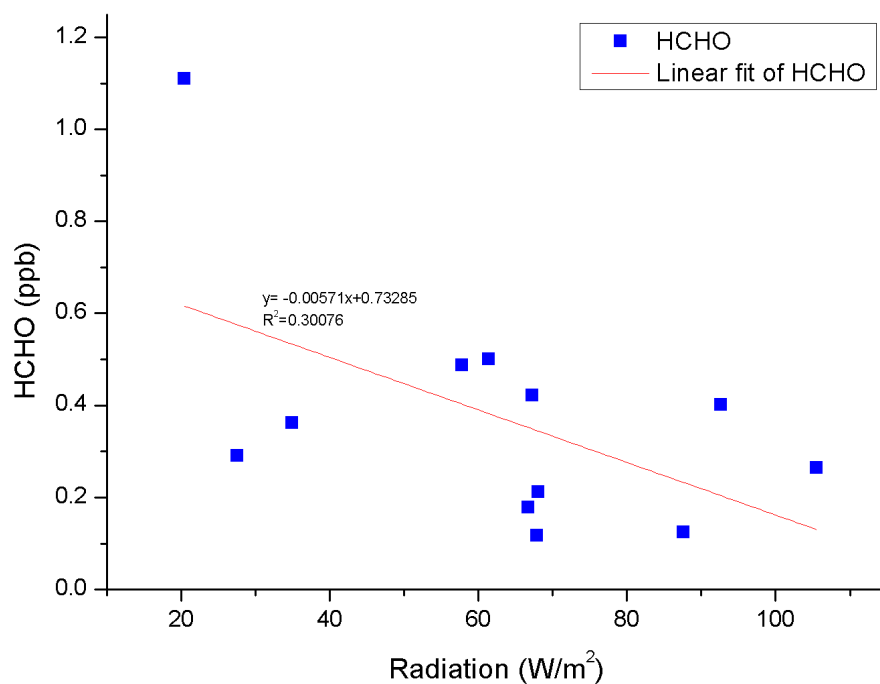
Figure 4-7 Correlation of formaldehyde and radiation in winter season at an urban Sydney site
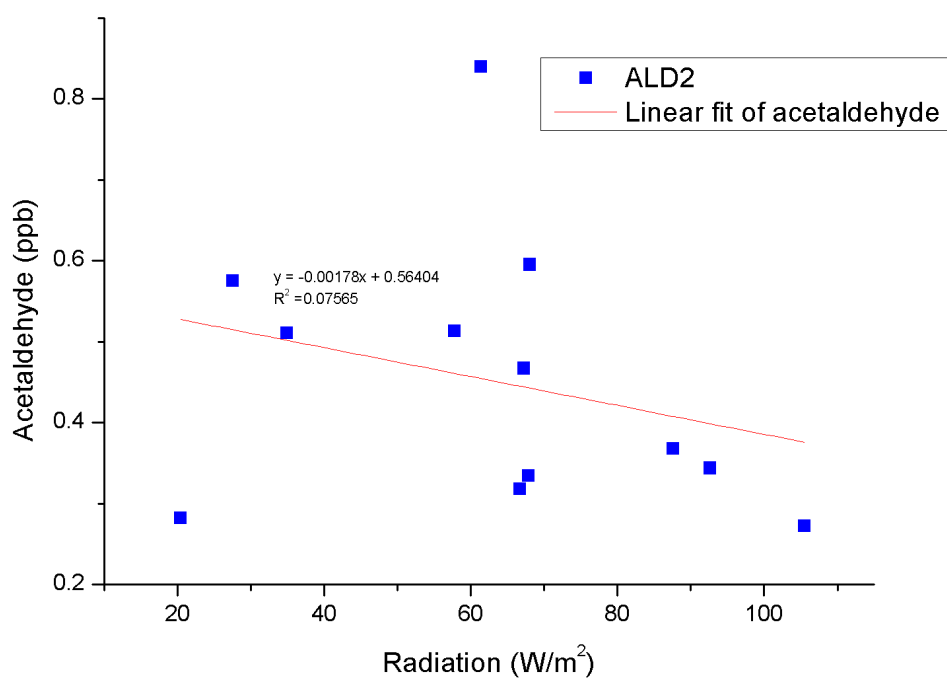
Figure 4-8 Correlation of acetaldehyde and radiation in winter season at an urban Sydney site

Formaldehye, Acetaldehyde, and Rainfall levels during 6 Jan to 5 Feb 2015 on MU site
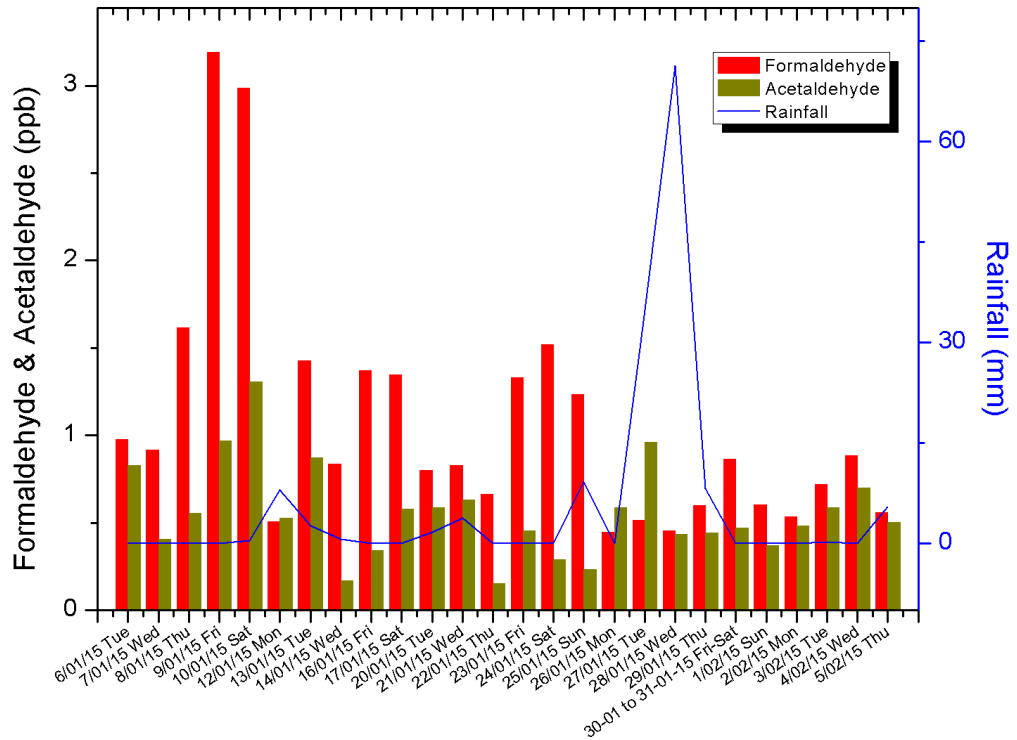
Figure 4-9 Formaldehyde, acetaldehyde, and rainfall during January and February 2015 at Macquarie University Site

Formaldehye, Acetaldehyde, and Rainfall levels during 8 Aug to 8 Sep 2014 on MU site
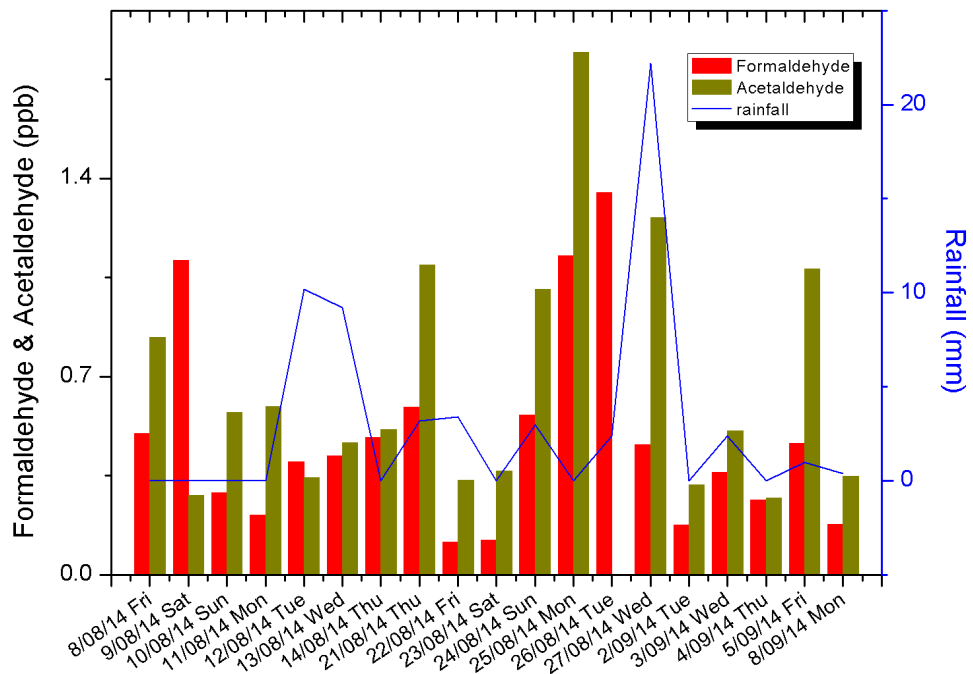
Figure 4-10 Formaldehyde, acetaldehyde, and rainfall during August and September 2014 at Macquarie University Site

65

4.5 Concentration Ratios

Previous studies have reported that the formaldehyde to acetaldehyde ratio (C1/C2) can be useful as an indication to measure biogenic sources of formaldehyde (Duan et al., 2012; Feng et al., 2005). This ratio has been reported to range from 1 to 2 at urban sites and to be about 10 in forested areas (Duan et al., 2012). The acetaldehyde to propionaldehyde ratio has been treated as an indicator for anthropogenic sources of ambient carbonyls (Feng et al., 2005; Grosjean, 1992). This ratio has been reported to be high in rural areas and low in polluted urban air (Feng et al., 2005). In this study, propionaldehyde was below the detectable limits in all samples from both the Macquarie University site and the Upper Hunter site. Therefore, only the formaldehyde to acetaldehyde ratio is considered in this section. The C1/C2 ratios of samples from summer and winter are listed in Table 4-7. The average values of this ratio were 2.23 and 0.80 at the Macquarie University site during summer and winter, respectively. The average ratio observed in summer was closer to the upper side of the C1/C2 ratio in urban areas, but much lower than the ratio in rural areas. This value indicates that anthropogenic sources may have an important influence on carbonyls levels. The ratio of the results from the Upper Hunter site was 1.07 on average with a range of 0.50 to 1.68. These values are in the range of the expected C1/C2 ratio for polluted urban areas, which reflects the impact of human activities on carbonyls levels. As the propionaldehyde value was not detectable, further comparison for anthropogenic sources of ambient carbonyls cannot be conducted in this study.

Table 4-7 Ratio of formaldehyde and acetaldehyde in summer and winter seasons

Sampling Site	Macquarie University		Upper Hunter Site
Sampling Period	Summer Sampling Jan & Feb 2015	Winter Sampling Aug & Sep 2014	Summer Sampling February 2015
Mean	2.23	0.80	1.07
Minimum value	0.54	0.34	0.50
Maximum value	5.28	3.94	1.68

Previous studies have also reported that photochemical reactions of carbonyls with the OH radical and ozone can change carbonyls levels in the atmosphere (Atkinson, 1997; Duan et al., 2012; Huang et al., 2008; Li et al., 2010). Photolysis with the OH radical is the dominant process for loss of carbonyls in polluted atmosphere (Atkinson, 1997; Atkinson, 2000). The calculated lifetimes of the reactions with OH radicals for formaldehyde, acetaldehyde, and propionaldehyde are 1.2 days, 8.8 hours, and 2.9 hours, respectively (Atkinson, 2000). As the lifetime of formaldehyde is longer than that of acetaldehyde in the atmosphere, this ratio

can be greater than the values reported in urban area (1-2) in areas where reaction with OH radicals play an important role in the atmosphere. In addition, formaldehyde is usually the dominant oxidation products from photochemical oxidation of hydrocarbons. A higher C1/C2 ratio has been reported as an implication of a positive impact of photochemical reactions of hydrocarbon (Duan et al., 2012). In summer, weather conditions in NSW often involve intensive sunlight and high temperature. It is more likely that more formaldehyde is formed from photochemical oxidation of hydrocarbon in summer than the other seasons. The higher ratio of C1/C2 in summer in this study compared to this value in winter is in agreement with positive impact of photochemical oxidation of hydrocarbon.

4.6 Comparison with overseas studies

Formaldehyde and acetaldehyde concentrations in MQ site and the Upper Hunter region site from this research were lower than the values in other countries. This research reviewed previous studies in the world. The aldehyde concentrations have wide ranges in different countries. In China, formaldehyde concentrations ranged from 10.39 to 62.34 ppb with mean value of 28.98 ppb in Beijing (Duan et al., 2012). The high concentrations in Beijing were observed during haze days. The high air pollution and stable boundary layer in summer were the significant factors to cause the high concentrations of aldehyde in Beijing. In New York City, U.S. the formaldehyde concentrations at the Queens College site was in a range of 0.4 - 7.5 ppb, with mean value of 2.2 ± 1.1 ppb in summer 2009 (Lin et al., 2012). Formaldehyde in Houston was 3.3 ppb on average between 12th August and 25th September, 2000 (Dasgupta et al., 2005). Formaldehyde concentrations at MQ site from this research were closer to the value at Queens College site in New York City. The Queens College has similar environmental conditions with the MQ site in this study. For example, The Queens College is surround by residential area, a busy interstate road and highways. MQ site was located in a hi-tech business parks. Many corporations have established regional headquarters in the area. In addition, the MQ site is surrounded by residential area, a motorway and a busy major road. These findings showed that high air pollution, stable boundary layers, and strong photochemical reactions may be the factors to cause high concentration of formaldehyde. The summary of formaldehyde concentrations in different cities worldwide including the results from this research are listed in Table 4-8.

Table 4-8 Summary of formaldehyde concentrations in different cities worldwide and this study

Location (ambient air)	Concentration (ppb)		Comment	References
New York City, USA	0.4-7.5	Range	15 July-3 August,2009	(Lin et al., 2012)
	2.2±1.1	Median	15 July-3 August,2009	(Lin et al., 2012)
Houston, USA	47	Maxima	August-September, 2000	(Dasgupta et al., 2005)
	3.3	Mean	August-September, 2000	(Dasgupta et al., 2005)
	30	Maxima	20 July-25 Sept. 2002	(Chen et al., 2004)
Nashville, USA	1.43-12.67	Range	26 June-07 July, 1999	(Dasgupta et al., 2005)
	4.78	Median	26 June-07 July, 1999	
Atlanta, USA	0.42-18.25	Range	03-31 August, 1999	(Dasgupta et al., 2005)
	7.82	Median	03-31 August, 1999	
Philadelphia, USA	0.33-9.53	Range	27 June-31 July, 2001	(Dasgupta et al., 2005)
	2.89	Median	27 June-31 July, 2001	
Tampa, USA	0.37-9.38	Range	25 April-01 June, 2002	(Dasgupta et al., 2005)
	2.32	Median	25 April-01 June, 2002	
Tijuana, Mexico	1-13.7	Range	15 May-30 June, 2010	(Zheng et al., 2013)
Mexico City, Mexico	3-27	Range	April-May, 2003	(Grutter et al., 2005)
	35	Maxima	2003, Monthly	(Volkamer et al., 2005)
	17	Maxima	Daily, 2003	(Molina et al., 2007)
Beijing, China	10.39-62.34	Range	August, 2006	(Duan et al., 2012)
	28.98±11.98	Average		
	15.85±7.24	Average	Urban Site, Aug.-Oct., 2005	(Pang and Mu, 2006)
	3.41±2.28	Average	Urban site, Nov.04-Jan. 05	
	24.15±7.80	Average	Transport site, Spring 2005	
	3.58±1.14	Average	Botanical park, Spring 2005	
Shanghai, China	9.9-40.4	Range	Mar. 2007, high air pollution	(Huang et al., 2008)
	23.96±7.41	Mean		
	25.91±5.93	Mean	Summer, 2007	
Guangzhou, China	3.75-5.99	Range	17-19 Nov. 2005, Clear days	(Lü et al., 2010)
	4.89	Mean		
	2.07-20.08	Range	30 Nov-2 Dec.2005, haze days	(Lü et al., 2010)
	11.87	Mean		
	54.45±12.11	Maxima	July-September, 2003	(Feng et al., 2005)
	11.22	Average		
Xi'an, China	8.05	Average	July-August, 2004	(Wang et al., 2007)
Hangzhou, China	18.05	Average	March-April, 2006	(Weng et al., 2009)
Guiyang, China	3.9	Average	Dec. 2008-Aug. 2009	(Pang and Lee, 2010)
Sydney, Australia	0.52-4.28	Range	18 Jan.-27 Feb.2007, Bringelly	(Galbally et al., 2008)
	0.04-4.24	Range	28 Feb-19 Mar2007,Randwick	
MQ site, Sydney, Australia	0.45-3.19	Range	Jan-Feb, 2015	This study
	1.07±0.69	Mean		

	0.12-1.35	Range	Aug. – Sep. 2014	This study
	0.48±0.35	Mean		
	1.10-3.11	Range	7-14 Nov. 2013	This study
	2.18±0.84	Mean		
	1.15-1.44	Range	29 May-1 Jun 2013	This study
	1.33±0.16	Mean		
The Upper Hunter, Australia	0.65-2.01	Range	17-22 Feb. 2015	This study
	1.75±1.65	Mean		
	0.85	Mean	13-14 Aug. 2015	This study

0.12-1.35 Range Aug. – Sep. 2014 This study

Chapter 5 Computer modelling development for atmospheric dispersion and movement of amines & degradation products

5.1 KPP model for kinetic functions of amines reactions in the atmosphere

5.1.1 KPP Model for amines chemical mechanism development

In order to benefit possible future development and assessment, a numerical method to solve the differential equations required to describe the reaction scheme was considered in model development. The Kinetic Preprocessor Model (KPP) (Sandu and Sander, 2005) is a tool to simulate chemical mechanisms for atmospheric chemistry. The KPP model was employed to generate FORTRAN codes for amine (MEA) photochemical reactions. The KPP model was treated as a box model where atmospheric chemistry occurs in the absence of dispersion, location, and seasonal variation. The mechanism and kinetic information for MEA and its oxidation products were based on previous EUPHORE chamber studies (Karl et al., 2012; Nielsen et al., 2011). Only gas phase reactions were considered in the model development. To reflect the background gas phase chemistry in the atmospheric environment, Carbon Bond mechanism version 6 was combined with the MEA sub-mechanism to perform the numerical integration. The Rosenbrock solver was used for integration of the differential equations of the gas phase reactions (Sander et al., 2011; Sandu and Sander, 2005). Initial concentrations of the main products were based on the concentrations in the EUPHORE chamber studies. For example, MEA was initially 410 ppb, formaldehyde was 2 ppb, nitramines were 0.1 ppb, and nitrosamines were zero. The KPP model was used to calculate concentrations of MEA, formaldehyde (FORM), nitrosamines and nitramines at time intervals of six minutes. The model was run for 12 hours commencing at 12:00 noon. As nitrosamine can degrade to non- toxic products (Bråten, 2008), the rate of degradation loss of nitrosamines was 1.91×10^{-2}/s which was used to setup the KPP run. In the KPP box model, wall loss of MEA is also considered for an individual run which is used to validate the results from KPP.

5.1.2 Results from KPP simulation

KPP was used to run two different scenarios: (1) simulation of the amine chemistry chamber experiments with wall loss of amine included; (2) simulation of amines chemistry in the atmospheric environment with wall loss removed. In considering wall loss in the chamber

experiment scenario, the KPP was run for 24 hours starting from mid-day 12:00 noon. Modelled output was calculated every six minutes during the process.

Figure 5-1 shows the concentrations change in wall loss of MEA to chamber surface scenario for the first 5 hours simulation. As concentrations of nitrosamines and nitramines were very low, the modeled nitrosamines and nitramines concentrations are scaled by a factor of 100 for better visibility. The results showed that MEA decreased sharply in the first 3 hours (180 minutes) after simulation started, in good agreement with the EUPHORE chamber experiment (Karl et al., 2012). Experiment 3 of the EUPHORE study (Karl et al., 2012) showed that nitramine concentrations reached their highest value 3 hours after initial exposure to sunlight. Using Proton Transfer Reaction Time-of-Flight Mass Spectrometer (PTR-TOF-MS), the highest nitrosamine concentration observed was 0.055 ppb, but the modeled result in Karl's study was 2.953 ppb. In KPP simulation of this study, the nitramines concentration increased to the highest value after 3 hours, which agrees with the observations (Karl et al., 2012). The highest value was only 0.00944 ppb. The over-prediction of this trace product could be due to loss of the nitrosamine to the sampling system. There are in addition differences in the reaction scheme used at EUPHORE and that used in the current study: the Module Efficiently Calculating the Chemistry of the Atmosphere (MECCA) included chemistry of C2-C4 alkanes, propene, isoprene and dimethyl sulphide. This study uses Carbon Bond version 6 chemistry scheme to run the simulation. Concentrations of nitrosamines and nitramines demonstrated fast increases at the beginning of the modeled experiment, then decreased slightly. Formaldehyde concentration increased after the model start and reached the highest value after about 4.5 hours from the start of the model run then began to decrease. The trend of formaldehyde concentration reflects secondary source contributions to the ambient formaldehyde concentrations. A previous study (Lin et al., 2012) measured formaldehyde concentrations in summer time. The study shows that the secondary sources became a major contributor to ambient HCHO concentration after 9 am, and 70% of the formaldehyde concentrations between 12 pm to 3 pm were from secondary HCHO (Lin et al., 2012).

In the case of the amine chemistry in the atmospheric scenario, the results showed that the concentration changes were slower than for the scenario incorporating wall loss. Figure 5-2 shows results for 8 hours model run time. The MEA concentration decreased initially but was

relatively constant but disappeared significantly slower than for the wall loss case as expected. Formaldehyde concentration reached its highest value of 5.4 ppb after about 6.5-7 hours of running time.
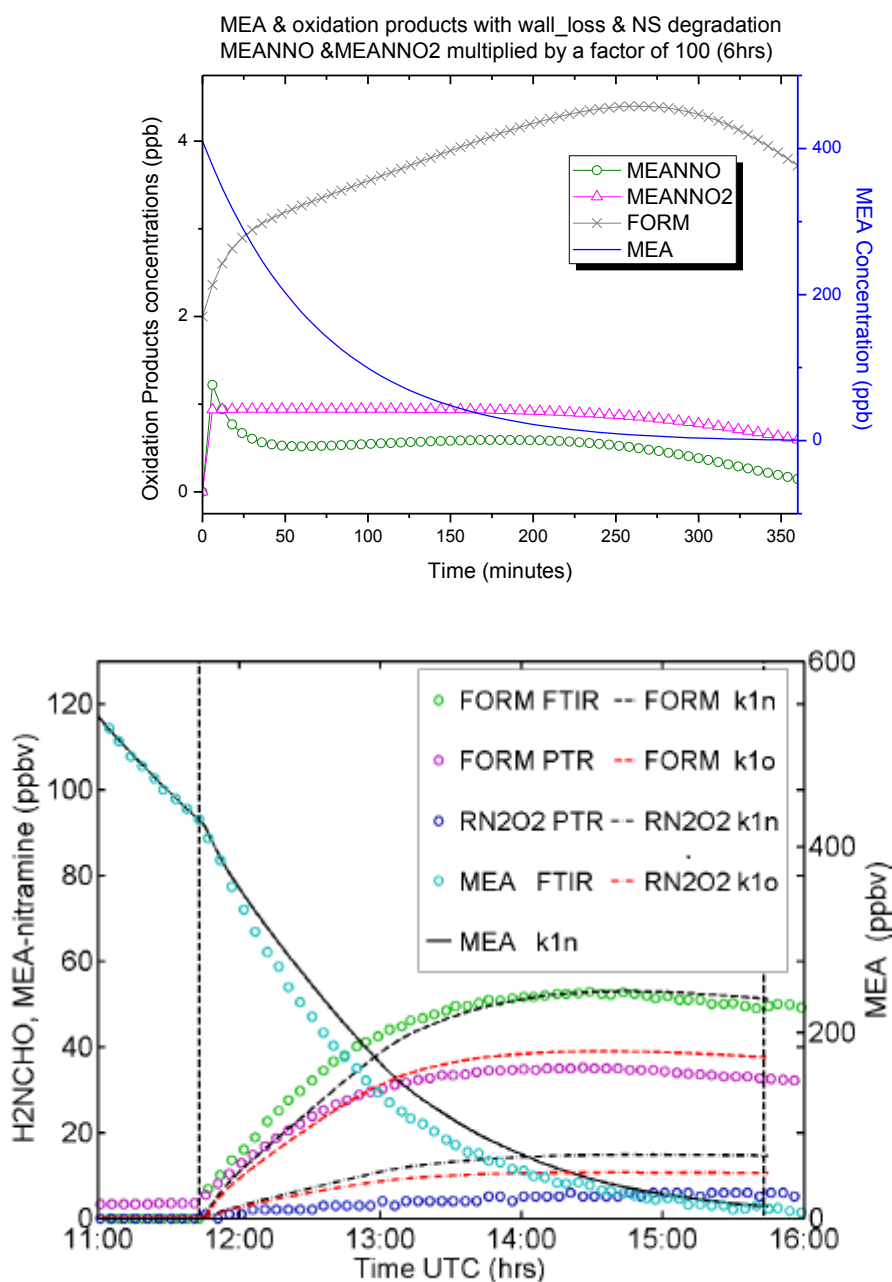
Figure 5-1 Above: MEA & oxidation products with wall loss & nitrosamines degradation. MEA: monoethanolamine; MEANNO: 2-(N-nitrosoamino)-ethanol; MEANNO2: 2-nitroamino ethanol; FORM: formaldehyde. MEANNO & MEANNO2 multiplied by a factor of 100. Below: Results of EUPHORE chamber study (Karl et al., 2012)
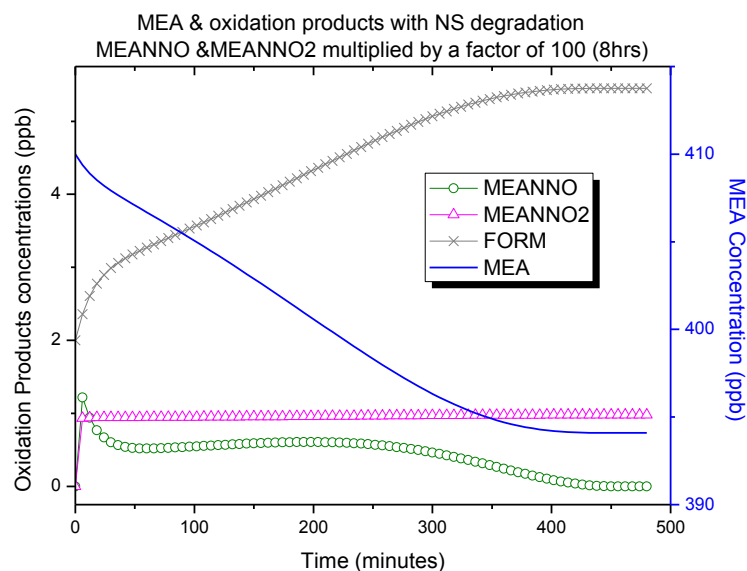
Figure 5-2 MEA & oxidation products with nitrosamines degradation. MEA: monoethanolamine; MEANNO: 2-(N-nitrosoamino)-ethanol; MEANNO2: 2-nitroamino ethanol; FORM: formaldehyde. MEANNO & MEANNO2 multiplied by a factor of 100.

5.2 TAPM model to generate meteorological data for CALMET

TAPM is employed to do meteorological data generation and atmospheric dispersion simulation for main compounds such as ammonia, formaldehyde, and particulate matter (PM). In this chapter, only meteorological data generation from TAPM will be discussed. The atmospheric dispersion simulation using TAPM model will be discussed in following chapters. There are three main components of the CALPUFF model: CALMET, CALPUFF, and CALPOST. CALMET is a model to generate meteorological data for wind and temperature fields. The data generated from CALMET is placed on a 3D gridded modeling domain. The meteorological data from CALMET can be used typically for CALPUFF domain setting or as an option (Scire et al., 2011). CALPUFF is a puff model to process dispersion, chemical transportation and deposition. CALPOST is a tool to process these files generated from CALPUFF and summarize results for highest or second or third highest values for each receptor. In this study, we used 3D meteorological data generated from TAPM as a basis to set up each CALMET run. The data from TAPM is an ASCII format file and machine-independent (Scire et al., 2011). To use the data to run CALMET, correct format files are needed. CALTAPM is a tool to transfer the data from TAPM to suitable format files for CALMET. The process was operated under DOS system.

In TAPM model set up, the study area selected was in the upper Hunter Valley, about 200 km north of Sydney. As discussed before, the Hunter valley is a region which includes extensive coal mining, power production and agricultural (mainly viniculture) operations, and two settlements of 10-20 000 inhabitants. The outer modeling grid which is 30 km X 30 km, was centered on -32°23.5" latitude and 150°57.0" longitude. TAPM was configured to have four nested grids at 30 km, 10 km, 3 km, and 1 km resolution. Each grid has 50 by 50 cells and 25 vertical levels. It was assumed that there were only two point sources from a full-scale coal-fired power station. The stack parameters were based on Bayswater Power Station located near the town of Muswellbrook in the upper Hunter, NSW, Australia. Emission rates for each chemical compounds were based on data determined by CSIRO (Thong et al., 2012) and corrected for the somewhat different parameters appropriate to Bayswater Power Station. The year 2000 was selected as a representation year for meteorological data simulation as the data of the year 2000 was the only available data at that time the simulation was set up. The year 2000 was in the La Niña climatological pattern. The TAPM model was run for each month of the year 2000. The detailed parameters for the TAPM model runs are shown in Table 5-1.

Table 5-1 Parameters for TAPM model meteorological data generation.

Parameters	Stack 1 & 2
Stack Diameter (m)	12
Stack Height (m)	248
Exit Velocity (m/s)	13.9
Temperature (K)	373
MEA emission rate (g/s)	1.2
Formaldehyde –HCHO emission rate (g/s)	2.4

After simulation, TAPM model generated meteorological data in ASCII format for each day in each nested grid. To make the output meteorology files of ASCII format from TAPM working in CALMET, CALTAPM model which is a tool in CALPUFF model package was employed to extract all TAPM 3D variances such as wind speed, wind direction, temperature, relative humidity, turbulent kinetic energy (Scire et al., 2011). TAPM is assumed to use UTM and Datum of WGS-84, which are used directly in CALTAPM 3D data files. CALTAPM was operated in DOS system with control file (caltapm.inp), data file from TAPM (.outa file), TAPM definition file (.def), surface file including terrain height, vegetation type, soil type and monthly leaf area index information (.top) in the running direction. The output 3D meteorological data from CALTAPM was stored in files with suffix of .m3d, which was produced for CALMET model.

5.3 CALPUFF model modification for amines reactions and results

5.3.1 CALPUFF model modification

CALPUFF is used to simulate chemical reactions in the atmosphere and to account for dispersion. In the original CALPUFF, there are seven chemical mechanisms provided as options (Scire et al., 2011). The existing nitrogen and sulphur oxides chemistry in CALPUFF gives a well validated platform to develop the amine chemical scheme for the simulations (Yiannoukas et al., 2011). Through studying the codes carefully, MCHEM =6 (Updated RIVAD scheme with ISORROPIA equilibrium) chemistry subroutines was selected as a foundation to modify and expand the FORTRAN codes as a new routine to be added into CALPUFF. The new routine is called mq_amines. The reaction mechanism with amine reactions was named as MCHEM=8. Only gas phase reactions in the atmosphere are considered in the MCHEM=8 mechanism. The chemical reactions of amines were based on a previously published reaction scheme (Karl et al., 2012). However, nitrosamines degradation was considered in addition according to previous reports (Fowler and Vernon, 2012b). As MEA was the only amine included in this case study, the rate constant for nitrosamine degradation was determined to be 1.91×10^{-2} cm^3/molecule/s for primary amines (Fowler and Vernon, 2012b). In this modified CALPUFF, only amine reaction related code was added as an additional module into the program codes, and the rest of the code remained unchanged. When the amine chemistry option was selected (MCHEM=8), this modified CALPUFF included 13 species in total, and 7 of which are amine chemistry participants: MEA (primary amines), MEAN (N-amino ethanol radical), MEABO2 (C2-amine peroxy radical), MEABO (C2-amine alkoxy radical), HCHO (formaldehyde), MEANNO2 (nitramines, also named NA), and MEANNO (nitrosamines, also called NS). The results after dispersion simulation focus on MEA, HCHO, and NS. The MEA mechanism was based on mechanism for OH-initiated oxidation of MEA in Karl et al. (2012) study. As this research focuses on MEA, HCHO, and NS concentrations, the mechanism was simplified and shown in Table 5-2.

Table 5-2 Parameters for TAPM model meteorological data generation.

No.	Reaction			Rate constant	Reference
1	$NH_2CH_2CH_2OH+OH$	→	$0.05\ H_2NCH_2CHO+0.8MEABO_2+0.15$ $MEAN+0.05\ HO_2$	3.58×10^{-11}	EPI Suite^{TM} V4.0
2	$MEABO2+NO$	→	$MEABO +NO_2$	$2.54 \times 10^{-12}exp\ (360/T)$	MCM*
3	$MEABO+O_2$	→	$H_2NCOCH_2OH+HO_2$	2.4×10^{-15}	(Karl et al., 2012)
4	$MEABO$	→	$H_2NCHO+HCHO$	2.0×10^5	(Karl et al., 2012)
5	$MEAN+NO_2$	→	$0.5MEANNO_2+0.5HNCHCH_2OH+0.5HONO$	1.4×10^{-13}	(Nielsen, 2010)

6	MEAN+O2	→	HNCHCH$_2$OH+HO$_2$	1.2×10^{-19}	(Nielsen, 2010)
7	MEAN+NO	→	MEANNO (also called NS)	8.5×10^{-14}	(Nielsen, 2010)
8	MEANNO2+OH	→	MEANHA+HO2	1.48×10^{-11}	EPI Suite^{TM} V4.0
9	MEANNO+hv	→	MEAN+NO	$j=0.33*j$(NO$_2$)	(Karl et al., 2012)
10	MEANNO degradation			1.91×10^{-2}	(Fowler and Vernon, 2012b)

*Master Chemical Mechanism (MCM) v3.1 (Bloss et al., 2005) available at http://mcm.leeds.ac.uk/MCMv3.1

5.3.2 Results from modified CALPUFF model

5.3.2.1 Concentration values from the modified CALPUFF model and seasonal variation

Meteorological data generated by TAPM for the finest resolution (1 km) were converted to a 3-Dimensional data output file for input to the CALMET model. The meteorological data from the CALMET model were employed in CALPUFF to simulate pollutant transport and dispersion in the atmosphere. The concentration data were averaged to give 1-hour & 24-hour averaging times for the 49 × 49 km domain area. The data were processed for individual months. In the case of CALPUFF output data, concentrations were calculated for three target chemical compounds: MEA, formaldehyde (HCHO) & nitrosamine (NS). The 1-hour and 24-hour average concentrations for the three compounds are shown in Figure 5-3, Figure 5-4, and Table 5-3. Meteorological data for the year 2000 were used in the case study. The three compounds in Figure 5-3 and Figure 5-4 show that the lowest average concentration values were observed in February and the highest average concentration was in December. The lowest average concentration of MEA was 2.9×10^{-5} µg/m^3 and 3.0×10^{-5} µg/m^3 for 1-hour and 24-hour averaged time, respectively. The lowest average concentration of NS was 6.3×10^{-7} ng/m^3 and 6.5×10^{-7} ng/m^3 for 1-hour and 24-hour averaged time, respectively. The highest concentration were 1.8×10^{-3} µg/m^3 & 1.9×10^{-3} µg/m^3 for MEA, and 4.0×10^{-5} ng/m^3 & 4.1×10^{-5} ng/m^3 for NS on 1-hour and 24-hour averaged time, respectively. Results from April to July show relatively low values compared to other months, detailed values are shown in Table 5-3.

Formaldehyde values were also modeled in the modified CALPUFF model. The value is mainly used to indicate concentration change during a year. Previous studies (Huang et al., 2008; Pang and Mu, 2006) measured formaldehyde concentration in China. Pang and Mu (Pang and Mu, 2006) observed that formaldehyde in summer time could be nearly 5 times higher than the value in winter time at a Beijing sampling site. Huang et al (Huang et al., 2008) indicated that the highest mean value was found in summer with a factor of 4.5 times

higher than the lowest mean value which was found in autumn. In the current study results consistent with these were observed apart for February. The highest average values of 3. 6×10^{-3} µg/m^3 and 3.6×10^{-3} µg/m^3 were recorded in December for 1-hour and 24-hour averaging times respectively. MEA and nitrosamine show similar seasonal trends to formaldehyde. In February 2000, historical meteorological data showed that the hottest month of 2000 was February with average daily temperature of 28 °C (WeatherSpark, 2000). However, the lowest calculated concentrations of all three compounds were observed in February. Particular meteorological features of the year 2000, including the temperature could be responsible for these observations. The historical data of 2000 also showed that the windiest month of 2000 was February, with an average wind speed of 6 m/s (WeatherSpark, 2000). The high speed wind could cause intensive atmospheric turbulence which can dilute the concentration values.
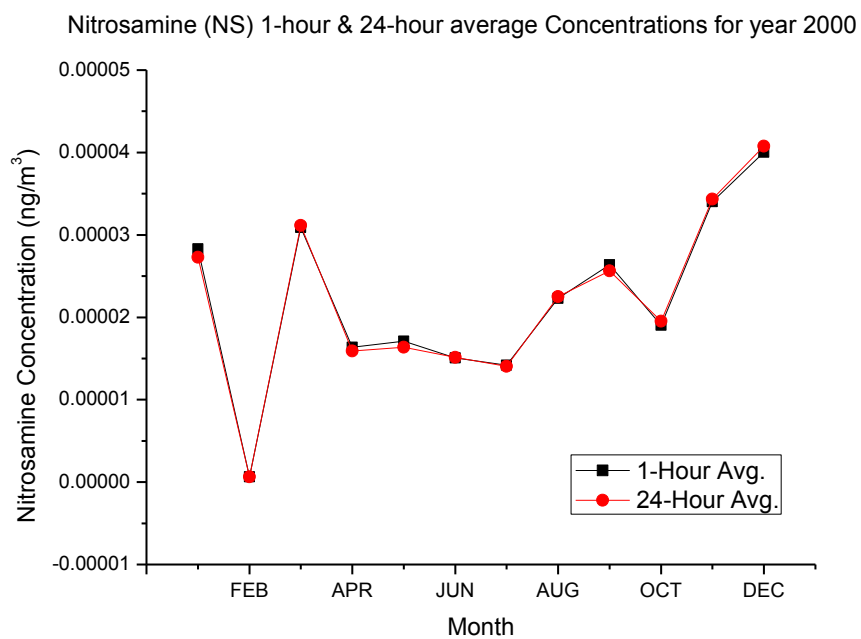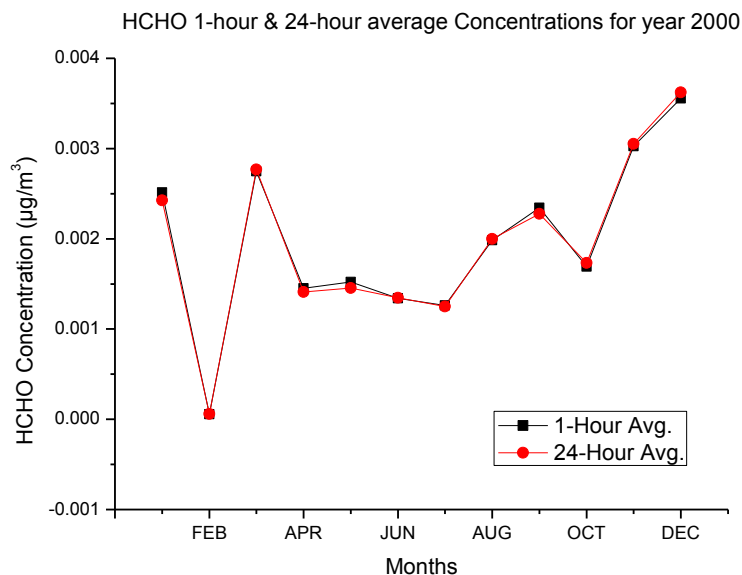
(a)
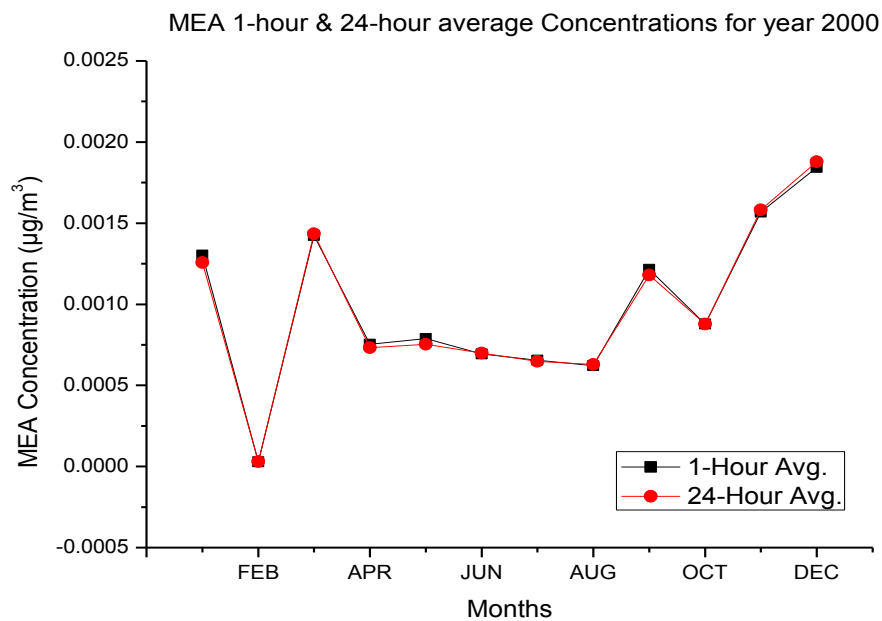
(b)

Figure 5-3 Results from modified CALPUFF model for year 2000: a) MEA 1-Hour & 24-Hour average concentration; b) Nitrosamines (NS) 1-Hour & 24-Hour average concentration.

Table 5-3 MEA & Nitrosamines 1-hour & 24-hour average concentrations from modified CALPUFF model

		MEA	NS	HCHO
	Average time	$\mu g/m^3$	ng/m^3	$\mu g/m^3$
JAN	1-Hour	1.3×10^{-3}	2.8×10^{-5}	2.5×10^{-3}
	24-Hours	1.3×10^{-3}	2.7×10^{-5}	2.4×10^{-3}
FEB	1-Hour	2.9×10^{-5}	6.3×10^{-7}	5.6×10^{-3}
	24-Hours	3.0×10^{-5}	6.5×10^{-7}	5.8×10^{-3}
MAR	1-Hour	1.4×10^{-3}	3.1×10^{-5}	2.7×10^{-3}
	24-Hours	1.4×10^{-3}	3.1×10^{-5}	2.8×10^{-3}
APR	1-Hour	7.5×10^{-4}	1.6×10^{-5}	1.5×10^{-3}
	24-Hours	7.3×10^{-4}	1.6×10^{-5}	1.4×10^{-3}
MAY	1-Hour	7.9×10^{-4}	1.7×10^{-5}	1.5×10^{-3}
	24-Hours	7.5×10^{-4}	1.6×10^{-5}	1.5×10^{-3}
JUN	1-Hour	6.9×10^{-4}	1.5×10^{-5}	1.3×10^{-3}
	24-Hours	6.9×10^{-4}	1.5×10^{-5}	1.3×10^{-3}
JUL	1-Hour	6.5×10^{-4}	1.4×10^{-5}	1.3×10^{-3}
	24-Hours	6.5×10^{-4}	1.4×10^{-5}	1.2×10^{-3}
AUG	1-Hour	1.0×10^{-3}	2.2×10^{-5}	2.0×10^{-3}
	24-Hours	1.0×10^{-3}	2.3×10^{-5}	2.0×10^{-3}
SEP	1-Hour	1.2×10^{-3}	2.6×10^{-5}	2.3×10^{-3}
	24-Hours	1.2×10^{-3}	2.6×10^{-5}	2.3×10^{-3}
OCT	1-Hour	8.8×10^{-4}	1.9×10^{-5}	1.7×10^{-3}
	24-Hours	9.0×10^{-4}	2.0×10^{-5}	1.7×10^{-3}
NOV	1-Hour	1.6×10^{-3}	3.4×10^{-5}	3.0×10^{-3}
	24-Hours	1.6×10^{-3}	3.4×10^{-5}	3.1×10^{-3}
DEC	1-Hour	1.8×10^{-3}	4.0×10^{-5}	3.6×10^{-3}
	24-Hours	1.9×10^{-3}	4.1×10^{-5}	3.6×10^{-3}

Figure 5-4 1-Hour & 24-Hour average concentration of Formaldehyde (HCHO) from modified CALPUFF model

5.3.2.2 Impact of stacks parameters on concentration values

To exam impacts of stack parameters on concentration values, worst case scenario was considered. The changes of stack parameters are shown in Table 5-4, only one parameter was assumed to be changed at each time in order to assess potential impacts of individual stack parameters. December data was selected for this task. Each scenario was run separately to generate concentrations of MEA, HCHO, and Nitrosamines (NS). The results are shown in Figure 5-5 and Figure 5-6 below. The nitrosamines result is shown separately as unit difference. The parameters were changed based on the conditions of a Norway PCC project (Fowler and Vernon, 2012b) . Figure 5-5 & Figure 5-6 show that changes to most of these parameters increased concentration values except for case DEC4 where the exit velocity was increased to 20 m/s from 13.9 m/s. In DEC4 case, the increased exit velocity decreases MEA, HCHO, and NS values by a factor of about 0.85. The results also indicated that DEC2 had highest increase comparing to other case scenarios. In DEC2, the changed parameter was stack height where was decreased to 65 meters from 248 meters for both stacks. The lower stacks result in reduced plume rise resulting as expected in higher calculated concentrations as expected. The results shown in this DEC2 scenario are higher than other scenarios. The concentration values in DEC2 were about 3.16 times higher than for the original parameters, reaching 1-hour average values of 0.005835 and 0.011256 $\mu g/m^3$ for MEA and HCHO respectively. The nitrosamines 1-hour average value was about 1.2664×10^{-4} ng/m^3. The DEC1 scenario indicates that the concentrations are higher than original setting with a factor of 1.87 while decreasing the diameters of stacks to half size of original. DEC3 had exit temperature decreased to 30 ˚C from 100 ˚C. The temperature change caused 2.41 times increase on three compounds values. The four case scenarios represent only a simple sensitivity analysis based on stack parameters.

Table 5-4 Different case scenarios for impact of stack parameters

Parameters	DEC	DEC1	DEC2	DEC3	DEC4
Stack Diameter (m)	12	6	12	12	12
Stack Height (m)	248	248	65	248	248
Exit Velocity (m/s)	13.9	13.9	13.9	13.9	20
Temperature (K)	373	373	373	303	373
MEA emission rate (g/s)	1.2441	1.2441	1.2441	1.2441	1.2441
Nitrosamines emission rate (g/s)	2.7×10^{-5}	2.7×10^{-5}	2.7×10^{-5}	2.7×10^{-5}	2.7×10^{-5}
HCHO emission rate (g/s)	2.3993	2.3993	2.3993	2.3993	2.3993

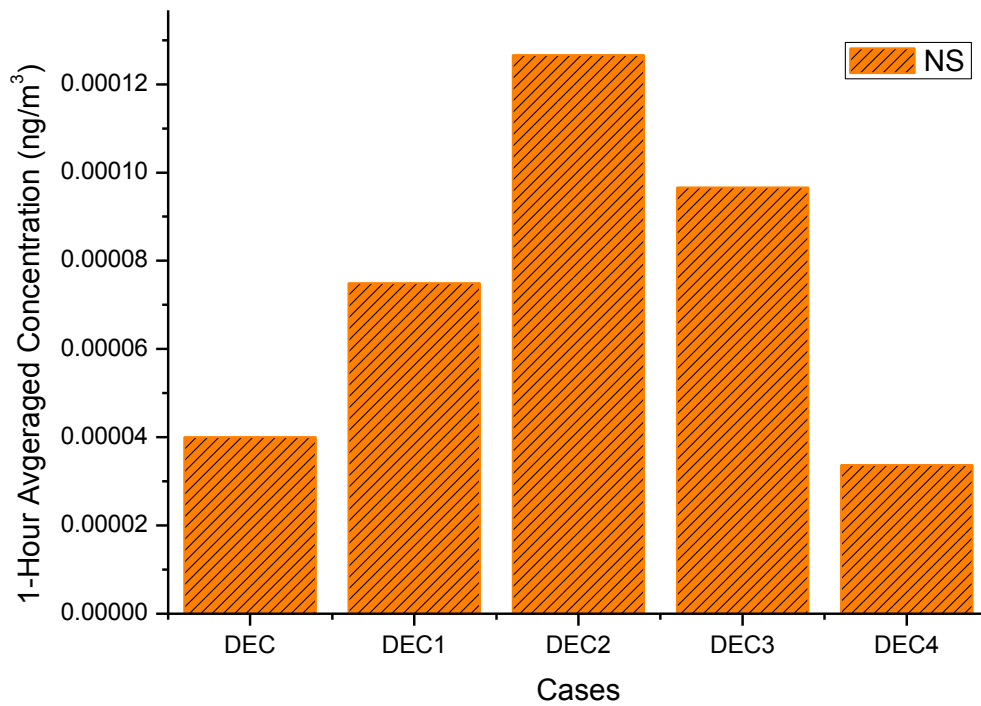Figure 5-5 Impact of stack parameters on MEA & HCHO concentrations of December data

Figure 5-6 Impact of stack parameters on Nitrosamines of December data

5.3.2.3 Health Effects based on concentration values

As mentioned in chapter 2, MEA has been recommended to have a threshold of 10 $\mu g/m^3$. The MEA maximum values modelled in this study was less than 1.844×10^{-3} $\mu g/m^3$ on 1-hour averaged monthly basis. The values are more than three orders of magnitude lower than the recommended threshold level. It is unlikely to have health effects based on the modelled concentrations.

USEPA and WHO both set inhalation risk limit on nitrosamines as a potential human carcinogenic compound. The value corresponding to 1 in 1,000,000 population is 0.07 ng/m^3 and 0.3 ng/m^3, respectively (Låg et al., 2009). In Norwegian studies (Berglen et al., 2010; Karl et al., 2011), worst case scenario was considered. The maximum concentration of nitrosamine was 0.032 ng/m^3 which is excess the inhalation risk limit WHO set. In CSIRO study (Emmerson et al., 2013), peak 1 hourly concentration of nitrosamines was predicted to be 2.46×10^{-11} ppb (about 7.3×10^{-8} ng/m^3 on dimethylnitrosamines) under CSIMEA scheme. The value from CSIRO study did not show much impacts on human health. In this research, the modelled concentration of nitrosamines were less than 4.001×10^{-5} ng/m^3 on 1-hour averaged time. The modelled value is about three orders of magnitude lower than USEPA limit. The cancer risk impact on human health is less concerned based on the simulation setting.

Formaldehyde has potential carcinogenicity on human health. USEPA also set risk limit of 0.08 $\mu g/m^3$ on 1 in 1,000,000 population for formaldehyde inhalation exposure. The value is much higher than the value from the modelled case study. Based on setting of the modified CALPUFF model, the background value of formaldehyde was not be considered. The ambient formaldehyde value could be higher than the result from the modified CALPUFF model which was aimed to simulate MEA and its oxidation products mainly. The more detailed simulation for other emissions like NH_3 and formaldehyde will be discussed in the next chapter using TAPM model.

# Chapter 6 Atmospheric dispersion of air pollutants in NSW using TAPM-CTM model

6.1 TAPM-CTM model configuration

6.1.1 Chemical transport modelling

The Air Pollution Model with Chemical Transport model (TAPM-CTM), developed by CSIRO, was employed in this study to simulate atmospheric movement and reactions of primary air pollutants. Nitrosamines, nitramines, and MEA are not considered in this model simulation due to minor formation and fast degradation of nitrosamines and nitramines in the atmopshere. The model system, which consists of a prognostic meteorological model and a chemical transport model, has been validated to provide reasonable simulations of atmospheric movement and reliable forecasts of near-surface concentration values (Hurley et al., 2005). The CTM has the capability to undertake complex chemical and aerosol transformation (Cope and Lee, 2009). The gas-phase chemical transformation was modelled using Carbon Bond 6 (CB-VI) mechanism with inorganic and organic aerosol chemistry. Previous studies assumed that the secondary inorganic aerosol chemistry occurred in thermodynamic equilibrium with gas-phase precursor (Cope et al., 2014; Fountoukis and Nenes, 2007). The chemistry was modelled using the ISORROPIA II model (Fountoukis and Nenes, 2007). The Volatility Basis Set approach is used to model secondary organic aerosols chemistry (Donahue et al., 2006). Plume-in-grid model was not used in this study as the study aims to simulate regional effect of emissions from PCC technology on health impacts. The meteorological data were based on the years 2011, 2014, and 2015, obtained from CSIRO.

The TAPM-CTM model was run separately to simulate a PCC case scenario and the base case scenario to understand potential impacts from post-combustion carbon capture projects. The outer grid domain spacing was 30 km × 30 km, centered on the Bayswater Power Station (32˚23.5"S, 150˚57"E). A nested grid system of four levels was used; with a domain spacing of 30 km, 10 km, 3 km, and 1 km. The most inner grid spacing captures the main Upper Hunter industrial area to the northwest, which includes Muswellbrook town with 16,167 people (NSW Health, 2010). Each grid domain has 30 × 30 grid cells with 25 vertical levels. In the CTM simulation, the vertical initial conditions and boundary conditions that were

provided by NSW EPA, also include 4.62 ppb NH_3 and 10 µg/m^3 $PM_{2.5}$. As the CB-VI mechanism including aerosol chemistry considers $PM_{2.5}$ specification, the concentration of 10 µg/m^3 of $PM_{2.5}$ were assigned into four main species: sulfate aerosol less than 2.5µm
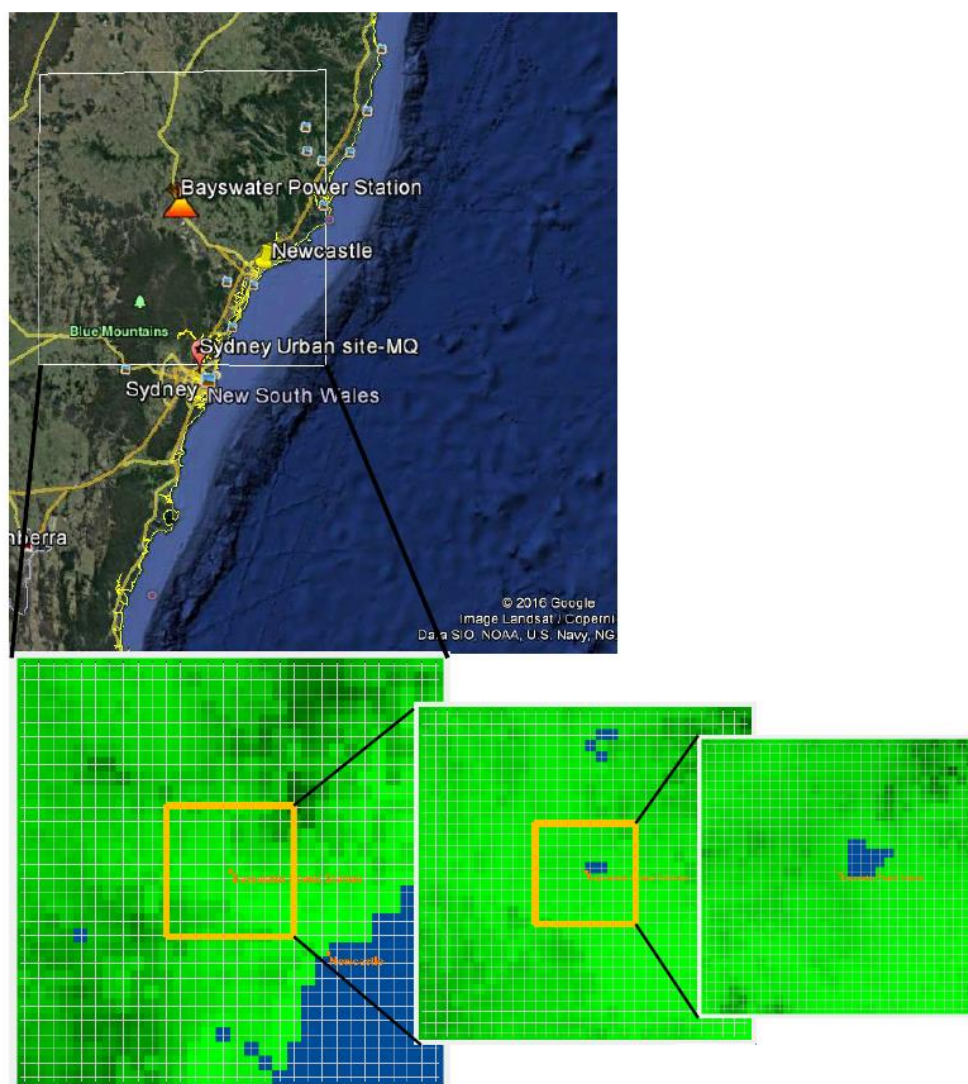
Figure 6-1 TAPM-CTM modelling domains used for this study region

(ASO4), $PM_{2.5}$ elemental carbon (EC25), $PM_{2.5}$ organic carbon (OC25), and $PM_{2.5}$ miscellaneous (OT25) with percentage of 5.69 %, 16.78 %, 17.84 %, and 59.69 % based on a previous Upper Hunter particle study (Hibberd et al., 2013). This study also considers gas phase ammonium nitrate and sulfate production to assess potential nitrate and sulfate aerosol impacts.

6.1.2 Emissions

The base case emission data provided by NSW EPA were based on the 2003 air emission inventory. Modeled base case emissions includes all anthropogenic sources, but turns off the

biogenic emissions. Anthropogenic sources include emissions from roadside, domestic, commercial and industrial sources for the Greater Sydney Metropolitan Region. The emissions are provided in three emission files, as domestic and commercial area sources, motor vehicles sources, and elevated industrial point sources. Species in the emissions inventory include NO_x, CO, SO_2, PART ($PM_{2.5}$ dominated particulate), and other main air pollutants. As this study considers impacts of NH_3 emissions from a PCC capture project, the NH_3 is added into the species list. The NSW EPA does not estimate the emission of ammonia for the greater Sydney region. The emission of ammonia was calculated by assuming a ratio of NH_3 to NO_x concentrations of 0.024: 1 (Cope et al., 2014; Emmerson et al., 2013). The NSW EPA inventory was originally created for use with the Carbon Bond 4 (CB-IV) mechanism for VOC emissions. CB-IV provides total particles, but does not specify $PM_{2.5}$ mass components. It is not possible to use the original NSW EPA 2003 air emission inventory for the CB-VI and aerosol mechanism. In order to undertake detailed speciation assessment of $PM_{2.5}$ emission, a method used in the Sydney Particle Study was used (Cope et al., 2014). This method uses emission factors to consider $PM_{2.5}$ speciation for all sources. These emission factors are shown in Table 6-1.

Table 6-1 Ratios of key components for speciation of $PM_{2.5}$

	OC25:PM25	EC25:PM25	OT25:PM25	ASO4:PM25
Motor Vehicle emission	0.430	0.283	0.239	0.048
Domestic and commercial area emission	0.391	0.202	0.206	0.200
Industrial point Sources emission	0.235	0.316	0.171	0.278

These ratios are based on units of mass (tonnes per year). However, the emission data in the NSW EPA 2003 inventory are in units of volume (ppmV/min). During simulation, TAPM converts the volume units to g/s using Equation 6.1 based on personal contact with Dr. Martin Cope, the developer of the TAPM-CTM model. This conversion takes into consideration the molecular weight of species when doing ratio assignment for detailed $PM_{2.5}$ speciation.

$$Q_{g/s} = Q_{ppmV/\min} \times mole_{air} \times MW\_\text{species} \times 10^{-6} \times \frac{1}{60} \qquad (6.1)$$

Where:

$Q_{g/s}$ = emission rate in unit of g/s

$Q_{ppmV/min}$ = emission rate in unit of ppmV/min

$mole_{air}$ = molecular weight of air

$MW\_species$ = molecular weight of species

6.1.3 Case scenario of TAPM-CTM simulation

The TAPM-CTM simulations were run for each individual month of year 2011, year 2014, and year 2015 to consider different meteorological impacts for PCC case scenario. The base case scenario was modelled using NSW EPA 2003 air emission inventory with additional calculated emission data of NH_3 and $PM_{2.5}$ species as described above. The PCC case scenario included the emissions of post-combustion technology. In the PCC scenario, NO_x emissions were assumed to be decreased by 70% and SO_2 emissions were decreased by 95% due to post-combustion capture technology. The NH_3, formaldehyde, and acetaldehyde emission rates included the additional emissions of these compounds from PCC technology. $PM_{2.5}$ emissions were kept same in the PCC case as the base case; it was assumed that there was no change on $PM_{2.5}$ emission due to PCC technology. The emission rates of these compounds were calculated from the findings of a previous study (Thong et al., 2012) and were converted to fit the Bayswater Power Station parameters. The Bayswater Power Station emissions under post-combustion case scenarios are hypothetical. The detailed emission rates of main chemical compounds are shown in Table 6-2.

Table 6-2: Emissions (per stack) from Bayswater Power Station before and after post-combustion carbon capture technology has been installed. The power station under PCC case scenario are hypothetical.

	Base (g/s)	PCC (g/s)
NO	381.8	114.5
NO_2	30.78	9.24
SO_2	1332.36	66.62
FORM	0.00	2.40
ALD2	0.00	2.67
NH_3	0.017	1.08
ASO4	0.18	0.18
EC25	0.29	0.29
OT25	0.16	0.16
OC25	0.22	0.22

6.1.4 Data processing

The simulations were generated in month-long periods, and results were processed and analysed using MatLab. The emission changes of NO_x, SO_2, NH_3, formaldehyde, acetaldehyde,

ASO$_4$ (Sulphate aerosol), and PM$_{2.5}$ by post-combustion carbon capture technology under different meteorological conditions was the primary focus of the analysis. Hourly concentrations of each compound were calculated for each day at each grid point. The daily peak value of each compound was maximum hourly average for each day at each grid point. The maximum monthly value was determined based on the daily maximum value for each compound at 1-km resolution 30×30 grid domain.

As PM$_{2.5}$ National Environmental Protection Measure (NEPM) standard is based on a 24-hour averaging time, PM$_{2.5}$ data was processed for the same 24-hour average time. The CTM breaks PM$_{2.5}$ into different species, such as ASO$_4$, EC$_{2.5}$, OT$_{2.5}$, SS$_{2.5}$, NH$_4$ (ammonium ions aerosol), NIT (aerosol nitrate), SOD (Sodium aerosols), MAG (Magnesium aerosols), CAL (Calcium aerosols), POT (Potassium aerosols), CL (Chlorine aerosols), and OC$_{2.5}$ (Organic carbon). The OC$_{2.5}$ was further broken down into 9 aerosol species, named as APA1, APA2 ...APA9. SS$_{2.5}$ indicates sea salt aerosol. EC$_{2.5}$ is elemental carbon, and OT$_{2.5}$ includes all other components that make up the balance of the aerosol emissions estimate. The modelled PM$_{2.5}$ concentrations are the sum of the individual modelled PM species using the following equations.

$$OC_{2.5} = APA_1 + APA_2 + ... + APA_9 \tag{6.2}$$

$$PM_{2.5}(CTM) = EC_{2.5} + 1.4 \times OC_{2.5} + OT_{2.5} + SS_{2.5} + ASO_4 + NH_4 + NIT \\ + SOD + MAG + CAL + POT + CL \tag{6.3}$$

Here OC$_{2.5}$ has been scaled by 1.4 to include the mass of associated hydrogen and oxygen groups"(Keywood et al., 2008). To calculate PM$_{2.5}$ concentration, MatLab generated data from NetCDF files on 24-hourly average basis for each day for each PM$_{2.5}$ species at 1-km resolution 30x30 grid domain. After calculating the sum of PM$_{2.5}$ using equation (6.3) for daily concentrations, the monthly peak value of PM$_{2.5}$ was derived from the maximum value of daily 24-hourly averaged values for each grid point from the whole month daily averaged value.

6.2 Analysis of atmospheric dispersion

This section presents the modelled results for each year. First, the January 2015 results will be compared with a previous study using the TAPM-CTM (Emmerson et al., 2013). After

that, the changes of atmospheric concentrations of each compound in monthly basis for each modelled year are discussed.

6.2.1 Comparison with a similar study

CSIRO has done a similar study (Emmerson et al., 2013) to determine the fate of PCC emissions into the atmosphere. The study was undertaken in a hypothetical power station in Wyong NSW, which is close to this study location. In the CSIRO study, 2003 NSW EPA air emissions inventory data were used in a model simulation of January 2004. In this Bayswater study, 2003 NSW EPA air emission inventory data and Carbon Bond 6 with aerosol mechanism were also employed in model simulation for whole study years. The detailed parameters for the CSIRO PCC power station (Emmerson et al., 2013) and Bayswater power station (this study) are both listed in Table 6-3.

Table 6-3 Comparison of the CSIRO PCC project and this study PCC project

Parameters	CSIRO study parameters	This study parameters
Stack height (m)	178	248
Stack radium (m)	5.2	6
Velocity (m/s)	17.7	13.9
Temperature (K)	395	307

To examine the reliability of the Bayswater study, the results in 3 km grid are placed in this section (Section 6.2.1) to obtain same resolution with CSIRO study. The results show the difference between the base case and PCC scenarios for criteria pollutants in the greater Sydney area. As the CSIRO study only considered one month (January 2004), only January 2015 3 km resolution results of this study are shown here. Full results that consider three years in 1 km resolution are discussed in Section 6.2.2.
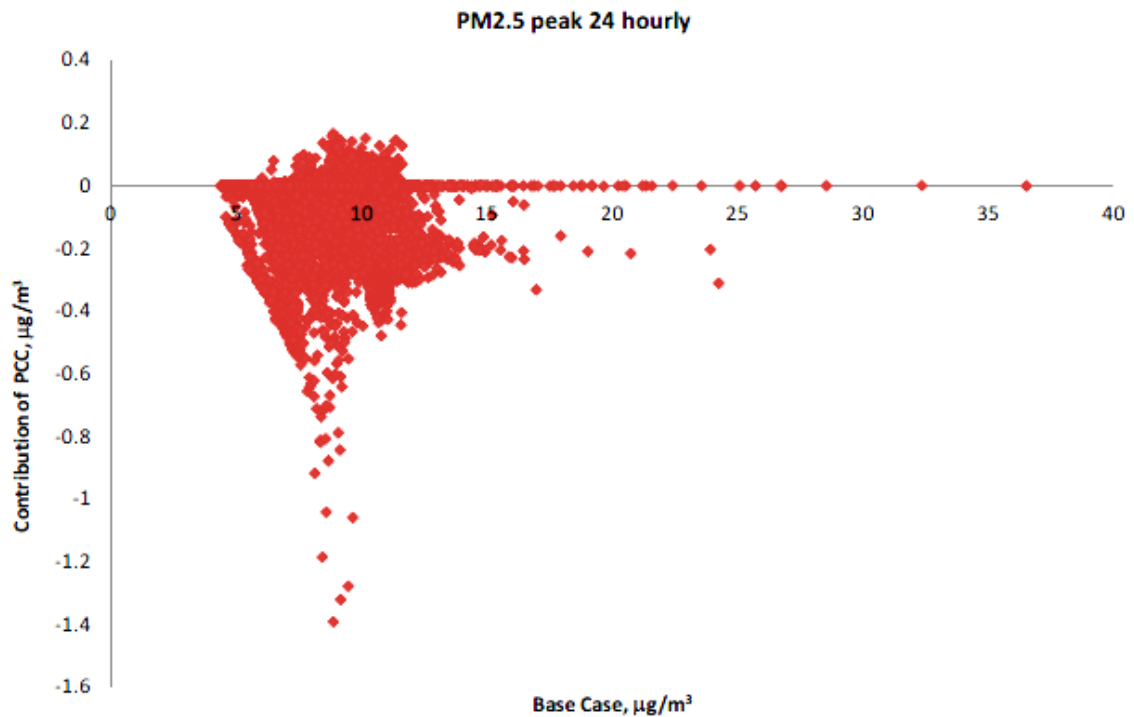
(a)
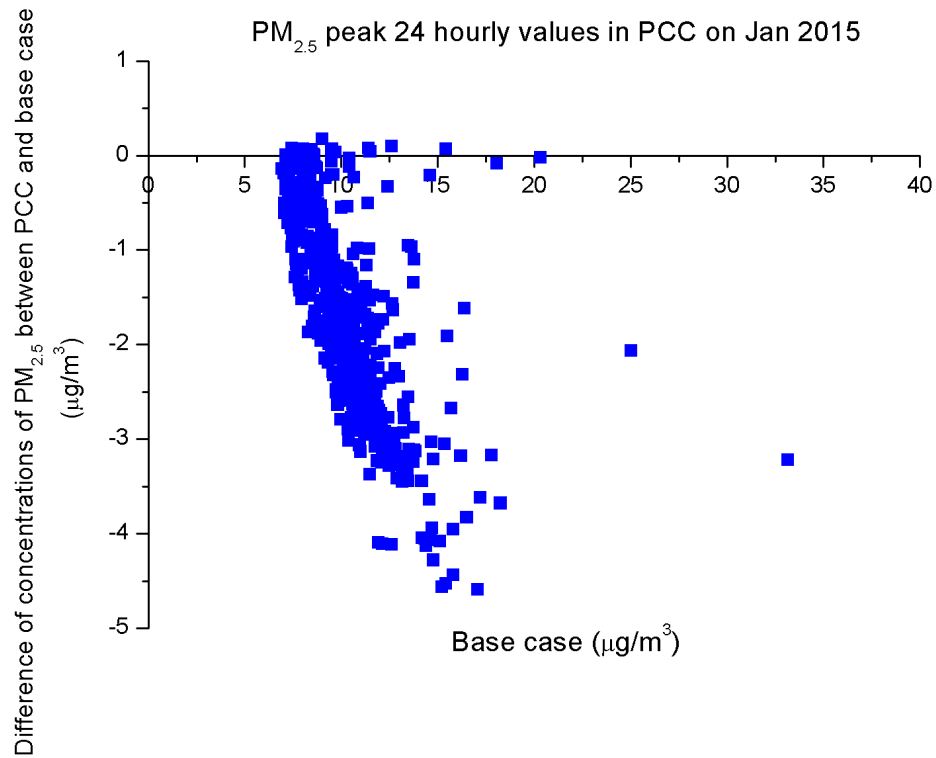
(b)

Figure 6-2: (a) Grid cell variation of this study PCC case contribution of PM2.5 to the Base Case; (b): the grid cell of variation of CSIRO study PCC contribution of PM2.5 to the base case run. plot (b) source from (Emmerson et al., 2013)

Peak 24- hourly average values of $PM_{2.5}$ from this study are shown in Figure 6-2 (a), and results from the CSIRO study are shown in Figure 6-2(b). The modeled 24-hourly concentration of $PM_{2.5}$ in this study decreased up to 4.6 μg/m^3 in January 2015 when a PCC plant was added to the region. The decrease is similar to CSIRO study, where $PM_{2.5}$ decreased up to 1.4 μg/m^3. The decrease in $PM_{2.5}$ is primarily due to the decrease of ASO_4, NIT, and NH_4 by decreasing emissions of SO_2 and NO_x from the PCC project. The peak 24-hourly concentrations of ASO_4, NIT, and NH_4 in PCC case scenario are decreased up to 52.4 μg/m^3, 7.0 μg/m^3, and 4.6 μg/m^3, respectively. The decreased range of ASO_4 (Figure 6-3) is larger than the decreased range reported by the CSIRO study, but it is considered to be reasonable as the parameters of the studied power station (Bayswater) and emission rates are different due to different capacities between these two studies. In addition, the modelled domain of this study is only 30×30 cells while the domain of the CSIRO study is 100×100 cells. The change in NH_4 between the base case and the inclusion of PCC technology, a decrease of up to 4.6 μg/m^3 (Figure 6-4) is larger than the decrease observed in the CSIRO study. The NIT change ranged from a decrease up to 7.0 μg/m^3 to an increase of up to 2.8 μg/m^3 (Figure 6-5). From these plots, it can be seen that when concentration of ASO_4 and NH_4 are low in the base case, the change in concentration is small with the addition of PCC technology. Higher concentrations in base case lead to high change in concentration. However, NIT values show more random changes corresponding to the concentration values.

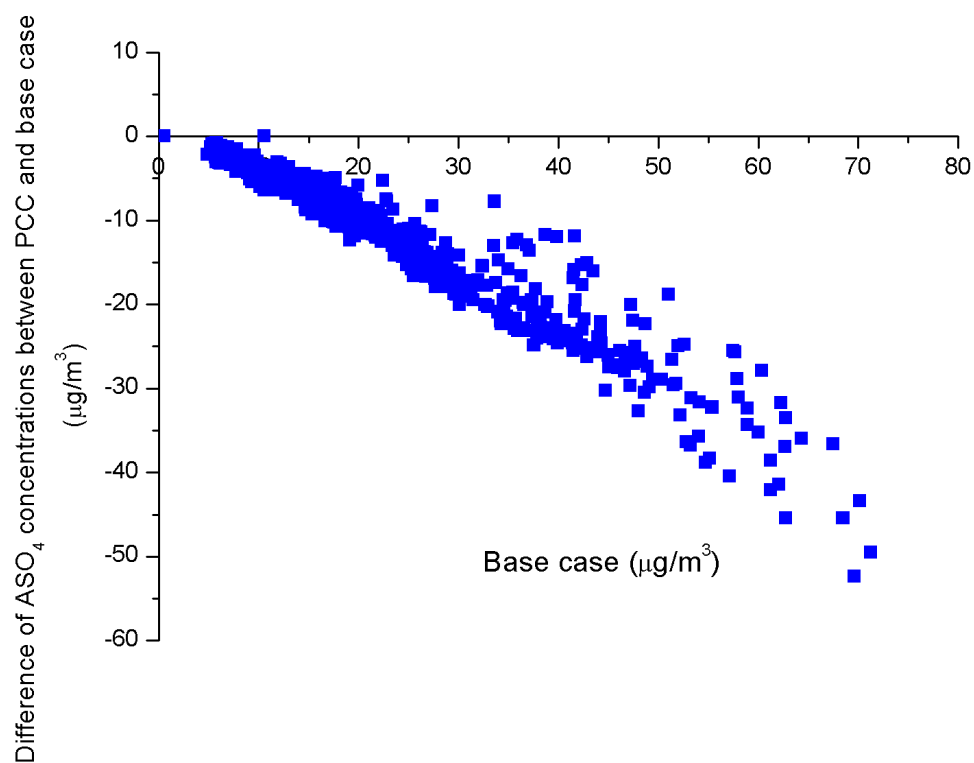**Figure 6-3 the grid cells of variation of this study PCC case contribution of ASO4 to the base case**
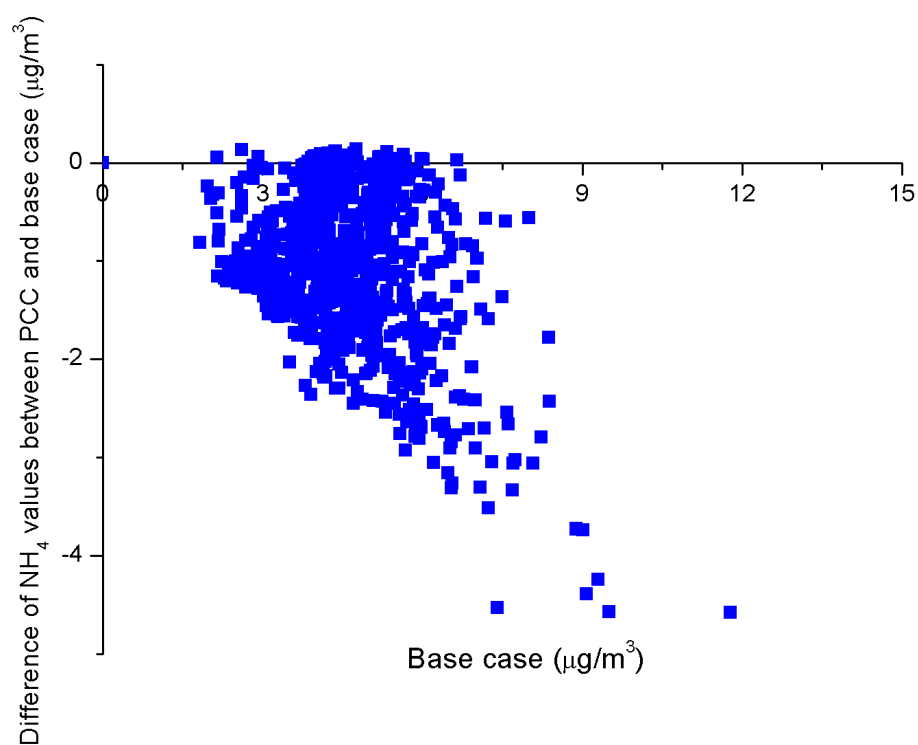
Figure 6-4 the grid cells variation of NH4 in this study comparing to the base case
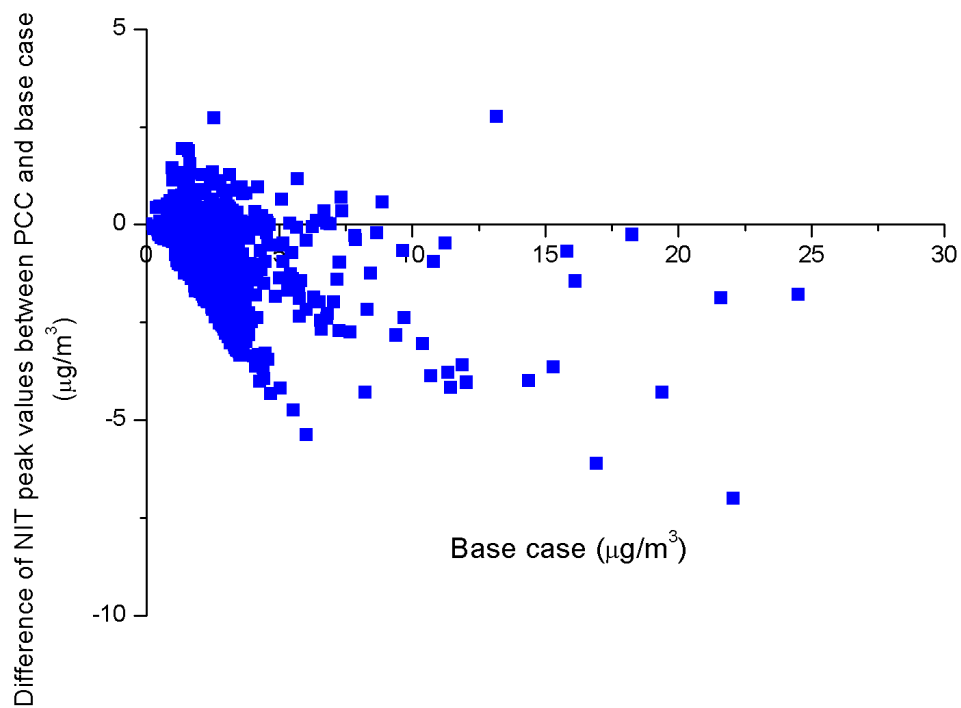
Figure 6-5 the grid cells variation of NIT in this study comparing to the base case

In the study, the NO_x and SO_2 emissions under the PCC case scenario were decreased by 70% and 95% respectively, and $PM_{2.5}$ emissions were kept the same as the base case. The modelled SO_2 peak 1-hourly value in January 2015 is shown in Figure 6-6(a), with the comparable CSIRO results shown in Figure 6-6(b).

The changes in SO_2 concentration between the base case and the addition of PCC technology in this study are similar to the results from the CSIRO study. In this study, the SO_2 1-hour average concentration was decreased up to 188 ppb as the emission of SO_2 was reduced by 95% in PCC cases. Comparing to the CSIRO study, the SO_2 value was decreased by up to 117 ppb. From the two plots in Figure 6-6, both SO_2 changes present a trend that the PCC technology has a more significant effect on SO_2 reduction at higher concentration levels.

The TAPM-CTM model has been proven to provide reliable simulations of air pollution (Cope et al., 2014; NSWEPA, 2005). The similar trends in these results demonstrate that the study using the TAPM-CTM model is reliable to examine the impacts of the PCC technology in air pollution.

(a)
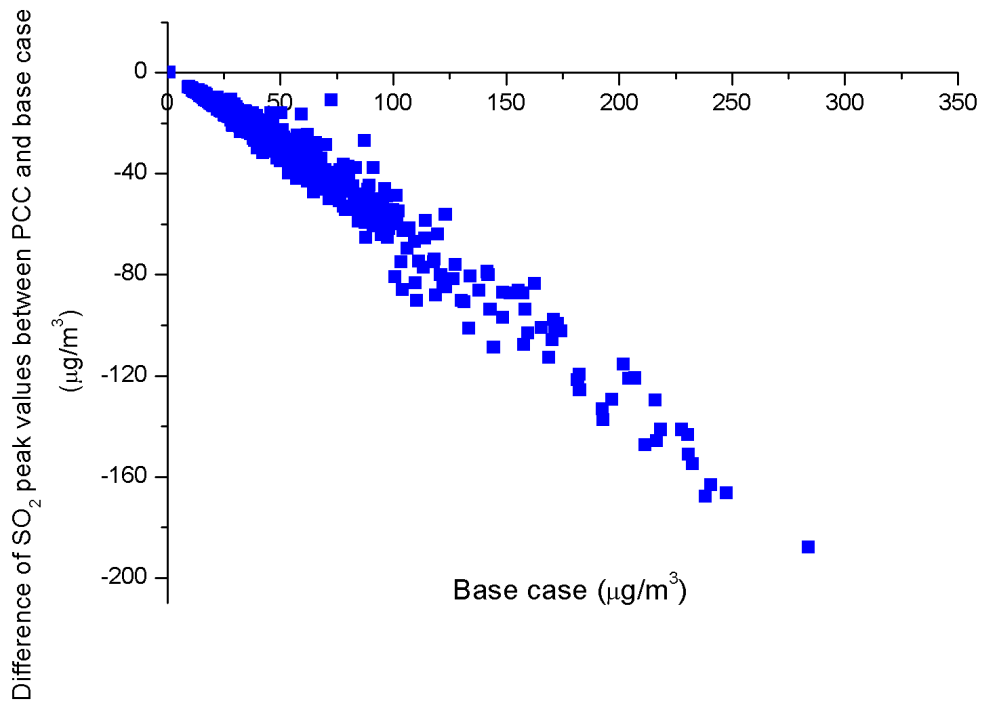
(b)

Figure 6-6 (a): the grid cells variation of SO₂ in this study comparing to the base case concentrations; (b): the grid cells variation of SO₂ in the CSIRO study comparing to the base case concentrations.
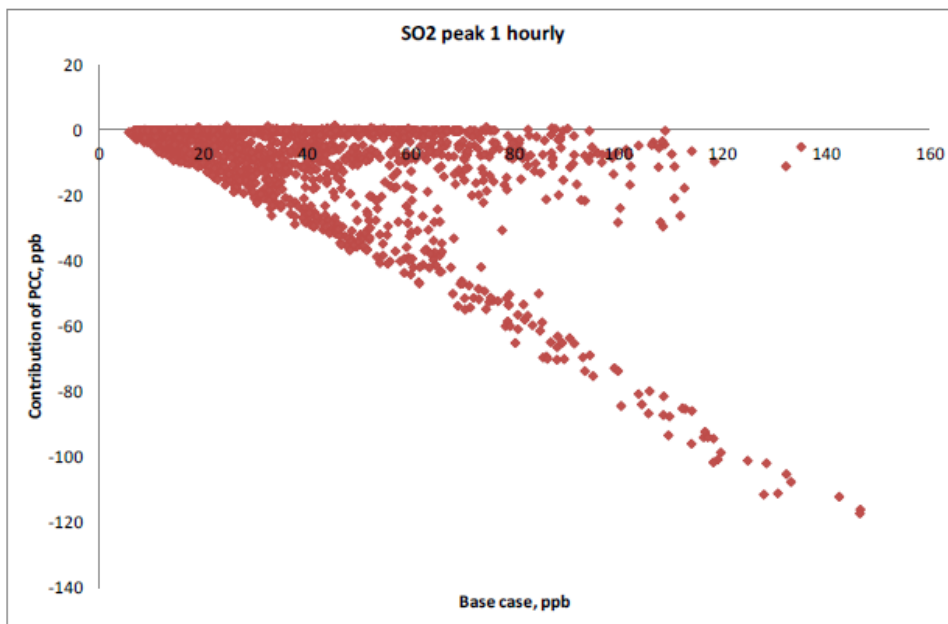
6.2.2 Results for each month of PCC case scenarios

In the TAPM-CTM simulation, three calendar years were selected for simulation: 2011, 2014, and 2015. These three years were selected for this study in order to provide the widest range of meteorological conditions that might affect the atmospheric concentrations of chemicals. 2011 was in the middle of La Niña event (2010-2012) according to Bureau of Meteorology (BOM) data. La Niña events normally bring wetter conditions to eastern and northern Australia (BOM, 2015b). In the La Niña pattern, higher than average rainfall occurred in the first three months and the last three months of year 2011, and dry conditions prevailed April to September 2011 under neutral El Niño Southern Oscillation (ENSO) conditions. 2011 was the second wettest year on record in Australia with an average rainfall of 708 mm (BOM, 2015b). 2014 was considered to be a normal year with a trend toward El Niño (BOM, 2014), and 2015 showed a clear El Niño signal. El Niño years normally have lower rainfall in winter and spring (June-November), and higher daytime temperatures over the southern half of Australia (BOM, 2015c). The results below are shown in 1 km resolution domain.

6.2.2.1 Nitrogen Oxides and Sulfur Dioxide

The maximum changes of peak values of NO, NO_2, and SO_2 have been shown in Figure 6-7, Figure 6-8, and Figure 6-9. These figures show maximum changes of peak values between PCC case and base case in 1 km resolution domain. The values above zero mean the maximum increase of peak values, and the values below zero represent the maximum decrease of peak values. As NO_x (NO + NO_2) and SO_2 emissions are assumed to be decreased by 70% and 95%, respectively, due to PCC technology, the averaged concentrations of peak values show a decrease in all modelled months. In 2011, the mean values of the modelled NO, NO_2, and SO_2 peak value changed in a range of -16. 6 ppb to -3.7 ppb, a range of -30.3 ppb to -4.4 ppb, and a range of -101.4 ppb to -26.5 ppb, respectively. In 2014, the decrease ranges were -18. 5 ppb to -5.0 ppb in NO, -27.4 ppb to -9.4 ppb in NO_2, and -99.3 ppb to -40.7 ppb in SO_2. In 2015, the modelled NO, NO_2, and SO_2 average peak value changed in the range of -16.0 ppb to -3.2 ppb, a range of -32.9 ppb to -6.0 ppb, a range of -99.7 ppb to -30.2 ppb, respectively.

According to these three years' simulations, the highest increases of NO concentration were in Jun 2015 with a value of 8.4 ppb, and the highest increases of NO_2 occurred on July 2015 with a value of 3.6 ppb. NO_x are important air pollutants in the atmosphere, as NO_2 reacts under bright light to form ground-level ozone which is a primary component of smog (Cox, 1999; Emmerson et al., 2013). In addition, NO can react with free radicals from the photo oxidation of VOCs to form NO_2 (Cox, 1999). CSIRO has reported that NO_2 and O_3 have a titration effect relationship (Emmerson et al., 2013). These simulations show the average NO_2 concentrations decreased largely in all months due to 70% emission decrease; the O_3 mean concentrations also show a decrease. The changes in concentration and the relationship of NO_2 and O_3 in the three study years are shown in Figure 6-10, Figure 6-11, and Figure 6-12. As the simulation used CB-VI, the mechanism's NO_x and O_3 reactions are shown below:

$$NO_2 \rightarrow NO + O \tag{6.4}$$

$$O + O_2 + M \rightarrow O_3 + M \tag{6.5}$$

$$O_3 + NO \rightarrow NO_2 \tag{6.6}$$

When NO_2 emission decreased, the reactions of NO_2 to oxygen singlet (O) reduced. As a result, the formation of ground-level O_3 in PCC was less than the formation in pre-PCC case scenario. As both ground-level O_3 and NO decrease, less NO_2 was formed in the atmosphere in PCC case scenario. From Figure 6-10, Figure 6-11, and Figure 6-12, the NO_2 mean peak values had a large amount of decrease, the main factor contributed to NO_2 decrease was the NO_x emission decreased by 70%.

Figure 6-7 Maximum changes of peak values of NO in 2011, 2014, and 2015 in 1 km resolution PCC1 case

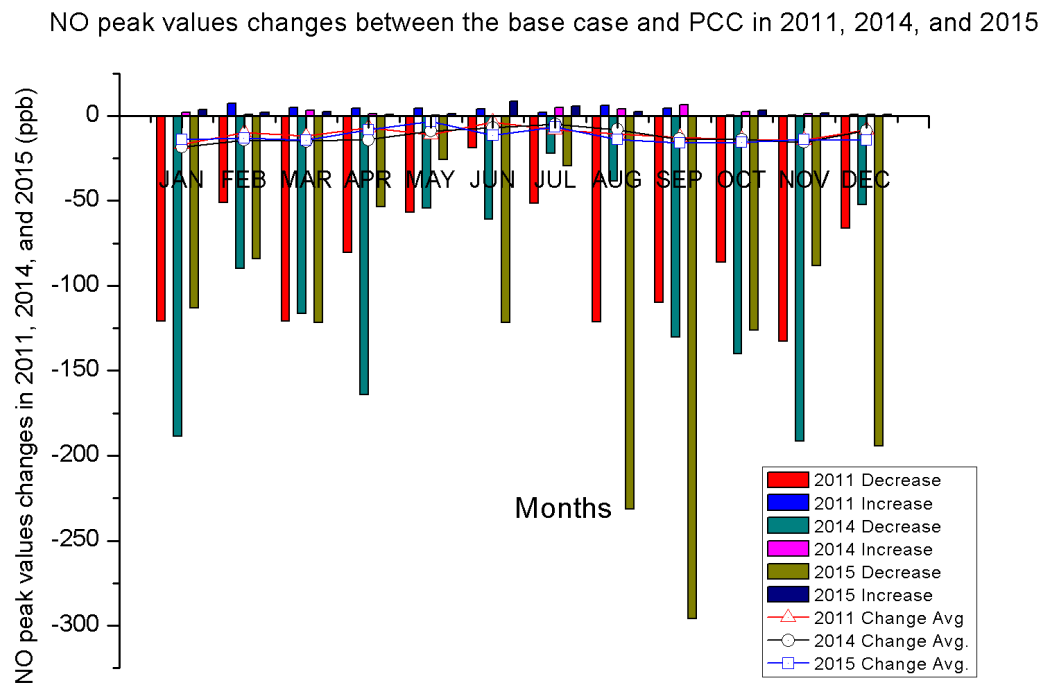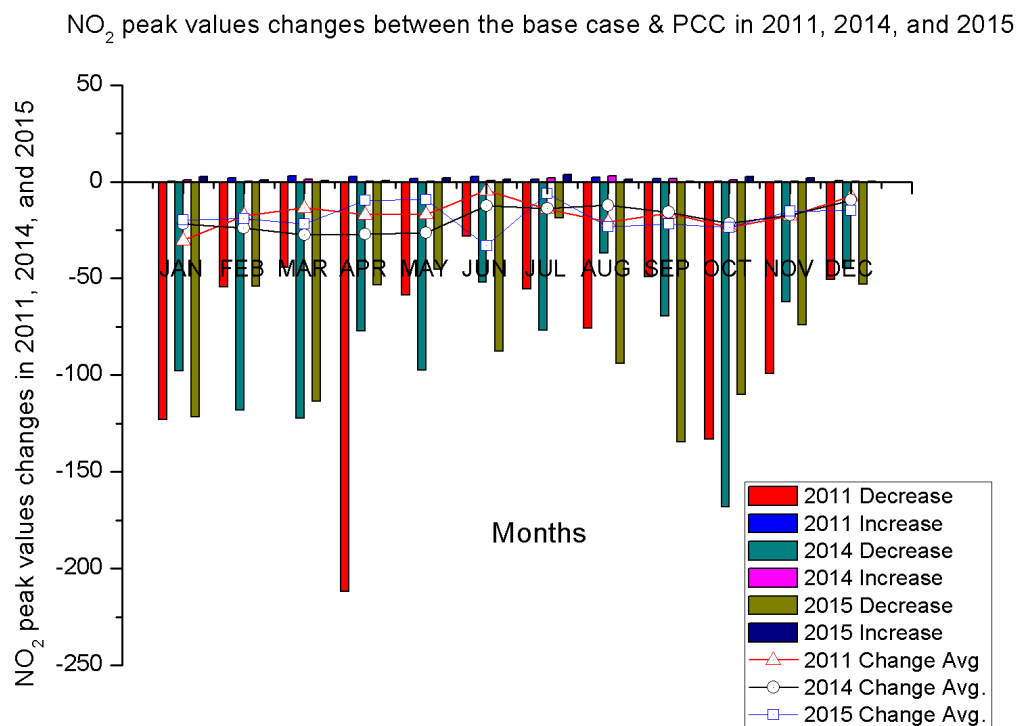**Figure 6-8 Maximum changes of peak values of NO₂ in 2011, 2014, and 2015 in 1 km resolution PCC1 case**
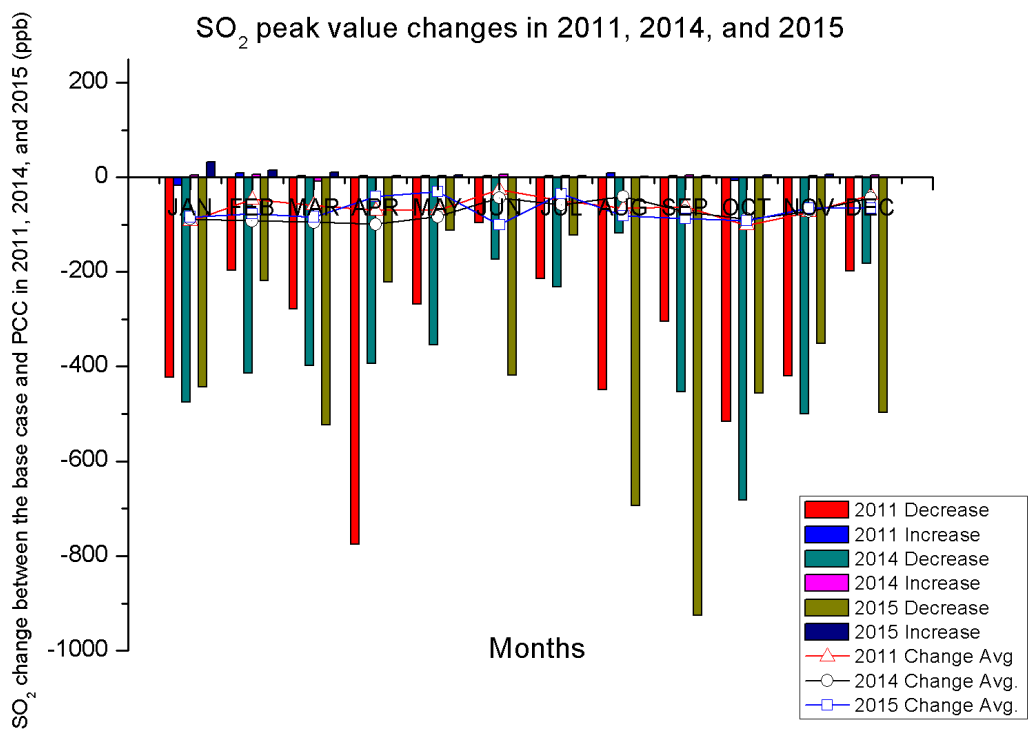
Figure 6-9 Maximum changes of peak values of SO₂ in 2011, 2014, and 2015 in 1 km resolution PCC1 case
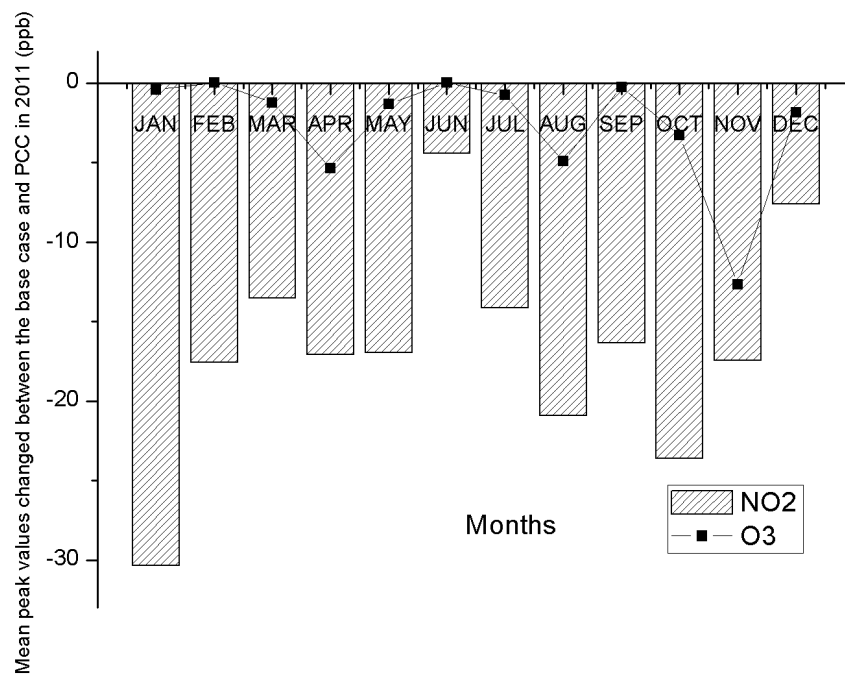
Figure 6-10 Change of mean peak values of NO$_2$ and O$_3$ between PCC and base case in 2011
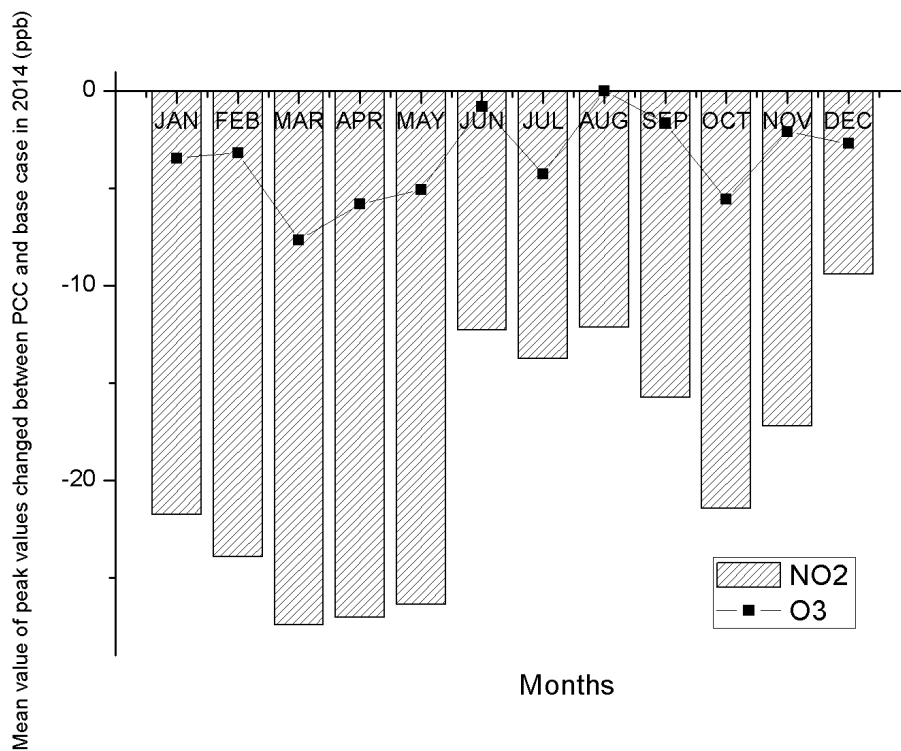
Figure 6-11 Change of mean peak values of NO$_2$ and O$_3$ between PCC and base case in 2014

101
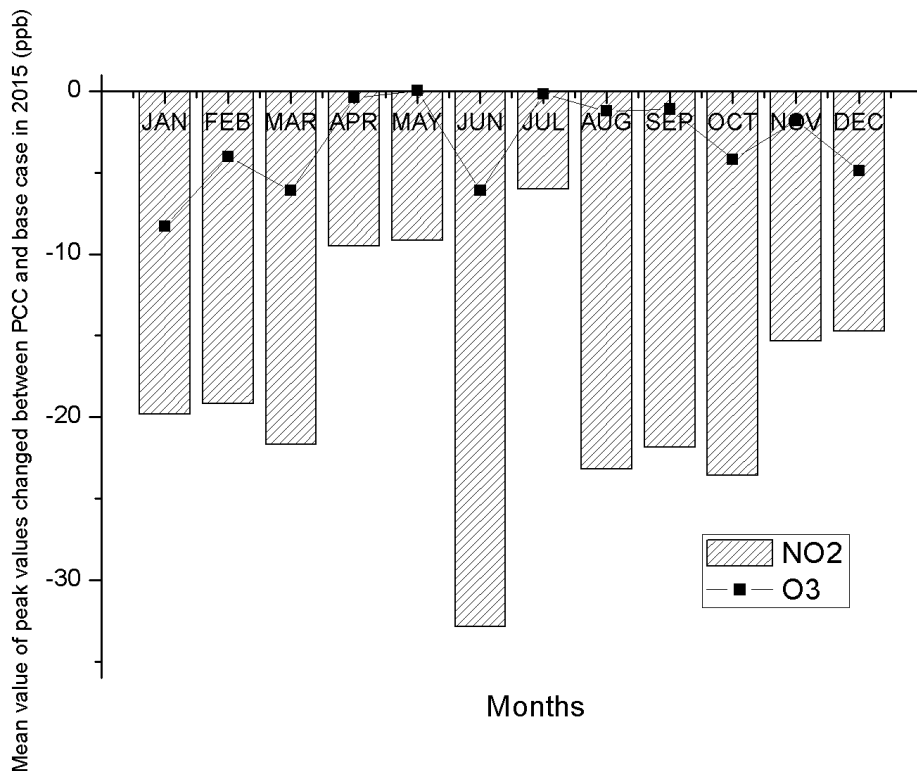
Figure 6-12 Change of mean peak values of NO$_2$ and O$_3$ between PCC and base case in 2015

Contour maps of NO, NO$_2$, and SO$_2$ in 2015 have been presented in Appendix 1-3 on a monthly basis. As the emission rates of NO$_x$ were assumed to decrease with the addition of PCC technology, most areas in the contour maps are showing decreases in concentrations. Clear decreases in NO concentrations were found near or within 5 km of the power station in every month of 2015 except May and July. Maximum decreases of NO concentrations in those two months were shown within 10-15 km of the power station. NO$_2$ concentrations showed more apparent decrease spread over the study domain, but the contour maps showed the maximum increase areas were around or within 10 km region of the power station in most months.

SO$_2$ emissions were assumed to decrease by 95%. Therefore, the decrease of concentrations in the study domain was more apparent. As discussed in previous work (Wu and Nelson, 2014), the dominant wind direction is southeast in summer and northwest in winter. The large decreases in 2015 (Appendix 3) were shown in the area around the power station in the direction of the dominant wind pattern, except in March, April and November, when the maximum decrease was to the west of the power station. Comparing the three different

meteorological conditions in Figure 6-9, the results showed that the average peak values were changed in a range of -101.4 ppb to -26.5 ppb, -99.3 ppb to -40.7 ppb, -99.7 ppb to -30.2 ppb in 2011, 2014, 2015 respectively. The meteorological conditions are likely to play a less significant impact on SO_2 concentrations under 95% emission decrease.

6.2.2.2 Aldehydes

Several studies have reported an increase of formaldehyde (HCHO) and acetaldehyde emissions when PCC technology is added to a power station (Emmerson et al., 2013; Morken et al., 2014; Thong et al., 2012). This study assumed that HCHO and acetaldehyde emission rates were increased by 2.4 g/s and 2.7 g/s, respectively. From the three year-long simulations, the peak values of HCHO were changed in a range of -19.2 ppb to 0.5 ppb, -13.6 ppb to 0.6 ppb, and -10.1 ppb to 0.4 ppb in 2011, 2014, and 2015, respectively. The emissions increase of HCHO did not result in a significant increase of atmospheric HCHO concentrations. The difference of acetaldehyde peak values was similar to the changes modelled in HCHO peak values. These differences of peak HCHO and acetaldehyde values are shown in Figure 6-13 and Figure 6-14.

The maximum increase of HCHO during the three modelled years that appeared in March 2014, was 0.6 ppb, and was located on about 11 km east of the stacks. In the same month, the monthly maximum decrease was about 10 km away from the power station, to the northwest (Figure 6-15). The maximum increase of acetaldehyde peak values occurred in August 2015 with a value of 0.8 ppb. The contour map of acetaldehyde peak values change in August 2015 is shown in Figure 6-16. The highest increase in August 2015 was around the power station, but most of the domain area showed a decrease in concentration. The increased emissions of HCHO and acetaldehyde did not cause large impacts on concentration change.

Formaldehyde peak values changes between the base case & PCC in 2011, 2014, and 2015
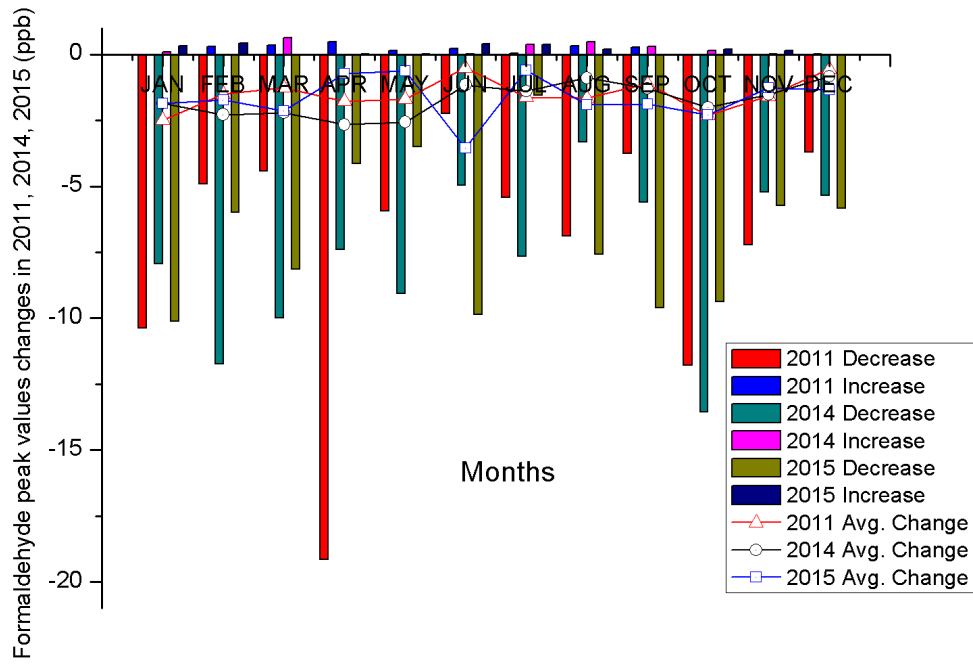
Figure 6-13 Maximum changes of formaldehyde in PCC1 case in 2011, 2014 & 2015

Acetaldehyde peak values changes between the base case & PCC in 2011, 2014, and 2015
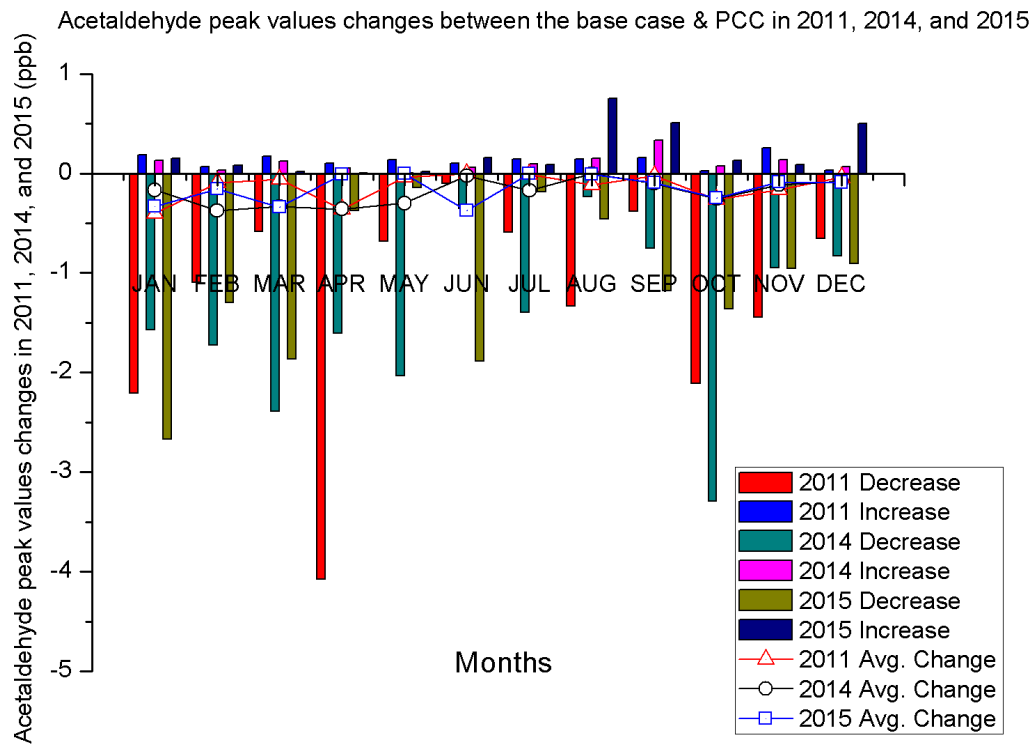
Figure 6-14 Maximum changes of acetaldehyde in PCC1 case in 2011, 2014 & 2015

Change of formaldehyde peak values in March 2014 between PCC and PrePCC (1 km resolution)
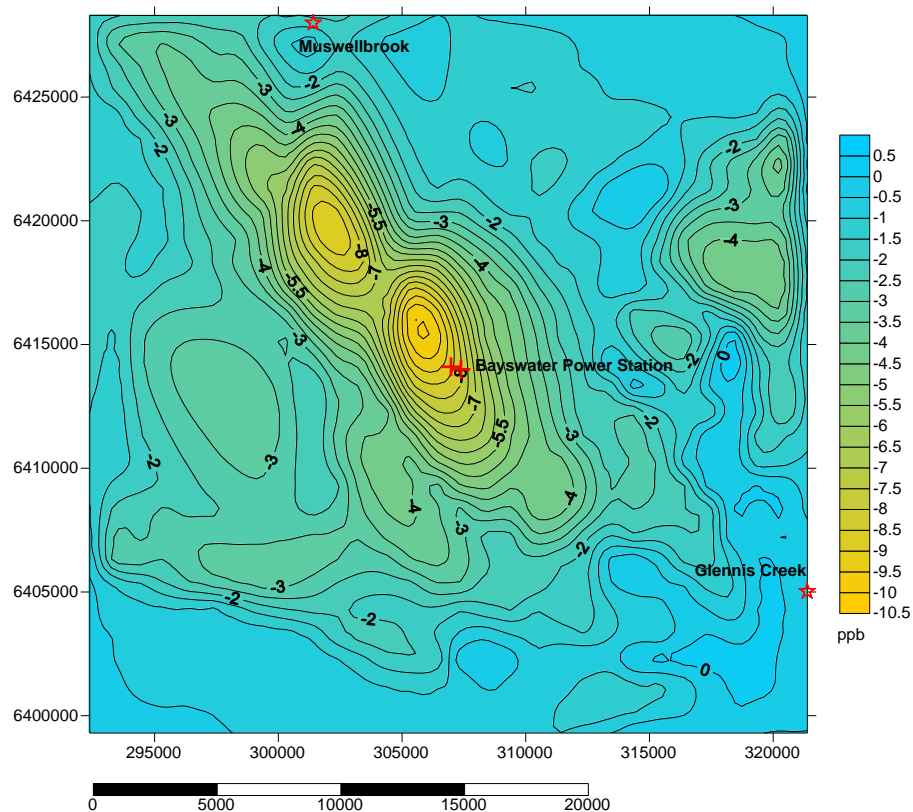
Figure 6-15 Change of formaldehyde peak values in March 2014 between PCC and base case (1 km resolution)

Change of acetaldehyde peak values in August 2015 between PCC and PrePCC (1 km resolution)
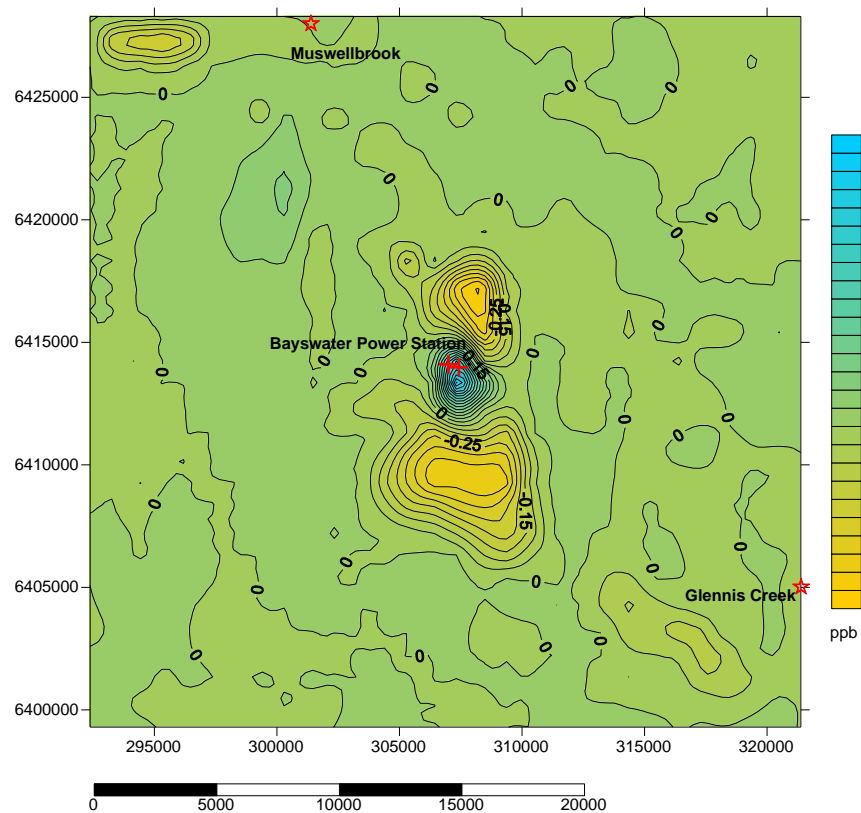
Figure 6-16 Change of acetaldehyde on August 2015 between PCC and base case (1 km resolution)

6.2.2.3 Ammonia

Ammonia (NH_3) is one of the products from amine-based (Ethanolamines (MEA) as solvent) post-combustion projects. This study assumed that the NH_3 emission from the hypothetical PCC project was increased from 11.63 g/s to 146.46 g/s. The data was based on the results of a previous study (Thong et al., 2012), and was converted to fit parameters of the Bayswater Power Station. The simulated NH_3 results from the three-year simulation are shown in Table 6-4, Table 6-5, and Table 6-5.

The three years of data demonstrate the maximum increase of peak concentration was 33.64 ppb occurred on June 2015, and the maximum decrease of 34.56 ppb occurred on July 2015. In the individual years, the maximum increase of NH_3 peak value occurred in March 2011, May 2014, and in June 2015.

NH_3 acts as a precursor for secondary aerosols by neutralizing atmospheric acids such as nitric acid and sulphuric acid (Ianniello et al., 2010). After acid neutralization, the inorganic secondary aerosol mainly exists as an aerosol nitrate or aerosol sulfate. Figure 6-17 shows relationship of difference of NH_3, NH_4, NIT (aerosol nitrate), and ASO_4 peak values from June 2015 simulation between PCC case and the base case in each grid point on 1 km resolution study domain. The NH_3 concentration difference is on X axis. The NH_4, NIT, and ASO_4 peak value change showing on Y axis correspond to the NH_3 difference. The plot (Figure 6-17) shows that only NIT concentrations recorded large increases when NH_3 concentrations changed within 5 ppb range. Most of the NH_4 and ASO_4 concentrations showed decreases regardless of the NH_3 change. The largest decrease was in sulfate aerosols, which decreased up to 72.9 $\mu g/m^3$. This large decrease of sulfate aerosols is mainly due to the 95% reduction in SO_2 emissions. In the atmosphere NH_3 first reacts with sulfuric acid to form sulfate aerosol. However, previous studies (Ansari and Pandis, 1998; Pinder et al., 2008) have reported that when there is an excess of NH_3, it will react with nitrate to form nitrate aerosol after neutralizing sulfuric acid. The situation is more likely with PCC case scenario as PCC emits ammonia. In addition, these studies have also reported that the nitrate aerosols are favored in low-temperature reactions (Ansari and Pandis, 1998; Heo et al., 2015; Pinder et al., 2008). This study focuses on the simulation in the southern hemisphere, June is early winter in Australia, and Figure 6-17 shows that the nitrate aerosol formation might be increased by additional ammonia emission in this time. In addition, a previous study (Heo et

al., 2015) reported that nitrate aerosol formation does not increase linearly with an increase in NH_3. The results from this study (Figure 6-17) also showed a good agreement with Heo et al's study results.

Table 6-4 the difference of NH_3 peak values in 2011 between PCC1 and the base case (ppb)

2011	JAN	FEB	MAR	APR	MAY	JUN	JUL	AUG	SEP	OCT	NOV	DEC
Min.	-0.55	-16.49	-12.04	-20.58	-6.29	-11.47	-6.49	-10.46	-13.86	-0.51	-0.47	-1.94
Max.	4.47	17.45	20.46	12.58	10.33	7.21	12.59	16.57	9.66	2.49	0.71	1.98
Mean	0.07	0.25	0.07	-0.02	0.22	-0.01	0.10	0.08	0.01	0.16	0.01	0.11
S.D.	0.36	2.04	1.58	2.15	1.26	1.46	1.02	2.19	1.23	0.34	0.08	0.31

Table 6-5 the difference of NH_3 peak values in 2014 between PCC1 and the base case (ppb)

2014	JAN	FEB	MAR	APR	MAY	JUN	JUL	AUG	SEP	OCT	NOV	DEC
Min.	-5.19	-0.24	-19.86	-0.35	-0.83	-1.09	-10.58	-19.16	-11.63	-5.10	-1.20	-0.31
Max.	4.52	6.38	16.27	7.83	25.69	2.86	16.34	10.79	15.56	5.34	4.32	1.78
Mean	0.04	0.10	0.42	0.23	0.50	0.10	0.04	0.03	0.04	0.05	0.09	0.02
S.D.	0.74	0.44	2.17	0.78	1.94	0.31	1.50	1.69	1.55	0.83	0.40	0.15

Table 6-6 the difference of NH_3 peak values in 2015 between PCC1 and the base case (ppb)

2015	JAN	FEB	MAR	APR	MAY	JUN	JUL	AUG	SEP	OCT	NOV	DEC
Min.	-7.03	-12.51	-0.48	-0.41	-0.78	-18.83	-34.52	-4.40	-0.47	-6.03	-0.27	-0.64
Max.	10.05	13.20	4.88	0.39	11.28	33.64	13.26	4.90	1.70	11.87	0.92	4.30
Mean	0.11	0.12	0.12	0.00	0.42	0.63	0.10	0.07	0.00	0.17	0.02	0.07
S.D.	1.15	1.12	0.51	0.07	1.21	3.34	2.15	0.77	0.11	1.46	0.07	0.45
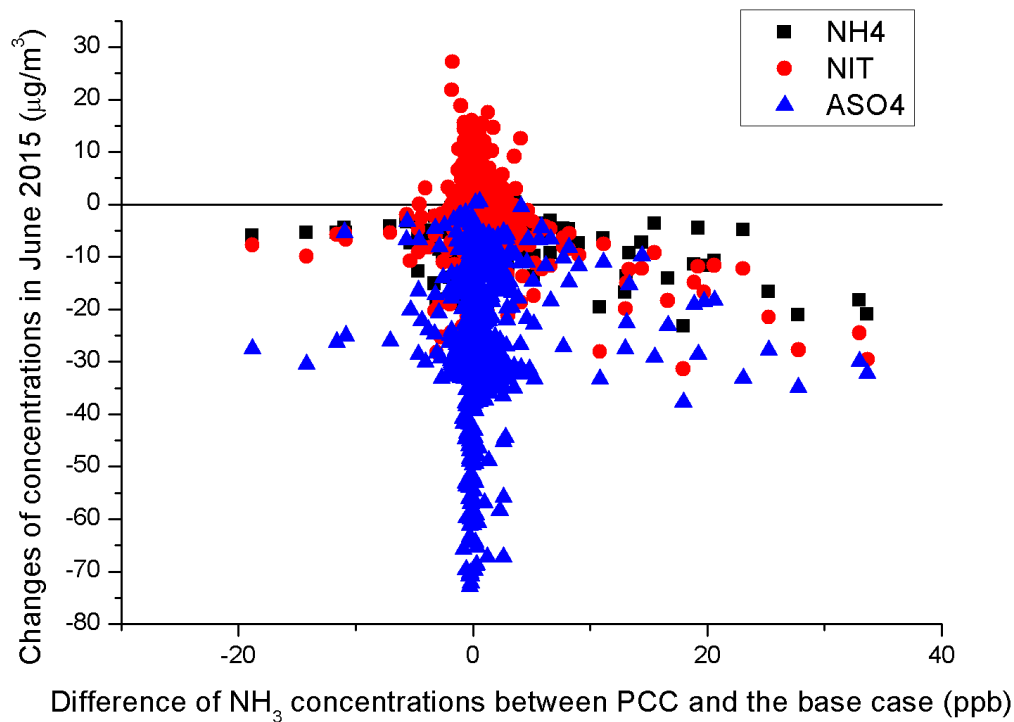
Figure 6-17 Relationship of concentration changes by PCC1 between NH₃, NH₄, NIT, and ASO₄ in June 2015

6.2.2.4 $PM_{2.5}$ and relative components

As July 2015 is the month with maximum increase on $PM_{2.5}$ peak value, the following

sections and next chapter will mainly focus on results from the July 2015 simulation. The July

2015 simulation generated atmospheric concentrations of detailed $PM_{2.5}$ components, and

the total $PM_{2.5}$ concentration was calculated using equation(6.3). In this part, the

relationships of each component and $PM_{2.5}$ concentration change are discussed in detail.

Figure 6-18 showed the change of $PM_{2.5}$ corresponding to a difference in NH_4 in the 1 km

resolution domain. NH_4 peak values showed decreases on most of the grid points. When the

NH_4 values increased, the $PM_{2.5}$ values did not show a linear relationship with NH_4

concentration change. The Figure 6-19 shows the relationship between $PM_{2.5}$ and nitrate

aerosol (NIT). The change in Figure 6-19 has similar distribution trend with the change in

Figure 6-18. As July is winter in Australia, the nitrate aerosol formation is more favorable

compared to sulfate aerosol formation during this time. Figure 6-19 and Figure 6-20 show

clearly that the sulfate aerosol formation was less than the nitrate aerosol formation in the

study domain. The lower sulfate aerosol concentration may be due either to lower sulfate

aerosol formation, or to the largely decreased SO_2 emission. The $PM_{2.5}$ change

corresponding to the difference of sulfate aerosols (ASO_4) in this July 2015 simulation did not show a clear relationship (Figure 6-20).

In the Upper Hunter region, a previous study (Hibberd et al., 2013) measured $PM_{2.5}$ speciation. In the Muswellbrook area, a town located in about 15 km northwest of the Bayswater Power Station, organic carbon (OC25) is the dominant component in $PM_{2.5}$ particles. When considering $PM_{2.5}$ concentration change by PCC emissions, this study also considered the impacts of $PM_{2.5}$ speciation including the previous nitrate aerosol and sulfate aerosol discussion. $OC_{2.5}$ did not show a clear linear relationship with the change of $PM_{2.5}$ concentrations. Figure 6-21 shows that $PM_{2.5}$ value increased while the $OC_{2.5}$ concentrations increased in small amount of the grid points in 1 km resolution domain. The remaining $PM_{2.5}$ components ($EC_{2.5}$, $OT_{2.5}$, $SS_{2.5}$, LEVO SOD, MAG, CAL, POT, CL) in equation (6.3) are shown in Figure 6-22. These components only show a slight positive relationship with $PM_{2.5}$ concentration change, but most of $PM_{2.5}$ increases appear in the grid points with no change in each component concentration.

In addition, these figures (Figure 6-18 to Figure 6-22) also show that some $PM_{2.5}$ values were increased at points with decreased $PM_{2.5}$ components. These results demonstrate that $PM_{2.5}$ concentration change mainly relied on concentration changes of nitrate aerosols, sulfate aerosols, and organic carbon, but also combined with impacts from each component.

6.3 Limitations of modelling analysis

This study converted data from a pilot plant to a hypothetical post-combustion project in the Bayswater Power Station. The pilot plant is a small scale project. Therefore, the emission data could be different from a commercial-scale project. To understand the potential risk from post-combustion project deeply, the emission data from a full scale project is needed for future study.
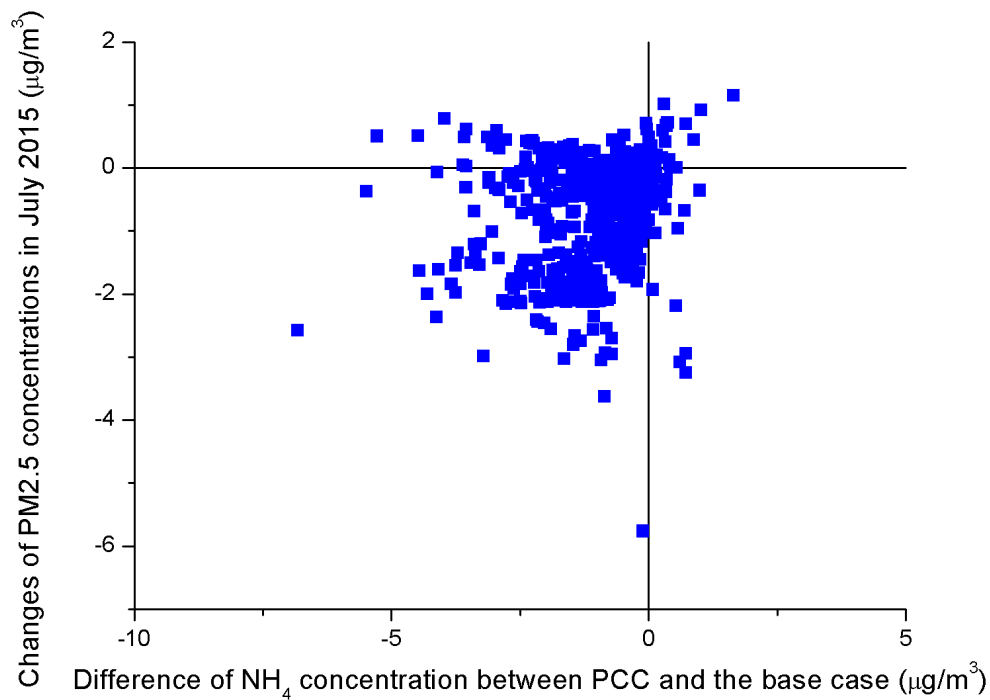
Figure 6-18 Relationship between change of PM₂.₅ and NH₄ in July 2015
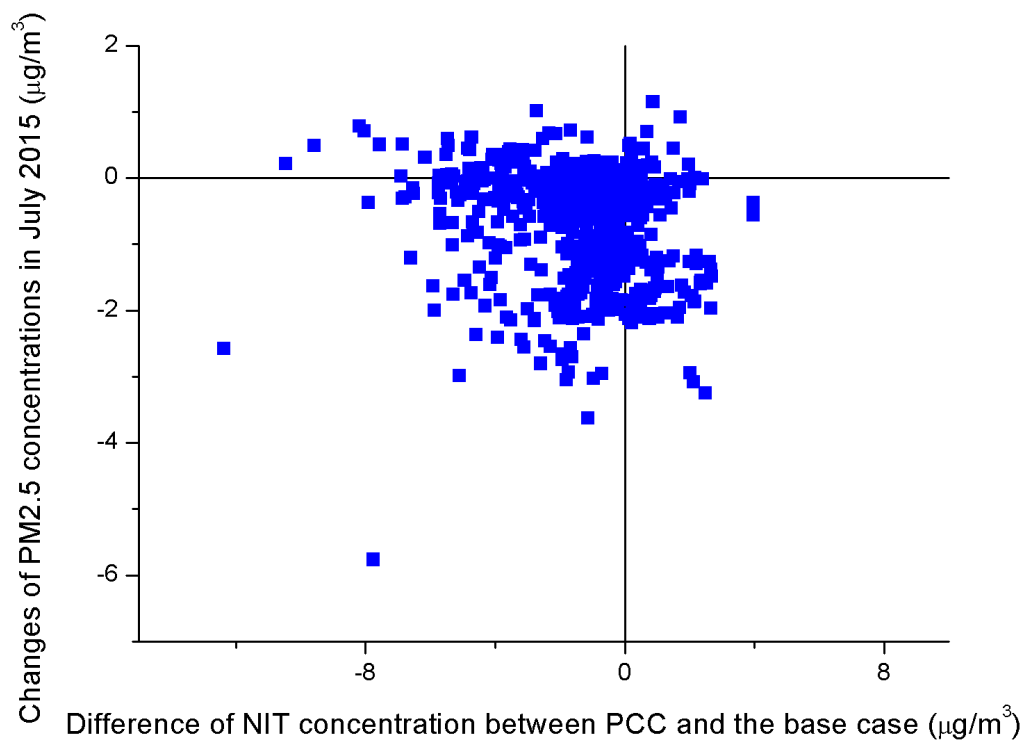
Figure 6-19 Relationship between change of PM₂.₅ and NIT in July 2015

110
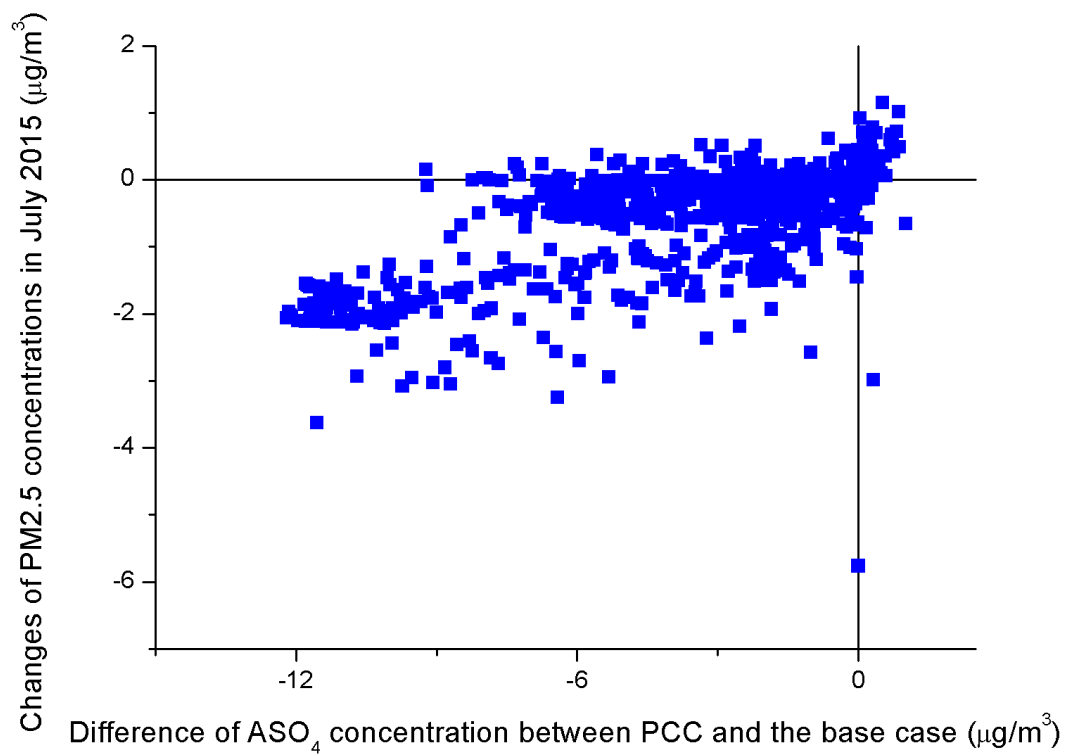
Figure 6-20 Relationship between change of PM2.5 and ASO4 in July 2015
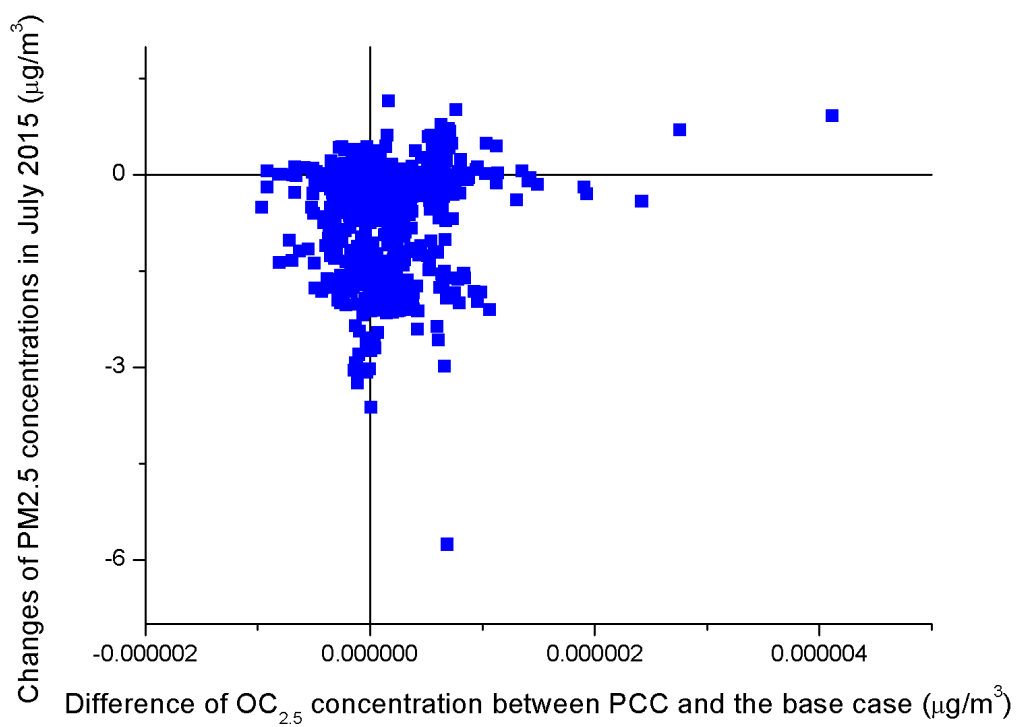
Figure 6-21 Relationship between change of PM2.5 and OC25 in July 2015

111
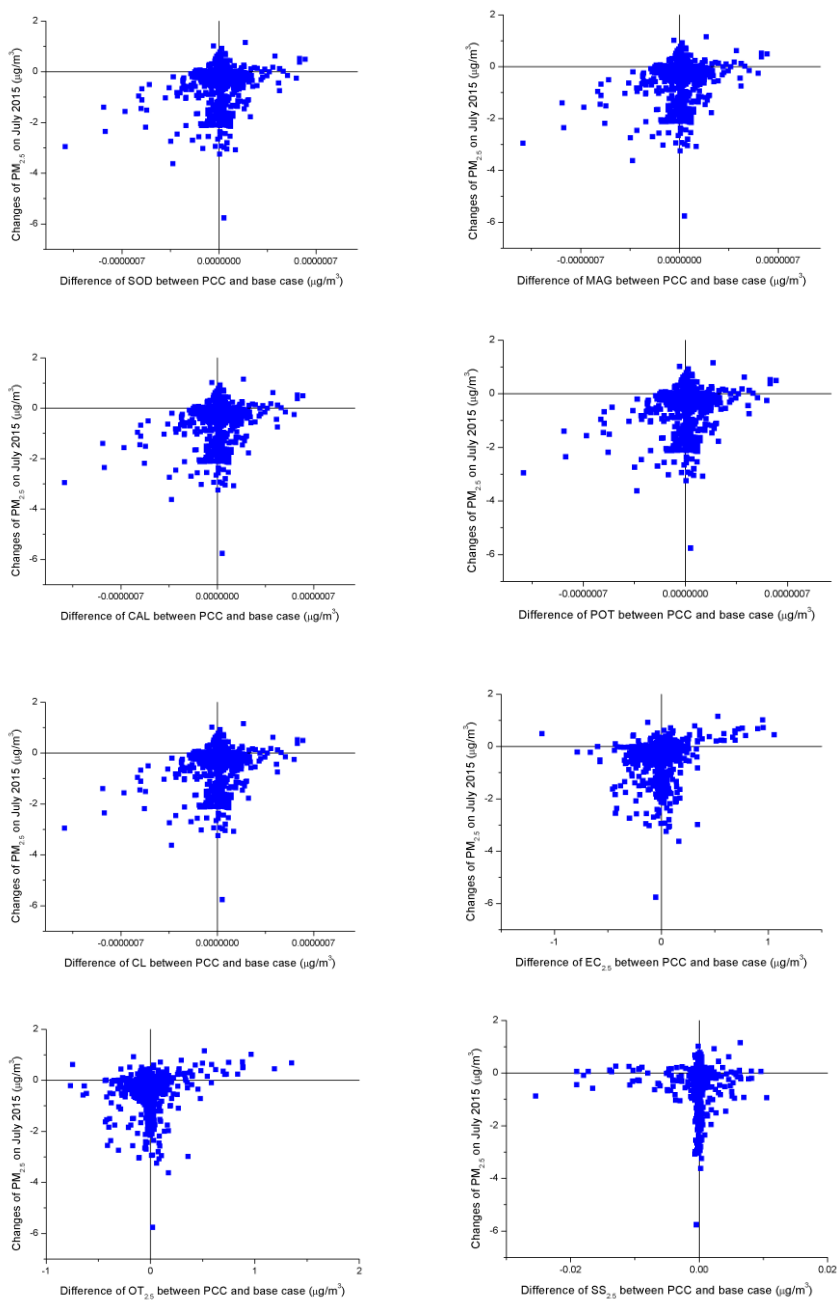
Figure 6-22 Relationship of PM$_{2.5}$ change and difference of each component in July 2015 case

Chapter 7 Sensitivity analysis & Risk assessment

7.1 Chemicals risk assessments protocol

As discussed in previous chapters, post-combustion carbon capture projects have the potential to emit toxic compounds into the atmosphere, such as formaldehyde (HCHO), ammonia (NH_3), nitrosamines etc. HCHO is a known carcinogen (Låg et al., 2009). NH_3 emitted into the atmosphere contributes to aerosol nitrate and aerosol sulfate formation, which contribute to $PM_{2.5}$ formation (Ansari and Pandis, 1998). Nitrosamines are suspected human carcinogens (Karl et al., 2011), and have been reported to cause tumors on lab animals (Låg et al., 2009). Although the atmosphere is capable of diluting the concentrations overall, atmospheric movement and oxidation reactions sometimes bring and increase concentration to some areas. When humans are located in these areas, they are at risk of exposure to these chemicals. Risk assessment is a way of analyzing scientific data to provide information regarding the form, extent, and likelihood of risk (Leeuwen and Vermeire, 2007). Risk assessments possess a broad range of characteristics and purposes. Some assessments are to assess impacts from a pollution incident. Others look for a prediction of potential future harm to humans and/or the environment (Leeuwen and Vermeire, 2007). In this study, the risk assessment focuses on anticipating potential future impacts from emissions of post-combustion carbon capture (PCC) projects. As the risk of chemical exposure can be international and can cross geopolitical borders, the United Nations Conference on Environment and Development (UNCED) recommended an international assessment with mutual acceptance of hazard and risk assessment methodologies (Leeuwen and Vermeire, 2007; United Nations, 1992). Currently, risk management in general consists of risk assessment and risk management as an objective/scientific part and as a subjective/political part of the process, respectively (Leeuwen and Vermeire, 2007). The process includes eight steps shown in Figure 7-1. The first four steps: hazard identification, exposure assessment, effects assessment, and risk characterization, are the risk assessment phase; the remaining steps belong to the risk management phase. This study focuses on the risk assessment phase.

Hazard identification is the identification of effects of a chemical that could cause environmental damage, injury, or disease (Leeuwen and Vermeire, 2007). Previous studies (Emmerson et al., 2013; Karl et al., 2008; Morken et al., 2014) have reported that PCC

technology mainly emits amines, formaldehyde (HCHO), acetaldehyde, and ammonia into the atmosphere based on pilot plant studies. Morken et al. (2014) reported that the nitrosamines and nitramines were below the detectable level. Amines, especially MEA and PIPA, have reproductive and development toxicity (Låg et al., 2009), while amines can also form more toxic compounds such as nitrosamines in the atmosphere under OH initiated degradation (Karl et al., 2012). Most nitrosamines are suspected human carcinogens (Karl et al., 2011; Låg et al., 2009). Låg et al. (2009) suggested that the exposure threshold to ambient MEA should be less than 10 µg/m^3. MEA and its oxidation products were modelled in Chapter 5, and the results showed the highest 1-hour ambient concentration of MEA after atmospheric dispersion using estimated PCC emission data was 1.844×10^{-3} µg/m^3. This is approximately three orders of magnitude less than the ambient level recommended by Låg et al. Based on results from the KPP modelling, nitrosamines were degraded quickly after formation. 8 hours after formation, the concentration had decreased to 5.3×10^{-11} ppb (about 1.58×10^{-7} ng/m^3 based on dimethylnitrosamine). In the CALPUFF dispersion model, the highest 1-hour ambient concentration of nitrosamines was 4.001×10^{-5} ng/m^3. The U.S. Environmental Protection Agency's (USEPA) Integrated Risk Information System states that concentration value of inhalation exposure to nitrosamines (N-Nitrosodimethylamine) corresponding to 1 in 1,000,000 and 1 in 10,000 risk of an adverse health or environmental effect is 0.07 ng/m^3 and 7 ng/m^3, respectively (USEPA, 2015c). The concentrations of nitrosamines found in the PCC simulations are far below the level where there is a 1 in 1,000,000 risk of an adverse health or environmental effect. The potential risk of MEA and nitrosamines to cause environmental damage and human health impacts in this simulation are very low based on current knowledge.
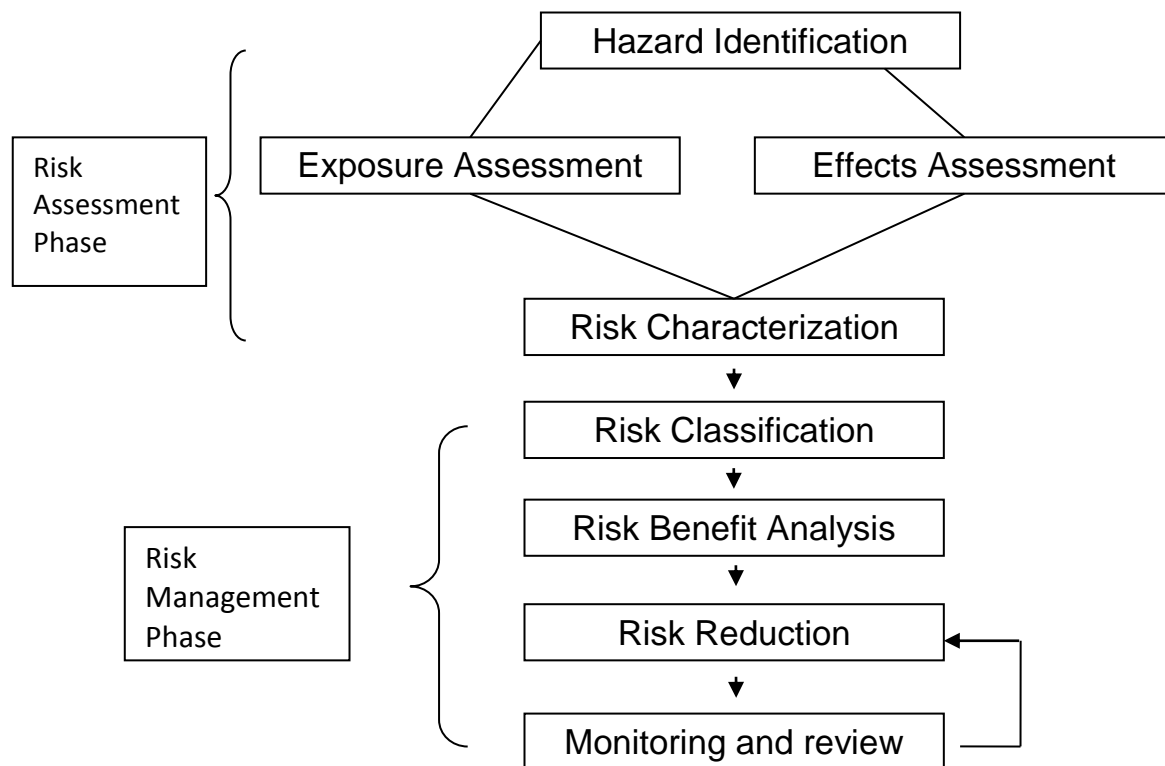
Figure 7-1 Risk Management Process

Epidemiological studies show the health effects associated with $PM_{2.5}$ include mortality, lung cancer, an increase of hospital admission, cardiovascular and respiratory diseases (Ostro, 2004; WHO, 2013). Health effects from short-term exposure to $PM_{2.5}$ include increased hospital admission for cardiovascular and respiratory events such as heart attack, stroke, and asthma attacks; and infant and child mortality linked to heart and lung diseases (US EPA, 2012; WHO, 2013). Health effects from long-term exposure to $PM_{2.5}$ include lung cancer, premature death, especially related to heart disease, and cardiovascular diseases (US EPA, 2012), Long-term $PM_{2.5}$ exposure may also be related to developmental and reproductive effects such as low birth weight (US EPA, 2012). Ammonia is a contributor to aerosol nitrate and sulfate formation, which contribute further to $PM_{2.5}$ formation (Ansari and Pandis, 1998). This study considers human health impacts from long term exposure to $PM_{2.5}$. HCHO as a carcinogenic compound and a primary emission from PCC technology is also considered in this risk assessment.

7.2 Methodology to assess exposure risk

This study aims to assess risks through inhalation exposure to HCHO and $PM_{2.5}$. US EPA classified formaldehyde as a potential human carcinogen and has ranked it in Group B1 (USEPA, 2012). This study considers cancer risk from inhalation exposure to formaldehyde after PCC technology has been installed. $PM_{2.5}$ consists of many species such as organic carbon, ammonium, chromium (Cr), and lead (Pb) et.al. (Hibberd et al., 2013). Some species have carcinogenic capability to cause cancer. However, no study reported that amines based PCC emission can change $PM_{2.5}$ speciation. Therefore, the long-term risk does not assess exposure risk to these detailed species, but only consider mortality risk of $PM_{2.5}$ as a whole.

In this study, the PCC technology is a hypothetical project at Bayswater Power Station. There is only a few of PCC emissions monitoring data available. In addition, PCC technology has not yet been implemented on a commercial scale. Only limited emission data are available from the PCC project. Therefore, this study employed the TAPM-CTM model to simulate atmospheric dispersion of emissions from a PCC project using emissions data from a pilot plant that has been scaled up into parameters suitable for the Bayswater Power Station. The ambient concentrations of HCHO and $PM_{2.5}$ from the TAPM-CTM simulations were then used to consider concentration distributions for each grid point in the study domain. The exposure risk assessment uses July 2015 simulation results to consider a lifetime (70 years) exposure to HCHO and a long-term exposure (30 years) to $PM_{2.5}$. The daily peak values of formaldehyde for July 2015 were used to generate concentration distributions for each grid point using the @RISK model. $PM_{2.5}$ concentration distributions were generated based on daily averaged values for the whole year, as the ambient air quality standard for $PM_{2.5}$ is calculated as a 24-hour average (NEPC, 2016). Both HCHO and $PM_{2.5}$ distribution types mainly include log-logistic, logistic, and normal distributions.

7.2.1 Quantification of cancer risk assessment

@RISK software was used to simulate uncertainties and understand potential risks due to HCHO and $PM_{2.5}$ exposure. Palisade @RISK uses a Monte-Carlo simulation to calculate risk values several thousand times to obtain an overall probability. The model calculates potential individual inhalation exposure doses and subsequent cancer risk in the study area. The inhalation exposure calculation follows the U.S. EPA risk assessment method by

considering concentrations of HCHO in the atmosphere, inhalation absorption factor, and daily breathing rate (USEPA, 1992).

The inhalation exposure dose is calculated using the following equation:

$$E_{in} = \frac{C \times DBR \times A}{BW} \times \frac{EF \times ED}{AT}$$

(7.1)

Where

A = inhalation absorption factor, unitless

C = atmospheric concentration value (simulated by TAPM-CTM), $\mu g/m^3$

EF = exposure frequency, unitless

ED = exposure duration, year

BW = body weight, Kg, and

AT = average time, days.

Table 7-1 Parameters used in risk calculations for HCHO inhalation exposure

Parameter	Distribution model & Model parameters	References
AT-Averaging Time	25550 days (70 years)	(USEPA, 1989)
ED-Exposure Duration	Adult: 70 years	(CalEPA, 2003)
BW- Body weight (kg)	Lognormal Adult: [66.44, 1.20]	(Arija V et al., 1996)
EF-exposure frequency (unitless)	Triangular [min, mode, max] [180, 345, 365]	(Smith, 1994)
A-inhalation absorption rate	1	(CalEPA, 2003)
DBR-Daily breathing rate (L/kg BW* day)	Gamma [Location, Scale, Shape] Adult:[193.99,31.27,2.46]	(CalEPA, 2003)

Atmospheric concentration values (C) was presented as distribution functions in each grid point. Regarding breathing rate and inhalation absorption factor, the California EPA recommended values for this equation are summarized in Table 7-1 (CalEPA, 2003). Data for other parameters in the exposure dose calculation were collected from published papers, and have also been shown in Table 7-1. The risk model was run through 1,000 iterations for this simulation.

The cancer risk (R_{in}) calculation is performed by multiplying the inhalation exposure dose by a cancer slope factor (*CSF*) of 0.021 (mg/kg/day)$^{-1}$ (OEHHA, 2009). Using this, cancer probabilities for individuals in the study area can be predicted by @RISK. The risk calculation estimates the incremental probability of cancer in an individual in response to a unit of formaldehyde increased when the exposure is via inhalation over a period of time. The final risk measurement is unitless, shown in equation (7.2).

$$R_{in} = E_{in} \times CSF \tag{7.2}$$

In considering individual risk on a particular group or population, the calculation becomes:

$$POP_{risk} = R_{in} \times population \tag{7.3}$$

The POP$_{risk}$ represents the number of individuals likely to be affected by inhalation exposure to a pollutant.

7.2.2 Quantification of mortality risk related to long-term exposure

Mortality risk associated with inhalation exposure to PM$_{2.5}$ has been conducted utilizing a WHO methodology (Ostro, 2004). The assessment of health endpoint impacts in response to exposure to PM$_{2.5}$ as summarised by the WHO (Ostro, 2004) consists of four components:

1. Estimates of the difference in PM$_{2.5}$ exposure levels between PrePCC (base case) and PCC case scenario using a computer model simulation;

2. The size of the population exposed to PM$_{2.5}$;

3. Baseline incidence of health effects in response to exposure to PM$_{2.5}$ (e.g. mortality rate in the population, in deaths per thousand people (Ostro, 2004)); and

4. Exposure-response functions from public health data expressed as a percentage change in health effects per µg/m^3 change in PM$_{2.5}$ exposure (Environmental Risk Sciences, 2014).

7.2.2.1 Exposure-response relationship
An exposure-response relationship employs mathematical function to express the relationship between the concentration of a pollutant and resulting health effects in response to the concentration level (Environmental Risk Sciences, 2014). Several studies (Dockery et al., 1993; Krewski et al., 2009; M Burgers and S Walsh, 2002; Pope III et al., 2002;

Pope III et al., 1995) have been undertaken to determine the relationship of long-term exposure to $PM_{2.5}$ to adverse health effects, including lung cancer, cardiopulmonary disease, and 'all-cause' disease and mortality (Ostro, 2004). For example, Pope III et al. (1995) reported that the range of $PM_{2.5}$ was from 7-30 μg/m^3 across 50 cities associated with both 'all-cause' mortality and cardiopulmonary mortality (Ostro, 2004). The risk assessment associated with exposure to $PM_{2.5}$ also contains the calculation of relative risk (Environmental Risk Sciences, 2014). Krewski et al. (2009) reported the relative risk (RR) per 10 μg/m^3 change in $PM_{2.5}$ in two time periods (1979-1983 and 1999-2000) based on US nationwide analysis. The relative risk per 10 μg/m^3 change in $PM_{2.5}$ was 1.03, 1.12, 1.06, and 1.08 for deaths from all causes, ischemic heart disease, cardiopulmonary disease, and lung cancer, respectively, between the years 1979-1983. The relative risk per 10 μg/m^3 change in $PM_{2.5}$ between 1999-2000 was 1.03, 1.15, 1.09, and 1.11 for deaths from all-causes, ischemic heart disease, cardiopulmonary disease, and lung cancer, respectively. Pope III et al. (1995) reported a linear function for the exposure-response relationship. A WHO study (Ostro, 2004) has adopted both linear and log-linear functions for exposure, and stated that the log-linear function can obtain more realistic results for long-term exposure. In addition, the study reported that the log-linear model generated slightly higher relative risk in the range of 10-30 μg/m^3, but lower relative risk below and above that range (Ostro, 2004). In this project, the concentrations of $PM_{2.5}$ in the study domain were between 5-32 μg/m^3. However, only 24 points out of a total of 900 grid points recorded concentrations above 10 μg/m^3. Therefore, this study utilises linear functions to provide a more conservative estimate for relative risk. The calculation of relative risk adopts the following equation used in linear model based on change of exposure concentration (Ostro, 2004).

$$RR = \exp[\beta \times (X - X_0)] \qquad\qquad (7.4)$$

Where: $X-X_0$ = the change in $PM_{2.5}$ concentration (μg/m^3), β = regression/slope coefficient, or the slope of the exposure-response function which can be expressed as the per cent change in response per 1 μg/m^3 increase in $PM_{2.5}$ (Environmental Risk Sciences, 2014), and RR = relative risk.

Previous epidemiological studies (Krewski et al., 2009; Pope III et al., 2002; Pope III et al., 1995) have reported the relative risk in response to different health effects due to 10 μg/m^3

increments in PM$_{2.5}$ concentrations. This study utilises the reported data to calculate the β values for different health effects. Therefore, the β coefficient calculation becomes the following equation.

$$\beta = \frac{\ln(RR)}{10} \tag{7.5}$$

Where *RR* = relative risk, and 10 = a 10 µg/m^3 increase in PM$_{2.5}$ exposure.

Based on the equation (7.5) and the reported results from previous studies, the β values associated with long-term exposure in response to mortalities from different health effects are shown in Table 7-2.

Table 7-2 Health impact factors in exposure-response relationships

Health endpoint	Exposure period	Published relative risk per 10 µg/m^3 change in PM$_{2.5}$	β coefficient for 1 µg/m^3 increase in PM$_{2.5}$	References
PM$_{2.5}$: Mortality, all causes	Long-term	1.06 95% CI [1.04-1.08]	0.0058 (0.58%)	Based on results from random Effects COX model during 1999-2000 study in nationwide analysis in US (Krewski et al., 2009)
PM$_{2.5}$: Cardiopulmonary Mortality	Long-term	1.13 95% CI [1.10-1.16]	0.0122 (1.22%)	
PM$_{2.5}$: Mortality, lung cancer	Long-term	1.14 95% CI [1.06-1.23]	0.0131 (1.31%)	
PM$_{2.5}$: Ischemic heart disease Mortality	Long-term	1.24 95% CI [1.19-1.29]	0.0215 (2.15%)	

7.2.2.2 Baseline incidence from local health statistic data, and relevant risk calculation

Once the relative risk is determined, the attributable fraction (*AF*) of health effects from air pollution can be calculated using the following equation, assuming only one exposure level applies to the population of one city.

$$AF = \frac{RR - 1}{RR} \tag{7.6}$$

To estimate the expected number of mortality cases due to exposure to PM$_{2.5}$, the equation (7.7) that used in Ostro (2004) study was adopted in this study.

$$E = AF \times B \times P \qquad (7.7)$$

Where E = the expected number of mortality cases due to exposure to PM$_{2.5}$, AF = attributable fraction, B = baseline incidence of health effects, and P = the relevant exposed population for the health effect.

As the incremental change in PM$_{2.5}$ is low in the most of the grid points, this study also utilized a simplified calculation of the equation (7.7) from a previous study (Environmental Risk Sciences, 2014) to calculate the expected number of health effects and the risk associated with the change of PM$_{2.5}$ concentrations. The simplified calculation is listed below.

$$E = \beta \times B \times \sum\nolimits_{mesh} (\Delta X_{mesh} \times P_{mesh}) \qquad (7.8)$$

Where β = Slope coefficient relevant to the per cent change in response to 1 µg/m^3 change in PM$_{2.5}$, B = baseline incidence of health effects, ΔX_{mesh} = change of PM$_{2.5}$ concentrations in µg/m^3 as average value in a small mesh block, and P_{mesh} = population in each small mesh block (Environmental Risk Sciences, 2014).

Furthermore, an additional risk is calculated as follow through dividing by total population (Environmental Risk Sciences, 2014).

$$Risk = \beta \times \Delta X \times B \qquad (7.9)$$

Where β = Slope coefficient relevant to the per cent change in response to 1 µg/m^3 change in PM$_{2.5}$, B = baseline incidence of health effects, and ΔX = change of PM$_{2.5}$ concentrations in µg/m^3 at the point of exposure.

In the above equations, baseline incidence of health effects as a main calculation factor were attained from local health department data. NSW Department of Health (NSW Health) has reported respiratory and cardiovascular diseases and cancer among residents in the Hunter New England Area Health Service using 2003-2007 data (NSW Health, 2010). This study region, the Upper Hunter area, is located within the larger Hunter New England area. Data from the Hunter New England area is utilized in this study to quantify exposure risk in the study region. The detailed data related to mortality are listed in Table 7-3.

Table 7-3 Baseline incidence of deaths in the Hunter New England area between 2003-2007

	People of all ages	Baseline incidence per person	Reference
Population	866,566		
Deaths from all causes	6413	0.0074	
Deaths from cardiovascular diseases	2543	0.0029	(NSW Health, 2010)
Deaths from lung cancer	1756	0.0020	

7.3 Cancer risk and probability

7.3.1 Cancer risk assessment of formaldehyde

The cancer risk assessment of HCHO uses daily averaged concentrations across the year 2015 to consider the exposure doses and relevant risks associated with lifetime exposure (70 years) to HCHO. The annual mean daily concentration of HCHO was 1.47 ppb with a range of 0.88 ppb to 4.91 ppb before the addition of PCC technology. The annual mean daily concentration after the PCC project was added decreased to 1.44 ppb, with the concentration ranging from 0.88 ppb to 3.49 ppb. Currently, there are no air quality standards for HCHO. The Australian Department of Environment sets up a monitoring investigation for five air toxics, including HCHO. In the future, the Department may have an air quality standard for HCHO.

The inhalation exposure dose calculation employs equation (7.1) and parameters in Table 7-1 to do the estimates. The difference in the average exposure dose between base case and PCC case did not show much change; they were both 0.00032 mg/kg/day. The maximum exposure doses for both scenarios also showed no change. The minimum exposure dose in the PCC scenario showed a slight decrease from 0.00030 mg/kg/day in base case to 0.00029 mg/kg/day. To consider cancer risk in response to exposure to HCHO, equation (7.2) was applied to calculate potential cancer risk based on the cancer slope factor for HCHO. The cancer risk was in a range of 6.20×10^{-6} to 8.01×10^{-6} in the base case, and was in a range of 6.15×10^{-6} to 7.94×10^{-6} in PCC case. The cancer risk from exposure to HCHO decreased slightly in the case with PCC technology added. All the cancer risks calculated were greater than U.S.EPA's target (1 in 10^{-6}), but well below the level where action is taken. Comparing the

base case and the PCC case, the mean cancer risk under the PCC case showed a slight decrease of 8.48×10^{-8}. HCHO is one of the air emissions from PCC projects. The decreased ambient concentrations and cancer risks may be led by the large decreases in NO_X emissions, which in turn causes less HCHO to be generated in the atmosphere. In addition, HCHO is a reactant in the photolytic processes in the atmosphere. The photolysis process could result in decreased ambient formaldehyde levels. As the cancer risk is above the targeted level, it is necessary to reduce the formaldehyde generation in the carbon capture process or install a flue gas cleaning device to decrease the potential ambient formaldehyde emission.

Most of the land in the study area is made up of industrial or coal mining sites. A small part of the town of Muswellbrook is located at the edge of the study area, and there is a small group of residential properties located in the study area. The entire Hunter New England region, as defined by the Department of Health, has a population of 866,566 people. The number of individuals is likely to be affected by inhalation exposure to HCHO from a nearby PCC project is about 6 in both the base case and the PCC case. The population in Muswellbrook was about 16,167 people in 2009, which is 1.9% of total Hunter New England population. The number of individuals likely be affected by inhalation exposure to HCHO is down to less than 1 person. The potential risk due to exposure to HCHO is quite low.

Table 7-4 formaldehyde levels, exposure dose, and cancer risk assessment in 2015 before PCC

	HCHO Concentration ($\mu g/m^3$)	Exposure dose – Life-time exposure(mg/kg/day)	Cancer risk – Lifetime exposure (unitless)
Mean	1.47	0.00032	6.77×10^{-6}
Minimum	0.88	0.00030	6.20×10^{-6}
Maximum	4.91	0.00038	8.01×10^{-6}

Table 7-5 formaldehyde levels, exposure dose, and cancer risk assessment in 2015 after PCC

	HCHO Concentration ($\mu g/m^3$)	Exposure dose – Lifetime exposure(mg/kg/day)	Cancer risk – Lifetime exposure (unitless)
Mean	1.44	0.00032	6.68×10^{-6}
Minimum	0.88	0.00029	6.15×10^{-6}
Maximum	3.49	0.00038	7.94×10^{-6}

7.3.2 Mortality risk assessment of $PM_{2.5}$

This study uses the simulation results from the year 2015 to consider potential health risks in response to exposure to $PM_{2.5}$. As this study only considers long-term exposure (30 years) and cardiopulmonary mortality data was lacking in the study region, only risks on mortality

from all-causes and lung cancer are available. In addition, the statistic health data are only available on all-age diseases. The risk assessment on exposure to $PM_{2.5}$ only focuses on all-ages assessment. The change of risk associated with $PM_{2.5}$ exposure between base case and PCC case are listed in Table 7-6.

Table 7-6 Change of risk associated with $PM_{2.5}$ exposure between base case and PCC

Change between base case & PCC	Mortality from all causes	Mortality from lung cancer
Mean	-9.26×10^{-6} 95%CI: [-1.47×10^{-6} - -3.24×10^{-6}]	-5.74×10^{-6} 95%CI: [-9.12×10^{-6} - -2.01×10^{-6}]
Maximum decrease on risk	-5.64×10^{-5}	-3.50×10^{-5}
Maximum increase on risk	9.16×10^{-5}	5.67×10^{-5}

The U.S. EPA has levels of concern associated with risk values ranging from one in a million to one in ten thousand (Gerba, 2006). The EPA's goal is to keep risk values below 1×10^{-6}, and the EPA takes action when the risk value is greater than one in ten thousand (Gerba, 2006). The mean potential risk changes after installing PCC were both decreased, by 9.26×10^{-6} and 5.74×10^{-6} on mortality from all causes diseases and mortality from lung cancer, respectively. The PCC technology is likely to improve atmospheric $PM_{2.5}$ concentrations due to a 70% decrease of NO_x emissions and 95% decrease of SO_2 emissions. The impacts of PCC technology may be different in other countries. In Australia, there is no specific control for NO_x and SO_2 emissions. The assumption of 70% decrease of NOx emission and 95% decrease of SO_2 emission has a positive impact in Australia. However, other locations such as U.S., Japan, European Union, employ flue gas desulphurisation (FGD) technology and NO_x control technology to scrub SO_2 and NO_x from flue gas. The decreases of NO_x and SO_2 due to the PCC technology may have a less significant impact on improving $PM_{2.5}$ concentrations. Further investigation needs to be conducted to understand the impacts of PCC technology under SO_2 and NO_x emission controls. The maximum increase of mortality risk from all causes and from lung cancer were 9.16×10^{-5} and 5.67×10^{-5}, respectively. The maximum increase from both mortality risks are in the range of the level of concern to EPA, but the increased risks are still below the level EPA should take an action. In addition, the 95% confidence interval of the risk change showed mortality risks were decreased on the both mortalities from all causes and from lung cancer. The change of risk from installing PCC technology is acceptable.

The whole study domain contour maps are shown in Figure 7-2 and Figure 7-3. The highest incremental risk on mortality from all causes and from lung cancer were both located on

about 10 km south from the power station, where is close to an open mining site. Most of the study domain showed mortality risk decrease after PCC technology installation.

Before the PCC technology installation, the mortality risks from both all causes disease and lung cancer were above 1×10^{-4}, which is the level EPA recommend action should be taken. In the Upper Hunter area, the public is concerned about exposure to particulate matter. The NSW EPA has already taken actions to improve air quality in the area. In the Upper Hunter Particles Action Plan (NSW EPA, 2013), the main actions involve reducing particle emissions from coal mining operation, using strategy planning and guidelines to improve air quality, reducing particle emissions from other sources, engaging and informing communities and stakeholders, and improve understanding of particles. The actions currently under development are listed below (NSW EPA, 2016).

- emissions control from diesel plant and equipment
- wood smoke abatement program
- actions to reduce emissions from exposed surfaces
- an integrated mining policy

After taking these actions, the air pollutant emissions could be decreased and further the ambient $PM_{2.5}$ concentrations could be decreased. According to Upper Hunter monitoring performance reports (NSW EPA, 2012c, 2014), the daily average $PM_{2.5}$ concentrations at centre of Muswellbrook was less than 25 $\mu g/m^3$ except for four days in 2011 and one day due to bushfire emergency in 2013. The daily ambient $PM_{2.5}$ levels have been improved under the air quality actions.
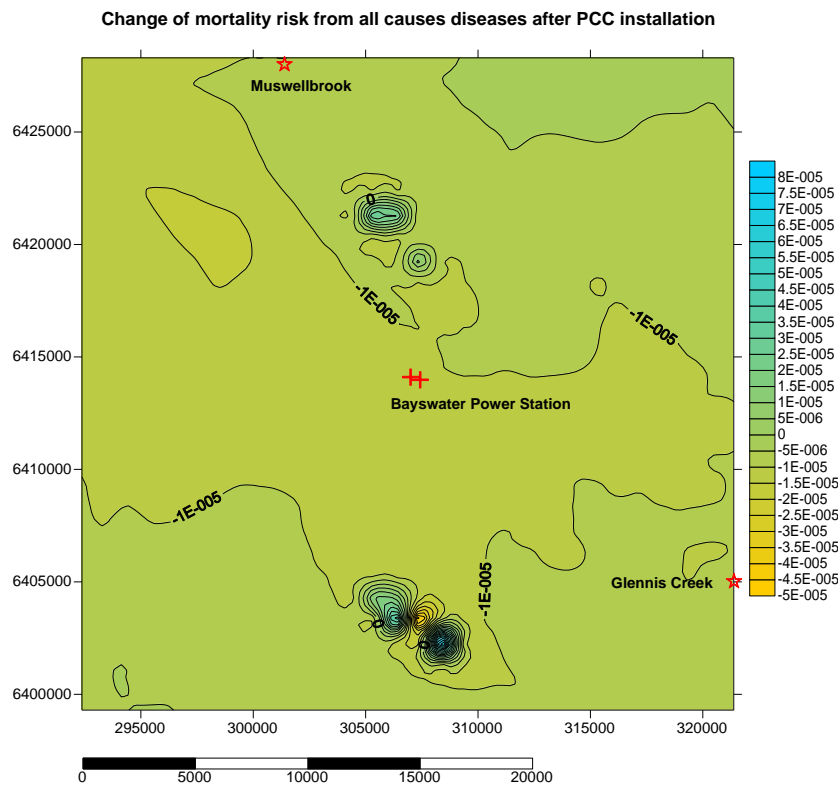
Figure 7-2 Change of risk on mortality risk from all causes diseases after PCC
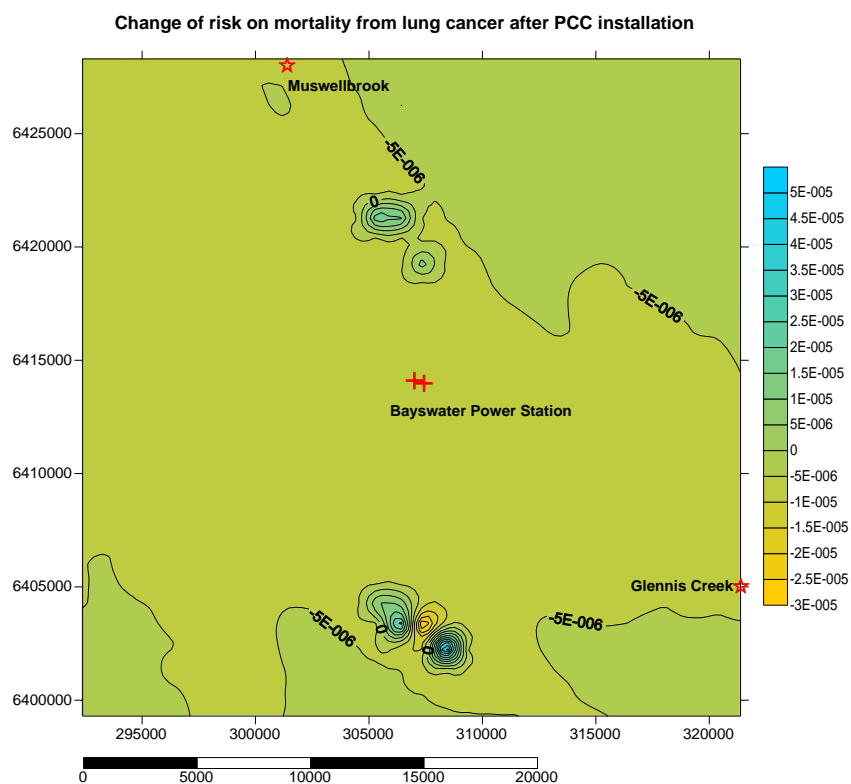
Figure 7-3 Change of risk on mortality risk from lung cancer after PCC

7.4 Summary

In this work an international, mutually accepted risk assessment method was used to analyse potential risk impacts from the prospective PCC project. The simulated 2015 daily ambient concentrations of specified air pollutants, HCHO and $PM_{2.5}$, which were generated from the TAPM-CTM model, were employed to obtain potential concentration distributions for each grid points in the study region under @RISK model. From the model analysis, the key findings in the risk assessment work are:

- Prior to the PCC installation, the cancer risk of HCHO exposure in the study domain were in excess of the EPA targeted level (one in a million). Additional emissions of HCHO from PCC should be concerning and appropriate flue gas control is necessary before emitting into the atmosphere, especially in polluted area.

- Prior to the PCC project, the mortality risk of $PM_{2.5}$ from both all-cause diseases and lung cancer were above one in a thousand which is the level the EPA should take action. Currently the NSW EPA has been taking actions to resolve the particle issues. The recent air quality monitoring has shown some positive progress.

- After installing the PCC technology, the mean HCHO concentration was decreased slightly regardless of the additional formaldehyde emission. The decreased HCHO level may be a result of the large decrease in NO_x emission.

- $PM_{2.5}$ risks were also decreased in PCC case under no $PM_{2.5}$ emission change. The large decreases in SO_2 emission restricted sulfate aerosols formation, in which reduced $PM_{2.5}$ level.

Chapter 8 Conclusions

Post-combustion carbon capture (PCC) technology is a facility installed in coal-fired power plants after the combustion units to capture carbon dioxide (CO_2) from flue gas. This technology in general employs amines, especially MEA, as a solvent to achieve carbon capture in the absorbing tower. The PCC technology can largely reduce CO_2 emissions into the atmosphere, but a drawback of the technology is that it also emits amine degradation products. Some emissions have the potential to increase risk to the environment and human health. This research uses published pilot plant data that were scaled up into parameters suitable for application to the Bayswater Power Station in the Upper Hunter Valley, NSW. The study aims to employ air pollution dispersion models to simulate atmospheric movement and dispersion in the region surrounding the power station, and further uses the modelled results in a risk assessment model to carry out cancer and mortality risk assessments. This chapter summarizes the study and the conclusions drawn from its various aspects, and further outlines suggestions and recommendations for future work.

8.1 Conclusions

An experimental study was carried out on the Macquarie University (MU) campus and in Glennies Creek, Upper Hunter area. In this study, air samples were collected to determine baseline values of formaldehyde (HCHO) and acetaldehyde. The measured average daily HCHO concentration was 2.2 ppb in late spring, 1.1 ppb in summer, 1.3 ppb in late autumn, and 0.5 ppb in winter on the MU campus. As only formaldehyde reference standard was available in late autumn and late spring, ambient acetaldehyde concentrations on the MU campus are only available in summer and winter with mean values of 0.6 ppb and 1.2 ppb, respectively. The HCHO average values were lower than the values measured in the same season in two other suburbs: Bringelly, which is located to the west of the Sydney metropolitan area, and Randwick, southeast of the city. However, the acetaldehyde mean value at MU was found to be higher than the mean value in Bringelly and Randwick. In the Upper Hunter area, the HCHO values were measured in summer and winter. The average concentration of ambient HCHO was 1.0 ppb and 0.9 ppb in summer and in winter, respectively. Acetaldehyde was only detected in summer with mean value of 1.8 ppb in the Upper Hunter area. The HCHO and acetaldehyde ratio can be an indicator to measure

biogenic sources of HCHO. Based on summer data from this research, the ratio at the MU site was 2.2 which is typical of an urban area. The Upper Hunter site is located in an industrial area surrounding by mining sites. The ratio of 1.1 in Upper Hunter site also indicates a polluted urban area. Formaldehyde is usually the dominant oxidation product from photochemical oxidation of hydrocarbons. The higher HCHO/acetaldehyde ratio was reported as an implication of positive impact of photochemical reactions of hydrocarbons (Duan et al., 2012).

In order to study amine degradation reactions in the atmosphere, a Kinetic PreProcess (KPP) simulation was undertaken to simulate amine's chemical mechanism in atmospheric chemistry. The KPP model was employed to simulate two scenarios: a chamber experiment and an ambient atmospheric scenario. In the chamber experiment, where wall losses need to be taken into consideration, the MEA decreased sharply in the first 3 hours, in good agreement with an EUPHORE chamber experiment (Karl et al., 2012). Nitramines and nitrosamines increased quickly at the beginning of the experiment, then decreased slightly. In the atmospheric scenario, the concentration changes were slower than the chamber experiment as there were no wall losses.

In order to consider atmospheric dispersion of amines and their degradation products in the atmosphere, this research added a box model of amine reactions onto the CALPUFF model to simulate atmospheric movement of amines and their degradation products. The simulation results indicated that the highest concentration of MEA, nitrosamine, and formaldehyde occurred in December 2000. The highest 1-hour average concentrations of MEA and nitrosamine were 1.8×10^{-3} µg/m³ and 4.0×10^{-5} µg/m³, respectively. The maximum values of MEA and nitrosamine are more than three orders of magnitude lower than the U.S. EPA's recommended threshold level for health impacts. The modelled HCHO is consistent with results reported in previous studies (Huang et al., 2008; Pang and Mu, 2006). The modelled results showed that the concentration of HCHO was higher in summer than in other seasons.

As the study area is located in an industrial area, detailed simulation, including criteria air pollutants, is necessary to obtain more understanding of the impacts of air quality from PCC technology. The CSIRO TAPM-CTM model was employed to achieve the purpose. The Carbon

Bond version VI (CB-VI) chemical mechanism was used to simulate atmospheric chemistry. The 2003 NSW emissions inventory was used to provide the surrounding emissions environment. The simulation was run for three individual years, representing El Niño, a normal year, and La Niña conditions in order to consider the impacts of different meteorological conditions on the change of near surface concentrations of air pollutants. The study assumed a 70% decrease of NO_x emissions and a 95% decrease of SO_2 emission from the selected Bayswater Power Station in the PCC case scenario based on pilot plant data. Emissions of ammonia (NH_3) and aldehydes including HCHO and acetaldehyde increased from the power station due to the installation of PCC technology. The modelled results demonstrated that meteorological conditions are likely to have a less significant impact on the change of near surface concentrations of NO_x and SO_2 due to largely decreased emissions of these compounds. The increase of aldehyde emissions did not significantly change concentrations.

As NH_3 is a contributor to $PM_{2.5}$ formation, reactions of NH_3 and formation of sulfate and nitrate were considered in this study. NH_3 is reported to be favored reacting with nitric acid to form nitrate aerosol (NIT) at low temperatures (Ansari and Pandis, 1998; Heo et al., 2015; Pinder et al., 2008). The study's results showed that the average change of NIT were smaller in winter than other months, which indicates that nitrate aerosol formation is favored in low temperature environments. The results from this study also showed a good agreement with Heo et al. (2015) study results, in which nitrate aerosol formation does not increase linearly with an increase in NH_3. When considering $PM_{2.5}$ formation with different components, the $PM_{2.5}$ formation did not show a linear relationship with NIT, NH_4, or ASO_4, but nitrate aerosol formation was more than the sulfate aerosol formation.

As modelled peak $PM_{2.5}$ concentration increased to a maximum of 1.2 µg/m^3 after PCC technology installation, a mortality risk assessment was used to analyse potential risk for environmental or human health impacts corresponding to the $PM_{2.5}$ change. HCHO as a potential carcinogenic compound was also considered in a cancer risk assessment. The @RISK model was employed to calculate the probability of life time risk. The results showed that cancer risk due to HCHO exposure decreased slightly after PCC technology installation. The risk of all cancers was above the US EPA's target, but well below the level where the EPA takes action. The mean potential risk changes after installing PCC decreased by 9.3×10^{-6} and

$5.7{\times}10^{-6}$ on mortality from all causes diseases and mortality from lung cancer, respectively. The PCC technology is likely to improve atmospheric $PM_{2.5}$ concentrations due to a 70% decrease of NO_x emission and 95% decrease of SO_2 emissions in Australia where the NO_x and SO_2 are not scrubbed from flue gas of power stations.

8.2 Recommendations for future work

In this study, computer modelling requires background values of air pollutants to provide reliable results. The background values of some air pollutants were obtained from a local monitoring network, but a few air pollutants such as HCHO and NH_3 do not have monitoring data. Sampling for these compounds was necessary to provide reasonable values for the model setup. The sampling period of aldehydes in this research project did not cover all four seasons. In addition, some samples collected during January and February 2015 were lost due to heavy rains. A sufficiently long sampling period across all four seasons would provide more understanding for existing ambient aldehyde concentrations and variation. Furthermore, the planned online continuous ammonia monitoring system in the Upper Hunter region was not successful due to ammonia analyser failure. Good equipment and a reliable monitoring system would provide the latest data to consider and analyse impacts and risk from a new technology under current environmental conditions.

Currently, the first commercial-scale PCC project has operated in Saskatchewan, Canada (Shell Global, 2014), but there is little emission data available from this project. This research uses emission data from a pilot plant that was scaled up into parameters suitable to an existing power station. This research, based on this limited emissions data, could not provide a comprehensive analysis and assessment on potential impacts from the installation of a PCC project. Further research that utilizes emissions data from the commercial-scale PCC project will provide more detailed information regarding potential emission of air pollutants.

In terms of computer dispersion modelling, this work employed the CSIRO TAPM-CTM model with 2003 NSW air pollutant emissions inventory files provided by the NSW EPA to simulate atmospheric dispersion due to limited emissions data. More recent emissions inventory data will provide a more realistic atmospheric environment to consider impacts from PCC projects. In addition, advanced atmospheric dispersion models including both CB VI and amine reactions can provide a more clear understanding of atmospheric formation and fate of

amine degradation products. With the additional understanding a more complete model would provide, a comprehensive risk assessment could be conducted for potential impacts from a commercial-scale PCC project.

Health risk assessments of air pollutants is a visual way to understand potential impacts from the PCC projects. This work conducted assessments for cancer risk from exposure to HCHO and mortality risk from $PM_{2.5}$. However, economic efficiency is also a significant factor in implementing PCC technology. Many studies (CSIRO, 2012; Global CCS Institute, 2009) have calculated the cost efficiency of the capture process. Decreased human health impacts benefit social communities and reduce social costs. Further research will be required to consider the cost efficiency from reduced human health impacts such as decreased mortality risk of $PM_{2.5}$ due to PCC projects.

Furthermore, this study conducted a risk assessment in an industrial area with a small population in Australia. The risk associated with PCC projects were acceptable in this local environment. However, HCHO and $PM_{2.5}$ concentrations in Australia are lower than many heavily polluted countries. A similar atmospheric dispersion simulation and risk assessment in a heavily polluted area would lead to different conclusions. Further research including risk assessments with different pollution levels and landscapes would provide a comprehensive understanding of potential human health impacts associated with the PCC projects.

This study investigated reaction schemes using a KPP kinetic model to understand the formation of degradation products of particular amines specifically nitramine and nitrosamine. The study calculated potential near-surface concentrations of primary air pollutants from PCC projects in year-long simulations under different meteorological conditions. A Monte-Carlo risk assessment was then conducted to analyse potential health risks corresponding to lifetime exposure to HCHO and $PM_{2.5}$. This study provides a reference case scenario for scientists and regulators working on implementing PCC technology to reduce CO_2 emission and reduce global warming.

References

Aarrestad, P.A., Gjershaug, J.O., 2009. Task 8 report-Effects on terrestrial vegetation soil and fauna of amines and possible degradation products, Phase I: CO2 and Amines Screening Study for Environmental Risks. Norwegian Institute for Nature Research, NO 7485 Trondheim, Norway.

AGEIS, 2013. National Greenhouse Gas Inventory - Kyoto Protocol classifications, Australian Greenhouse Emissions Information System (AGEIS). Department of Environment, Australia, http://ageis.climatechange.gov.au/.

Andreini, B.P., Baroni, R., Galimberti, E., Sesana, G., 2000. Aldehydes in the atmospheric environment: evaluation of human exposure in the north-west area of Milan. Microchemical Journal 67, 11-19.

Ansari, A.S., Pandis, S.N., 1998. Response of Inorganic PM to Precursor Concentrations. Environmental science & technology 32, 2706-2714.

Arija V, S.J., Fernandez-Ballart J, C.G., C., M.-H., 1996. Consumption, dietary habits and nutritional status of the Reus population (IX)--Evolution of food consumption, energy and nutrient intake and relationship with the socioeconomic and cultural level,1983-1993. Med Clin (Barc) 106, 174-179.

Atkinson, R., 1997. Gas-phase tropospheric chemistry of volatile organic compiunds: q alkanes and alkenes. Journal of Physical and Chemical Reference Data 26, 215-290.

Atkinson, R., 2000. Atmospheric chemistry of VOCs and NOx Atmospheirc Environment 34, 2063-2101.

Australian Bureau of Statistics, 2012. Regional Population Growth, Australia, 2011-12, http://www.abs.gov.au/ausstats/abs@.nsf/Products/3218.0~2011-12~Main+Features~New+South+Wales?OpenDocument#PARALINK0.

Baez, A.P., Belmont, R.D., Padilla, H., 1995. Measurements of formaldehyde and acetaldehyde in the atmosphere of Mexico City. Environmental Pollution 89, 163-167.

Berglen, T.F., Tønnesen, D., Dye, C., Karl, M., Knudsen, S., Tarrasón, L., 2010. CO2 Technology Centre Mongstad-updated air dispersion calculations-Update of OR 12-2008 TCM NILU report 2010. Norwegian Institute for Air Research.

Bieniarz, K., Epler, P., Kime, D., Sokolowska-Mikolajczyk, M., Popek, W., Mikolajczyk, T., 1996. Effects of N,N-dimethylnitrosamine (DMNA) on in vitro oocyte maturation and embryonic development of fertilized eggs of carp (Cyprinus carpio L.) kept in eutrophied ponds. Journal of Applied Toxicol 16, 153.

Blackall, T.D., Wilson, L.J., Bull, J., Theobald, M.R., Bacon, P.J., Hamer, K.C., Wanless, S., Sutton, M.A., 2008. Temporal variation in atmospheric ammonia concentrations above seabird colonies. Atmospheric Environment 42, 6942-6950.

Bloss, C., Wagner, V., Jenkin, M.E., Volkamer, R., Bloss, W.J., Lee, J.D., Heard, D.E., Wirtz, K., Martin-Reviejo, M., Rea, G., Wenger, J.C., Pilling, M.J., 2005. Development of a detailed chemical mechanism for the atmospheric oxidation of aromatic hydrocarbons. Atmos. Chem. Phys. 5, 641-664.

BOM, 2014. Near El Niño conditions persist in tropical Pacific Ocean (Issued on 23 December 2014). Bureau of Meteorology, http://www.bom.gov.au/climate/enso/archive/ensowrap_20141223.pdf.

BOM, 2015a. Definitions for 9am and 3pm statistics. Bureau of Meteorology, http://www.bom.gov.au/climate/cdo/about/definitions9and3.shtml.

BOM, 2015b. La Niña – Detailed Australian Analysis. Bureau of Meteorology, http://www.bom.gov.au/climate/enso/lnlist/.

BOM, B.o.M., 2015c. ENSO wrap-UP_20150526. Bureau of Meteorology, http://www.bom.gov.au/climate/enso/archive/ensowrap_20150526.pdf.

Borweina, J., Howlettb, P., Piantadosi, J., 2014. Modelling and simulation of seasonal rainfall using checkerboard copulas of maximum entropy. Mathematics and Computers in Simulation https://www.carma.newcastle.edu.au/jon/matcom.pdf.

Bråten, H.B., Bunkan, A. J., Bache-Andreassen, L., Solimannejad, M. and Nielsen, C. J., 2008. Final Report on a Theoretical Study on the Atmospheric Degradation of Selected Amines, Oslo/Kjeller.

Bringmann, G., Kuhn, R., 1980. Comparison of the toxicity thresholds of water pollutants to bacteria, algae, and protozoa in the cell multiplication inhibition test Water Res 14, 231-241.

Brooks, S., 2008. The Toxicity of Selected Primary Amines and Secondary Products to Aquatic Organisms: A review, in: Research, N.I.f.W. (Ed.), Phase I: CO2 and Amines Screening Study for Environmental Risks, Norwegian Institue for Water Research.

CalEPA, 2003. The Air Toxics Hot Spots Program Guidance Manual for Preparation of Health Risk Assessments, in: Office-of-Environmental-Health-Hazard-Assessment (Ed.), California.

Chen, J., So, S., Lee, H., Fraser, M.P., Curl, R.F., Harman, T., Tittel, F.K., 2004. Atmospheric Formaldehyde Monitoring in the Greater Houston Area in 2002. Applied Spectroscopy 58.

Chi, S., Rochelle, G.T., 2002. Oxidative Degradation of Monoethanolamine. Industrial & Engineering Chemistry Research 41, 4178-4186.

Climate Change Authority, 2014. Reducing Australia's Greenhouse Gas Emissions—Targets and Progress Review Final Report. Climate Change Authority, Melbourne Australia.

Coffey, 2000. Summary Report Of The Review Of Fuel Quality Requirements For Australian Transport, in: Department_of_Environment (Ed.). Australia Department of Environment, http://www.environment.gov.au/resource/summary-report-review-fuel-quality-requirements-australian-transport.

Cope, M., Keywood, M., Emmerson, K., Galbally, I., Boast, K., Chambers, S., Cheng, M., Crumeyrolle, S., Dunne, E., Fedele, R., Gillett, R., Griffin, A., Harnwell, J., Katzfey, J., Hess, D., Lawson, S., Miljevic, B., Molloy, S., Powell, J., Reisen, F., Ristovski, Z., Selleck, P., Ward, J., Zhang, C., Zeng, J., 2014. Sydney Particle Study--Stage II, CSIRO and NSW Office of Environmental Heritage (OEH).

Cope, M., Lee, S., 2009. TAPM-CTM_UserManual, in: CSIRO (Ed.).

Cox, L., 1999. Technical Bulletin--Nitrogen Oxides (NOx): why and how they are controlled. U.S. Environmental Protection Agency, Research Triangle Park, North Carolina 27711.

CSIRO, 2012. Assessing Post-Combustion Capture for Coal-fired Power Stations in Asia-Pacific Partnership Countries, Final report to the Department of Resources, Energy and Tourism. CSIRO, Newcastle.

Dai, N., Mitch, W.A., 2014. Effects of flue gas compositions on nitrosamine and nitramine formation in postcombustion CO2 capture systems. Environmental science & technology 48, 7519-7526.

Dasgupta, P.K., Li, J., Zhang, G., Luke, W.T., Mcclenny, W.A., Stutz, J., Fried, A., 2005. Summertime-ambient-formaldehyde-in-five-U.S.-metropolitan-areas-Nashville,-Atlanta,-Houston,-Philadelphia,-and-Tampa_2005_Environmental-Science-and-Technology. Environmental science & technology 39.

de Koeijer, G., Talstad, V.R., Nepstad, S., Tønnessen, D., Falk-Pedersen, O., Maree, Y., Nielsen, C., 2013. Health risk analysis for emissions to air from CO2 Technology Centre Mongstad. International Journal of Greenhouse Gas Control 18, 200-207.

De'Ath, G., Fabricius, K., Sweatman, H., Puotinen, M., 2012. 'The 27-year decline of coral cover on the Great Barrier Reef and its causes'. Proceedings of the National Academy of Science 109, 17,995-999.

Department of Environment, 2005a. Air Toxics Air Quality Fact Sheet. Department of Environment, Australia, http://www.environment.gov.au/protection/publications/air-toxics.

Department of Environment, 2005b. Nitrogen dioxide (NO2) Air Quality Fact Sheet. Department of Environment, Australia, http://www.environment.gov.au/protection/publications/factsheet-nitrogen-dioxide-no2.

Department of Environment, 2005c. Sulfur dioxide (SO2) Air Quality Fact Sheet. Department of Environment, Australia, http://www.environment.gov.au/protection/publications/factsheet-sulfur-dioxide-so2.

Dockery, D., Pope III, C.A., Xu, X., Spengler, J., Ware, J., Fay, M., Ferris, B., Speizer, F., 1993. An association between air pollution and mortality in six US cities. New England Journal of Medicine 329, 1753-1759.

Donahue, N.M., Robinson, A.L., Stanier, C.O., Pandis, S.N., 2006. Coupled partitioning, dilution,and chemical aging of semivolatile organics. Environmental Science and Technology 40, 2635-2643.

Duan, J., Guo, S., Tan, J., Wang, S., Chai, F., 2012. Characteristics of atmospheric carbonyls during haze days in Beijing, China. Atmospheric Research 114-115, 17-27.

Emmerson, K., Cope, M., White, S., Angove, D., Azzi, M., 2013. 3D Dispersion Modelling of Monoethanolamine (MEA) from a Hypothetical Power Station. Deliverable 4.3: Determination of the fate of PCC emissions into the atmosphere. Prepared for ANLEC R&D CSIRO, Australia.

Environmental Risk Sciences, 2014. Technical working paper: Human health risk assessment-Appendix H, Technical working paper: Human health risk assessment--NorthConnex.

Feng, Y., Wen, S., Chen, Y., Wang, X., Lu, H., Bi, X., Sheng, G., Fu, J., 2005. Ambient levels of carbonyl compounds and their sources in Guangzhou, China. Atmospheric Environment 39, 1789-1800.

Ferm, M., Hellsten, S., 2012. Trends in atmospheric ammonia and particulate ammonium concentrations in Sweden and its causes. Atmospheric Environment 61, 30-39.

Fostås, B., Gangstad, A., Nenseter, B., Pedersen, S., Sjøvoll, M., Sørensen, A.L., 2011. Effects of NOx in the flue gas degradation of MEA. Energy Procedia 4, 1566-1573.

Fountoukis, C., Nenes, A., 2007. ISORROPIA II: a computationally efficient thermodynamic equilibrium model for K+-Ca2+-Mg2+-NH(4)(+)-Na+-SO42--NO3--Cl--H2O aerosols. Atmospheric Chemistry and Physics 7, 4639-4659.

Fowler, T., Vernon, G., 2012a. Atmospheric chemistry modelling of Components from Post-combustion Amine-Based CO2 Capture_Executive Summary, in: Veritas, D.N. (Ed.), Report for GASSNOVA SF Modelling air quality impacts of post-combustion amine-based CO2 capture. Det Norske Veritas, Norway.

Fowler, T., Vernon, G., 2012b. Report for Atmospheric chemistry modelling of Componets from post-combustion amine-based CO2 capture --Final Report. Det_Norske_Veritas.

Galbally, I., Cope, M., Lawson, S., Bentley, S., Cheng, M., Gillett, R., Selleck, P., Petraitis, B., Dunne, E., Lee, S., 2008. Sources of Ozone Precursors and Atmospheric chemistry in a typical australian city. CSIRO Marine and Atmospheric Research.

Gerba, C.P., 2006. Risk Assessment, in: Pepper, I.L., C.P. Gerba, Brusseau, M.L. (Eds.), Environmental and Pollution Science. Elsevier Inc., , Amsterdam pp. 212-232.

Gillner, M., Loeper, I., 1993. Health effects of selected chemicals 2-Ethanolamine, in: Ministers, N.C.o. (Ed.), København, pp. 49-73.

Global CCS Institute, 2009. Report 2 Economic assessment of carbon capture and storage technologies, Strategic Analysis of the Global Status of Carbon Capture and Storage Global CCS Institute, Canberra, Australia.

Global CCS Institute, 2012. Pre Combustion Capture, CO2 Capture Technologies July 2011. Global Carbon Capture and Storage Institute, Canberra, Australia. , https://hub.globalccsinstitute.com/sites/default/files/publications/29756/co2-capture-technologies-pre-combustion-capture.pdf.

Goff;, G.S., Rochelle, G.T., 2004. Monoethanolamine degradation: O2 mass transfer effects under CO2 capture conditions. Industrial & Engineering Chemistry Research 43, 6400-6408.

Gong, L., Lewicki, R., Griffin, R.J., Tittel, F.K., Lonsdale, C.R., Stevens, R.G., Pierce, J.R., Malloy, Q.G.J., Travis, S.A., Bobmanuel, L.M., Lefer, B.L., Flynn, J.H., 2013. Role of atmospheric ammonia in particulate matter formation in Houston during summertime. Atmospheric Environment 77, 893-900.

Goodall, C.M., Kennedy, T.H., 1976. Carcinogenicity of dimethylnitramine in NZR rats and NZO mice. Cancer Letter 1, 295-298.

Gouedard, C., Picq, D., Launay, F., Carrette, P.L., 2012. Amine degradation in CO2 capture. I. A review. International Journal of Greenhouse Gas Control 10, 244-270.

Greene, N.A., Morris, V.R., 2006. Assessment of Public Health Risks Associated with Atmospheric Exposure to PM2.5 in Washington, DC, USA. International Journal of Environmental Research and Public Health 3, 86-97.

Grosjean, D., 1992. Discussion: amospheric concentrations and temporal variations of C1-C3 carbonyl compounds at two rural sites in central Ontario. Atmospheirc Environment 26A, 349-351.

Grosjean, D., Grosjean, E., LMoreira, L.F.R., 2002. Speciated-ambient-carbonyls-in-Rio-de-Janeiro,-Brazil_2002_Environmental-Science-and-Technology. Environmental Science and Technology 36, 1389-1395.

Grutter, M., Flores, E., Andraca-Ayala, G., B ez, A., 2005. Air pollution monitoring with two optical remote sensing techniques in Mexico City. Atmospheirc Environment 39, 1027-1034.

He, K., Yang, F., Ma, Y., Zhang, Q., Yao, X., Chak, K.C., Steven, C., Chan, T., Patricia, M., 2001. The characteristics of PM2.5 in Beijing, China. Atmospheric Environment 35, 4959-4970.

Hellsten, S., Dragosits, U., Place, C.J., Misselbrook, T.H., Tang, Y.S., Sutton, M.A., 2007. Modelling seasonal dynamics from temporal variation in agricultural practices in the UK ammonia emission inventory. . Water, Air, and Soil Pollution, Focus 7, 3-13.

Heo, J., McCoy, S.T., Adams, P.J., 2015. Implications of ammonia emissions from post-combustion carbon capture for airborne particulate matter. Environmental science & technology 49, 5142-5150.

Herzog, H., Meldon, J., Hatton, A., 2009. Advanced Post-Combustion CO2 Capture-Prepared for the Clean Air Task Force MIT.

Hibberd, M., Selleck, P., Keywood, M., Cohen, D., Stelcer, E., Atanacio, A., 2013. Upper Hunter Valley Particle Characterization Study. CSIRO, Australia.

Ho, S.S.H., Ho, K.F., Liu, W.D., Lee, S.C., Dai, W.T., Cao, J.J., Ip, H.S.S., 2011. Unsuitability of using the DNPH-coated solid sorbent cartridge for determination of airborne unsaturated carbonyls. Atmospheric Environment 45, 261-265.

Ho, S.S.H., Ip, H.S.S., Ho, K.F., Dai, W.-T., Cao, J., Ng, L.P.T., 2013. Technical Note: Concerns on the Use of Ozone Scrubbers for Gaseous Carbonyl Measurement by DNPH-Coated Silica Gel Cartridge. Aerosol and Air Quality Research.

Hodzic, A., Jimenez, J.L., 2011. Modeling anthropogenically controlled secondary organic aerosols in a megacity: a simplified framework for global and climate models. Geosci. Model Dev. 4, 901-917.

Huang, J., Feng, Y., Li, J., Xiong, B., Feng, J., Wen, S., Sheng, G., Fu, J., Wu, M., 2008. Characteristics of carbonyl compounds in ambient air of Shanghai, China. Journal of Atmospheric Chemistry 61, 1-20.

Hurley, P., 2006. An Evaluation And Inter-Comparison Of Ausplume, Aermod And Tapm For Seven Field Datasets Of Point Source Dispersion. Clean Air and Environmental Quality 40, 45-50.

Hurley, P., 2008a. TAPM version 4 technical Description Part1., in: CSIRO (Ed.). CSIRO Marine and Atmospheric Research, CSIRO.

Hurley, P., 2008b. tapm_v4_user_manual, in: CSIRO (Ed.), CSIRO Marine and Atmoshpheric Research Internal Report No. 5.

Hurley, P.J., Physick, W.L., Luhar, A.K., 2005. TAPM: a practical approach to prognostic meteorological and air pollution modelling. Environmental Modelling & Software 20, 737-752.

Ianniello, A., Spataro, F., Esposito, G., Allegrini, I., Rantica, E., Ancora, M.P., Hu, M., Zhu, T., 2010. Occurrence of gas phase ammonia in the area of Beijing (China). Atmospheric Chemistry and Physics 10, 9487-9503.

IEA, 2015. Energy and Climate Change: World Energy Outlook Special Report, World Energy Outlook. International Enegy Agency (IEA), France.

IEAGHG, 2012. Gaseous Emissions from Amine Based post combustion CO2 capture processes and their deep removal, in: Azzi, M., Sharma, S., Dave, N., Feron, P., Day, S., Attalla, M., French, D., Do, T., Yu, H., Khare, S. (Eds.), IEAGHG report 07/2012, IEAGHG UK.

IPCC, 2013. Working Group I Contribution to the IPCC Fifth Assessment Report, Climate Change 2013—The Physical Science Basis, Final Draft Underlying Scientific-Technical Assessment, Cambridge and New York, http://ipcc.ch/report/ar5/wg1/. .

Jones, N.B., Riedel, K., Allan, W., Wood, S., Palmer, P.I., Chance, K., Notholt, J., 2009. Long-term tropospheric formaldehyde concentrations deduced from ground-based fourier transform solar infrared measurements. 9, 7131–7142.

Karl, M., Brooks, S., Wright, R., Knudsen, S., 2008. Amines Worst Case Studies-- Worst Case Studies on Amine Emissions from CO2 Capture Plants, in: NILU (Ed.).

Karl, M., Dye, C., Schmidbauer, N., Wisthaler, A., Mikoviny, T., D'Anna, B., Müller, M., Borrás, E., Clemente, E., Muñoz, A., Porras, R., Ródenas, M., Vázquez, M., Brauers, T., 2012. Study of OH-initiated degradation of 2-aminoethanol. Atmospheric Chemistry and Physics 12, 1881-1901.

Karl, M., Wright, R.F., Berglen, T.F., Denby, B., 2011. Worst case scenario study to assess the environmental impact of amine emissions from a CO2 capture plant. International Journal of Greenhouse Gas Control 5, 439-447.

Keywood, M., Cope, M., Iinuma, Y., 2008. Appendix C--Development of Tools for the Identification of Secondary Organic Aerosol in Australian Cities, Progress Report 3: Aerosol Microphysics, Organic Speciation and Modelling. CSIRO, Department of Environment, Water Heritage and Arts.

Knaak, J.B., Leung, H.W., Stott, W.T., Busch, J., Bilsky, J., 1997. Toxicology of mono-, di-, and triethanolamine. Rev. Environ. Contam. Toxicol., 1-86.

Krewski, D., Jerrett, M., Burnett, R., Ma, R., Hughes, E., Shi, Y., Turner, M., Pope, C.r., Thurston, G., Calle, E., Thun, M., Beckerman, B., DeLuca, P., Finkelstein, N., Ito, K., Moore, D., Newbold, K., Ramsay, T., Ross, Z., Shin, H., Tempalski, B., 2009. Extended follow-up and spatial analysis of the American Cancer Society study linking particulate air pollution and mortality, Research Report No.140. Health Effects Institute, Boston, Massachusetts.

Låg, M., Andreassen, Å., Instanes, C., Lindeman, B., 2009. Health effects of different amines and possible degradation products relevant for CO2 capture, Nydalen, Norway.

Leeuwen, C.J.v., Vermeire, T.G., 2007. Risk Assessment of Chemicals-An Introduction. Springer, Netherlands.

Lei, W., de Foy, B., Zavala, M., Volkamer, R., Molina, L.T., 2007. Characterizing ozone production in the Mexico City Metropolitan Area: a case study using a chemical transport model. Atmospheric Chemistry and Physics 7, 1347–1366.

Lei, W., Zavala, M., Foy, B.d., Volkamer, R., Molina, M.J., Molina, L.T., 2009. Impact of primary formaldehyde on air pollution in the Mexico City Metropolitan Area. Atmospheric Chemistry and Physics 9, 2607-2618.

Lepaumier, H., da Silva, E.F., Einbu, A., Grimstvedt, A., Knudsen, J.N., Zahlsen, K., Svendsen, H.F., 2011. Comparison of MEA degradation in pilot-scale with lab-scale experiments. Energy Procedia 4, 1652-1659.

Lepaumier;, H., Picq;, D., Carrette;, P.-L., 2009. New Amines for CO2 Capture. II. Oxidative Degradation Mechanisms. Industrial & Engineering Chemistry Research 48, 9068-9075.

Li, Y., Shao, M., Lu, S., Chang, C.-C., Dasgupta, P.K., 2010. Variations and sources of ambient formaldehyde for the 2008 Beijing Olympic games. Atmospheirc Environment 44, 2632-2639.

Lin, Y.C., Schwab, J.J., Demerjian, K.L., Bae, M.-S., Chen, W.-N., Sun, Y., Zhang, Q., Hung, H.-M., Perry, J., 2012. Summertime formaldehyde observations in New York City: Ambient levels, sources and its contribution to HOx radicals. Journal of Geophysical Research 117.

Lü, H., Cai, Q., Wen, S., Chi, Y., Guo, S., Sheng, G., Fu, J., Antizar-Ladislao, B., 2009. Carbonyl compounds in the ambient air of hazy days and clear days in Guangzhou, China. Atmos. Res. 94, 363-372.

Lü, H., Cai, Q.Y., Wen, S., Chi, Y., Guo, S., Sheng, G., Fu, J., 2010. Seasonal and diurnal variations of carbonyl compounds in the urban atmosphere of Guangzhou, China. The Science of the total environment 408, 3523-3529.

Luecken, D.J., Hutzell, W.T., Strum, M.L., Pouliot, G.A., 2012. Regional sources of atmospheric formaldehyde and acetaldehyde, and implications for atmospheric modeling. Atmospheric Environment 47, 477-490.

M Burgers, S Walsh, 2002. Exposure Assessment and Risk Characterissation for the Development of a PM2.5 Standard, prepared for National Environment Protection Council Service Corporation. Environment Protection Authority of Victoria, Melbourne.

MacIntosh, D.L., Stewart, J.H., Myatt, T.A., Sabato, J.E., Flowers, G.C., Brown, K.W., Hlinka, D.J., Sullivan, D.A., 2010. Use of CALPUFF for exposure assessment in a near-field, complex terrain setting. Atmospheric Environment 44, 262-270.

Manins, P., Ayers, G., Bohm, M., Raupach, M., Williams, D., Carras, J., 1996. Hunter Valley dry deposition Study, A report to Pacific Power CSIRO, p. 175p.

Martins, L.D., Andrade, M.F., Ynoue, R.Y., De Albuquerque, E.L., Tomaz, E., Vasconcellos, P.C., 2008. Ambiental volatile organic compounds in the Megacity of Sao Paulo. Quimica Nova 31, 2009-2013.

Meng, Z.Y., Lin, W.L., Jiang, X.M., Yan, P., Wang, Y., Zhang, Y.M., Jia, X.F., Yu, X.L., 2011. Characteristics of atmospheric ammonia over Beijing, China. Atmospheric Chemistry and Physics 11, 6139-6151.

Molina, L.T., Kolb, C.E., de Foy, B., Lamb, B.K., Brune, W.H., Jimenez, J.L., Ramos-Villegas, R., Sarmiento, J., Paramo-Figueroa, V.H., Cardenas, B., Gutierrez-Avedoy, V., Molina, M.J., 2007. Air quality in North America's most populous city – overview of the MCMA-2003 campaign. Atmos. Chem. Phys. 7, 2447-2473.

Molina, L.T., Molina, M.J., (Eds.), 2002. Air Quality in the Mexico Megacity: An Integrated Assessment. Kluwer Academy Publishers.

Morken, A.K., Nenseter, B., Pedersen, S., Chhaganlal, M., Feste, J.K., Tyborgnes, R.B., Ullestad, Ø., Ulvatn, H., Zhu, L., Mikoviny, T., Wisthaler, A., Cents, T., Bade, O.M., Knudsen, J., de Koeijer, G., Falk-Pedersen, O., Hamborg, E.S., 2014. Emission Results of Amine Plant Operations from MEA Testing at the CO2 Technology Centre Mongstad. Energy Procedia 63, 6023-6038.

Moser, P., Schmidt, S., Stahl, K., 2011. Investigation of trace elements in the inlet and outlet streams of a MEA-based post-combustion capture process results from the test programme at the Niederaussem pilot plant. Energy Procedia 4, 473-479.

Muswellbrook Shire Council, 2015. Climate of Muswellbrook Shire. Muswellbrook Shire Council, http://www.muswellbrook.nsw.gov.au/index.php/about-muswellbrook-shire/climate.

Na, K., Cocker, D.R., 2008. Fine organic particle, formaldehyde, acetaldehyde concentrations under and after the influence of fire activity in the atmosphere of Riverside, California. Environ Res 108, 7-14.

NEPC, 2016. Ambient air quality standards. National Environment Protection Council https://www.environment.gov.au/protection/air-quality/air-quality-standards.

Nielsen, C.J., D' Anna, B., Dye, C. George, C., Graus, M., Hansel, A., Karl, M., King, S., Musabila, M., Müller, M., Schmidbauer, N., Stenstrom, Y., Wisthaler, A., 2010. Atmospheric Degradation of Amines. Summary Report: Gas phase oxidation of 2-aminoethanol (MEA). CLIMIT project no. 193438, NILU OR 8/2010. Norwegian Institute for Air Research, Kjeller, Norway.

Nielsen, C.J., D'Anna, B., Dye, C., Graus, M., Karl, M., King, S., Maguto, M.M., Müller, M., Schmidbauer, N., Stenstrøm, Y., Wisthaler, A., Pedersen, S., 2011. Atmospheric chemistry of 2-aminoethanol (MEA). Energy Procedia 4, 2245-2252.

NIPH, 2015 Access. Health effects of amines and derivatives associated with CO2 capture: Nitrosamines and nitramines. Norwegian Institue of Public Health, http://www.fhi.no/dav/872795158b.pdf.

NSW EPA, 2012a. 2008 Calendar Year Air Emissions Inventory for the Greater Metropolitan Region in NSW. NSW Environment Protection Authority, http://www.epa.nsw.gov.au/air/airinventory2008.htm.

NSW EPA, 2012b. Air Emissions Inventory for the Greater Metropolitan Region in New South Wales - 2008 Calendar Year. Technical Report No. 1 - Consolidated Natural and Human-Made Emissions: Results. NSW Environment Protection Authority, Sydney NSW, Australia.

NSW EPA, 2012c. Upper Hunter Air Quality Monitoring Network-- Interim Performance Report December 2010-August 2011. NSW Environment Protection Authority, http://www.environment.nsw.gov.au/resources/aqms/120164uhaqmnintrepdecaug.pdf.

NSW EPA, 2013. Upper Hunter Air Particles Action Plan, in: (EPA), N.E.P.A. (Ed.). NSW Environment Protection Authority (EPA), Sydney, p. 23.

NSW EPA, 2014. Upper Hunter Air Quality Monitoring Network Annual Report 2013. NSW Environment Protection Authority, http://www.environment.nsw.gov.au/resources/air/140855UHAQMNAnnualReport2013.pdf.

NSW EPA, 2015. Atmosphere--New South Wales State of the Environment 2015, in: New South Wales Environment Protection Authority (Ed.). New Southe Wales Environment Protection Authority, Sydney.

NSW EPA, 2016. Upper Hunter Air Particles Action Plan. NSW Environment Protection Authority, http://www.epa.nsw.gov.au/aqms/130158uphuntap.htm.

NSW Health, 2010. Respiratory and Cardiovascular Diseases and Cancer Among Residents in the Hunter New England Area Health Service. NSW Department of Health, http://www.health.nsw.gov.au/environment/Publications/HNE-Respi-Cardio-Disease.pdf.

NSWEPA, 2005. Approved Methods for the Modelling and Assessment of Air Pollutants in NSW, in: NSWEPA (Ed.). New South Wale Environment Protection Authority, http://www.epa.nsw.gov.au/air/appmethods.htm.

NSWEPA, 2012. New South Wales State of the Environment 2012 in: New_South_Wales_Environment_Protection_Authority (Ed.). New Southe Wales Environment Protection Authority, Sydney.

Ochs, S.d.M., Albuquerque, F.C., Massa, M.C.G.P., Pereira Netto, A.D., 2011. Evaluation of C1–C13 carbonyl compounds by RRLC-UV in the atmosphere of Niterói City, Brazil. Atmospheric Environment 45, 5183-5190.

OEHHA, 2009. OEHHA Cancer Potency Values. The Office of Environmental Health Hazard Assessment (OEHHA), California, USA.

Office of Fossil Energy, 2016. PRE-COMBUSTION CARBON CAPTURE RESEARCH. US_Department_of_Energy, http://energy.gov/fe/science-innovation/carbon-capture-and-storage-research/carbon-capture-rd/pre-combustion-carbon.

Olajos, E., Coulston, F., 1978. Comparative Toxicology of N-Nitroso compounds and their carcinogenic potential to man. Ecotox Environ Safety 317-367.

Ostro, B., 2004. Outdoor Air Pollution: Assessing the environmental burden of disease at national and local levels, Enrionmental Burden of Disease Series. World Health Organization, Geneva.

Palisade, 2013. Guide to using @RISK version 6 : Risk Analysis and Simulation Add-In for Microsoft Excel. Palisade Corporation, Newfield NY USA.

Palisade, 2015. @RISK webpage. Palisade, http://www.palisade.com/risk/.

Pang, X., Mu, Y., 2006. Seasonal and diurnal variations of carbonyl compounds in Beijing ambient air. Atmospheric Environment 40, 6313-6320.

Pang, X.B., Lee, X., 2010. Temporal variations of atmospheric carbonyls in urban ambient air and street canyons of a Mountainous city in Southwest China. Atmospheirc Environment 44, 2098-2106.

Pedersen, S., SjØvoll, M., Fostås, B.F., 2010. Flue Gas Degradation of Amines", IEA GHG Workshop, 16th February, 2010, Oslo, Norway.

Peng, C.-Y., Yang, H.-H., Lan, C.-H., Chien, S.-M., 2008. Effects of the biodiesel blend fuel on aldehyde emissions from diesel engine exhaust. Atmospheric Environment 42, 906-915.

Pinder, R.W., Dennis, R.L., Bhave, P.V., 2008. Observable indicators of the sensitivity of PM2.5 nitrate to emission reductions—Part I: Derivation of the adjusted gas ratio and applicability at regulatory-relevant time scales. Atmospheric Environment 42, 1275-1286.

Pinder, R.W., Walker, J.T., Bash, J.O., Cady-Pereira, K.E., Henze, D.K., Luo, M., Osterman, G.B., Shephard, M.W., 2011. Quantifying spatial and seasonal variability in atmospheric ammonia with in situ and space-based observations. Geophysical Research Letters 38, n/a-n/a.

Pope III, C.A., Burnett, R.T., Thun, M.J., Calle, E.E., Krewski, D., Ito, K., Thurston, G.D., 2002. Lung cancer, cardiopulmonary mortality, and long-term exposure to fine particulate air pollution. Journal of the American Medical Association 287, 1132-1141.

Pope III, C.A., Thun, M., Namboodiri, M., Dockery, D., Evans, J., Speizer, F., Health, C.J., 1995. Particulate air pollution as a predictor of mortality in a prospective study of US adults. American Journal of Respiratory and Critical Care Medicine 151, 669-674.

Possanzini, M., Palo, V., Cecinato, A., 2002. Sources and photodecomposition of formaldehyde and acetaldehyde in Rome ambient air. Atmospheirc Environment 36, 3195-3201.

Puchalski, M.A., Sather, M.E., Walker, J.T., Lehmann, C.M., Gay, D.A., Mathew, J., Robarge, W.P., 2011. Passive ammonia monitoring in the United States: comparing three different sampling devices. Journal of environmental monitoring : JEM 13, 3156-3167.

Qiu, C., Wang, L., Lal, V., Khalizov, A.F., Zhang, R., 2011. Heterogeneous reactions of alkylamines with ammonium sulfate and ammonium bisulfate. Environmental science & technology 45, 4748-4755.

Ras, M.R., Marcé, R.M., Borrull, F., 2009. Characterization of ozone precursor volatile organic compounds in urban atmospheres and around the petrochemical industry in the Tarragana region. Sci. Total Environ. 407, 4132-4319.

Rochelle, G.T., 2009. Amine scrubbing for CO2 capture. Science 325, 1652-1654.

Salas, L.j., Singh, H.B., 1986. Measurements of formaldehyde and acetaldehyde in the urban ambient air. Atmospheirc Environment 20, 1301-1304.

Sander, R., Baumgaertner, A., Gromov, S., Harder, H., Jöckel, P., Kerkweg, A., Kubistin, D., Regelin, E., Riede, H., Sandu, A., Taraborrelli, D., Tost, H., Xie, Z.Q., 2011. The atmospheric chemistry box model CAABA/MECCA-3.0. Geoscientific Model Development 4, 373-380.

Sandu, A., Sander, R., 2005. kpp-2.1 Users Manual.

Sather, M.E., Mathew, J., Nguyen, N., Lay, J., Golod, G., Vet, R., Freise, J., Hathcoat, A., Sakizzie, B., King, M., Lee, C., Oliva, S., Miguel, G.S., Crow, L., Geasland, F., 2008. Baseline ambient gaseous ammonia concentrations in the Four corners area and eastern Oklahoma USA. Journal of Environmental Monitoring 10, 1319-1325.

Schauer, e.a., 1999. Measurement of Emissions from Air Pollution Sources, C1 through C30 Organic Compounds from Medium Duty Diesel Trucks. Environ. Sci. Technol 33, 1578-1587.

Scire, J.S., Strimaitis, D.G., Yamartino, R.J., 2011. CALPUFF Version 6 User Instructions. the Atmospheric Studies Group at TRC Solutions.

Seinfeld, J.H., Pandis, S.N., 1998. Atmospheric Chemistry and Physics : From Air Pollution to Climate Change. Wiley.

Sexton, A.J., Rochelle, G.T., 2011. Reaction Products from the Oxidative Degradation of Monoethanolamine. Industrial & Engineering Chemistry Research 50, 667-673.

Shao, R., Stangeland, A., 2009. Bellona report - Amines used in CO2 capture, in: Foundation, T.B. (Ed.).

Shell Global, 2014. SHELL CANSOLV TECHNOLOGY USED AT THE FIRST COMMERCIAL-SCALE POST-COMBUSTION CARBON CAPTURE AND STORAGE PLANT. Shell Global, http://www.shell.com/business-customers/global-solutions/shell-cansolv-gas-absorption-solutions/cansolv-news-and-media-releases/shell-cansolv-media-releases/shell-cansolv-technology.html#vanity-aHR0cDovL3d3dy5zaGVsbC5jb20vZ2xvYmFsL3Byb2R1Y3RzLXNlcnZpY2VzL3NvbHV0aW9ucy1mb3ItYnVzaW5lc3Nlcy9nbG9iYWwtc29sdXRpb25zL2NhcmJvbi1jYXB0dXJlLWFuZC1zdG9yYWdlL2NhbnNvbHYuaHRtbA/LW5ld3MtbGdlLacmFyeS9zaGVsbC1jYW5zb2x2LW1lZGlhLXJlbGVhc2VzL3NoZWxsLWNhbnNvbHYtdGVjaG5vbG9neS0yMDE0MTAwMi5odG1s.

Smith, R.L., 1994. Use of monte carlo simulation for human exposure assessment at a superfund site. Risk Analysis 14, 433-439.

Strazisar, B.R., Anderson, R.R., White, C.M., 2003. Degradation pathways for monoethanolamine in a CO2 capture facility. Energy and Fuels 17, 1034-1039.

Sun, Y.L., Zhuang, G.S., Tang, A.H., Wang, Y., An, Z.S., 2006. Chemical characteristics of PM2.5 and PM10 in haze–fog episodes in Beijing. Environmental Science and Technology 40, 3148-3155.

Tang, X., Bai, Y., Duong, A., Smith, M.T., Li, L., Zhang, L., 2009. Formaldehyde in China: production, consumption, exposure levels, and health effects. Environment international 35, 1210-1224.

Thong, D., Dave, N., Feron, P., Azzi, M., 2012. Activity 3: Estimated emissions to the atmosphere from amine based PCC processes for a black coal fired power station based on literature and

modelling., Environmental Impact of Amine-based CO2 Post-combustion Capture (PCC) Process--Deliverable 3.2 Progress Report. CSIRO.

Todoroski, A., Kjellberg, D., 2013. Lower Hunter Air Quality Review of Ambient Air Quality Data for State of NSW and the Environment Protection Authority, in: Ltd, T.A.S.P. (Ed.). Todoroski Air Sciences Pty Ltd.

U.S.EPA, 2008. National Emissions Inventory (NEI) Data Version 2, http://www.epa.gov/ttn/chief/net/2008inventory.html.

United Nations, 1992. Environmentally sound management of toxic chemicals including prevention of illegal international traffice in toxic and dangerous products, Agenda 21, Chapter 19. United Nations Conference on Environment and Development, Rio de Janeiro, Brazil.

US EPA, 2012. PARTICLE POLLUTION AND HEALTH, https://www3.epa.gov/airquality/particlepollution/2012/fshealth.pdf.

US EPA, 2016. Ozone, AIRTrends 1995 Summary. US EPA, https://www3.epa.gov/airtrends/aqtrnd95/o3.html.

USEPA, 1989. Risk Assessment Guidance for Superfund - Human Health Evaluation Manual (Part A) Interim Final. Office of Emergency and Remedial Response, Washington, DC.

USEPA, 1992. Guidelines for Exposure Assessment (US-EPA), in: Agency, U.S.E.P. (Ed.). U.S.Environmental Protection Agency, Washington, DC.

USEPA, 2012. Integrated Risk Information System-Formaldehdye, http://www.epa.gov/iris/subst/0419.htm.

USEPA, 2013. Integrated Risk Information System (IRIS). The U.S. Environmental Protection Agency (EPA) www.epa.gov/iris/index.html.

USEPA, 2015a. Acetaldehyde, Integrated Risk Information System, http://www.epa.gov/iris/subst/0290.htm.

USEPA, 2015b. Formaldehyde, Integrated Risk Information System. US EPA, http://www.epa.gov/iris/subst/0419.htm.

USEPA, 2015c. N-Nitrosodimethylamine (Nitrosamines), Integrated Risk Information System. USEPA, http://www.epa.gov/iris/subst/0045.htm.

Verna, L., Whysner, J., Williams, G., 1996. N-nitrosodiethylamine mechanistic data and risk assessment: Bioactivation, DNA-adduct formation, mutagenicity, and tumor initiation. Pharmacol Ther, 57-81.

Volkamer, R., Molina, L.T., Molina, M.J., Shirley, T., Brune, W.H., 2005. DOAS measurement of glyoxal as an indicator for fast VOC chemistry in urban air. Geophys. Res. Lett. 32.

Wang, B., Lee, S.C., Ho, K.F., 2007. Characteristics of carbonyls: concentrations and source strengths for indoor and outdoor residential microenvironments in China. Atmospheirc Environment 41, 2851-2861.

Wang, Y., Zhuang, G., Sun, Y., An, Z., 2006. The variation of characteristics and formation mechanisms of aerosols in dust, haze, and clear days in Beijing. Atmospheirc Environment 40, 6579-6591.

WeatherSpark, 2000. Historical Weather For 2000 in Sydney, Australia - WeatherSpark. Weather Spark, http://weatherspark.com/history/34088/2000/Sydney-New-South-Wales-Australia.

Weeks, M.H., Downing, T.O., Musselman, N.P., Carson, T.R., Groff, W.A., 1960. The effect of continous exposure of animals to ethanolamine vapour. J. Am. Ind. Hyg. Assoc., 374-381.

Weng, M., Zhu, L., Yang, K., Chen, S., 2009. Levels and health risks of carbonyl compounds in selected public places in Hangzhou, China. J. Hazard. Mater. 164, 700-706.

WHO, 1998. Urban Traffic Pollution, in: Scewela, D., Zali, O. (Eds.). World Health Organization, Routledge, London.

WHO, 2013. Health effects of Particulate Matter--Policy implication for countries in eastern Europe, Caucasus and central Asia. World Health Organization, Denmark.

Wikipedia, 2012. Geography of New South Wales, http://en.wikipedia.org/wiki/Geography_of_New_South_Wales.

Wikipedia, 2013. Houston, http://en.wikipedia.org/wiki/Houston#cite_note-port_ranking-12.

Wikipedia, 2014. Geography of Sydney, http://en.wikipedia.org/wiki/Geography_of_Sydney.

Wikipedia, 2015a. Hunter Region, http://en.wikipedia.org/wiki/Hunter_Region.

Wikipedia, 2015b. Sydney, http://en.wikipedia.org/wiki/Sydney.

William, T., Winberry, J., Tejada, S., Lonneman, B., Kleindienst, T., 1999. Compendium of Methods for the Determination of Toxic Organic Compounds in Ambient Air (Method TO-11A), in: U.S.EPA (Ed.). U.S.EPA, Cincinnati, OH 45268.

Wilson, S.M., Serre, M.L., 2007a. Examination of atmospheric ammonia levels near hog CAFOs, homes, and schools in Eastern North Carolina. Atmospheric Environment 41, 4977-4987.

Wilson, S.M., Serre, M.L., 2007b. Use of passive samplers to measure atmospheric ammonia levels in a high-density industrial hog farm area of eastern North Carolina. Atmospheric Environment 41, 6074-6086.

Wu, Y., Nelson, P.F., 2014. Using Computer Modelling to Simulate Atmospheric Movement and Potential Risk of Pollutants from Post-combustion Carbon Capture Projects. Energy Procedia 63, 976-985.

Yamada, T., Uchiyama, S., Inaba, Y., Kunugita, N., Nakagome, H., Seto, H., 2012. A diffusive sampling device for measurement of ammonia in air. Atmospheric Environment 54, 629-633.

Yamamoto, N., Nishiura, H., Honjo, T., Ishikawa, Y., Suzuki, K., 1995. A long-term study of atmospheric ammonia and particulate ammonium concentrations in Yokohama, Japan. , . Atmospheric Environment 29, 97-103.

Yiannoukas, S., Morale, G., Vernon, G., 2011. Report for Atmospheric chemistry modelling of Componets from post-combustion amine-based CO2 capture --First approach. Det_Norske_Veritas.

Zbieranowski, A.L., Aherne, J., 2012. Spatial and temporal concentration of ambient atmospheric ammonia in southern Ontario, Canada. Atmospheric Environment 62, 441-450.

Zbieranowski, A.L., Aherne, J., 2013. Ambient concentrations of atmospheric ammonia, nitrogen dioxide and nitric acid in an intensive agricultural region. Atmospheric Environment 70, 289-299.

Zhao, M., Wang, S., Tan, J., Hua, Y., Wu, D., Hao, J., 2016. Variation of Urban Atmospheric Ammonia Pollution and its Relation with PM2.5 Chemical Property in Winter of Beijing, China. Aerosol and Air Quality Research 16, 1390-1402.

Zheng, J., Ma, Y., Chen, M., Zhang, Q., Wang, L., Khalizov, A.F., Yao, L., Wang, Z., Wang, X., Chen, L., 2015. Measurement of atmospheric amines and ammonia using the high resolution time-of-flight chemical ionization mass spectrometry. Atmospheric Environment 102, 249-259.

Zheng, J., Zhang, R., Garzón, J.P., Huertas, M.E., Levy, M., Ma, Y., Torres-Jardón, R., Ruiz-Suárez, L.G., Russell, L., Takahama, S., Tan, H., Li, G., Molina, L.T., 2013. Measurements of formaldehyde at the U.S.–Mexico border during the Cal-Mex 2010 air quality study. Atmospheric Environment 70, 513-520.

Zhu, L., Schade, G.W., Nielsen, C.J., 2013. Real-time monitoring of emissions from monoethanolamine-based industrial scale carbon capture facilities. Environmental science & technology 47, 14306-14314.

Appendix 1 contour maps of changes of NO peak value in 2015

Change of NO peak values in Jan 2015 between PCC and PrePCC (1 km resolution)
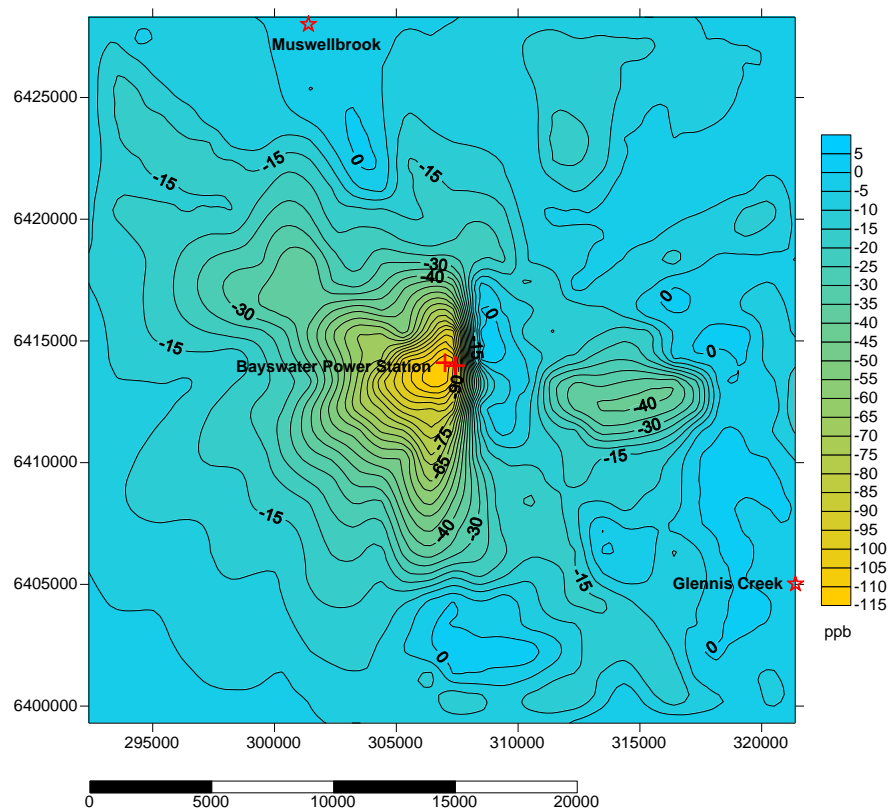
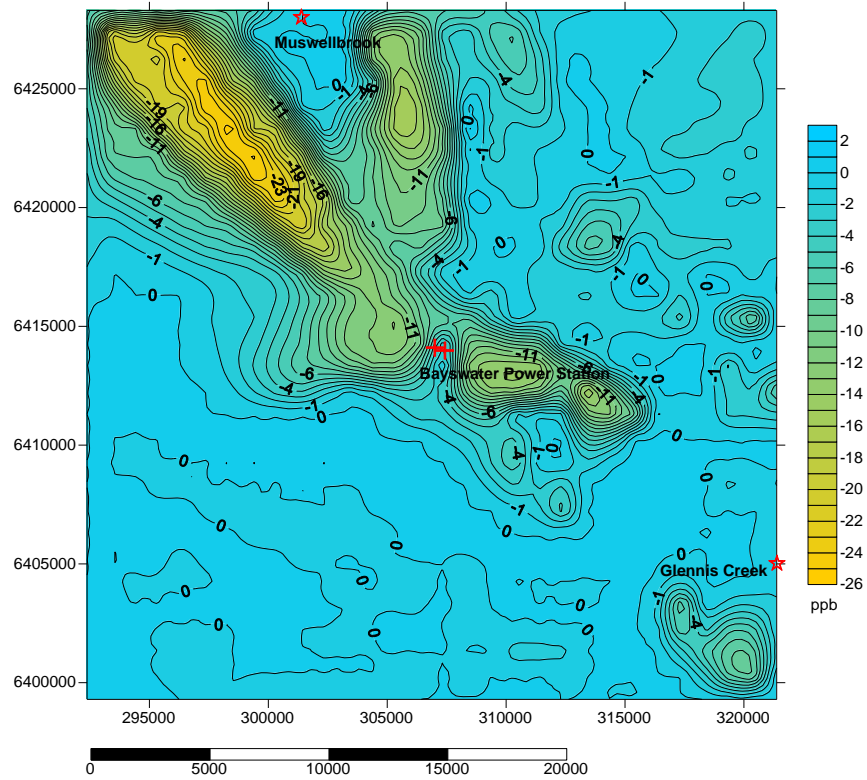**Change of NO peak value in Feb 2015 between PCC and PrePCC (1 km resolution)**
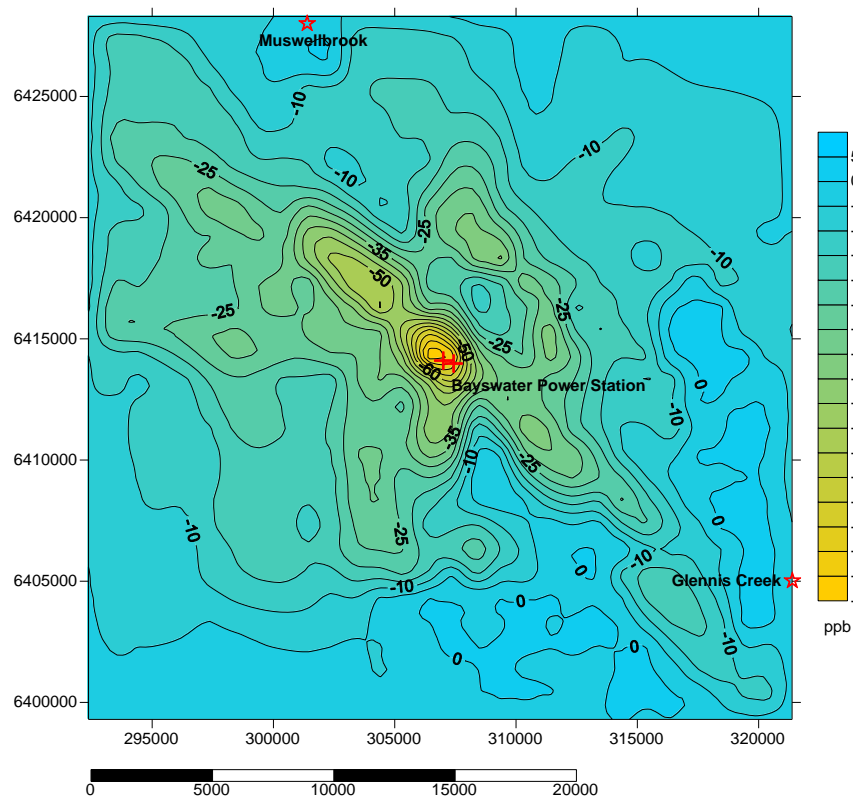
Change of NO peak values in March 2015 between PCC and PrePCC (1 km resolution)
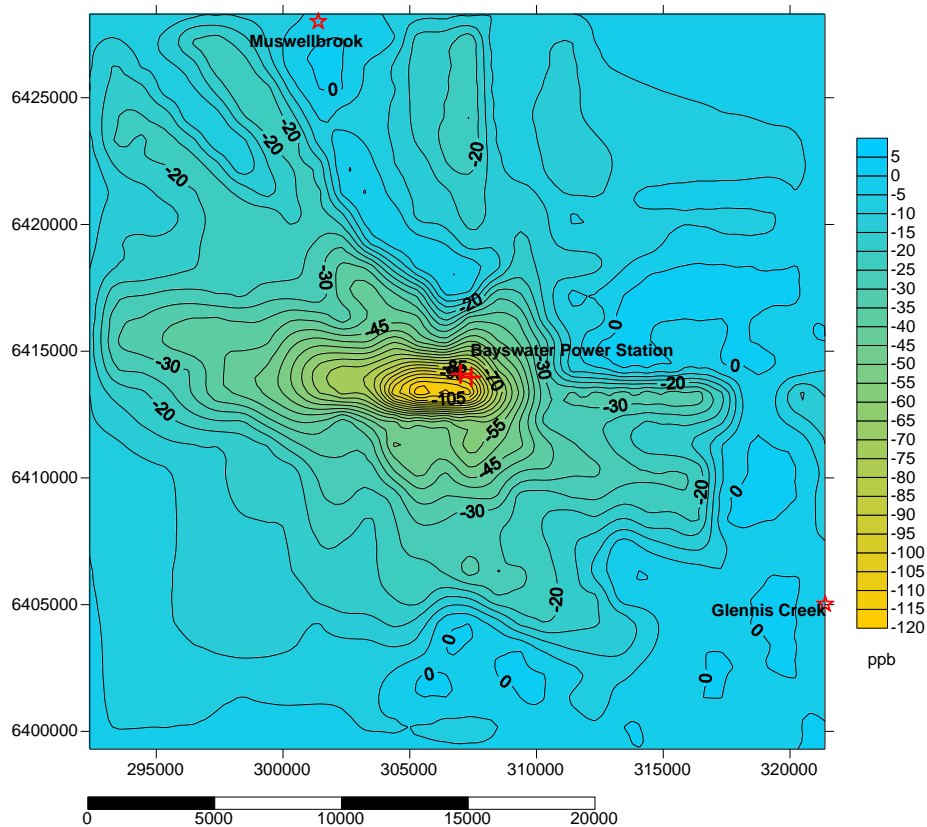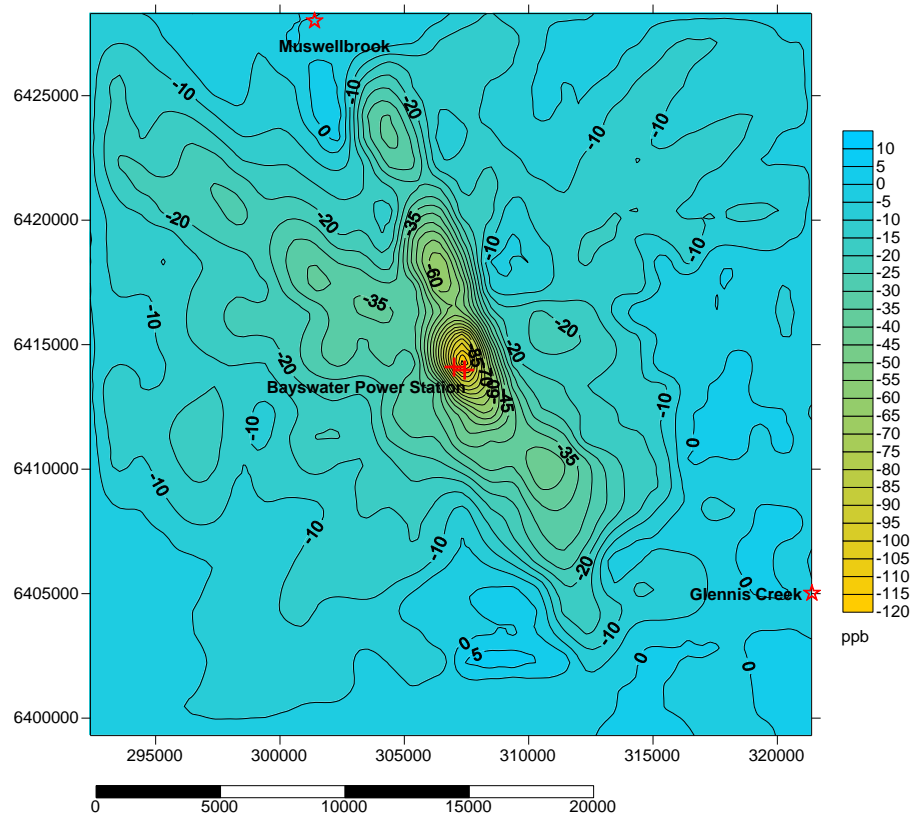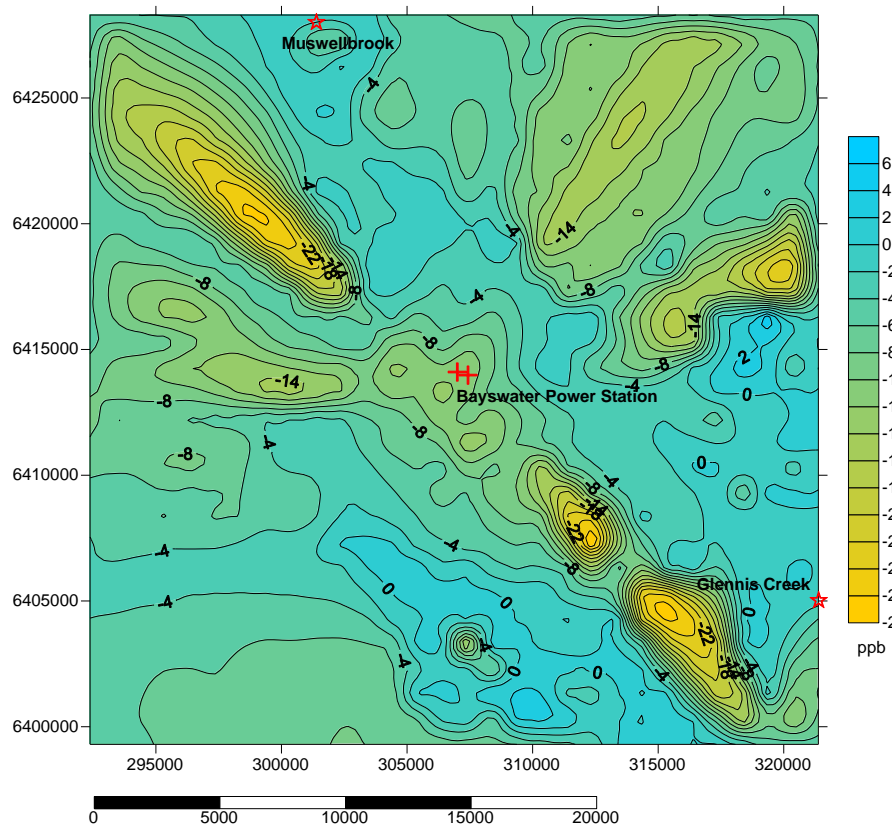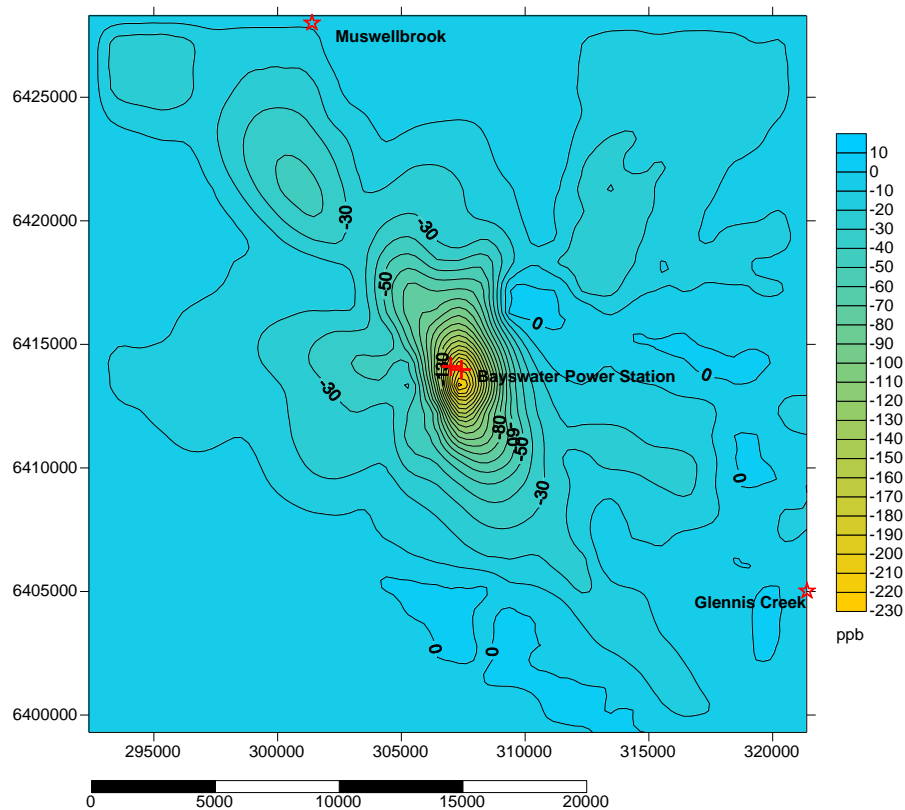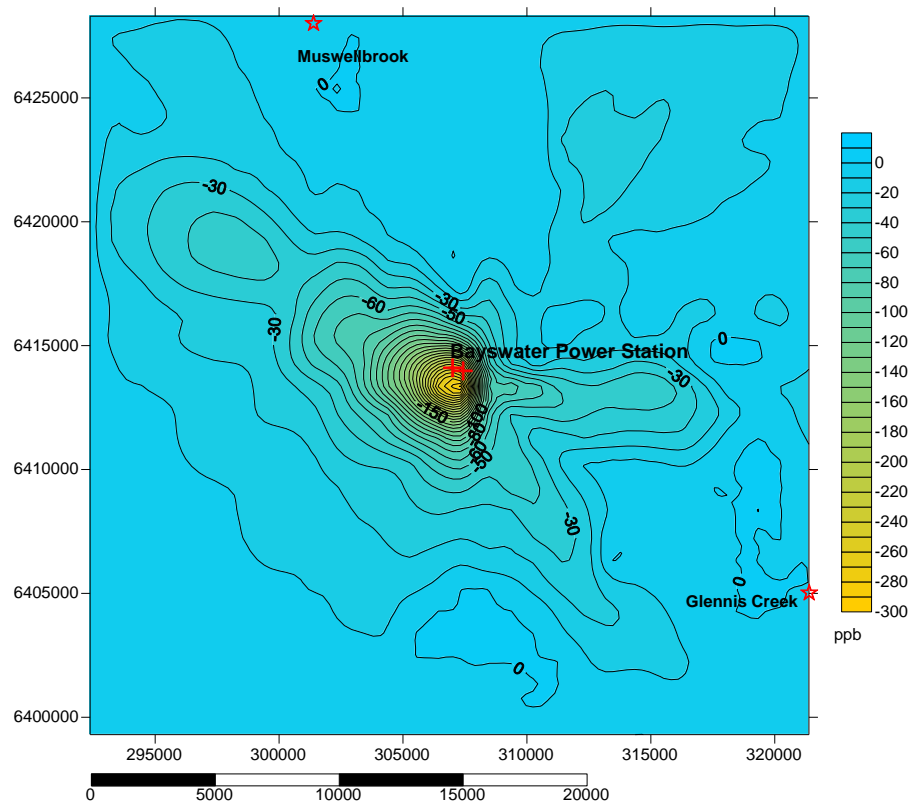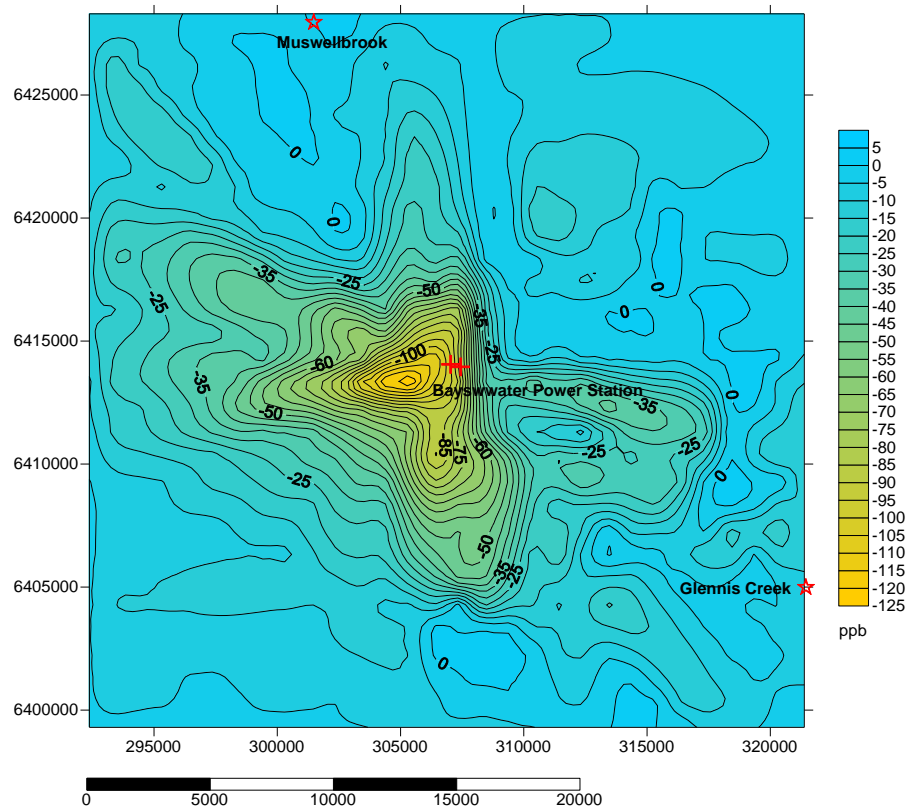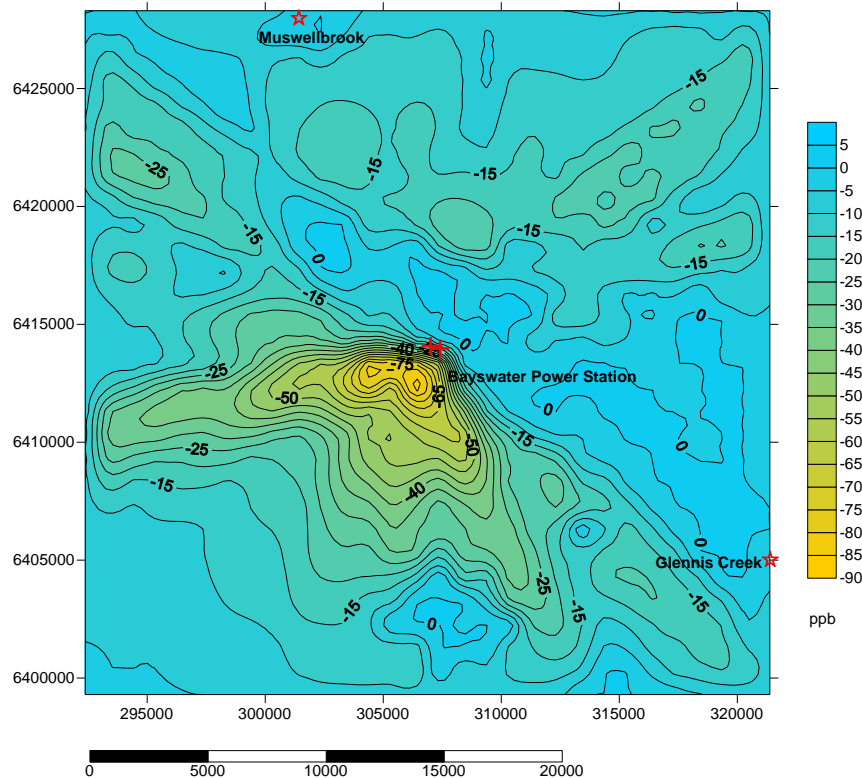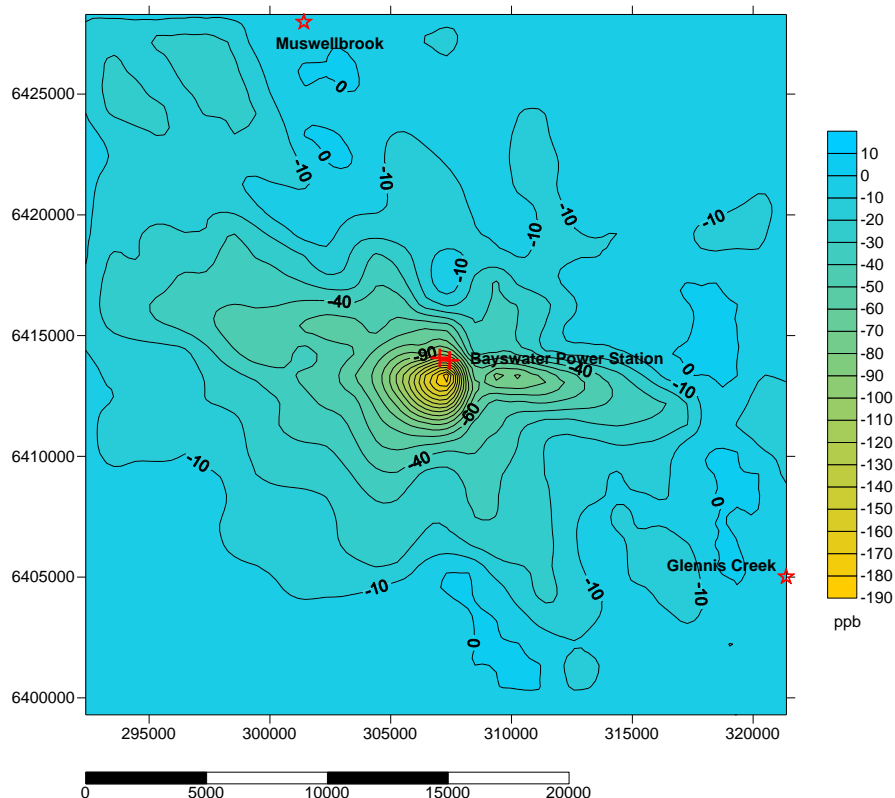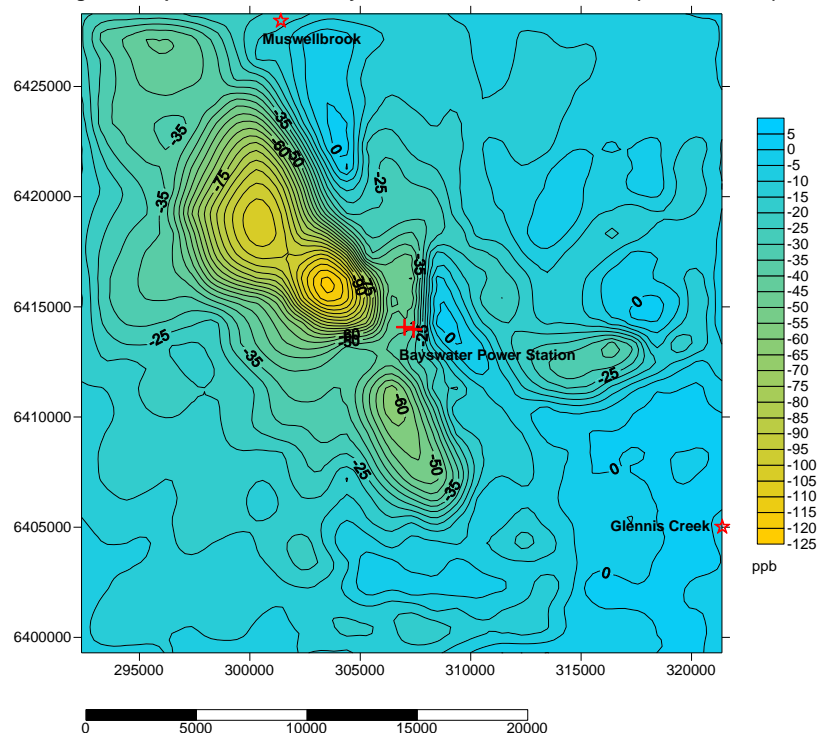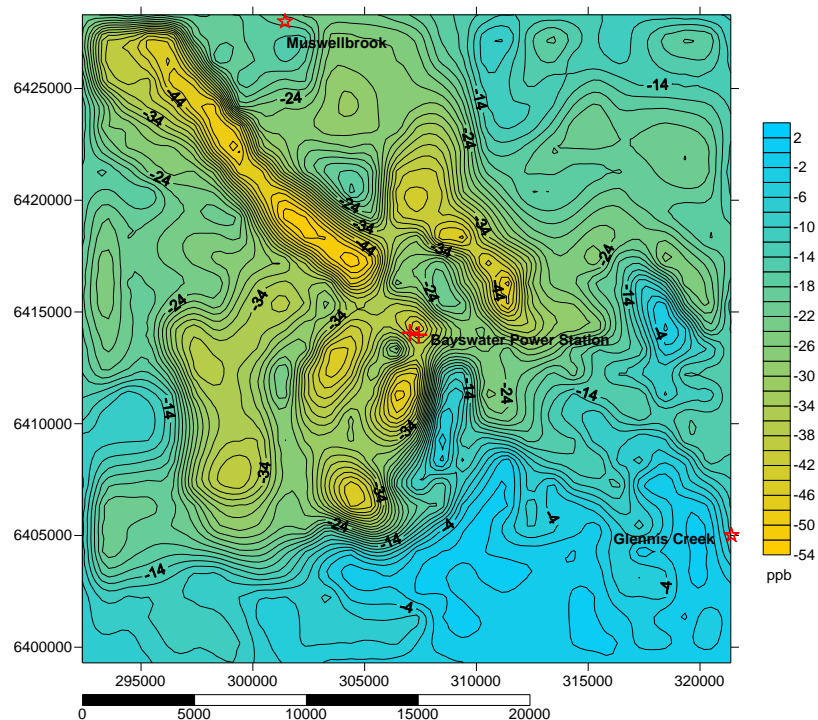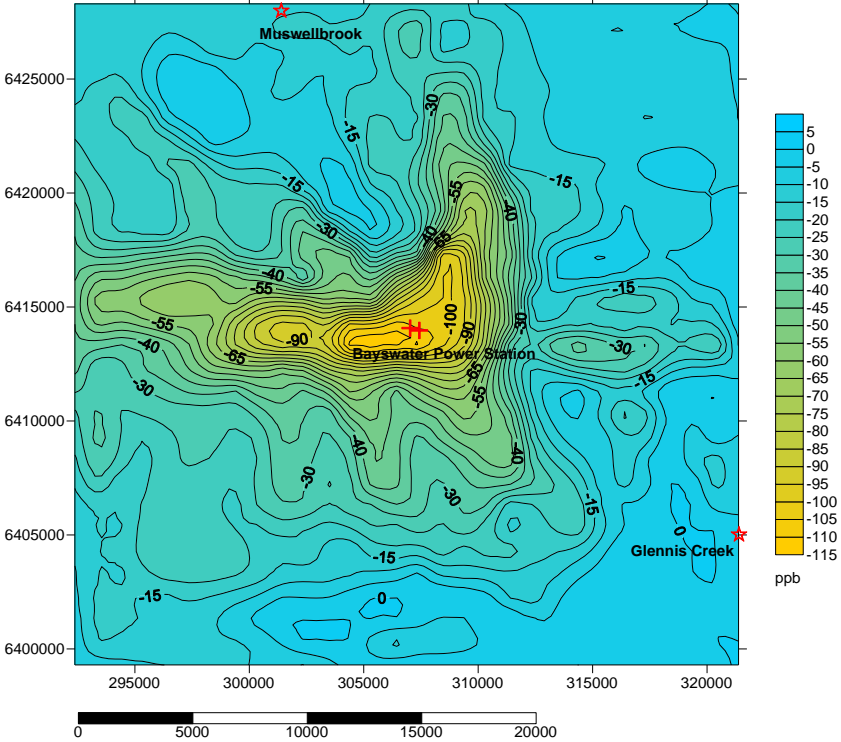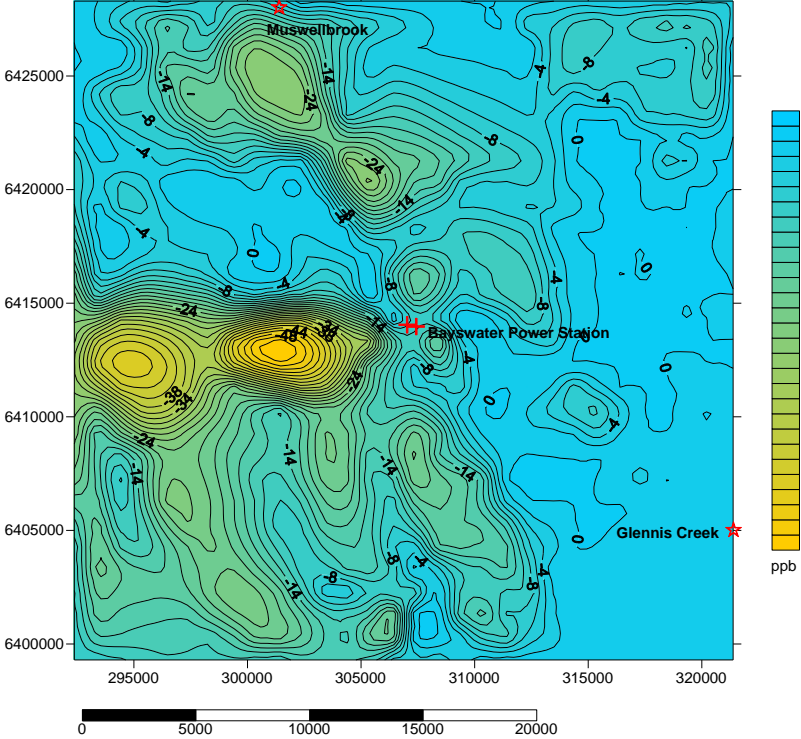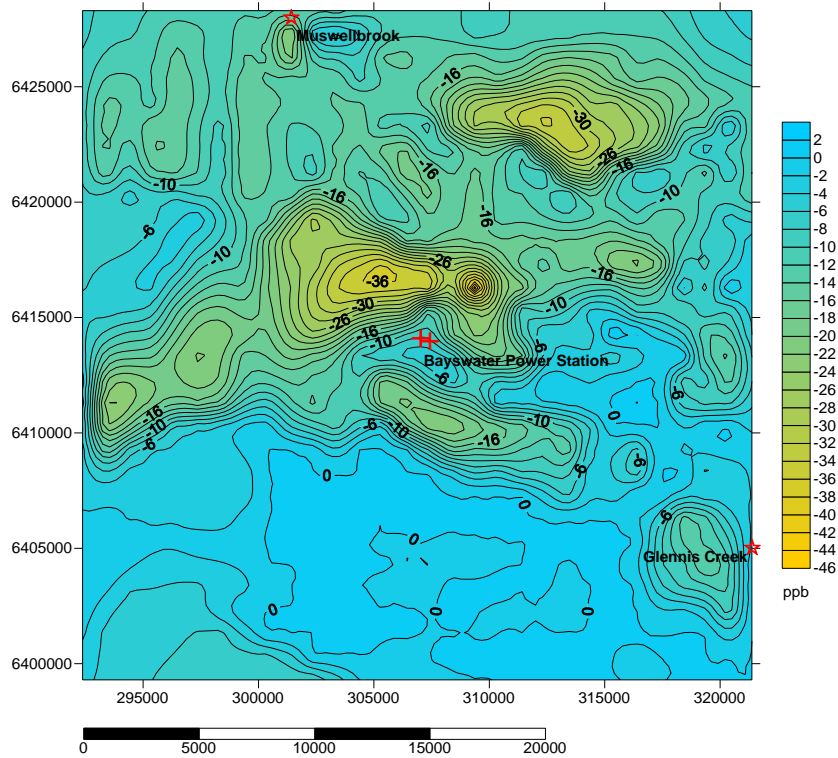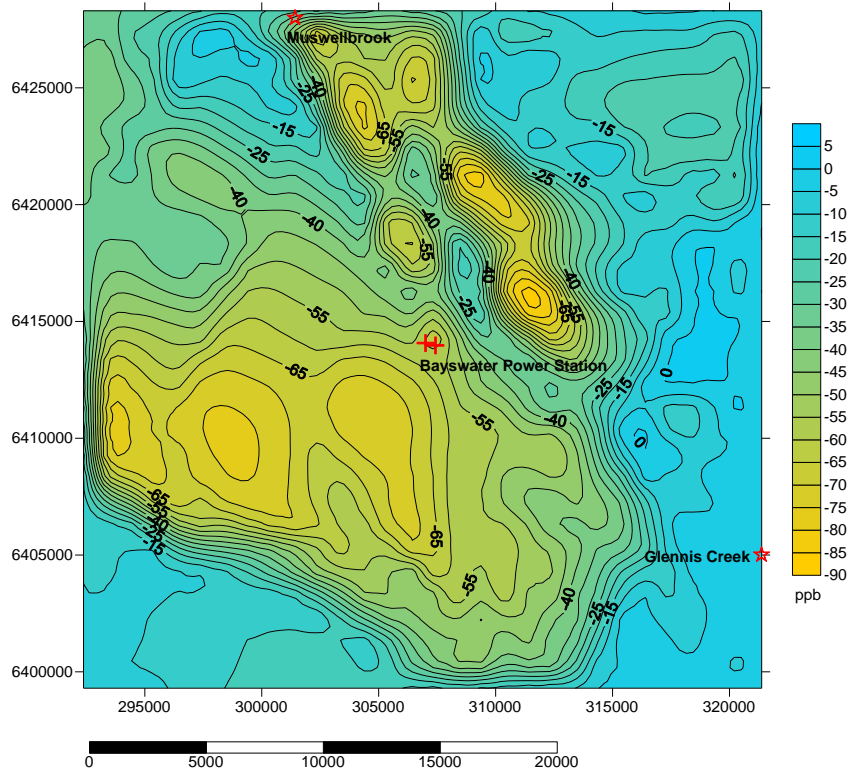

Change of NO peak values in April 2015 between PCC and PrePCC (1 km resolution)
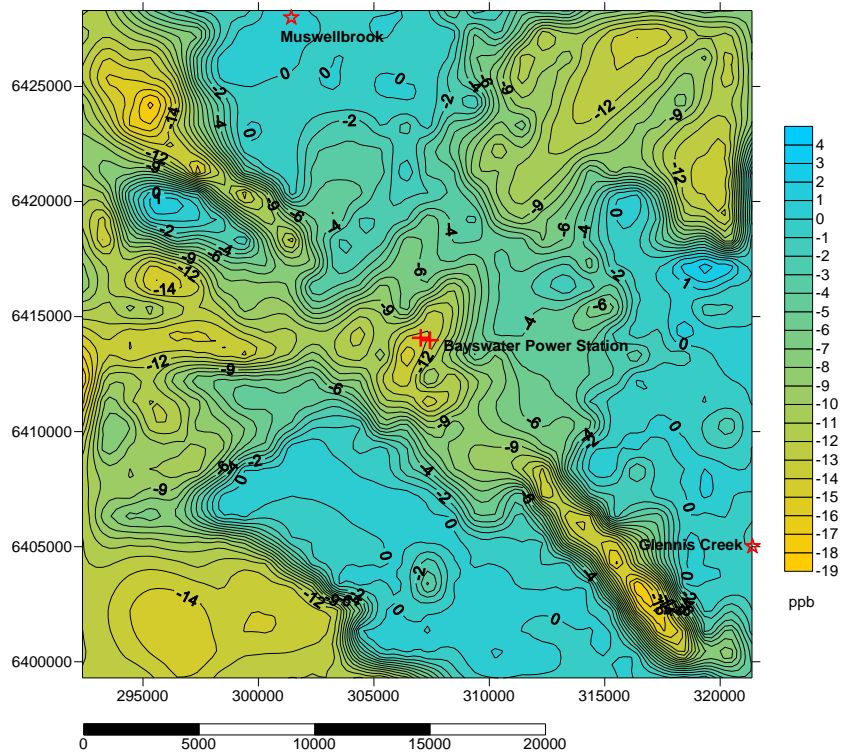

146
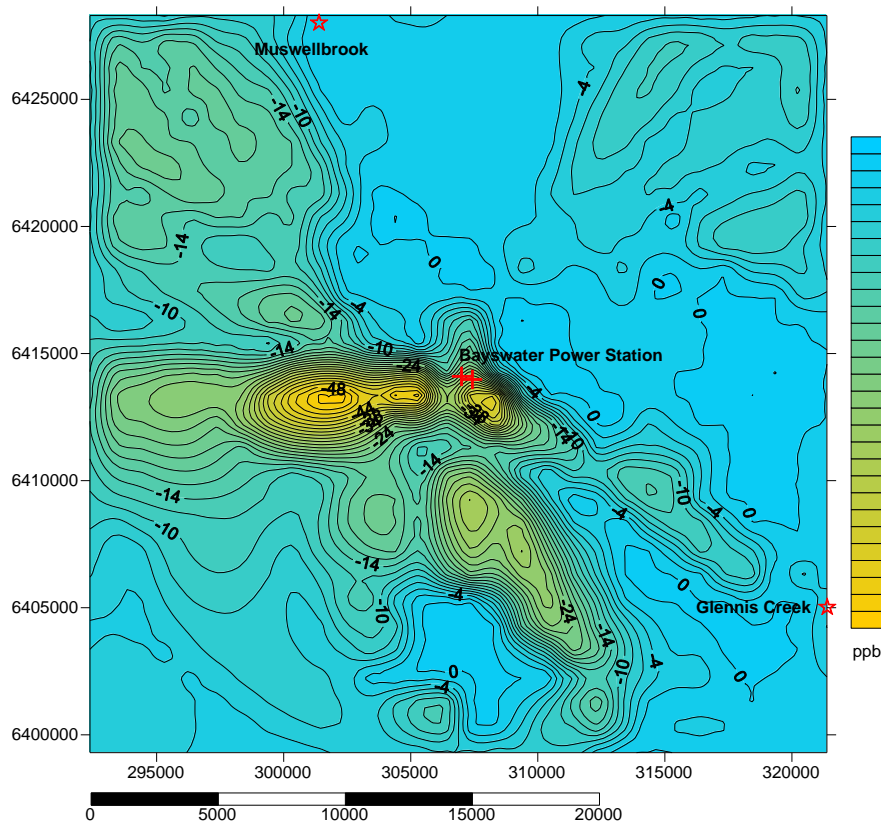
Change of NO peak values in May 2015 between PCC and PrePCC (1 km resolution)

Change of NO peak values in June 2015 between PCC and PrePCC (1 km resolution)
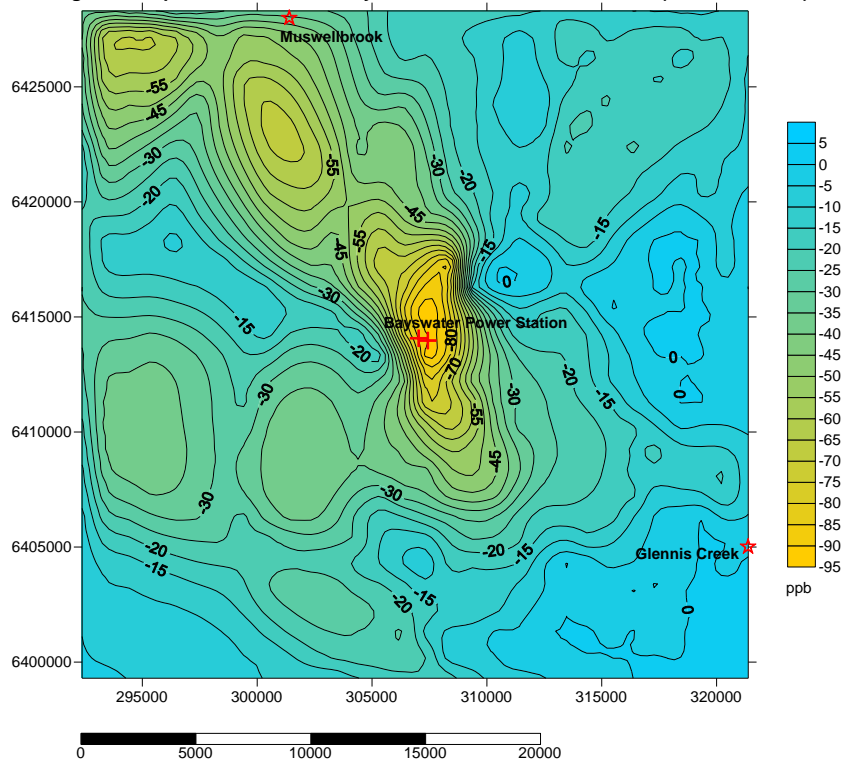

147

Change of NO peak values in July 2015 between PrePCC and PCC (1 km resolution)

Change of NO peak values in August 2015 between PCC and PrePCC (1 km resolution)

148

Change of NO peak values in September 2015 between PCC and PrePCC (1 km resolution)

Change of NO peak values in October 2015 between PCC and PrePCC (1 km resolution)

149

Change of NO peak values in November 2015 between PCC and PrePCC (1 km resolution)

Change of NO peak values in December 2015 between PCC and PrePCC (1 km resolution)

150

Appendix 2 contour maps of changes of NO₂ peak value in 2015

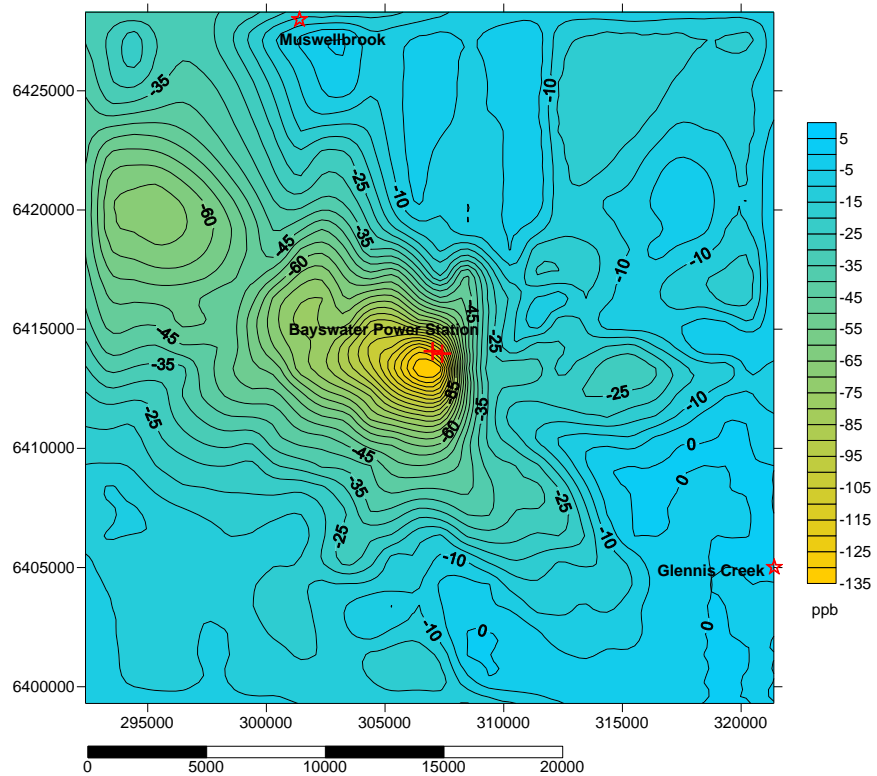**Change of NO2 peak values in January 2015 between PCC and PrePCC (1 km resolution)**

Change of NO2 peak values in February 2015 between PCC and PrePCC (1 km resolution)

Change of NO2 peak values in March 2015 between PCC and PrePCC (1 km resolution)

Change of NO2 peak values in April 2015 between PCC and PrePCC (1 km resolution)

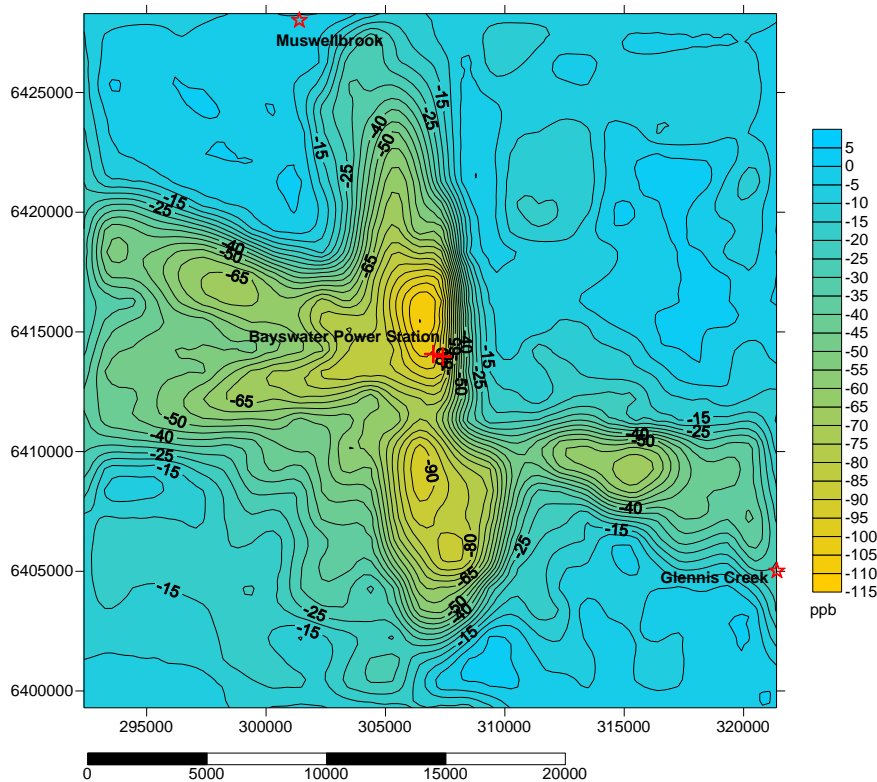**Change of NO2 peak values in May 2015 between PCC and PrePCC (1 km resolution)**

Change of NO2 peak values in June 2015 between PCC and PrePCC (1 km resolution)

153

Change of NO2 peak values in July 2015 between PCC and PrePCC (1 km resolution)

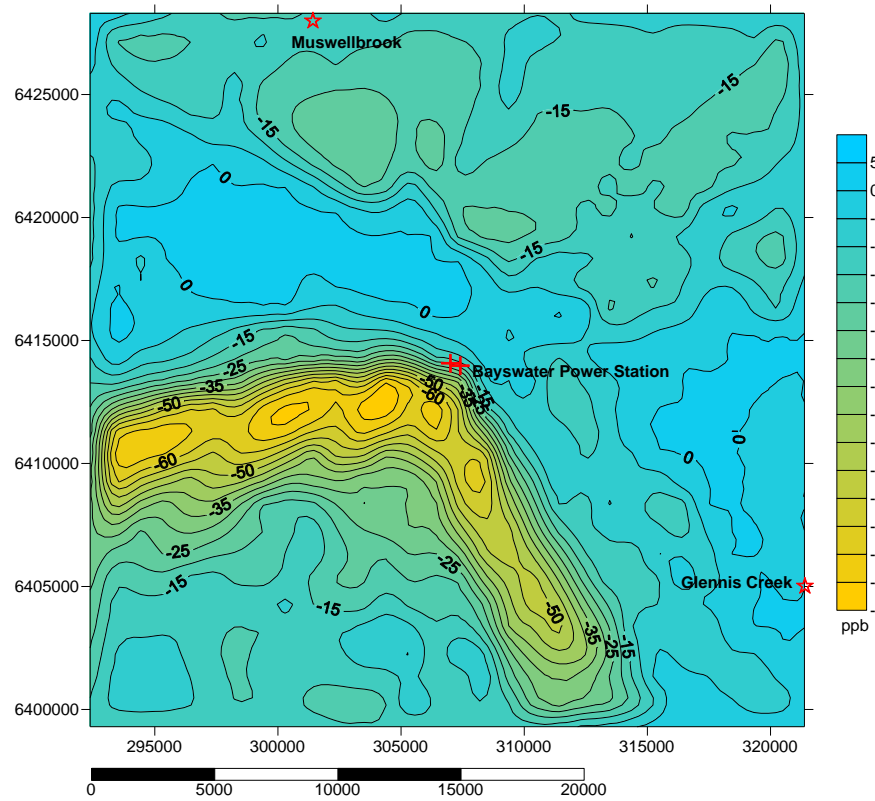Change of NO2 peak values in February 2015 between PCC and PrePCC (1 km resolution)

154

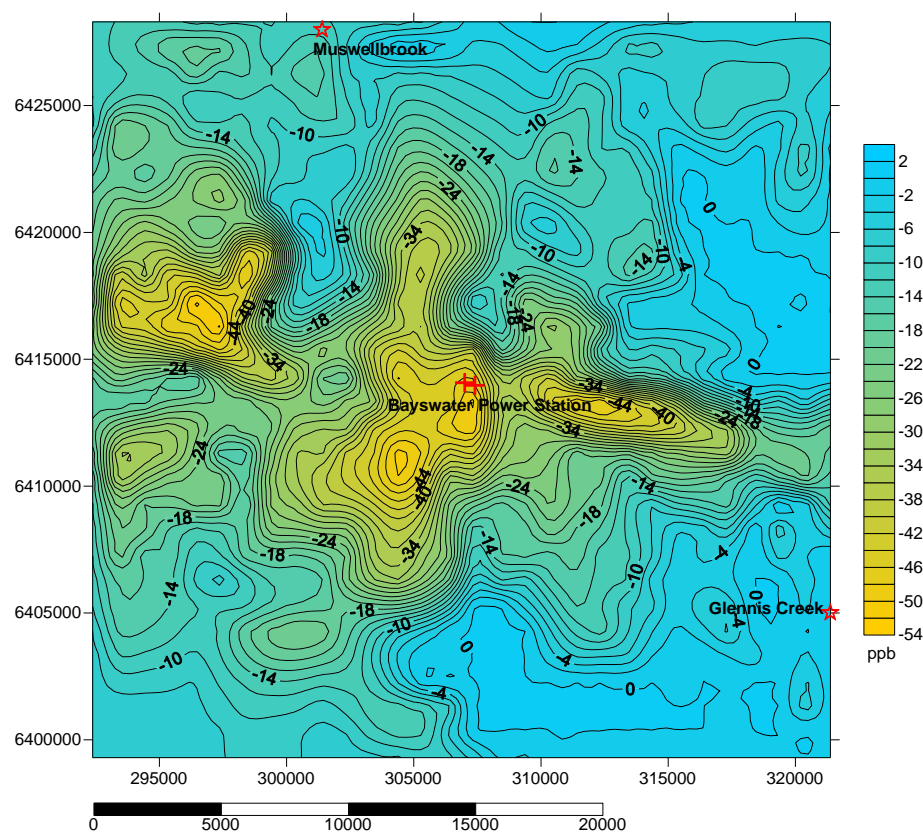**Change of NO2 peak values in September 2015 between PCC and PrePCC (1 km resolution)**

Change of NO2 peak values in February 2015 between PCC and PrePCC (1 km resolution)

155

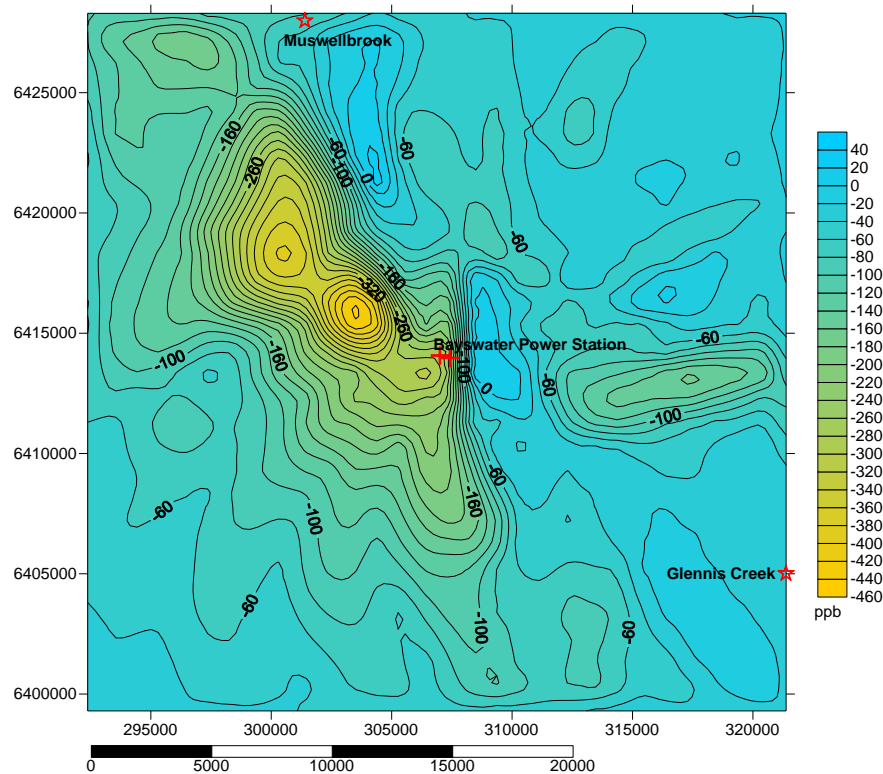**Change of NO2 peak values in November 2015 between PCC and PrePCC (1 km resolution)**

Change of NO2 peak values in December 2015 between PCC and PrePCC (1 km resolution)
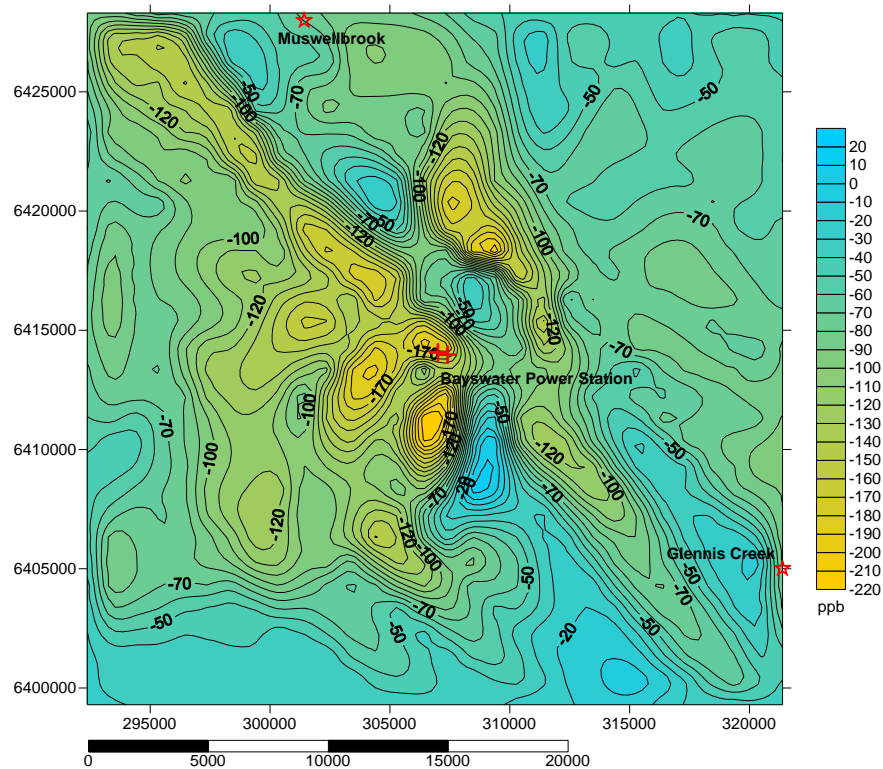
156

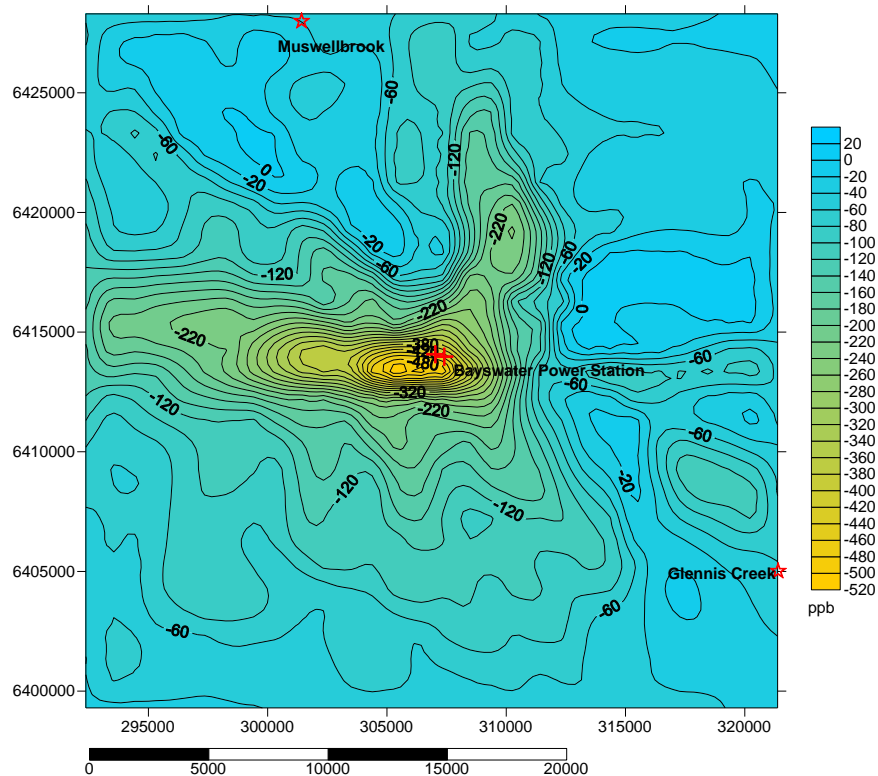# Appendix 3 contour maps of changes of SO₂ peak value in 2015

Change of SO2 peak values in January 2015 between PCC and PrePCC (1 km resolution)
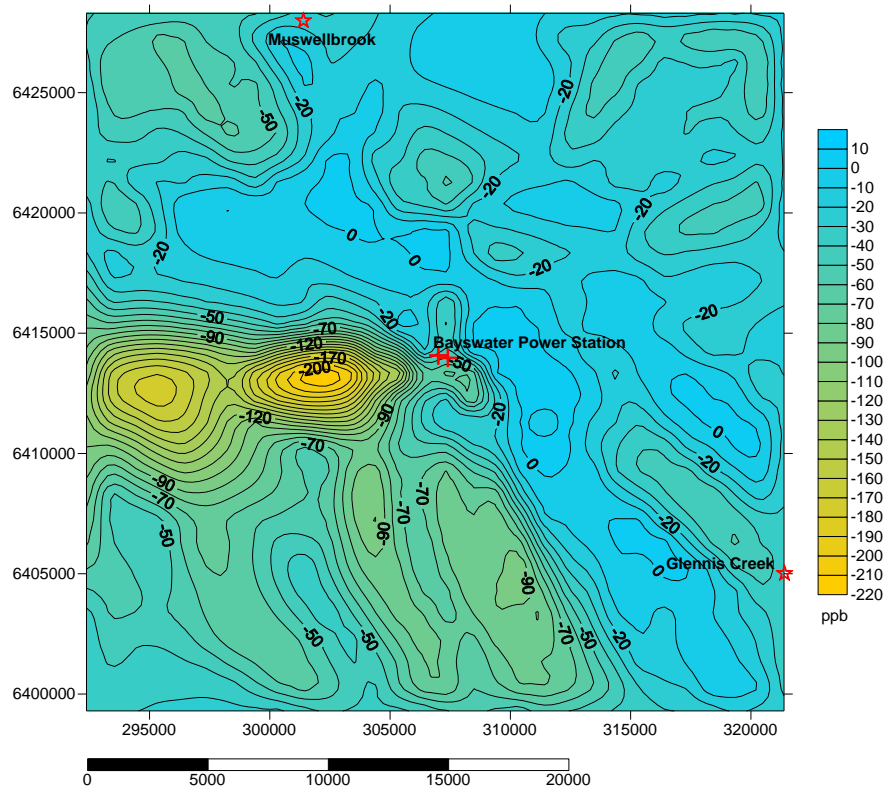

Change of SO2 peak values in February 2015 between PCC and PrePCC (1 km resolution)

Change of SO2 peak values in March 2015 between PCC and PrePCC (1 km resolution)

Change of SO2 peak values in April 2015 between PCC and PrePCC (1 km resolution)

158

Change of SO2 peak values in May 2015 between PCC and PrePCC (1 km resolution)

Change of SO2 peak values in June 2015 between PCC and PrePCC (1 km resolution)
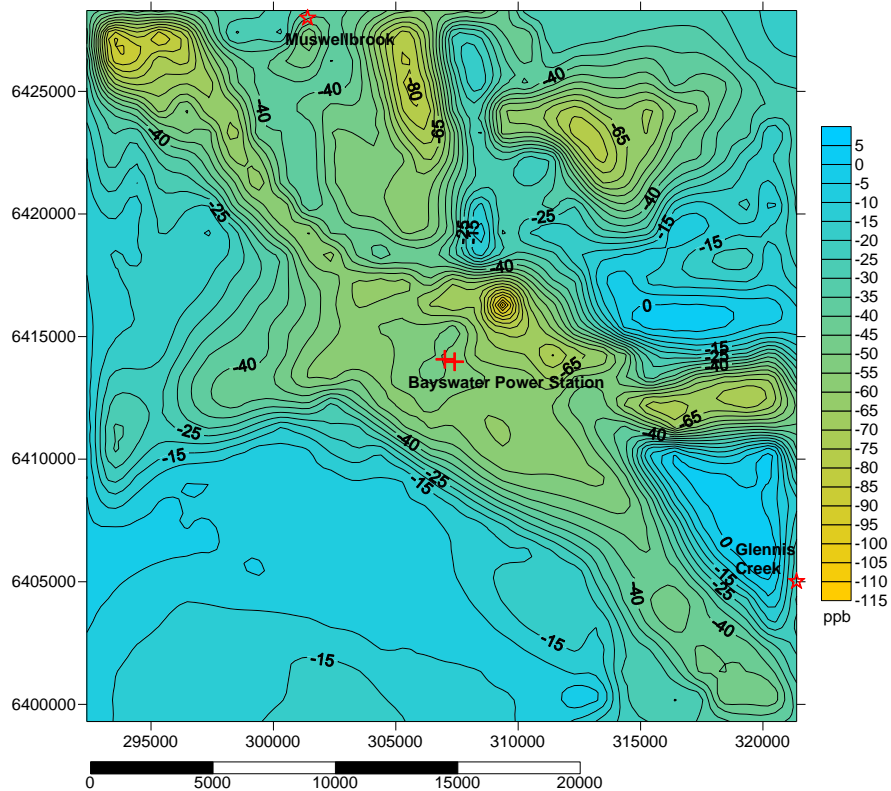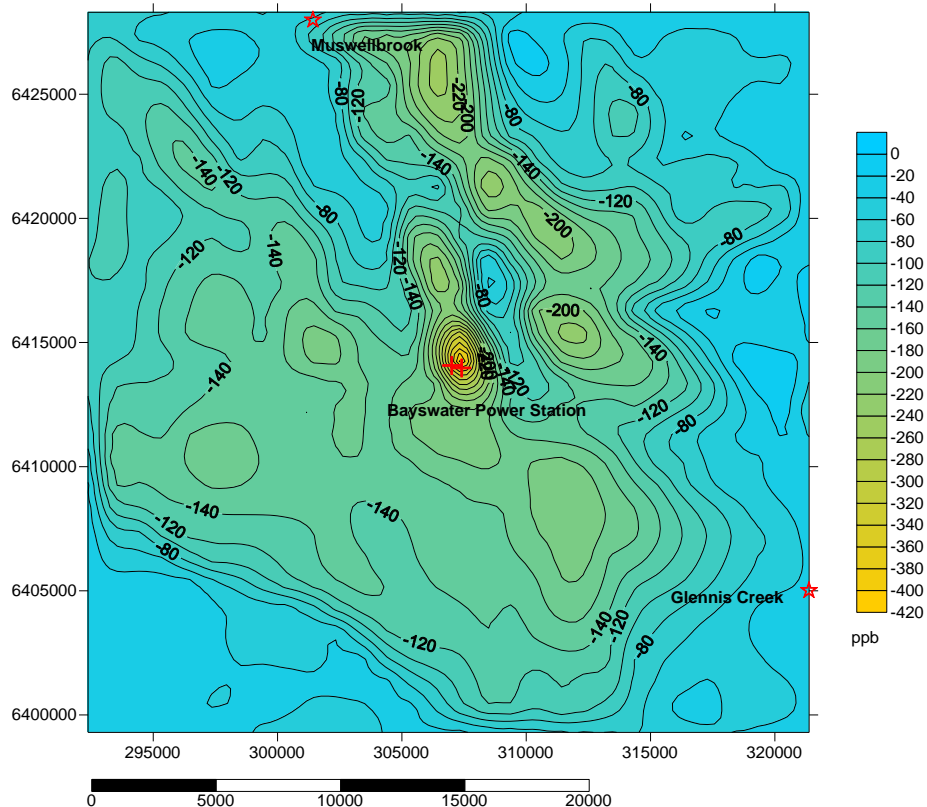
159

Change of SO2 peak values in July 2015 between PCC and PrePCC (1 km resolution)

Change of SO2 peak values in August 2015 between PCC and PrePCC (1 km resolution)
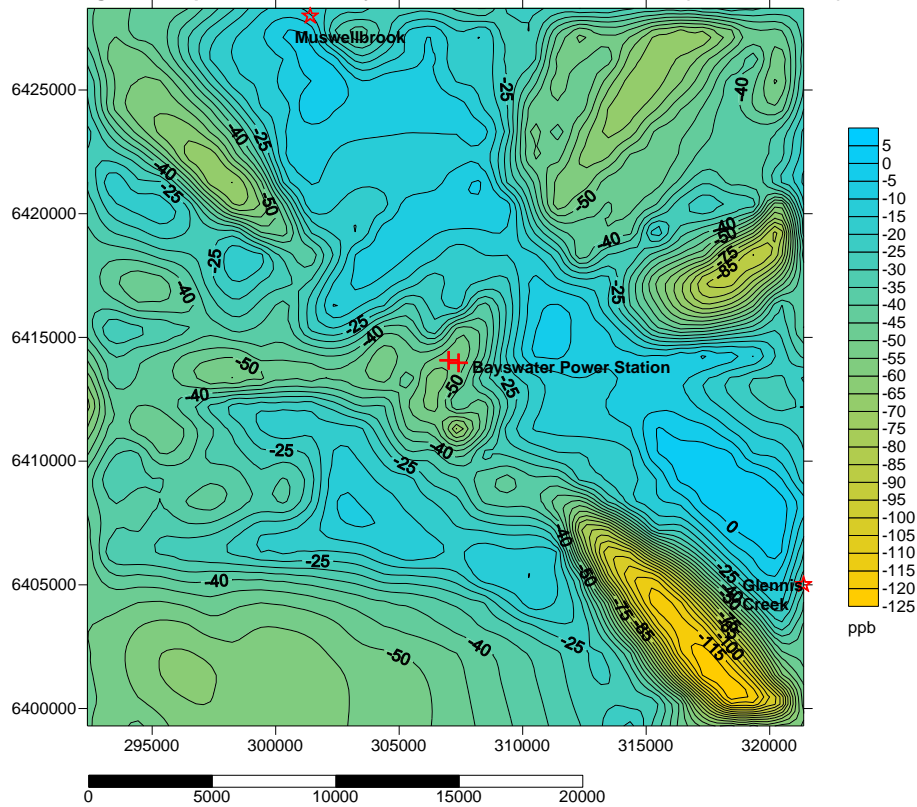
160

Change of SO2 peak values in September 2015 between PCC and PrePCC (1 km resolution)

Change of SO2 peak values in October 2015 between PCC and PrePCC (1 km resolution)

161
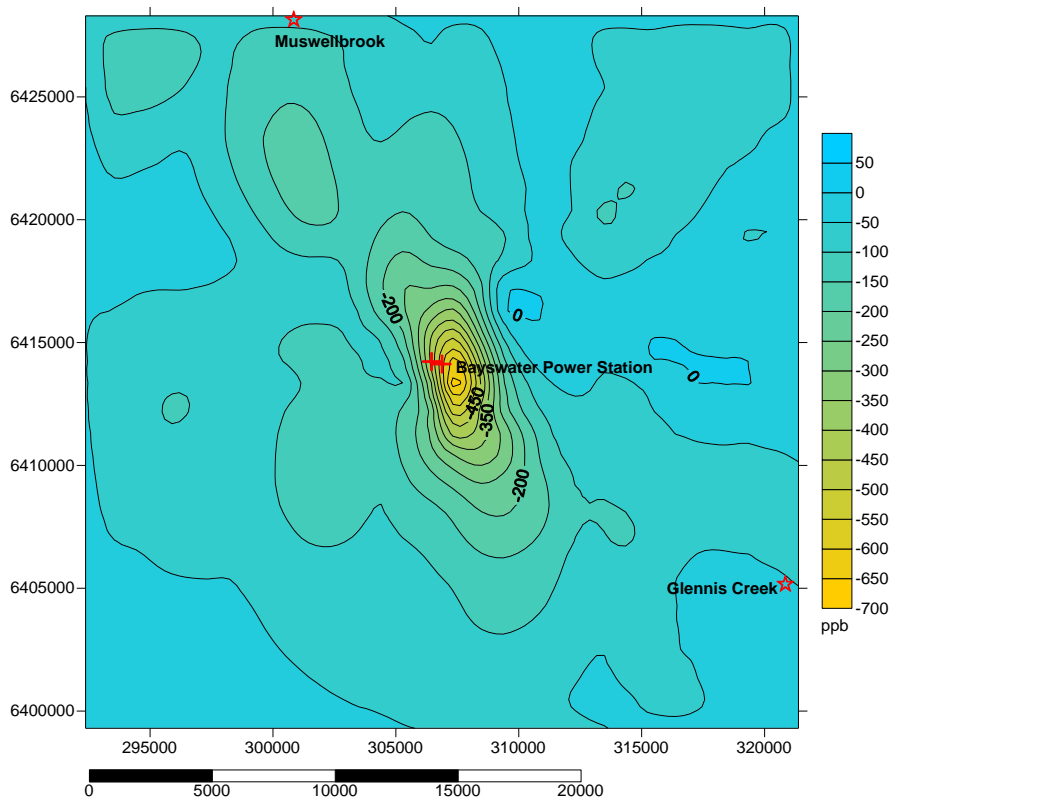
Change of SO2 peak values in November 2015 between PCC and PrePCC (1 km resolution)

Change of SO2 peak values in December 2015 between PCC and PrePCC (1 km resolution)
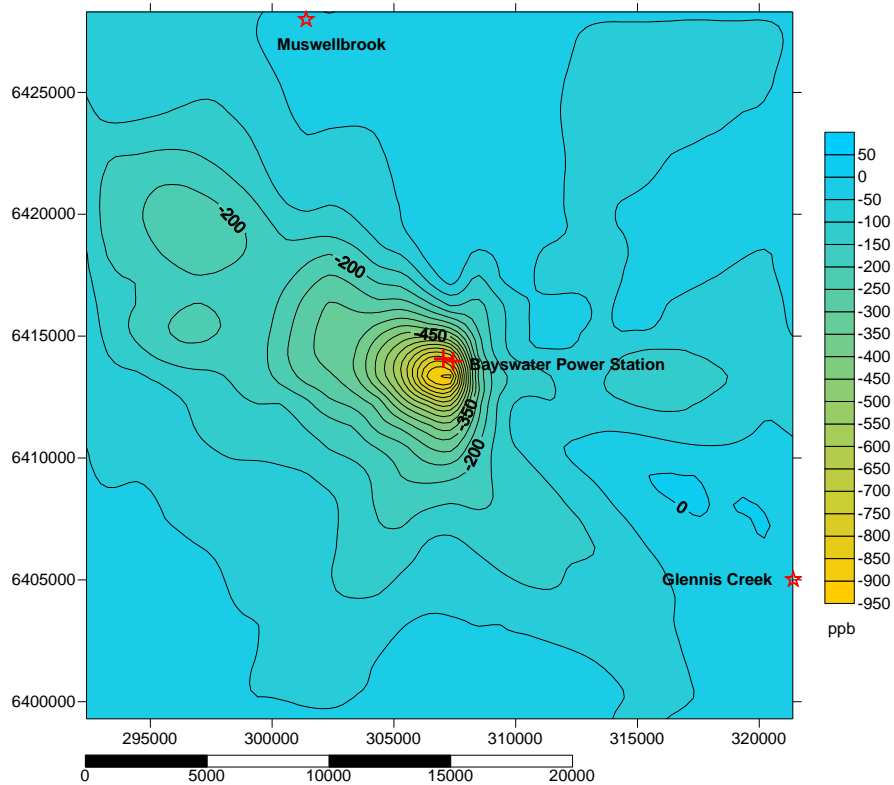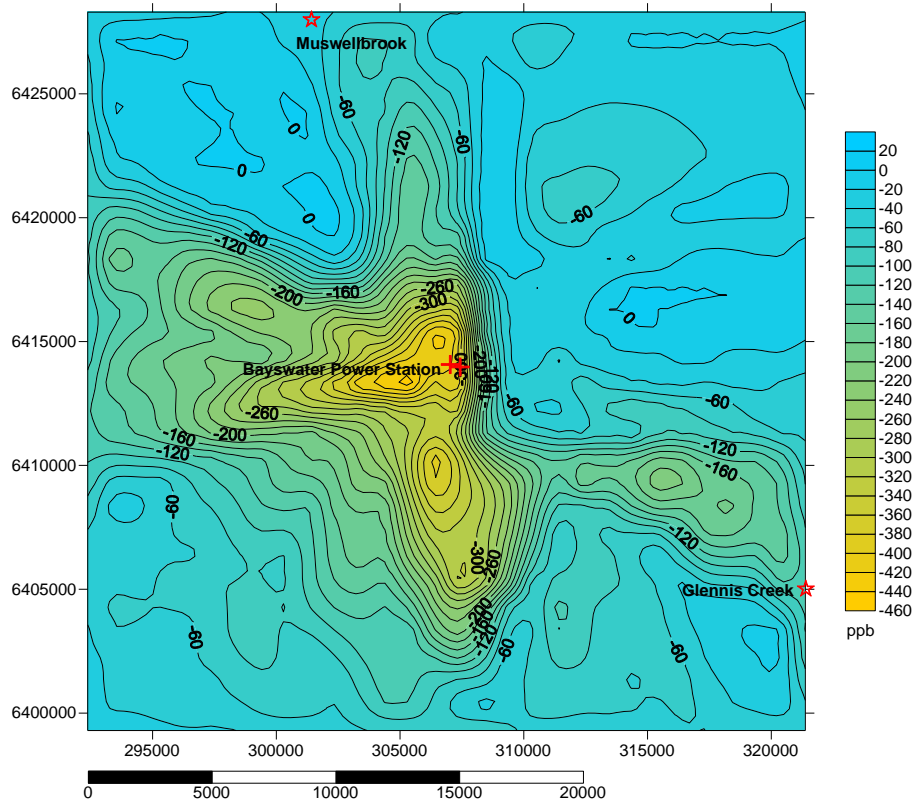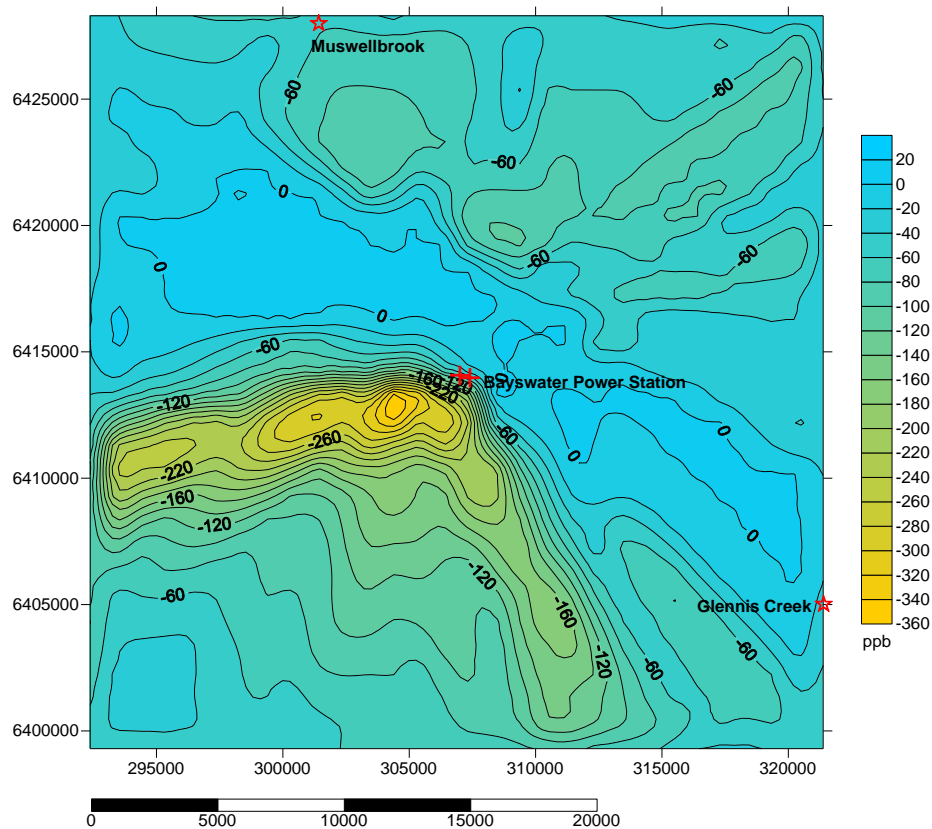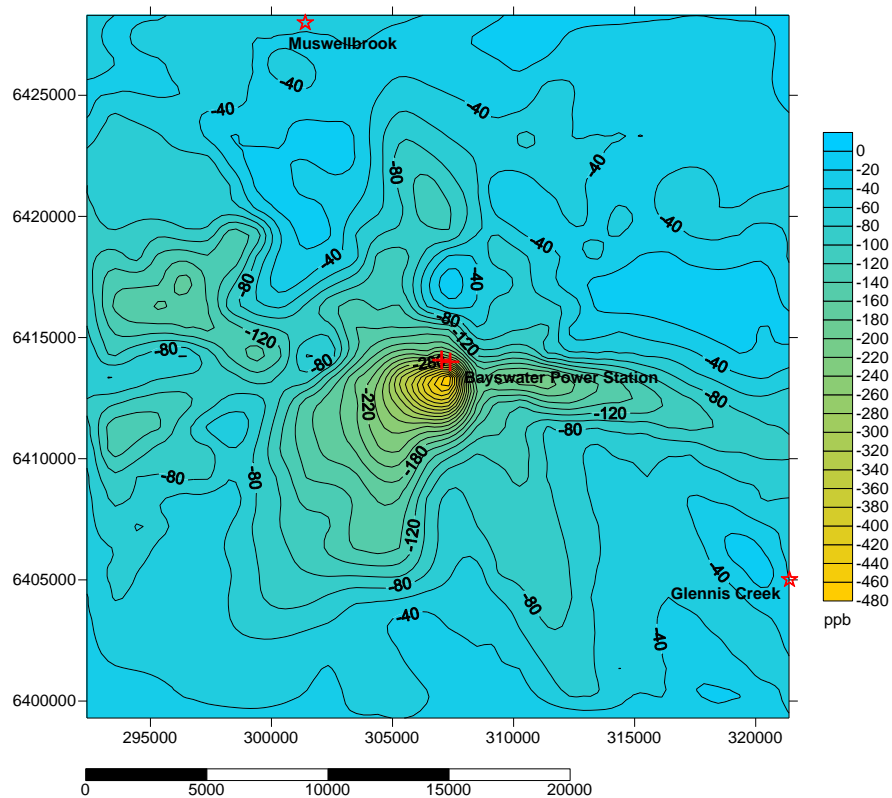

162

Publication

GHGT-12

Using computer modelling to simulate atmospheric movement and potential risk of pollutants from post-combustion carbon capture projects

Ye Wu*, Peter F. Nelson

Department of Environment & Geography, Macquarie University, NSW, 2109, Australia

Abstract

This study focuses on simulating atmospheric transport and risk of pollutant emissions from a potential post-combustion carbon capture project using computer modelling. Meteorological data for the year 2000 was used and the CSIRO TAPM model was employed to generate input meteorological data to calculate ground level concentrations of target species. CALMET which is a diagnostic meteorological model was used to restructure 3D wind and temperature data for CALPUFF model using prognostic data from TAPM. CALPUFF was then used to simulate atmospheric dispersion and movement of pollutants. The results showed that concentration values in December were the highest values based on 2000 meteorological data. Sensitivity analysis focused on simulating pollutant movement and dispersion in December using different values for relevant power station operating parameters. The study found that these parameters station can have a large impact on modelled concentration values. The introduction of post-combustion technology at a commercial scale will require appropriate regulations and power station design.

Keywords: Post-combustion, Nitrosamines, formaldehyde, CALPUFF, risk assessment

1. Introduction

Post-combustion carbon capture (PCC) is an innovative technology to remove carbon dioxide (CO_2) from the flue gas of coal fired power stations. The main solvent predicted to be used to capture CO_2 is an aqueous solution of monoethanolamine (MEA) [1], e.g. conventional 30% w/w MEA [2]. This amine-based solvent can release volatile organic compounds, ammonia, and amines during absorption process due to the degradation of the solvent in use [1, 2]. After emission to the atmosphere, these compounds can degrade into toxic compounds such as nitrosamines through reaction with OH radicals or photolysis [3]. Most nitrosamines have exhibited carcinogenic effects in laboratory animals and bioassay studies [4]. Formaldehyde is not only emitted from PCC projects, is but also formed in the atmosphere by amines reacting with OH radicals [3, 5]. Formaldehyde is a suspected carcinogen [6]. As commercial scale PCC projects have not yet been widely installed, there are still uncertainties on potential products from PCC projects, and environmental and human health impacts.

---

* Corresponding author. Tel.: +61-2-9850-8427; fax: +61-2-9850-8420.
E-mail address: ye.wu@mq.edu.au

To understand the uncertainties and to assess potential risks, previous studies have used computer modelling and European Photochemical Reactor (EUPHORE) chamber experiments to predict impacts of carbon capture projects. CSRIO has conducted carbon capture process using Aspen-Plus process simulation package to estimate potential emissions based on Tarong coal-fired power station [2]. In the simulation, a post-combustion plant can emit a maximum of 885 mg formaldehyde while capturing one tonne of CO_2 and a maximum of 8.9 µg nitrosamines (nitrosomorpholine) per tonne CO_2 captured [2]. Karl, et al and Nielson, et al [3, 5] have used EUPHORE chamber to simulate atmospheric reactions and to analyse potential oxidation products in the atmosphere. A mechanism for OH initiated oxidation of MEA has been used to simulate chamber experiments [3]. The mechanism includes formation of nitrosamines, and degradation of nitrosamines by sunlight. Nitrosamines have not been detected in any experiments from MEA [5]. However, MEA with NOx presence in capture process can degrade to secondary amines [2] which are confirmed to form nitrosamines from previous research [7]. The nitrosamines would be emitted into the atmosphere with the flue gas. In the atmosphere complex processes of dispersion, transport, and chemical transformation determine the concentrations and fate of the chemical compounds emitted from industrial stacks. These processes are affected by the local terrain and meteorology effects. Computer models have been employed to simulate the movement and dispersion. We have used TAPM model to investigate transport of these species but TAPM does not currently include amine chemistry. CALPUFF is an alternative model to solve the chemistry problem. CALPUFF is a Gaussian puff model which was developed by the Atmospheric Studies Group at TRC Solutions[8]. CALPUFF provides accurate simulation for pollutants in complex terrain domains [8, 9].

This paper presents the development of amine chemistry for input into computer models, and provides results from the KPP pre-processor [10] on amine chemical mechanism in complex atmospheric environment. The paper also provides details on the modification and use of the CALPUFF model for gas phase amine chemistry, and gives results for different input parameters in a sensitivity analysis. The study also considers risk assessment on chemical compounds related to PCC emission as nitrosamines and formaldehyde are carcinogenic.

2. Methods

In the previous study[11], TAPM-CTM which is a Gaussian model developed by CSRIO was used to do a simple simulation for amines dispersion and movement without considering atmospheric reactions after emission. To understand generation of amines and their degradation products, it is necessary to include atmospheric reactions of amines and degradations. As CALPUFF is an open source model using FORTRAN codes, the CALPUFF model was chosen for related simulation by adding an amine reactions scheme to it.

2.1. KPP box model for MEA related reactions

In order to benefit possible future development and assessment, a numerical method to solve the differential equations required to describe the reaction scheme was considered in model development. The Kinetic Pre-Processor KPP (KPP) was employed to generate FORTRAN codes for amine (MEA) photochemical reactions. The KPP model was treated as a box model where atmospheric chemistry occurs in the absence of dispersion, location, and seasonal variation. The mechanism and kinetic information for MEA and its oxidation products were based on previous EUPHORE chamber studies [3, 5]. Only gas phase reactions were considered in the model development. To reflect the background gas phase chemistry in the atmospheric environment, Carbon Bond mechanism version 6 was combined with the MEA sub-mechanism to perform the numerical integration. The Rosenbrock solver was used for integration of the differential equations of the gas phase reactions [12, 13]. Initial concentrations of the main products were based on the concentrations in the EUPHORE chamber studies. For example, MEA was initially 410 ppb, formaldehyde was 2 ppb, nitramines were 0.1 ppb, and nitrosamines were zero. The KPP model was used to calculate concentrations of MEA, formaldehyde (FORM), nitrosamines and nitramines at time intervals of six minutes. The model was run for 12 hours commencing at 12:00 noon. As nitrosamine can degrade to non- toxic products [14], the rate of degradation loss of nitrosamines was 1.91×10^{-2} cm³/molecule/s which was used to setup the KPP run. In the KPP box model, wall loss of MEA is also considered for an individual run which is used to validate the results from KPP.

2.2. Develop simple chemical scheme for CALPUFF simulation

There are three main components of the CALPUFF model: CALMET, CALPUFF, and CALPOST. CALMET is a model to generate meteorological data for wind and temperature fields. The data generated from CALMET is placed on a 3D gridded modeling domain. The meteorological data from CALMET can be used typically for CALPUFF domain setting or as an option [8]. CALPUFF is a puff model to process dispersion, chemical transportation and deposition. CALPOST is a tool to process these files generated from CALPUFF and summarize results for highest or second or third highest values for each receptor. In this study, we used 3D meteorological data generated from TAPM as a basis to set up each CALMET run. The data from TAPM is an ASCII format file and machine-independent [8]. To use the data to run CALMET, correct format files are needed. CALTAPM is a tool to transfer the data from TAPM to suitable format files for CALMET. The process was operated under DOS system.

In TAPM model set up, the study area selected was in the upper Hunter Valley, about 200 km north of Sydney. The Hunter valley is a region which includes extensive coal mining, power production and agricultural (mainly viniculture) operations, and

two settlements of 10-20 000 inhabitants. The outer modeling grid which is 30 km X 30 km, was centered on -32°23.5" latitude and 150°57.0" longitude. TAPM was configured to have four nested grids at 30 km, 10 km, 3 km, and 1 km resolution. Each grid has 50 by 50 cells and 25 vertical levels. It was assumed that there were only two point sources from a full-scale coal-fired power station. The stack parameters were based on Bayswater Power Station, NSW, Australia, located near the town of Muswellbrook in the upper Hunter. Emission rates for each chemical compounds were based on data determined by CSRIO [2] and corrected for the somewhat different parameters appropriate to Bayswater Power Station. The year 2000 was selected as a representation year for meteorological data simulation. The TAPM model was run for each month of the year 2000. The detailed parameters for the TAPM model runs are shown in Table 1.

Table 1. Parameters for TAPM model runs.

Parameters	Stack 1 & 2
Stack Diameter (m)	12
Stack Height (m)	248
Exit Velocity (m/s)	13.9
Temperature (K)	373
MEA emission rate (g/s)	1.2
Formaldehyde –HCHO emission rate (g/s)	2.4

CALPUFF is used to simulate chemical reactions in the atmosphere and to account for dispersion. In the original CALPUFF, there are seven chemical mechanisms provided as options [8]. The existing nitrogen and sulphur oxides chemistry in CALPUFF gives a well validated platform to develop the amine chemical scheme for the simulations [15]. Through studying the codes carefully, we decided to use MCHEM =6 chemistry subroutines as a foundation to modify and expand the FORTRAN codes as a new routine to be added into CALPUFF. The new routine is called mq_amines. The reaction mechanism with amine reactions was named as MCHEM=8. Only gas phase reactions in the atmosphere are considered in the MCHEM=8 mechanism. The chemical reactions of amines were based on a previously published reaction scheme [3]. However, nitrosamines degradation was considered in addition according to previous reports [9]. As MEA was the only amine included in this case study, the rate constant for nitrosamine degradation was determined to be 1.91×10^{-2} cm³/molecule/s for primary amines [9]. In this modified CALPUFF, only amine reaction related code was added as an additional module into the program codes, and the rest of the code remained unchanged. When the amine chemistry option was selected (MCHEM=8), this modified CALPUFF included 13 species in total, and 7 of which are amine chemistry participants: MEA (primary amines), MEAN (N-amino ethanol radical), MEABO2 (C2-amine peroxy radical), MEABO (C2-amine alkoxy radical), HCHO (formaldehyde), NA (nitramines), and NS (nitrosamines). The results after dispersion simulation focus on MEA, HCHO, and NS.

2.3. Model sensitivity analysis

As full scale post-combustion carbon capture technology has not been widely used in commercial operation, it was necessary to perform a sensitivity analysis to understand concentration changes due to varying parameters of the power station stacks. After running simulation using Bayswater Power Station parameters, the model parameters were changed to determine the effects of these different parameters on modelled concentrations. Only one variable was changed at any one time in the CALPUFF simulation, other parameters were maintained at the values that existed for Bayswater Power Station. The variables include stack diameter, stack height, exit temperature, and exit velocity. The details of varied parameters are shown in Table 2. Comparison of the concentration values focus on 1-hour average values.

Table 2. Parameters variables in each case scenario

Case scenario	Parameters changed
DEC	Original parameters of Bayswater Power Station (see Table 1)
DEC1	Stack Diameter = 6 meters
DEC2	Stack Height = 65 meters
DEC3	Exit temperature = 303K
DEC4	Exit velocity = 20 m/s

2.4. Risk assessment and Monte-Carlo model

Risk assessment follows the method of our previous study [11], @RISK software which is Monte-Carlo simulation model was employed to simulate the risk assessment model for uncertainties and probability of cancer risk caused by exposure to pollutants. The model focused on inhalation exposure and cancer risk probabilities. The inhalation exposure calculation followed the US EPA method by considering atmospheric concentrations, inhalation absorption factor, daily breathing rate, and body weight [16]. The equation for inhalation exposure is shown in eq. (1) below. The risk value calculated by cancer slope factor is shown in equation (2). Equations (3) & (4) show the conversion between cancer risk and unit risk factors [17], and risk value calculated by unit risk factor. Values for these variables are listed in Table 3. Parameters for setting up the risk model were based on different probability distribution functions according to uncertainties, and are also shown in Table 3.

$$E_{in} = \frac{C_a \times DBR \times A \times EF \times ED}{AT} \tag{1}$$

$$Risk_i = E_{in} \times CSF \times ADAF_i \tag{2}$$

$$CSF = \frac{URF}{DBR} \tag{3}$$

$$Risk_i = \frac{C_a \times A \times URF \times EF \times ED}{AT} \times ADAF_i \tag{4}$$

Where:

C_a=Atmospheric concentration value of chemical compounds (simulated by CALPUFF),
EF=Exposure frequency,
ED=Exposure duration,
BW=Body weight,
AT=Average time.
A =Inhalation absorption factor,
DBR =Daily breathing rate,
CSF = Cancel slope factor,
URF = Unit risk factor,
$ADAF_i$ = Age-dependent adjustment factor for age bin I (unit less)

Table 3. Parameter Distribution Functions and values

Parameter	Distribution model & Model parameters	References
AT-Averaging Time	25550 days	[18]
ED-Exposure Duration	Adult: 70 years	[19]
BW- Body weight (kg)	Lognormal Adult: [66.44, 1.20]	[20]
EF-exposure frequency (unitless)	Triangular [min, mode, max] [180, 345, 365]	[21]
A-inhalation absorption rate	1	[19]
ADAFi	1	[22]
DBR-Daily breathing rate (L/kg BW* day)	Gamma [Location, Scale, Shape] Adult:[193.99,31.27,2.46]	[19]

Cancer risk is calculated by multiplying inhalation exposure dose by cancer unit risk factor for toxic compounds. As most nitrosamines are carcinogenic [4], inhalation unit risk factor of N-Nitrosodimethylamine was used for the calculations in this study. The unit risk factor of nitrosamine used was 1.4×10^{-2} $(\mu g/m^3)^{-1}$[23]. Formaldehyde inhalation risk factor is 1.3×10^{-5} $(\mu g/m^3)^{-1}$[24]. The cancer probabilities for individuals was predicted by the @RISK model, using 1000 iterations for the simulation.

3. Results and discussion

3.1. Simulation results from KPP pre-processor

KPP was used to run two different scenarios: (1) simulation of the amine chemistry chamber experiments with wall loss of amine included; (2). simulation of amines chemistry in the atmospheric environment with wall loss removed. In considering wall loss in the chamber experiment scenario, the KPP was run for 24 hours starting from mid-day 12:00 noon. Modelled output was calculated every six minutes during the process.

Figure 1 (a) shows the concentrations change in wall loss of MEA to chamber surface scenario for the first 5 hours simulation. As concentrations of nitrosamines and nitramines were very low, the modeled nitrosamines and nitramines concentrations are increased by a factor of 100 for better visibility. The results show that MEA decreased sharply in the first 3 hours (180 minutes) after simulation started, in good agreement with the EUPHORE chamber experiment [3]. Experiment 3 of this study showed that nitramine concentrations reached their highest value 3 hours after initial exposure to sunlight. Using Proton_Transfer_Reaction Time-of-Flight Mass Spectrometer (PTR-TOF-MS), the highest nitrosamine concentration observed was 0.055 ppb, but the modeled result was 2.953 ppb. In KPP simulation of this study, the nitramines concentration increased to the highest value after 3 hours, which agrees with the observations [25]. The highest value was only 0.00944 ppb. The over-prediction of this trace product could be due to loss of the nitrosamine to the sampling system. There are in addition differences in the reaction scheme used at EUPHORE and that used in the current study: the Module Efficiently Calculating the Chemistry of the Atmosphere (MECCA) included chemistry of C2-C4 alkanes, propene, isoprene and dimethyl sulphide. This study uses Carbon Bond version 6 chemistry scheme to run the simulation. Concentrations of nitrosamines and nitramines demonstrated fast increases at the beginning of the modeled experiment, then decreased mildly. Formaldehyde concentration increased after the model start and reached the highest value at about 4.5 hours from the beginning then began to decrease. The trend of formaldehyde concentration reflects secondary source contributions to the ambient formaldehyde concentrations. Previous study [26] measured formaldehyde value in summer time. The study shows that the secondary sources became a major contributor to ambient HCHO concentration after 9 am, and 70% of the formaldehyde concentrations between 12 pm to 3 pm were from secondary HCHO [26].

In the case of the amine chemistry in the atmospheric scenario, the results show that the concentration changes were slower than for the scenario including with wall loss. Figure 1 (b) shows results for 8 hours model run time. The MEA concentration decreased initially but was relatively constant but disappeared significantly slower than for the wall loss case as expected. Formaldehyde concentration reached its highest value of 5.4 ppb after about 6.5-7 hours of running time.
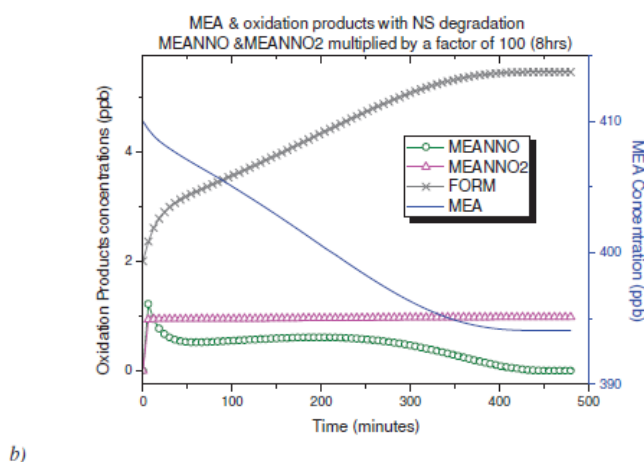

a)

b)
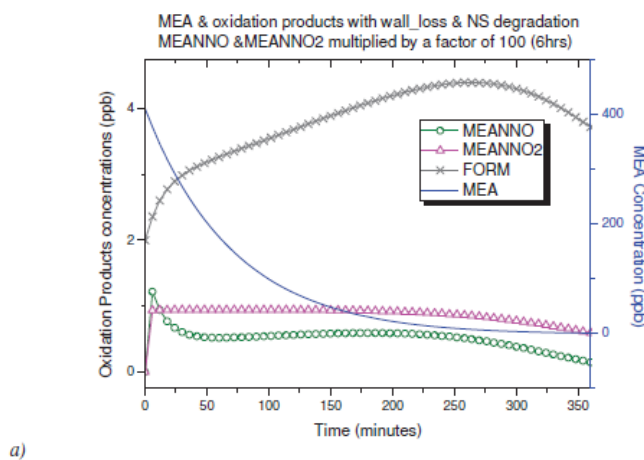
Fig. 1. (a) MEA and oxidation products with wall loss and nitrosamines degradation. (b) MEA and oxidation products with nitrosamines degradation. MEA: monoethanolamine; MEANNO: 2-(N-nitrosoamino)-ethanol; MEANNO2: 2-nitroamino ethanol; FORM: formaldehyde.

3.2. Results from modified CALPUFF model

Meteorological data that TAPM generated for the finest resolution (1 km) were converted to a 3-Dimensional data output file for input to the CALMET model. The meteorological data from the CALMET model were employed in CALPUFF to simulate pollutant transport and dispersion in the atmosphere. The concentration data were averaged to give 1-hour 24-hour averages time for the 49 × 49 km domain area. The data were processed for individual months. In the case of CALPUFF output data, concentrations were calculated for three target chemical compounds: MEA, HCHO & nitrosamine (NS). The 1-hour and 24-hour average concentrations for the three compound are shown in Figure 2. Meteorological data for the year 2000 were used in the case study. The three compounds in Figure 2 show that the lowest concentration values were observed in February and the highest concentration in December. Results from April to July show relative low values compared to other months. Previous studies [27, 28] measured formaldehyde concentration in China. Pang and Mu [27] observed that formaldehyde in summer time could be near 5 times higher than the value in winter time at a Beijing sampling site. Huang et al [28] indicated that the highest mean value was found in summer with a factor 4.5 times higher than the lowest mean value which was found in autumn. In the current study results consistent with these were observed apart for February. The highest average values of 0.003556 and 0.003624 µg/m³ were recorded in December for 1-hour and 24-hour averaging times respectively. MEA and nitrosamine show similar seasonal trends to formaldehyde. The highest value of MEA were found in December with 0.001844 & 0.001879 µg/m³ for 1-hour and 24-hour averages respectively. For nitrosamine, the highest values were 4.00145×10^{-5} and 4.07735×10^{-5} ng/m³, respectively. In February 2000, historical meteorological data showed that the hottest month of 2000 was February with average daily temperature of 28 ℃ [29]. However, the lowest calculated concentrations of all three compounds were observed in February. Particular meteorological features of the year 2000, including the temperatures could be responsible for these observations. The historical data of 2000 also showed that the windiest month of 2000 was February, with an average wind speed of 6 m/s [29]. The high speed wind could cause intensive atmospheric turbulence which can dilute the concentration values.
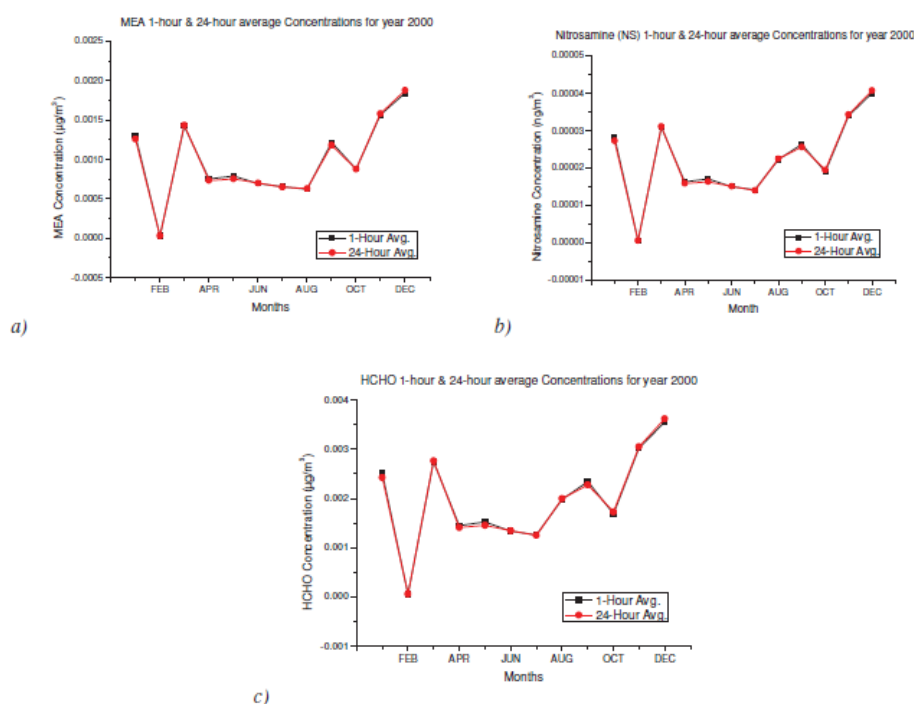
a)

b)

c)

Figure 2 Results from modified CALPUFF model for year 2000: a) MEA 1-Hour & 24-Hour average concentration; b) Nitrosamines (NS) 1-Hour & 24-Hour average concentration; c) Formaldehyde (HCHO) 1-Hour & 24-Hour average concentration.

3.3. Sensitivity analysis

In this case study, we consider the worst case scenario in sensitivity analysis. December data was selected for this task. Each scenario was run separately to generate concentrations of MEA, HCHO, and Nitrosamines (NS). The results are shown in Figure 3 below. The nitrosamines result is shown separately as unit difference. The parameters were changed based on the conditions of a Norway PCC project [9] . Figure 3 shows that changes to most of these parameters cause concentration values to increase except for case DEC4 where the exit velocity was increased to 20 m/s from 13.9 m/s. In DEC4 case, the increased exit velocity decreases MEA, HCHO, and NS by a factor of about 0.85. Figure 3 indicates that DEC2 has highest increase comparing to other case scenarios. In DEC2, the changed parameter is stack height where was decreased to 65 meters from 248 meters for both stacks. The lower stacks result in reduced plume rise resulting as expected in higher calculated concentrations as expected. The results shown in this DEC2 scenario are higher than other scenarios. The concentration values in DEC2 were about 3.16 times higher than for the original parameters, reaching 1-hour average values of 0.005835 and 0.011256 $\mu g/m^3$ for MEA and HCHO respectively. The nitrosamines 1-hour average value was about 1.2664×10^{-4} ng/m³. The DEC1 scenario indicates that the concentrations are higher than original setting with a factor of 1.87 while decreasing the diameters of stacks to half size of original. DEC3 had exit temperature decreased to 30 ºC from 100 ºC. The temperature change caused 2.41 times increase on three compounds values. The four case scenarios represent only a simple sensitivity analysis; in future work calculations will be performed for different months and by changing multiple parameters.
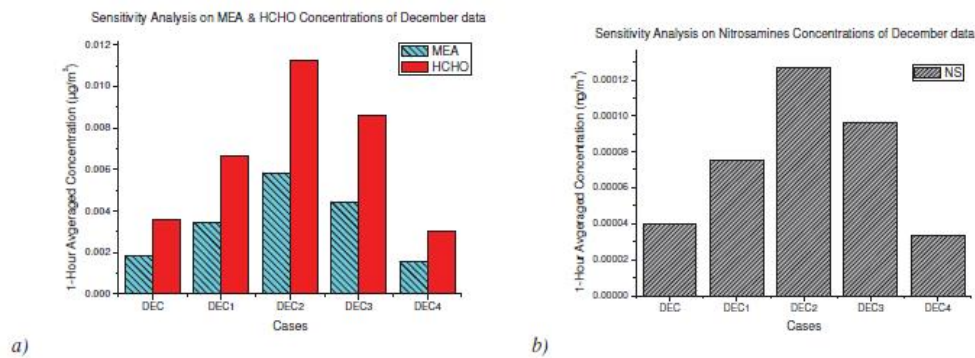
Figure 3 Results for sensitivity analysis based on December data: a) MEA & HCHO 1-Hour average concentration; b) Nitrosamines (NS) 1-Hour average concentration.

3.4. Risk Assessment

As concentration values in December were the highest observed, we only use December data to consider risk assessment. The @RISK model was employed to calculate risk distribution in the study domain relying on the parameters in Table 3. The risk distributions are shown in Figure 4. USEPA has levels of concern associated with risk values ranging from one in a million to one in ten thousand [30]. EPA's goal is to keep risk value below 1×10^{-6}. EPA takes action when the risk value is greater than one in ten thousand [30]. All risk values are below 1×10^{-6}. The maximum risk value of nitrosamine was 2.383×10^{-9} which is near three orders of magnitudes below 1×10^{-6}. The formaldehyde maximum risk value was 1.967×10^{-7} which is one order of magnitude below the USEPA level. The average risk value of formaldehyde was 3.758×10^{-8}. The values are well below the level where action is required. The impact of introduction of PCC technology is small. Figure 4 also shows that the risk distribution was determined by the dominant wind direction which is southeast in summer and northwest in winter [31].
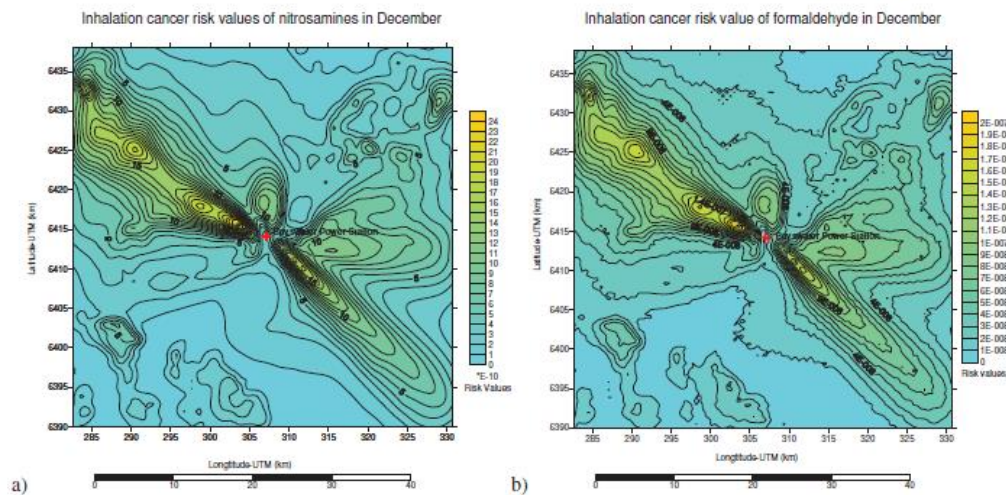

Figure 4 Inhalation cancer risk in December: a) Nitrosamines, value to be multiplied by 10^{-10}, b) Formaldehyde

4. Conclusion

The study indicates that amine-based post combustion carbon capture technology does not cause large impact on environment and human health. Sensitivity analysis demonstrates power station parameters can have impacts on concentration changes. As nitrosamines and formaldehyde are carcinogenic, further sensitivity analysis may be required to provide appropriate guidance for the development of effective regulation of PCC and hence the implementation of commercial scale projects.

Acknowledgements

References

[1] Karl M, Castell N, Simpson D, Solberg S, Starrfelt J, Svendby T, et al. Uncertainties in assessing the environmental impact of amine emissions from a CO2 capture plant. Atmospheric Chemistry and Physics Discussions 2014;14:8633-93.
[2] Thong D, Dave N, Feron P, Azzi M. Activity 3: Estimated emissions to the atmosphere from amine based PCC processes for a black coal fired power station based on literature and modelling. In: Portfolio C-ACT, editor. Environmental Impact of Amine-based CO2 Post-combustion Capture (PCC) Process: CSIRO; 2012.
[3] Karl M, Dye C, Schmidbauer N, Wisthaler A, Mikoviny T, D'Anna B, et al. Study of OH-initiated degradation of 2-aminoethanol. Atmospheric Chemistry and Physics 2012;12:1881-901.
[4] Låg M, Andreassen Å, Instanes C, Lindeman B. Health effects of different amines and possible degradation products relevant for CO2 capture. Nydalen, Norway2009.
[5] Nielsen CJ, D'Anna B, Dye C, Graus M, Karl M, King S, et al. Atmospheric chemistry of 2-aminoethanol (MEA). Energy Procedia 2011;4:2245-52.
[6] Larsen A, Jentoft NA, Greibrokk T. Determination of ppb levels of formaldehyde in air. The Science of the total environment 1992;120:261-9.
[7] Pitts JN, Grosjean D, Vanmcauwenberghe K, Schmidt JP, Fitz DR. Photooxidation of aliphatic amines under simulated atmospheric conditions: Formation of nitrosamines, nitramines, amides, and photochemical oxidant. Environ Sci Technol 1978;12:946-53.
[8] Scire JS, Strimaitis DG, Yamartino RJ. CALPUFF Version 6 User Instructions. the Atmospheric Studies Group at TRC Solutions; 2011.
[9] Fowler T, Vernon G. Report for Atmospheric chemistry modelling of Componets from post-combustion amine-based CO2 capture --Final Report. Det_Norske_Veritas; 2012.
[10] Sandu A, Sander R. Technical note: Simulating chemical systems in Fortran90 and Matlab with the Kinetic PreProcessor KPP-2.1. Atmos Chem Phys 2006;6:187-95.
[11] Wu Y, Nelson PF. Environmental Risk Assessment Of Formaldehyde Emission From Amines-Based Post-Combustion Carbon Capture Projects. 2013 CASANZ conference. Sydney: CASANZ-Clear Air Society of Australia & New Zealand; 2013.
[12] Sandu A, Sander R. kpp-2.1 Users Manual. 2005.
[13] Sander R, Baumgaertner A, Gromov S, Harder H, Jöckel P, Kerkweg A, et al. The atmospheric chemistry box model CAABA/MECCA-3.0. Geoscientific Model Development 2011;4:373-80.
[14] Bråten HB, Bunkan, A. J., Bache-Andreassen, L., Solimannejad, M. and Nielsen, C. J. Final Report on a Theoretical Study on the Atmospheric Degradation of Selected Amines. Oslo/Kjeller2008.
[15] Yiannoukas S, Morale G, Vernon G. Report for Atmospheric chemistry modelling of Componets from post-combustion amine-based CO2 capture –First approach. Det_Norske_Veritas; 2011.
[16] USEPA. Guidelines for Exposure Assessment (US-EPA). In: Agency USEP, editor. Washington, DC: U.S.Environmental Protection Agency; 1992.
[17] Protection NJDoE. Inhalation exposure pathway soil remediation standards--basisi and background. New Jersey http://www.state.nj.us/dep/srp/regs/rs/bb_inhalation.pdf: New Jersey Department of Environmental Protection; 2008.
[18] USEPA. Risk Assessment Guidance for Superfund. Human Health Evaluation Manual (Part A) Interim Final. Washington, DC.: Office of Emergency and Remedial Response; 1989.
[19] California-EPA. The Air Toxics Hot Spots Program Guidance Manual for Preparation of Health Risk Assessments. In: Office-

171

of-Environmental-Health-Hazard-Assessment, editor. California2003.

[20] Arija V SJ, Fernandez-Ballart J CG, C. M-H. Consumption, dietary habits and nutritional status of the Reus population (IX)--Evolution of food consumption, energy and nutrient intake and relationship with the socioeconomic and cultural level,1983-1993. Med Clin (Barc) 1996;106:174-9.

[21] Smith RL. Use of monte carlo simulation for human exposure assessment at a superfund site. Risk Analysis 1994;14:433-9.

[22] USEPA. Cancer Risk Calculations. Handbook for Implementing the Supplemental Cancer Guidance at Waste and Cleanup Sites. http://www.epa.gov/oswer/riskassessment/sghandbook/riskcalcs.htm: USEPA Website; 2012.

[23] EPA U. Hazard Summary-N-Nitrosodimethylamine. In: U.S.EPA, editor. http://www.epa.gov/ttn/atw/hlthef/nitrosod.html.2000.

[24] USEPA. Integrated Risk Information System-Formaldehdye. http://www.epa.gov/iris/subst/0419.htm2012.

[25] Karl M, Dye C, Schmidbauer N, Wisthaler A, Mikoviny T, D'Anna B, et al. Study of OH-initiated degradation of 2-aminoethanol. Atmos Chem Phys 2012;12:1881-901.

[26] Lin YC, Schwab JJ, Demerjian KL, Bae M-S, Chen W-N, Sun Y, et al. Summertime formaldehyde observations in New York City: Ambient levels, sources and its contribution to HOx radicals. Journal of Geophysical Research 2012;117.

[27] Pang X, Mu Y. Seasonal and diurnal variations of carbonyl compounds in Beijing ambient air. Atmospheric Environment 2006;40:6313-20.

[28] Huang J, Feng Y, Li J, Xiong B, Feng J, Wen S, et al. Characteristics of carbonyl compounds in ambient air of Shanghai, China. Journal of Atmospheric Chemistry 2008;61:1-20.

[29] WeatherSpark. Historical Weather For 2000 in Sydney, Australia - WeatherSpark. http://weatherspark.com/history/34088/2000/Sydney-New-South-Wales-Australia: Weather Spark; 2000.

[30] Gerba CP. Risk Assessment. In: Pepper IL, C.P. Gerba, Brusseau ML, editors. Environmental and Pollution Science. Amsterdam Elsevier Inc., ; 2006. p. 212-32.

[31] Meteorology ABo. Climate statistics for Australian locations. http://www.bom.gov.au/climate/averages/tables/cw_061086.shtml ,2014.

172